Molecular Toxicological Mechanisms of New Psychoactive Substances *In Vitro*

Inauguraldissertation

zur Erlangung der Würde eines Doktors der Philosophie

vorgelegt der

Philosophisch-Naturwissenschaftlichen Fakultät

der Universität Basel

von

Xun Zhou

aus China

Basel, 2020

Genehmigt von der Philosophisch-Naturwissenschaftlichen Fakultät
auf Antrag von

Prof. Dr. Stephan Krähenbühl, Erstbetreuer

Prof. Dr. Jörg Huwyler, Zweitbetreuer

Dr. Evangelia Liakoni, externer Experte

Basel, den 17.03.2020

Prof. Dr. Martin Spiess

Dekan der Philosophisch-Naturwissenschaftlichen Fakultät

TABLE OF CONTENTS

Acknowledgement

Three years ago, I came to Switzerland from China. This was the first time I left my hometown and went abroad. At the end of my exciting and memorable journey, I would like to express my sincere thanks to the people that have been accompanying me along the way.

First of all, my foremost and sincere gratitude goes towards my PhD supervisor Prof. Stephan Krähenbühl. You offered me great opportunities to join your outstanding lab three years ago. You also opened a new door to academic research for me that has greatly influenced my way of thinking about science. Thank you for providing me with fantastic research conditions. Thank you for your purposive lead and your regular motivations. Thank you for your encouragement and inspiration. I feel extremely lucky to have had such an incredible supervisor.

I would like to express my gratitude to Prof. Jörg Huwyler, Dr. Evangelia Liakoni and Prof. Alex Odermatt for joining my thesis committee. Thanks for your invaluable support, encouragement and insightful comments.

My sincere thanks also go to my additional supervisor and best friend, Riccardo. Thank you for your valuable comments and help with my research plans, statistical analysis and scientific writing. Your enthusiasm for science and data mining has greatly influenced me. Mille Grazie! I'm glad you like my dumplings and hope to invite you to have various dumplings in China.

A big thank you goes to each colleague of the “Lab 410”. You make our lab become such a fun and inspiring place. I would like to thank Jamal. Thank you for your help at the beginning of my PhD study, which let me start my experiment smoothly. Thank you for sharing your opinions and valuable experiences with me. Additionally, your French desserts are really delicious. Dino introduced me into the work with mitochondrial dysfunction. Dino, Deborah and I had a very pleasant experience to attend the congress in Bucharest. Gerda is the Western Blot expert of our lab, thanks for your help with my Western Blot experiment, and I was really enjoying your birthday party and durian sugar. I want to thank Karolina and Noëmi for your personal support and encouragement during my difficult moments, especially when I had stress from my family. Urs and Miljenko, thank you for good ideas about my project and thank you for inviting me to your party. I also appreciated the funny talks with Fabio and David during lunch and breaks. Bea, thanks for helping me the orderings and sharing your pictures to me.

Franziska introduced me into the Seahorse work, this is an important part of my project during the three years. Moreover, I would like to thank all master students, I enjoyed working and talking with you. Working in the lab 410 was a great pleasure for me!

I am grateful for Evelyne, you helped me find the apartment and had the “first” cup of coffee when I arrived in Switzerland.

Last but not least I would like to express my gratitude towards my family. To support me as a PhD student is not an easy decision for traditional Chinese parents. However, my parents have always supported my decision, even they have to face some opposition. I love you!

我非常感谢你们的支持与帮助! 这三年是我人生中美好和难忘的回忆。

Abbreviations

ACD	Autophagic cell death
ADHD	Attention deficit hyperactivity disorder
ADP	Adenosine diphosphate
AO	Acridine orange
APAF-1	Apoptotic protease activating factor 1
ATP	Adenosine triphosphate
AV	Autophagic vacuole
AVO	Acidic vacuolar organelle
BBB	Blood-brain barrier
BDNF	Brain-derived neurotrophic factor
CARD	Caspase recruitment domain
CNS	Central nervous system
COX	Cytochrome *c* oxidase
CPK	Creatine phosphokinase
CYPs	Cytochromes P450
DA	Dopamine
DAT	Dopamine transporter
DNA	Deoxyribonucleic acid
DR	Death receptor
EMCDDA	European monitoring centre for drugs and drug addiction
ETC	Electron transport chain
FADH$_2$	Reduced form of flavin adenine dinucleotide
FCCP	Carbonyl cyanide *p*-(trifluoromethoxy) phenylhydrazone
HEK 293	Human embryonic kidney 293 cells
Hsp 70	70 Kilodalton heat shock proteins

IAP	Inhibitor of apoptosis protein
IC_{50}	Half maximal inhibitory concentration
LSD	Lysergic acid diethylamide
LC3	Microtubule-associated proteins light chain 3
MAO	Monoamine oxidases
MC	Methcathinone
MDMA	3,4-Methylenedioxymethamphetamine
MDPV	Methylenedioxypyrovalerone
METH	Methamphetamine
Methylone	3,4-Methylenedioxymethcathinone
mPTP	Mitochondrial permeability transition pore
NADH	Ubiquinone oxidoreductase
Naphyrone	Naphthylpyrovalerone
NE	Norepinephrine
NET	Norepinephrine transporter
NPS	New psychoactive substance
OCR	Oxygen consumption rate
OXPHOS	Oxidative phosphorylation
PCA	4-Chloroamphetamine
PI	Propidium iodide
PS	Phosphatidylserine
ROS	Reactive oxygen species
RA	Retinoic acid
SOD	Superoxide dismutase
TCA	Tricarboxylic acid cycle

UCP3	Uncoupling protein 3
UQH2	Ubiquinol
VMAT2	Vesicular monoamine transporter 2
3-MMC	3-Methylmethcathinone
4-CMC	4-Chloromethcathinone
4-FA	4-Fluoroamphetamine
4-FMC	4-Fluoromethcathinone
4-MMC	4-Methylmethcathinone (mephedrone)
5-HT	5-Hydroxytryptamine
5-HTT	5-Hydroxytryptamine
α-PVP	α-Pyrrolidinopentiophenone
Δψm	Mitochondrial membrane potential
Δp	Electrochemical proton dynamic
ΔpHm	Mitochondrial pH gradient

Summary

In recent years, many “new psychoactive substances” (NPS), such as amphetamine and synthetic cathinone derivatives, have dramatically appeared on the illegal market, and the abuse of these drugs is now a global crisis. The mechanisms of cytotoxicity associated with NPS are still unclarified. The aims of this thesis were to comprehensively evaluate the mechanisms of NPS-induced myotoxicity, hepatotoxicity and neurotoxicity *in vitro,* and as well as to assess the role of hyperthermia on methcathinone-induced neurotoxicity. Therefore, we treated human hepatoma HepG2 cells, mouse muscle C2C12 cells, and human neuroblastoma SH-SY5Y cells with amphetamines and synthetic cathinones at concentrations from 50-2000 μM.

In the first paper, we focused on the toxicological effects in C2C12 cells of the following synthetic cathinones: 3,4-methylenedioxymethcathinone (methylone), 4-methylmethcathinone (4-MMC, mephedrone), 3-methylmethcathinone (3-MMC), methylenedioxypyrovalerone (MDPV), α-pyrrolidinopentiophenone (α-PVP), and naphthylpyrovalerone (naphyrone). All the investigated synthetic cathinones showed a concentration-dependent impairment of the cell membrane integrity, a drop in intracellular adenosine triphosphate (ATP) content, and an increase of mitochondrial superoxide concentrations. α-PVP and naphyrone impaired basal and maximal cellular respiration and inhibited the activities of complex I and II of the electron transport chain (ETC). These results indicated mitochondrial dysfunction associated with these drugs. In conclusion, α-PVP and naphyrone showed mitochondrial toxicity after 24 h exposure. In comparison, the cytotoxic effects of methylone, 4-MMC (mephedrone), 3-MMC and MDPV were related to an impairment of glycolysis rather than inhibition of mitochondrial pathways.

The goal of the second paper was to investigate the pharmacological profile and the potential hepatotoxicity of *para*-halogenated amphetamines and cathinones *in vitro*. We determined the pharmacological profile in transporter-transfected human embryonic kidney 293 cells (HEK 293). Amphetamine, 4-fluoroamphetamine (4-FA), 4-chloroamphetamine (PCA), methcathinone (MC), 4-fluoromethcathinone (4-FMC) and 4-chloromethcathinone (4-CMC) inhibited the norepinephrine transporter (NET) and the dopamine transporter (DAT). Moreover, the inhibition of these compounds on the dopamine *versus* the serotonin transporter, showed selectivity in their activity, which decreased together with the increasing size of the *para*-substituents, resulting in an inhibition of the serotonin uptake. Concerning the assessment

of hepatocellular toxicity, we found that all substances induced membrane toxicity, depletion of the intracellular ATP content and formation of reactive oxygen species (ROS) in HepG2 cells. The decrease in the ATP content was at a lower concentration than the damage of the cell membrane integrity, which suggests mitochondrial toxicity. Furthermore, amphetamines and 4-CMC impaired the mitochondrial respiratory chain, confirming their nature as mitochondrial toxicants. Finally, both 4-FA and 4-CMC induced apoptosis and necrosis in HepG2 cells. Taken together, *para*-halogenation of amphetamines and cathinones increase the risk for serotonergic neurotoxicity, which may induce hyperthermia *in vivo*. The toxicity rank of the substitutes was the following: chloride > fluoride > hydrogen.

The purpose of the third study was to characterize the mechanisms of neurotoxicity of amphetamine, 4-FA, PCA, methcathinone (MC), 4-FMC and 4-CMC. 4-FA, PCA and 4-CMC strongly impaired membrane integrity, depleted ATP intracellular content and decreased the mitochondrial membrane potential of undifferentiated and differentiated neuronal SH-SY5Y cells, indicating mitochondrial toxicity. Moreover, PCA and 4-CMC inhibited the function of the ETC, increased ROS and induced apoptosis for both cell types. Besides that, caspase 3 and 9 were activated after 4-CMC exposure. In conclusion, PCA and 4-CMC impaired the function of mitochondria and induced apoptosis in undifferentiated and differentiated SH-SY5Y cells, while 4-FA depleted ATP content, increased ROS formation, and decreased mitochondrial membrane potential in undifferentiated SH-SY5Y cells. This study further supported the toxicity rank of *para*-halogenated amphetamines and cathinones (Cl > F > H).

In the last study, we investigated the effects of hyperthermia (40.5 °C) on the neurotoxicity of MC, 4-MMC and 4-CMC in SH-SY5Y cells. We found that 4-MMC and 4-CMC caused cell membrane damage, decreased intracellular ATP content, impaired the function of ETC, and increased ROS levels at both thermic conditions. At the hyperthermic condition (40.5 °C), SH-SY5Y cells exposed to test drugs were more sensitive than at the normothermic condition (37 °C). MC also induced an increase of ROS and inhibited ETC, however only at the hyperthermic condition. Moreover, hyperthermia reduced drug-induced apoptosis by promoting the expression of the 70 kilodalton heat shock proteins (Hsp70), but was associated with late autophagy and cell death. In conclusion, hyperthermic conditions increased the neurotoxic properties of methcathinones due to enhanced impairment of mitochondrial function and induced late autophagy and cell death when early protective measures were overwhelmed.

Introduction

1. Psychoactive Drugs

Psychoactive drug is a generic term referring to some chemical substance that can act on the function of the nervous system and lead to psychological effects such as changes in perception, mood, feelings, awareness and/or behaviour. Psychotropic drugs are mainly classified into three groups [1]:

- Stimulants: substances that can excite the body's central nervous system (CNS) and can cause anxiety, psychosis, paranoia, hyperthermia, depression, heart failure, stroke, seizures and even death. Common stimulants include nicotine, amphetamines, cocaine, ritalin, methamphetamine, ecstasy, caffeine [2].
- Depressants: substances that can slow down the CNS. The abuse of depressants can increase sluggish thinking, induce sedation and sleep and are associated with dependence after repetitive ingestion with withdrawal symptoms. Examples of depressants include benzodiazepines such as flunitrazepam, diazepam and midazolam, the benzodiazepine-like Z-drugs such as zolpidem and the barbiturates benzodiazepines [3].
- Hallucinogens: substances that can distort the communication within different areas of the brain. Users report some immediate impact as rapidly shifting emotions, flashbacks, distorted cognition, paranoia, hallucinations, anxiety, nausea. Examples of hallucinogens include LSD, mescaline, "magic mushrooms", ecstasy, cathinones, and cannabis [4, 5].

1.1. New Psychoactive Substances (NPS)

New psychoactive substances (NPS) are a wide variety of psychoactive compounds which are not controlled by the 1961 Convention on Narcotic Drugs or the 1971 Convention of Psychotropic Substances [6]. They are also known as "legal highs", "bath salts", "plant food", "herbal highs", "party pills" or "research chemicals". Since the 2000s, a large number of NPS has begun to appear on the illicit market and over the internet for recreational use. The drug manufacturers create novel compounds to circumvent the ban of drugs in some countries, in order to stay ahead of the law [7]. However, NPS are not innocuous recreational substances, they can be as harmful as illicit drugs to users. A large part of NPS is represented

by derivatives of amphetamine and synthetic cathinones [6]. The structures of some amphetamine and cathinone derivatives are shown in Figure 1.

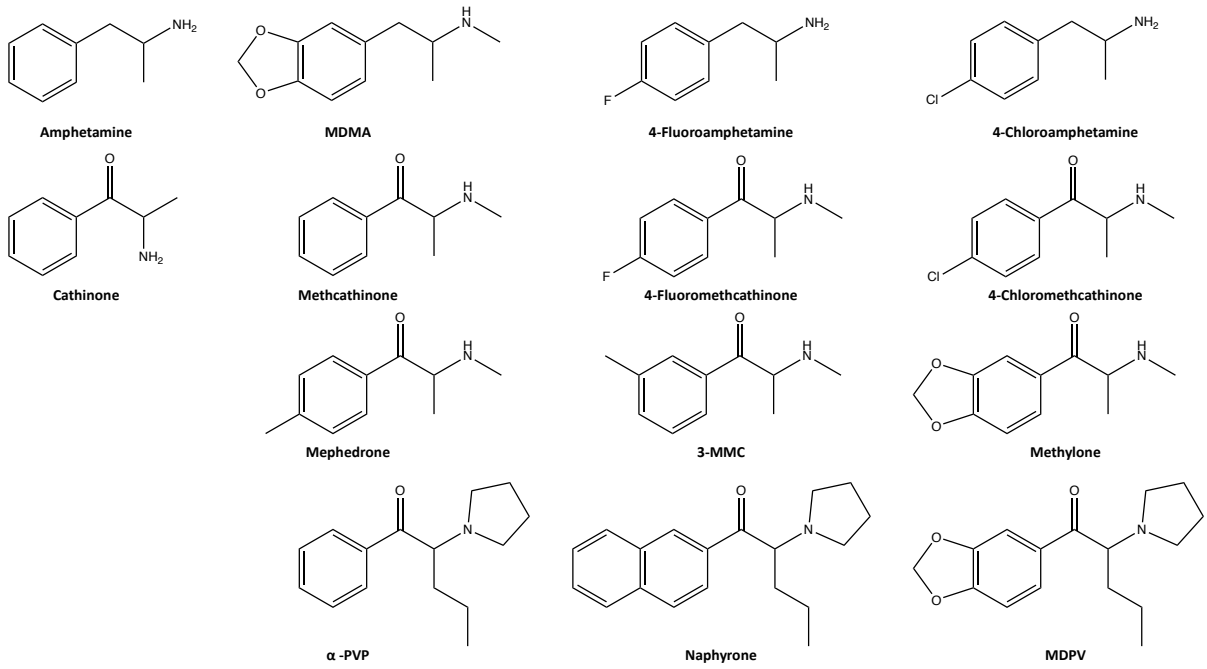

Figure 1. Chemical structure of some amphetamines and synthetic cathinones.

1.2. Halogenation

Halogenation is an easy and effective method for modification of known compounds in order to change their solubility and their pharmacological properties. Chlorination and bromination are the predominant modification, while fluorination and iodination are performed more rarely [8]. The introduction of halogenated substituents into many natural compounds can profoundly affect their biological activity [9], and can modify membrane binding and cell permeation [10].

Halogenation is also an effective tool to create NPS, since many common psychoactive drugs have been banned in many countries. For instance, *para*-halogenated amphetamines and methcathinones, 4-FA, PCA, 4-FMC and 4-CMC, have recently appeared on the illegal drug market [11-15]. As mentioned above, halogenation can change the pharmacological and toxicological profile of psychoactive drugs. PCA has an increased serotonergic toxicity when compared to amphetamine *in vitro* [16-18]. In a microdialysis study of the nucleus accumbens in rats, *para*-halogenated methcathinones (-F, -Cl or -Br)

increased dopamine (DA) and 5-hydroxytryptamine (5-HT) release with different potencies compared to methcathinone [19].

1.3. Amphetamines

Amphetamines form a family of structurally similar drugs [20], including natural alkaloids and chemically synthesized derivatives [21]. Natural amphetamines have been used as plant products for more than thousand-years and extracted from various genus of the plant *Ephedra* and from the tree *Catha edulisor* [21]. Since Lazar Edeleanu produced the first synthetic amphetamine in 1887 [22], many chemically synthesized amphetamine derivatives have appeared, for instance methamphetamine (METH) and 3,4-methylenedioxymethamphetamine (MDMA, ecstasy) [21, 23]. The structural definition of amphetamines was reported by J.H. Biel and B.A. Bopp in 1978 [24]: (1) an unsubstituted phenyl ring, (2) a two-carbon side chain between the phenyl ring and nitrogen, (3) an α-methyl group, and (4) a primary amino group [25] (Figure 2).

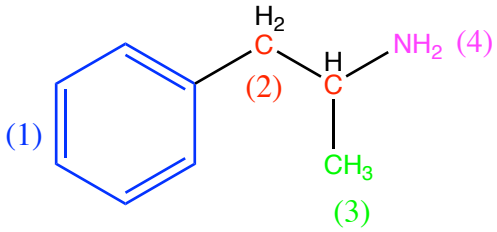

Figure 2. The generic structure for amphetamines.

General pharmacological properties of amphetamines are shown in Figure 3. Amphetamines predominantly enter into the cell cytoplasm through neuronal monoamine transporters [26]. Amphetamines can affect the peripheral and central human nervous system through their interaction with the presynaptic monoamine transporters of dopamine (DAT), serotonin (SERT) and noradrenaline (NAT) [20]. Moreover, amphetamines act as competitive substrates for transporters in the uptake of biogenic amines such dopamine (DA), norepinephrine (NE), and serotonin (5-HT) [27]. Furthermore, amphetamines have different affinity for DAT, NAT and SERT [20]. The selectivity of amphetamines also corresponds to the specific neurotoxic effects of these drugs [20]. They can bind to intracellular vesicular monoamine transporter 2 (VMAT 2), thereby reducing vesicular monoamine storage. Amphetamines can also inhibit monoamine oxidase (MAO)-mediated monoamine breakdown, thereby increasing cytoplasmic monoamine concentrations [28]. Eventually, excessive extracellular noradrenaline, dopamine and serotonin lead to acute toxicity [29]. An

obvious clinical manifestation is the α- and β-adrenergic receptor-mediated sympathomimetic toxidrome [29].

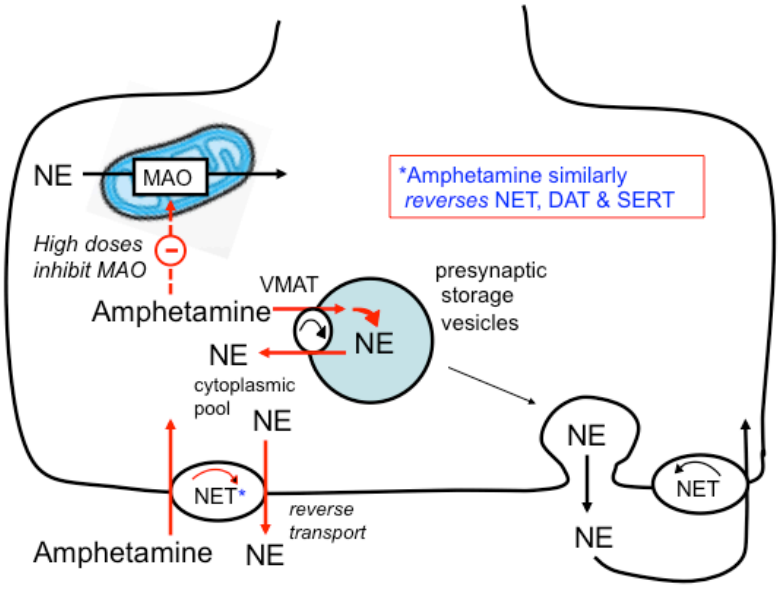

Figure 3. Mechanism of action of amphetamines on synaptic terminal of neurons [30].

Amphetamine (Figure 4) was first synthesized in 1887, and initially it has primarily been used as a stimulant [31]. Since 1930, amphetamine was being prescribed to treat narcolepsy and obesity [31, 32]. It was also noted in the 1930s that amphetamine is able to cross the blood brain barrier (BBB) and induce a wide range of behavioral changes, such as euphoria and pleasurable effects [31]. These effects resulted in a widespread prescription and also in drug abuse [31]. After the addictive potential of amphetamine had been observed and described, amphetamine was classified under the Convention on Psychotropic Substances as a Schedule II drug in the US and internationally [33].

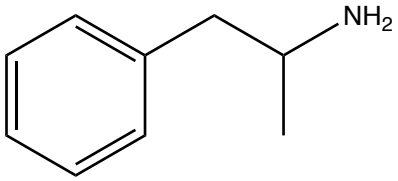

Figure 4. Chemical structure of amphetamine.

MDMA (3,4-methylenedioxymethamphetamine, Figure 5), is an amphetamine-derivative and was initially synthesized as a member of new haemostatic substances in 1912 by Merck [23]. In the 1970s, MDMA was used as medicine to enhance

the effect of psychotherapy, then, it became popular as recreational drug for decades [34]. Although MDMA is not a novel psychoactive substance, it still occupies one of the largest shares of recreational use. MDMA is a stimulant and enhances sociability [35], such as emotional empathy, trust and extroversion [36, 37]. MDMA has a significant higher affinity for 5-HTT and NAT over DAT, due mainly to the addition of the 3,4-methylenedioxy group to the phenyl ring [38]. For this reason, MDMA is considered a primarily serotonergic drug, with less sympathomimetic effects than amphetamine at low doses [29]. The low activity for DAT explains its low or lacking addictive potential, which is different from amphetamine.

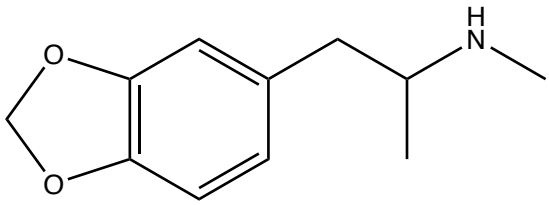

Figure 5. Chemical structure of MDMA

4-Fluoroamphetamine (4-FA, Figure 6) is a *para*-substituted amphetamine, which has been synthesized in the 1940s [39]. It was first used as a recreational drug in 2003 [40]. In a survey among the users, 4-FA shares comparable subjective effects with amphetamine and MDMA [41]. In animal studies, 4-FA can induce the release of NE, DA and 5-HT and inhibit their reuptake in the brain [41-44]. Different from other *para*-halogenated compounds, 4-FA does not deplete the neuronal 5-HT in the brain of rats [45]. This may reflect the fact that 4-FA, due to the fluoride in the p-position, is metabolized differently compared to amphetamine.

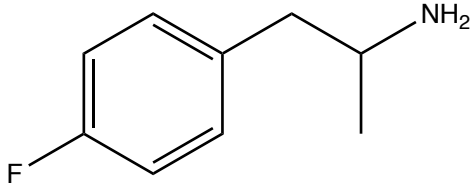

Figure 6. Chemical structure of 4-FA.

4-Chloroamphetamine (PCA, Figure 7) is another *para*-substituted derivative of amphetamine, known as depletor of brain serotonin [46], since it selectively toxic on serotonergic neurons in animal studies [16]. The clinical effects of PCA are considered to be similar to MDMA, however, it shows a higher neurotoxicity due to the effects of its

metabolites [16]. In addition to acute reversible neurotoxicity, PCA has as well long-term effects, including tryptophan hydroxylase inactivation and neuronal destruction [16].

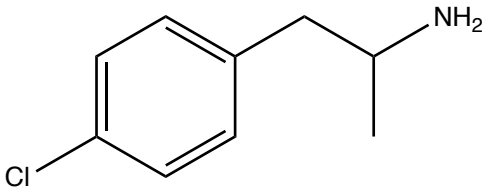

Figure 7. Chemical structure of PCA

1.4. Synthetic Cathinones

Cathinone (Figure 8A) is an alkaloid that has been first isolated from the fresh leaves of khat shrub (*Catha edulis*) in 1975. Cathinones are β-keto amphetamine derivatives [47], which psychostimulant effects [48]. Many experiments have demonstrated that cathinone has a pharmacological profile on the CNS and sympathomimetic effects close to amphetamine [49]. However, isolated cathinone degrades rapidly. For clinical use, a growing number of synthetic cathinone derivatives have been synthesized, such as bupropion, which was introduced as an antidepressant in 1985.

Synthetic cathinones (Figure 8B), which were designated as "legal highs", have recently emerged and rapidly grown into the NPS scene [50]. Nowadays, nearly more than one hundred different synthetic cathinones were detected by the European Union Early Warning System from 2005 to 2017 [51, 52].

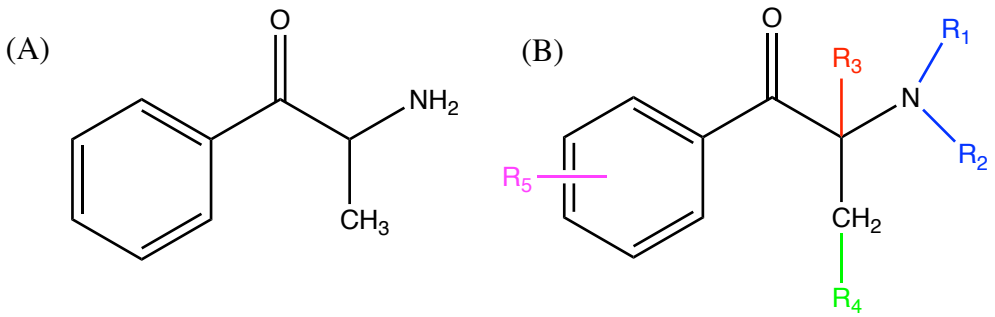

Figure 8. Chemical structure of (A) cathinone and general structure of (B) synthetic cathinones [50].

In vitro studies of synthetic cathinones have shown that they can penetrate the BBB easily [53]. Increasing concentration of catecholamines into the inter-synaptic space can stimulate the CNS and sympathetic nerve system, and their effects are usually stronger than for amphetamines, despite their structures are similar [54]. Similar to amphetamine, synthetic

cathinones can inhibit some monoamine transporters, including the dopamine transporter (DAT), the noradrenaline transporter (NAT), and the serotonin transporter (SERT) [54]. According to the mechanisms of action, synthetic cathinones can be classified into three groups [53, 54]:

- Cocaine-MDMA-mixed cathinone group. This group can non-selectively inhibit monoamine uptake (similar to cocaine) and promote serotonin liberation (similar to MDMA) (e.g. 4-MMC, methylone).
- Methamphetamine-like cathinone group. This group can preferentially inhibit the reuptake of catecholamines and induce the release of DA (e.g. methcathinone, 4-FMC and 4-CMC).
- Pyrovalerone-cathinone group. Members of this group are potent and selective inhibitors of the DA and NA transporter (e.g. MDPV and α-PVP).

Methcathinone (MC, Figure 9), commonly known as ephedrone, is a methyl derivative of cathinone [55]. It was first developed during the processes of synthesis of ephedrine in Germany and France in the early 1920s [56]. During the 1930s and 1940s, it was used as an antidepressant in the Soviet Union [57]. Between the 1950s and the 1960s, methcathinone was studied as a potential appetite suppressant, but its strong addictive potential was gradually revealed and the clinical applications were stopped [58]. During the 1970s and 1980s, methcathinone had a widespread recreational use under the name of "Jeff" in the USSR [59]. Subsequently, it appeared in the USA in the early 1990s, where its popularity increased rapidly [59]. In 1993, it was added to the Federal Controlled Substances Act [60]. Finally, in 1994, it was included under the Schedule I of the UN Convention on Psychotropic Substances [59]. Methcathinone has a similar pharmacological mechanisms as amphetamine with a comparable monoamine transporter inhibition profile [53].

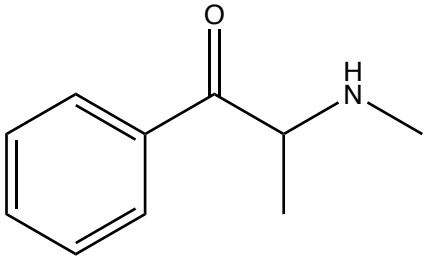

Figure 9. Chemical structure of methcathinone.

4-Methylmethcathinone (mephedrone, 4-MMC, Figure 10) was first reported by Saem de Burnaga Sanchez in 1929 [61]. 4-MMC has remained in obscurity until 2003, when clandestine chemists rediscovered it and communicated it online [62]. It became widely abused as an alternative to MDMA in the subsequent decade, due to its low price and low harm potential [63, 64]. Since more and more reports of hospital admissions and overdose deaths appeared with time, mephedrone has been classified as a Class B substance under the Misuse of Drugs Act in 2010 [65]. Following that, it was banned by all European Monitoring Centre for Drugs and Drug Addiction (EMCDDA) member states in 2010 and by the USA in 2011 [66, 67].

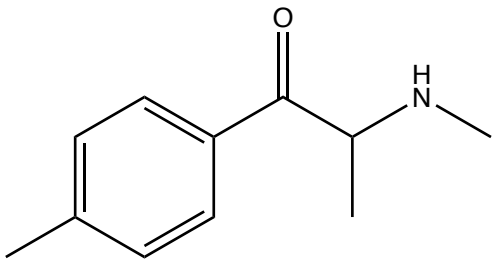

Figure 10. Chemical structure of 4-MMC

3-Methylmethcathinone (3-MMC, Figure 11) is a synthetic cathinone and a structural isomer of mephedrone, which was reported in 2012 by the Swedish Poisons Information Centre in 2012 [68]. It is one of the most popular NPS around the world [69]. Due to its sweet liquorice-like taste, it was also called as *sladoled*, ice cream [70, 71]. It is a substitute of mephedrone, with similar psychostimulant properties and weaker toxicological effects than its mephedrone [69, 71-73].

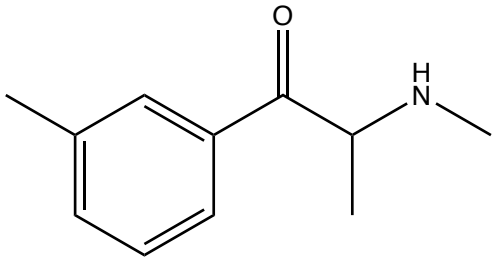

Figure 11. Chemical structure of 3-MMC

Methylone (3,4-methylenedioxymethcathinone, MDMC, βk-MDMA, Figure 12), is a cathinone derivative and an analogue of MDMA. It was first developed by Peyton Jacob III and Alexander Shulgin, and patented as a potential antidepressant in 1996 [74, 75]. At around 2004, methylone began to emerge online under the name “Explosion” and was then abused in

several countries, such as Japan, USA, and also in Europe [76, 77]. Since 2007, it became illegal in Sweden, and then it has also been banned in the UK and France in 2010 and 2012, respectively [75]. Compared to MDMA, methylone has subtle differences on the effects of recreational use [78], with which it shares similar risks and adverse effects [75, 79]. The pharmacological profile is similar to 4-MMC [53].

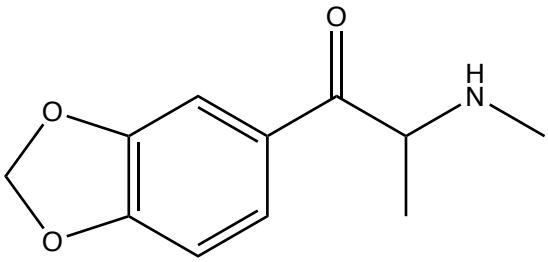

Figure 12. Chemical structure of methylone

Methylenedioxypyrovalerone (MDPV, Figure 13) is a stimulant and member of the cathinone class. It was first synthesized by Boehringer Ingelheim in 1969 [80]. Until 2004, MDPV was reported as a new designer drug and then sold as the major component of "bath salts" [81, 82]. Since 2010, MDPV became a controlled substance in the UK, Australia, and in some European countries [83]. Moreover, it is controlled in the USA as Schedule I controlled substance (2011) [84]. Structurally, MDPV is similar to MDMA. They both contain a 3,4-methylenedioxy ring and the phenyl group, while MDPV presents a pyrrolidine ring. MDPV is a blocker of DAT and NET [53, 85, 86]. Due to the pyrrolidine ring, the pharmacological properties of MDPV are distinct from other synthetic cathinones [82, 87]. In this regard, MDPV is pharmacologically much similar to cocaine rather than to cathinone [82, 87].

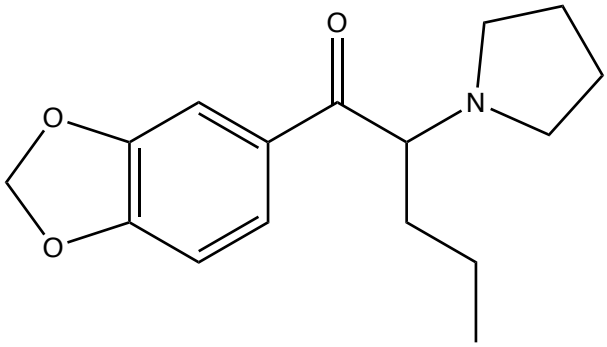

Figure 13. Chemical structure of MDPV

α-Pyrrolidinopentiophenone (α-PVP, "gravel" or "flakka", Figure 14) is a pyrrolidine-type cathinone derivative and known as a component of "bath salts" [88]. It was

developed by Boehringer Ingelheim in the 1960s as CNS stimulant and pressor agent [88]. Since α-PVP has been reported to cause human fatalities, it was placed by the US DEA under Schedule I in a temporary scheduling action in 2014 [89-91].

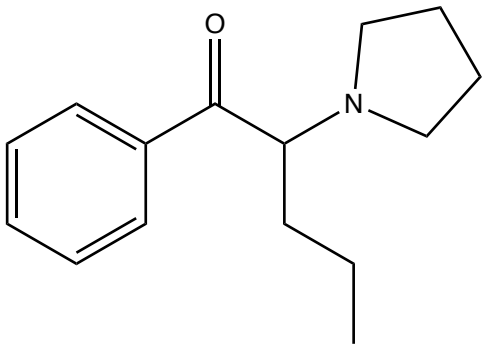

Figure 14. Chemical structure of α-PVP

Naphyrone (Figure 15**)**, which is also well known as NRG-1 or O-2482, is derived from pyrovalerone [92]. It was first synthesized in 1964 and then sold as a triple reuptake inhibitor with stimulant effects [93]. To date, naphyrone is scheduled as Class B drug in the UK since 2010 [94]. Due to its structure, naphyrone has higher lipophilicity than other synthetic cathinones, and it can easier permeate brain increasing its exposure *in vivo* [95]. Currently, there are little data about the toxicology of naphyrone, since is usually used in mixture with other cathinones [96]. The monoamine uptake transporter inhibition profile of naphyrone is very similar to the one of cocaine [53]. Moreover, naphyrone is not a monoamine releaser [53].

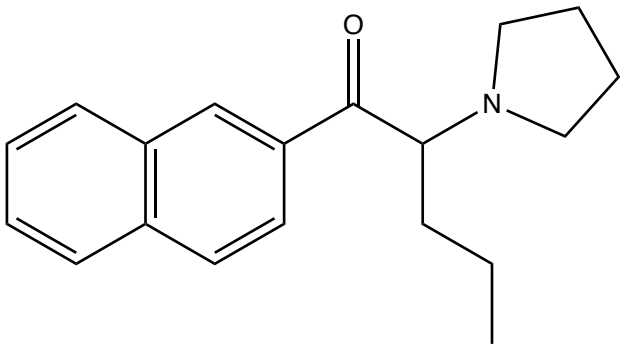

Figure 15. Chemical structure of naphyrone.

4-Fluoromethcathinone (4-FMC, flephedrone, Figure 16) was first reported in 1952 as a potentially antibacterial, antithyroidal and bacteriostatic medicine [97, 98]. Since 2010, many countries have listed 4-FMC as illegal substance [99]. It is also listed as Schedule I controlled substance in the US [91]. 4-FMC belongs to "methamphetamine-like cathinones"

group, and it has similar pharmacological profile with 4-FA [43]. 4-FMC can inhibit DAT but not 5-HTT, it is also a potent releaser of DA but not of 5-HT [43].

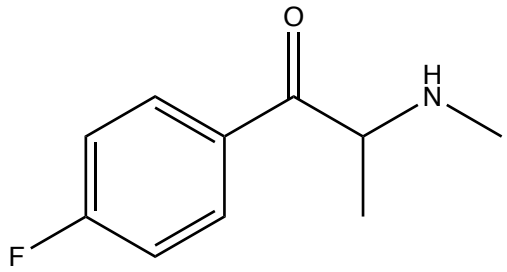

Figure 16. Chemical structure of 4-FMC

4-Chloromethcathinone (4-CMC, Figure 17) is a chlorine-substituted cathinone, which appeared in the internet as a designer drug since 2014 [14]. It is strictly controlled in many countries, such as Germany, China and the USA [100]. There is little data about its pharmacokinetic, pharmacological and toxicological effects [101]. It is often sold with MDMA or even as a fake MDMA [11]. The effects on the users depend on the route of administration: oral ingestion leads to a euphoric effect, while snorting can increase concentration and self-confidence [101].

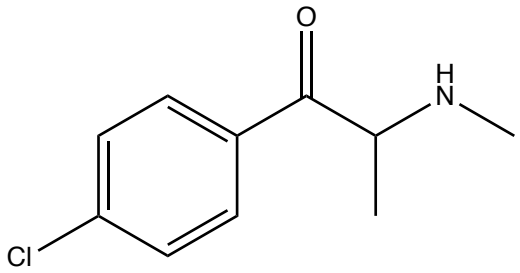

Figure 17. Chemical structure of 4-CMC

2. Toxicology

2.1. Clinical Effects

Amphetamine abuse leads to a wide range of clinical manifestations. Clinical effects of acute and chronic use of amphetamines and synthetic cathinones are summarized in Table 2 [29, 79].

Table 2. Clinical manifestations of amphetamines and synthetic cathinones toxicity.

System	Amphetamines	Synthetic Cathinones
Cardiovascular	Tachycardia, hypertension, aortic dissection, arrhythmias, vasospasm, acute coronary syndrome, hypotension (late sign), acute cardiomyopathy	Palpitations, shortness of breath, chest pain
Neurologic	Agitation, paranoia, euphoria, hallucinations, bruxism, hyperreflexia, intracerebral haemorrhage, choreoathetoid movements, anorexia, hyperthermia, seizures, coma	Aggressiveness, bruxism, dizziness, headache, lightheadness, memory loss, tremor, seizures, Anger, anxiety, auditory and visual hallucinations, depression, dysphoria, empathy, euphoria, fatigue, formication, increased energy, increased and decreased concentration, loquaciousness, panic, paranoia, perceptual distortions, restlessness
Gastrointestinal	Nausea, vomiting, diarrhoea, gastrointestinal ischaemia	Abdominal pain, anorexia, nausea, vomiting
Pulmonary	Non-cardiogenic pulmonary oedema/adult respiratory distress syndrome, tachypnoea	Shortness of breath
Musculoskeletal	Muscle rigidity, rhabdomyolysis	Arthralgias, extremity changes—coldness, discoloration, numbness, tingling, muscular tension and cramping
Ophthalmologic	Mydriasis, nystagmus, visual hallucinations (rarely)	Blurred vision, mydriasis, nystagmus
Genitourinary	Erectile dysfunction	Anorgasmia, erectile dysfunction, increased libido
ENT	Auditory hallucinations (rarely)	Dry mouth, epistaxis, nasal pain, “nose burns”, oropharyngeal pain, tinnitus
Chronic Toxicity	Behavioural/psychiatric illness, cardiomyopathy, cardiac valve disease, pulmonary hypertension, vasculitis	Depression, infrequent hallucinations, impaired inhibition (similar to alcohol), increased risk of myocardial infarction (heart attack), psychosis in extreme cases in the genetically predisposed
Others	Hepatitis, hyponatraemia (dilutional/syndrome inappropriate anti diuretic hormone), acidosis, diaphoresis,	Body odor “mephedrone stink”, diaphoresis, fever, insomnia, nightmares, skin rash

2.1.1. Myotoxicity

In some reports from poison control centres, users who abused amphetamines present increased muscle tension and increased serum levels of creatine phosphokinase (CPK) [102]. Long-term use of amphetamines and its analogues can cause muscle ache, increase muscle tension and provoke spasms [103, 104]. *In vivo* studies in mice have shown that the combination of MDMA and exercise can induce skeletal muscle toxicity and even lead to rhabdomyolysis [105]. MDMA-induced skeletal muscle toxicity may be caused by an increase in mitochondrial proton leakage *in vivo* through the expression of the uncoupling protein 3 (UCP3) [106]. Users of synthetic cathinones also reported clinical effects on muscle such as numbness, tingling, muscular tension and cramping [79]. These drugs also elevate serum creatinine kinase levels and may cause rhabdomyolysis [79].

2.1.2. Hepatoxicity

Overdose of amphetamines and synthetic cathinones is considered as a potential cause that may induce acute liver injury [107]. In some Western countries, as amphetamines and synthetic cathinones become more and more popular as recreational drugs, they have

become one of the main causes of acute hepatitis and acute liver failure [108]. Histological changes in the liver after amphetamines exposure include individual cell necrosis, centrilobular necrosis and even massive hepatic necrosis, which may be related with acute hepatic failure [109-111]. Some users developed jaundice in addition to elevation of transaminases, which may reflect potentially fatal fulminant liver failure [112-115]. There is also experimental evidence for amphetamine-induced hepatotoxicity in animal studies. Amphetamines, especially MDMA, have been observed to cause liver necrosis in mice and rats [116, 117]. *In vitro* studies verified that mitochondrial dysfunction and apoptosis contribute to hepatotoxicity associated with amphetamines [118-120]. For synthetic cathinones, hepatotoxicity data are currently scarce. A case of acute liver failure has been reported after ingestion of MDPV [121]. Moreover, MDPV and methylone have been shown to be toxic for rat hepatocytes, HepG2 cells and HepaRG cells, affecting mitochondrial function and inducing oxidative stress [122-124].

2.1.3. Neurotoxicity

The acute neurologic effects of amphetamines include positive subjective effects, like euphoria, increased alertness, an increased state of arousal, and increases in energy and ability to talk. Negative effects include anxiety, paranoia, auditory and visual hallucinations [125, 126]. Long-term abuse of amphetamines may impair memory, attention, and decision-making, and induce psychosis and aggressiveness [127]. In some *in vivo* studies, acute and high doses of amphetamines altered dopaminergic (amphetamine and methamphetamine) or serotonergic neurons (MDMA) [128-131]. Some studies have shown that high-doses of amphetamines increased chromatolysis in medullary neurons in cats, and induced hemorrhage, hyperemia and glial proliferation in monkeys [132, 133]. Parenteral administration of these drugs in rats and mice can reduce the number of dopaminergic axons and terminals, and lead to serotonin deficits [129]. The clinical neurologic manifestations of synthetic cathinones in users include agitation, aggression, altered mental status, collapse, confusion, dizziness, drowsiness, dystonia, headache, hyperreflexia, myoclonus, seizures, tremor [79]. It has been shown in *in vivo* studies that synthetic cathinones such as 4-MMC, methylone and MDPV may trigger inflammatory processes in mice brain areas, leading to neuronal degeneration [134]. Most synthetic cathinones can alter monoaminergic system via altering the transporters and receptors of DA and 5-HT [135], and can induce neuron toxicity via oxidative stress [135].

2.2. *In vitro* cell models

2.2.1. C2C12 cell line

The **C2C12 cell line** (Figure 18) is an immortalized murine myoblast cell line, which was derived from the C2 (C3H strain) cell line [136]. The original C2 cell line was obtained by Yaffe and Saxel in 1977 by establishing primary cultures from the thigh leg muscle of 2-month-old normal C3H mice [136]. The C2C12 cells are very proliferative muscle satellite cells, commonly used as the standard model for skeletal or cardiac muscle [136-138]. The C2C12 cell line has also been used to study mechanistic biochemical pathways and to understand the early myogenesis [139]. Moreover, the C2C12 cell line is a useful model to study the cell cycle since it has a high division rate [140].

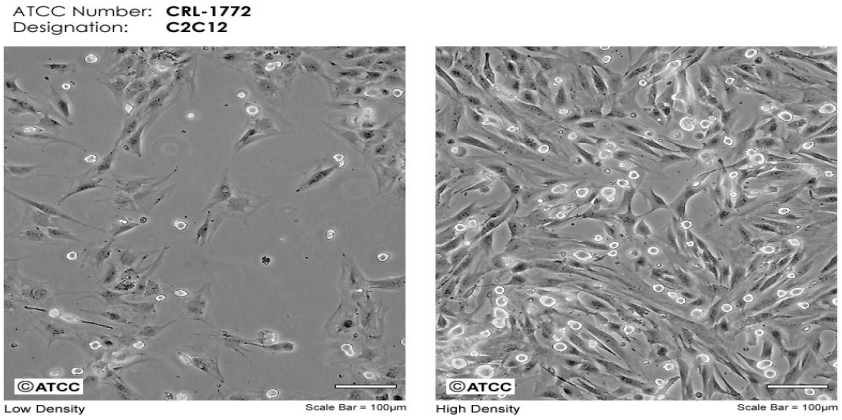

Figure 18. C2C12 myoblast under microscope, 100x magnification [141].

2.2.2. HepG2 cell line

Hepatic cell lines have been widely used *in vitro* for the studies of hepatocellular functions and toxicity [142]. In comparison to primary cultured human hepatocytes, the advantages of hepatic cell lines include continuous growth, unlimited lifespan, stable phenotype, easy availability, simple culture conditions, and standardized methods among laboratories. Additionally, some hepatic cell lines retain, at least in part, a differentiated adult phenotype. However, the expression of biotransformation activities on hepatic cell lines is limited, at least in HepG2 cells [143].

The human hepatoma HepG2 cell line (Figure 19) was derived from the liver tissue biopsy of a 15 years old boy with a well-differentiated hepatocellular carcinoma [144]. It is the most widely used *in vitro* model for polarized human hepatocytes [144]. The HepG2 cell line has many liver-specific functions and also can express conjugating enzymes [143]. It also can secrete many major plasma proteins, such as albumin, α1-antitrypsin, α2-macroglobulin, plasminogen and transferrin. However, HepG2 cells do not express most of the relevant human liver cytochromes P450 (CYPs) [145]. Besides that, this cell line can be used to study the cellular trafficking and dynamics of lipids, sinusoidal membrane proteins and bile canaliculi in hepatocytes, which is important for human liver diseases that are induced by an incorrect subcellular distribution of liver cell surface proteins [146, 147].

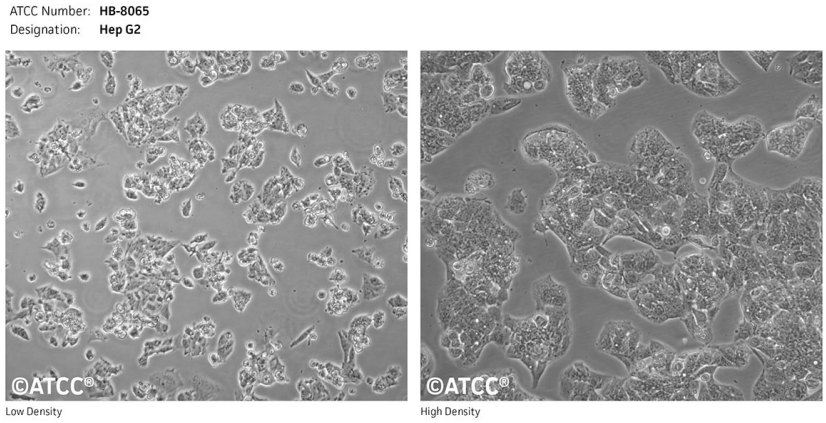

Figure 19. HepG2 cells under microscope, 100x magnification [148].

2.2.3. SH-SY5Y cell line

The human neuroblastoma SH-SY5Y cell line (Figure 20) was originally derived from the SK-N-SH cell line, which was subcloned from a bone marrow biopsy of a 4 years old girl with neuroblastoma [149]. The SH-SY5Y cell line is an adrenergic and dopaminergic neuronal cell line that has been utilized as a model for neuroscience researches *in vitro* [150]. The SH-SY5Y cell line is also useful in the fields of some neurological disease and disorders such as Parkinson's and Alzheimer's, and in toxicological studies [151-153]. The advantages of SH-SY5Y cells are the following:

- They are human-derived cells, which can express many human-specific proteins and protein isoforms.
- They are easy to culture with low cost.

- They have the capacity for large-scale expansion, which can overcome the propagate-limitation of human mature neurons.
- They can differentiate into different neurons as needed, with adrenergic or dopaminergic phenotype.
- It is a cell-line, avoiding ethical concerns of primary cell cultures [154].

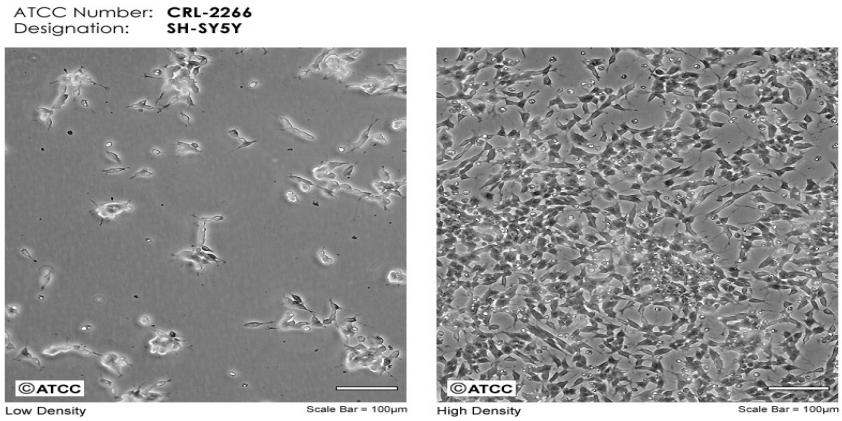

Figure 20. SH-SY5Y cells under microscope, 100x magnification [155]

In order to obtain nearly pure human neuron‐like cells, all-trans-retinoic acid (ATRA) and brain-derived neurotrophic factor (BDNF) in can be used to differentiate SH-SY5Y cells [156]. Using this method, plenty of cell with a neuronal morphology can be obtained (Figure 21) [156, 157].

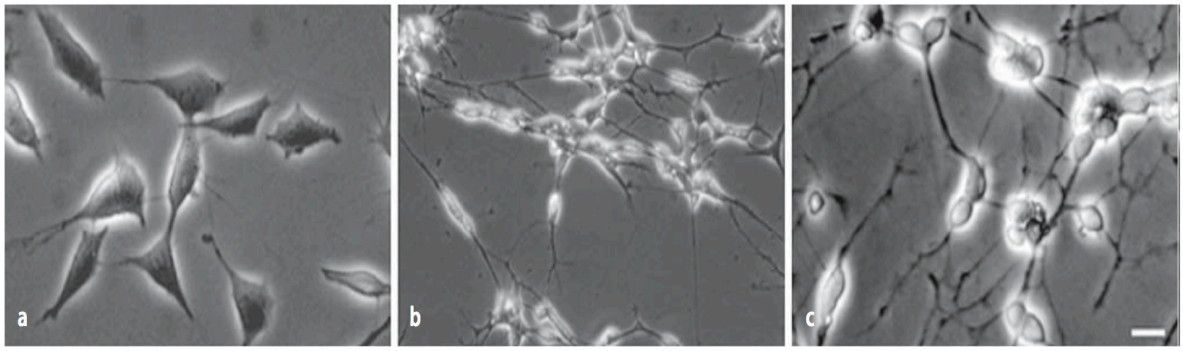

Figure 21. Cell differentiation effects of sequential treatment of SH-SY5Y cells with ATRA. (a) Neuroblastoma cell line SH-SY5Y cells. (b) Cells incubated with ATRA. (c) Cell incubated with ATRA followed by BDNF, 200x magnification [157].

2.3. Mitochondrial Function

Mitochondria (Figure 22) are rod-shaped organelles with a two-layer membrane, which are considered as the “power house” of cells. They measure only 0.5 to 1.0 microns,

but they can be considered the most important oxidative phosphorylation (OXPHOS) machinery and metabolic signaling center of cells [158]. Mitochondria have many important biological functions: (1) first of all they produce energy in the form of ATP, (2) they maintain cytosolic homeostasis of calcium ions within the compartments of the cell, (3) they participate in the synthesis of lipids, (4) they produce iron-sulphur clusters, (5) they build certain components of blood, and hormones like testosterone and estrogen, (6) they have functional enzymes to detoxify ammonia in the liver and to degrade fatty acids, and finally (7) they can regulate the process of apoptosis [159-162]. Mitochondria play therefore an important role in biological homeostasis of cells. Mitochondrial dysfunction can cause cell death, which can affect the function of organs and potentially in a variety of human diseases or death [163]. In toxicological studies on psychoactive drugs, mitochondria have been considered as the main target organs of these drugs [164].

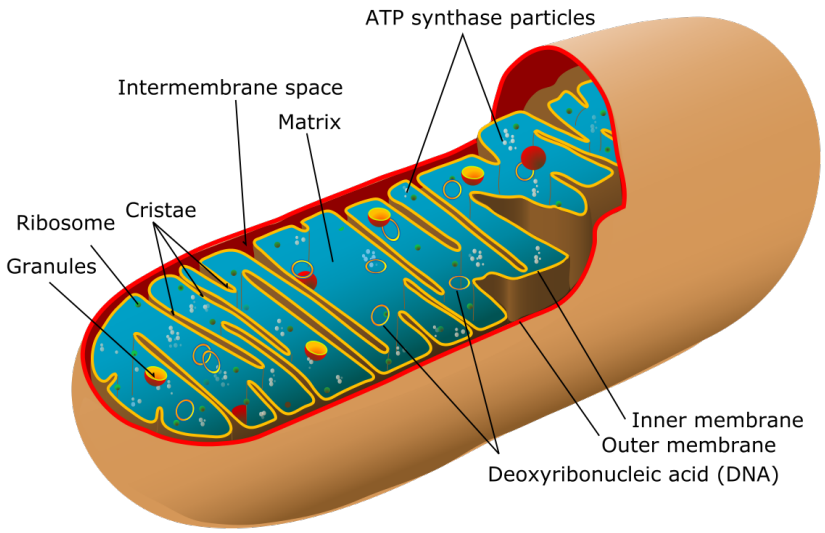

Figure 22. Schematic representation of a mitochondrion.

The most prominent role of mitochondria is to convert oxygen and nutrients into ATP, in fact mitochondria provide more than 90% of the ATP used by cells. ATP is the "molecular unit of currency" of cells since it provides the power to drive most cellular metabolic activities [165]. Mammalian cells produce ATP by two metabolic pathways: oxidative phosphorylation and glycolysis. For OXPHOS, the generation of ATP is accomplished *via* enzyme complexes the electron transport chain and the F_1F_0-ATPase. On the other hand, glycolysis is the first metabolic pathway used to extract energy when glucose is available.

2.3.1. Mitochondrial electron transfer chain

The mitochondrial electron transfer chain (ETC) is located in the inner membrane of mitochondria and consists of complex I, complex II, complex III and complex IV [166].

Complex I (NADH: ubiquinone oxidoreductase) is the largest complex and the first enzyme of the mitochondrial electron transport chain (ETC). It has a L-shaped architecture with a membrane arm and a peripheral arm. In addition to participating in the oxidative phosphorylation process, complex I also plays an important role in the formation of mitochondrial ROS and in the pathogenesis of a large number of genetic and degenerative disorders [167].

Complex II (SQR: succinate ubiquinone oxidoreductase) has four nuclear-encoded subunits: SDHA, SDHB, SDHC and SDHD. It lacks subunits encoded by the mitochondrial genome, thus it is distinguished from the other 3 complexes. Complex II is not only involved in the ETC but also closely related to the TCA cycle [168]. The function of complex II in oxidative phosphorylation has been described before the description of the succinate dehydrogenase (SDH) activity. Complex II contributes significantly to the TCA cycle by the oxidation of succinate to fumarate [169].

Complex III (ubiquinol: cytochrome c oxidoreductase) is considered to be another producer of superoxide and derived ROS besides complex I. Studies have shown that complex III generates superoxide at the ubiquinol oxidation center (Q_o site, center P), suggesting that electrons are transferred from reduced cytochrome b_L to oxygen *via* ubiquinone in a reverse reaction rather than through ubiquinone during a forward Q cycle reaction [170].

Complex IV (cytochrome *c* oxidase) is the terminal electron acceptor of the mitochondrial ETC, which is formed by cytochrome *c* oxidase (COX) embedded in the mitochondrial inner membrane [171]. Complex IV is a complex metalloprotein, which can catalyze the transfer of electrons from reduced cytochrome *c* to molecular oxygen [172]. In addition, it has proton-pumping activity that preserves the free energy released in this extra-energetic reaction by maintaining a transmembrane proton gradient, which is used to drive the synthesis of ATP or transmembrane transport [172, 173].

2.3.2. Oxidative Phosphorylation

The processes of oxidative phosphorylation are the following (Figure 23): (1) the tricarboxylic acid cycle (TCA) generates NADH and $FADH_2$, which are electron donors for the electron transport chain. NADH and $FADH_2$ are high-energy molecules that are shuttled through the ETC. NADH and $FADH_2$ transfer energy to protein complex I and complex II, respectively. During this process, NADH and $FADH_2$ will lose electrons due to oxidation. (2) Matrix protons (H^+) are pumped into the intermembrane space by complex I, while the electrons are given to another membrane-bound electron carrier (ubiquinone Q). The complexes III and IV also repeat this proton-pumping process and accumulate protons in the intermembrane space, which results in a pH gradient and creates a proton-motive force. (3) UQH_2 transfers the electrons to complex III. (4) Then, cytochrome *c* picks up the electrons from complex III. This process also pumps protons into the intermembrane space. (5) The electrons are then carried to complex IV by cytochrome *c*, accompanied by the proton-pumping process. Then oxygen, the final electron acceptor, receives the electrons and combines them with protons to form H_2O. (6) The proton-pumping process and the electron transport create an electrical gradient (mitochondrial membrane potential, $\Delta\psi m$), which allows the proton transfer through the F_1F_0ATP synthase. Finally, the ATP is synthesized by adding Pi to adenosine diphosphate (ADP) [174-176].

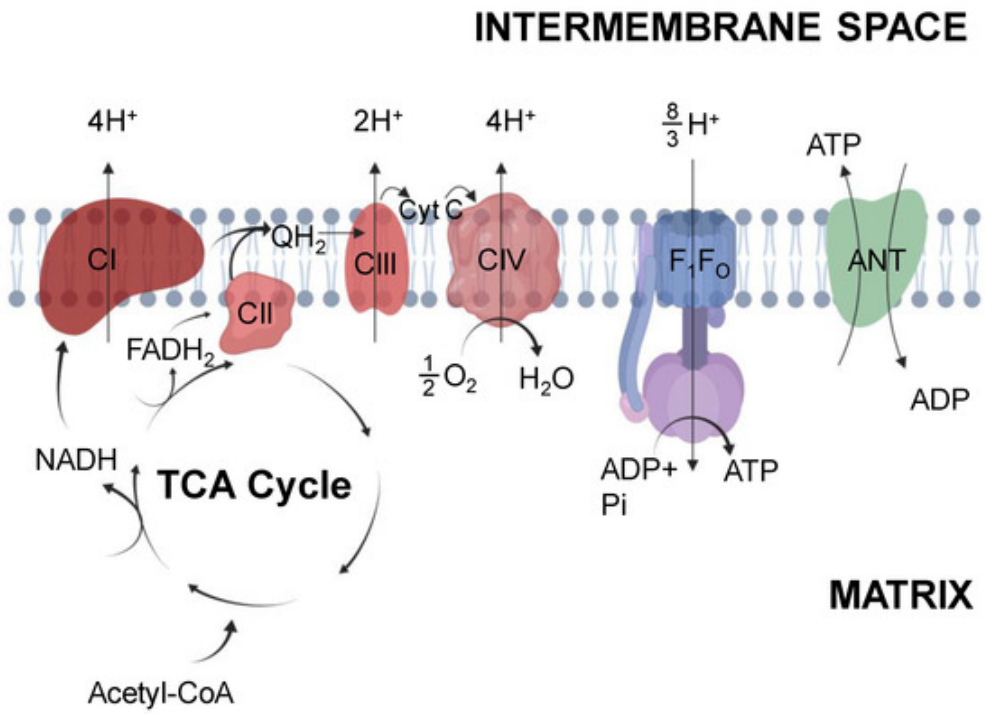

Figure 23. Mitochondrial oxidative phosphorylation [166].

2.3.3. Mitochondrial Respiratory Activity

Cellular oxygen consumption generally reveals mitochondrial respiratory activity, which represents a fundamental mitochondrial function. Quantification of the oxygen consumption rate (OCR, Figure 24) is one of the best choices to detect mitochondrial dysfunction [177]. The basal oxygen consumption rate reflects the coupled mitochondrial respiration (ATP formation), the uncoupled consumption of oxygen (formation of heat or of ROS) and oxygen consumption at non-mitochondrial sites. It is possible to distinguish between coupled and uncoupled respiration by inhibiting ATP synthase (oligomycin) and to determine non-mitochondrial oxygen consumption by using the complex I inhibitor rotenone. The maximal oxygen consumption rate caused by the addition of mitochondrial uncoupling agents (carbonyl cyanide p-(trifluoromethoxy) phenylhydrazone (FCCP)) provides an indication on the energy storage capacity [178, 179].

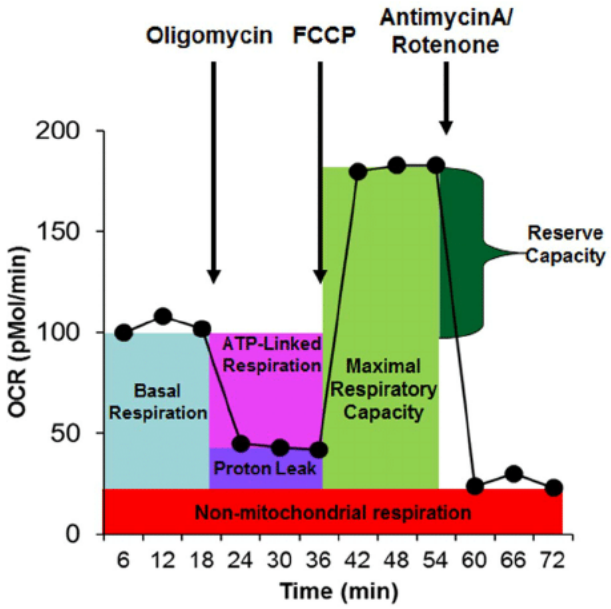

Figure 24. Oxygen consumption rate (OCR) is measured by Seahorse assay [180].

2.3.4. Mitochondrial Membrane Potential

The electrical potential difference between the mitochondrial matrix and the cytosol is one of the postulates of the chemiosmotic theory of oxidative phosphorylation [181, 182]. Nowadays, it is well known as mitochondrial membrane potential ($\Delta\psi m$) [183].

Mitochondria use proton electrochemical gradient potential or electrochemical proton dynamics (Δp) to generate ATP [184, 185]. The Δp is a combination of mitochondrial membrane potential ($\Delta\psi m$) and mitochondrial pH gradient (ΔpHm) [184, 185]. Δp provides is the driving force for bioenergy (ATP) production, while the $\Delta\psi m$ provides the charge

gradient required for mitochondrial Ca^{2+} storage and regulates the production of ROS [186]. During cell stress, $\Delta\psi m$ can be altered by the imbalance of intracellular ionic charge, affecting Δp and the production of ATP [185, 186]. For this reason $\Delta\psi m$ can be considered a marker of cell health or injury [185].

2.4. Oxidative Stress

In addition to ATP synthesis, mitochondria are also the major intracellular sources and target of ROS in most cell types [187]. Superoxide is considered as the main form of ROS, which is generated in mitochondria by incomplete reduction of molecular oxygen during oxidative phosphorylation [188, 189]. The main source of ROS appears to be the redox cycle ubiquinone in complex III. Another source is complex I, which also has many redox centres (Figure 25) [187]. Manganese superoxide dismutase (SOD2, an enzyme located ion the mitochondrial matrix) can convert superoxide to H_2O_2. H_2O_2 is more stable than superoxide and lipid-soluble and can be released by mitochondria easily. Although mitochondria-derived ROS plays a signalling role in cells, ROS may be harmful due to oxidative modification of proteins, nucleic acids, and lipid membranes [187]. An excess of ROS can lead to oxidative stress, a harmful process that can damage several cellular structures, such as proteins, lipids, lipoproteins, membranes and DNA [190-194]. At this point, cells need specific mechanisms to eliminate ROS in order to restore normal physiological conditions [194]. The superoxide dismutase (SOD) family can be used to catalyze the initial reaction of ROS to water through glutathione peroxidase and catalase (Figure 25) [195]. Many studies *in vivo* have supported the involvement of oxidative stress in drug-induced toxicity [27, 196].

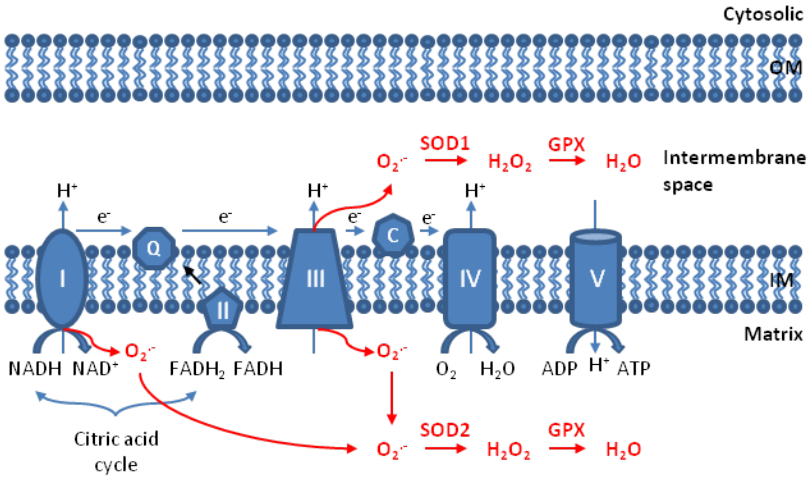

Figure 25. The production and elimination of mitochondrial ROS.

2.5. Mechanisms of Cell Death

There are mainly three forms of cell death: necrosis, apoptosis, and autophagy-associated cell death [197]. A comparison of necrosis, apoptosis, and autophagy is presented in Table 3 [197, 198].

Table 3. Comparison of necrosis, apoptosis and autophagy.

Characteristic	Necrosis	Apoptosis	Autophagy
Causative factors	Severe oxidative stress Ischemia Hyperthermia Hypoxia High concentrations of toxic substances Chemotherapy(?)	Moderate oxidative stress Deficiency of growth factors HIV Chemotherapy Irradiation Induction of death receptors	Nutrient deprivation Growth factor depletion Hypoxia Endoplasmic reticulum stress Pathogen infection
Morphological Characteristics	Chromatin flocculation Membrane damage Disintegration of organelles Cell swelling Cell lysis Secondary necrosis can occur in the late stage of apoptosis	Condensation of chromatin Intact cell membrane with blebs but the membrane may be damaged in the late stage in vitro Shrinkage of cell Apoptotic body formation	Double- or multiple-membrane enclosed vesicles in the cytoplasm Engulf portions of cytoplasm and/or organelles such as mitochondria and endoplasmic reticulum. Vesicles fuse with lysosomes
Biochemical/Immunological Characteristics	Impaired ion homeostasis ATP is not required DNA gives a smear pattern in agarose gel electrophoresis Total cell death markers (LDH, M65) are released Lysosomal enzymes are released and inflammation occurs	ATP is required Internucleosomal DNA fragmentation(ladder pattern in agarose gel electrophoresis) Caspase-cleaved cytokeratin 18 (M30 antigen) is released Inflammation does not occur	Caspase activation very late if at all Primary proteases are cathepsins or proteasomal proteins DNA fragmentation very late if at all Exteriorization of phosphatidylserine No inflammation
Methods to Assess	M65 ELISA assay (detects both necrosis+apoptosis) Lactate dehydrogenase (LDH) determination Cytochrome c release	M30 ELISA assay Caspase-3 activation Sub G_1 peak inflow cytometry	Electron microscopy Immuno-gold labeling on ultrathin cryosections LC3 determination

2.5.1. Necrosis

Necrosis (Figure 26) is a classical mechanism of cell death, which can occurred by factors external to the cell or tissue [199]. The morphological characteristics of necrosis are cell swelling and lysis, chromatin flocculation, disintegration of organelles, extensive DNA hydrolysis, vacuolation of the endoplasmic reticulum, and organelle breakdown [199, 200].

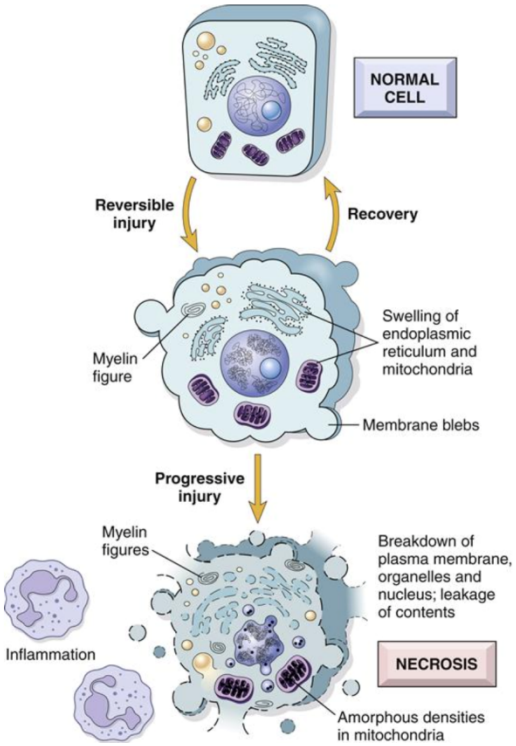

Figure 26. The cellular changes in necrosis [201].

2.5.2. Apoptosis

Apoptosis (Figure 27) is a programmed form of cell death first identified and named by John Kerr and Andrew Wyllie in 1972 [202]. It is far distinct from necrosis and can occur under physiological and pathological conditions. Morphologically, apoptotic cells decerase the cellular and nuclear volume, condense the chromatin, show cell shrinkage and loss of surface microvilli, have an intact cell membrane with blebs and internucleosomal DNA fragmentation [203]. ATP is required for this process.

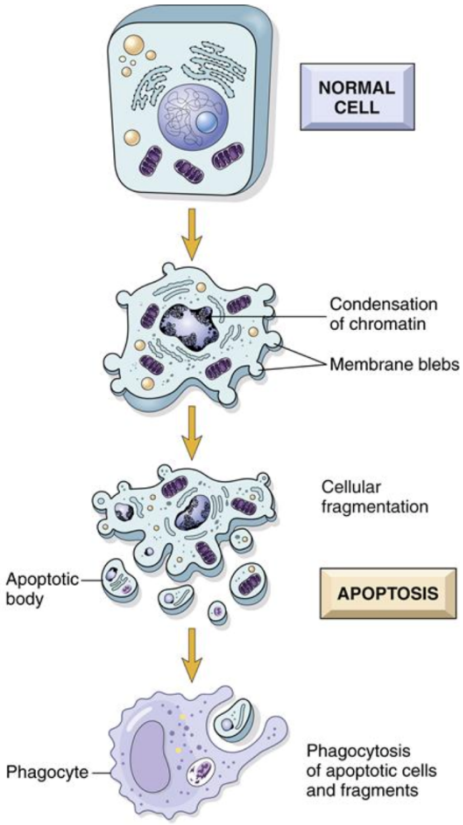

Figure 27. The cellular changes in apoptosis [201].

At the molecular level, apoptosis can occur by two signaling mechanisms (Figure 28): intrinsic pathway and extrinsic pathway. The intrinsic pathway is initiated by internal sensors of severe cell distress, and regulated by Bcl-2 family proteins [204]. These triggers are collectively called "stress signals" and include DNA damage, loss of cellular adhesion, growth factor withdrawal, cytoskeleton disruption, hypoxia, endoplasmic reticulum stress, macromolecular synthesis inhibition and many more. The extrinsic pathway is triggered by extracellular specific ligands through the engagement of death receptors (DR) at the cell surface [205]. It also means that both physiological and pathological conditions can result in cell apoptosis. Downstream effects of the two pathways lead to the activation of the executioner caspases (cysteine-aspartic acid protease) [206]. Furthermore, mitochondrial dysfunction also can trigger apoptosis [207].

Caspases are a family of endoproteases that play essential roles in regulating cell death and controlling inflammation [208]. The most important function of them is to participate in programmed cell death (apoptosis, pyroptosis and necroptosis) and inflammation. Caspases are divided into two categories due to their roles in apoptosis (caspase 3, 6, 7, 8, and 9 in mammals) and inflammation (caspase 1, 4, 5, 12 in humans and

caspase 1, 11, and 12 in mice). During apoptotic processes, caspases can disassembly the cell into apoptotic bodies. Caspases 8, 9 and 3 are considered as key pivots to initiate the apoptotic pathways.

Caspase 8 is responsible for the extrinsic apoptosis pathway [209]. The extrinsic apoptosis pathway is triggered by the external ligand binding to the death receptors (DRs). When a ligand binds to a DRs, it results in the dimerization and activation of caspase 8 by the adapter proteins (FADD/TRADD) [208].

Caspase 9 plays an important role in the intrinsic apoptosis pathway (mitochondrial apoptosis) [210]. The process of caspase 9 activation is as follows: first, cellular stresses lead to the release of cytochrome *c* from the mitochondria and to the formation of apoptosome [211]. Then, the binding of cytochrome *c* to apoptotic protease activates factor 1 (APAF-1) monomer and results into conformational changes with exposure of a nucleotide-binding site and oligomerization of APAF-1. Next, the caspase recruitment domain (CARD) of caspase 9 binds to APAF-1. Finally, the extra-mitochondrial cytochrome *c*, caspase 9, ATP and APAF-1 form the apoptosome which activates caspase 3 [211] [212].

Caspase 3 is a key death protease that amplifies signals of caspase 8 and caspase 9 to commit disassembly of vital cellular proteins or other caspases [213, 214]. It can be activated by both extrinsic and intrinsic apoptosis pathways [215, 216]. Caspase 3, also known as the executioner caspase, can be triggered by mitochondrial cytochrome *c* release and by caspase 8 and 9 activity [208, 217]. Caspase 3 is also essential to maintain the development of the brain [208].

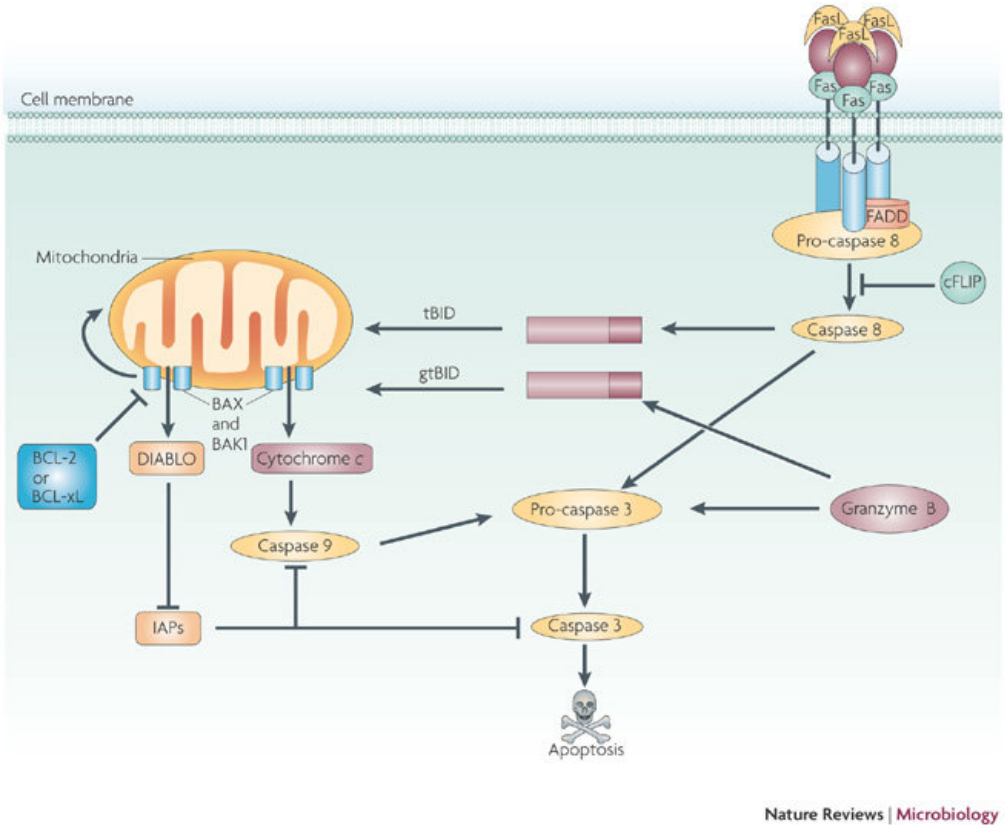

Figure 28. Caspase-dependent apoptosis [218].

5.3.3. Autophagy

Autophagy is a physiological process to maintain the balance between anabolism and catabolism in normal cell growth and development [219]. Autophagy plays an important role in the response of cells to stresses, starvation, poison, and radiation [220, 221]. Autophagy is a strictly regulated process (Figure 29) [222, 223], it can provide substrates for energy or new synthesis *via* turning over non-essential cytoplasmic components (including organelles) [224]. During autophagic processes, intracellular cytoplasm, proteins, lipids, and organelle regions are sequestered in a double-membrane limited vacuole (autophagosomes) [225, 226]. Mature autophagosomes are single-membrane phagosomes and autophagosomes may become autolysosomes when they are acidified and acquire proteolytic enzymes by fusion with late endosomes or lysosomes [227, 228]. Moreover, when cells are fused with autophagosomes, these endocytosed substances can also trigger the autophagy pathway [229, 230]. The autophagic vacuole (AV) contains all the lysosomal compartments [231].

Autophagy acts as a surveillance system when cells are stressed or injured, and it can remove damaged mitochondria or other organelles which may otherwise trigger apoptosis

[232-234]. Moreover, autodigestion caused by acute up-regulation of autophagy is also a form of programmed cell death [235, 236]. It is different from apoptosis but shares some characteristics [236]. Autophagy-induced cell death has been defined as a caspase-independent form of apoptosis, some cathepsins can trigger or mediate aspects of apoptosis and necrosis in various pathological conditions [237, 238].

It is noteworthy that autophagy and apoptosis interact in various ways, since (1) autophagy plays an essential role in the occurrence of apoptosis, (2) but autophagy may also prevent apoptosis, and (3) apoptosis and autophagy may appear independently [239], moreover, inhibition of apoptosis may induce autophagic cell death, and *vice versa* [240].

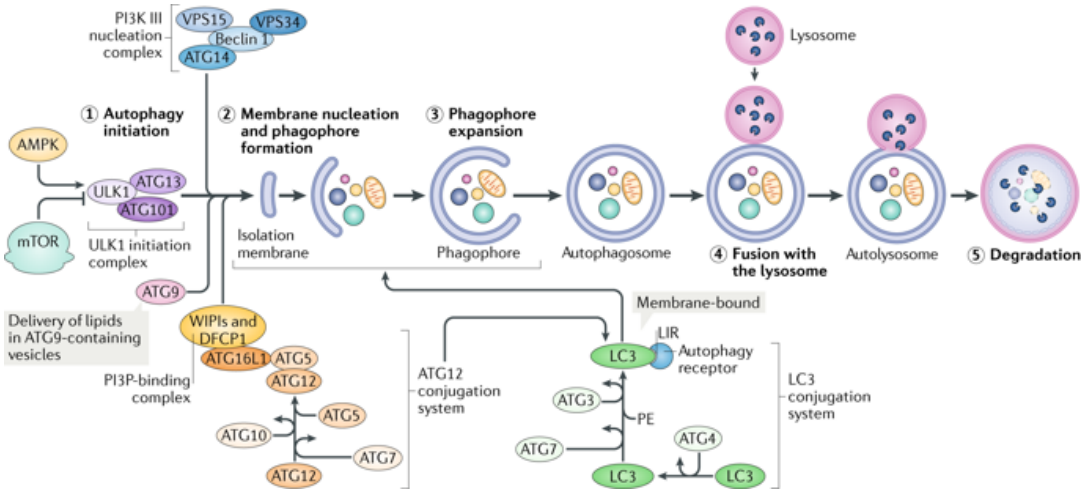

Figure 29. The macro-autophagy process [241].

2.6. Hyperthermia

Hyperthermia, also known as “overheating”, is the prominent manifestations of stimulant drug abuse and even the primary reason for user-death [242]. The symptoms of stimulant drug-induced hyperthermia resembles heat stroke, the clinical manifestation is body temperature beyond normal [243]. According to clinical case reports, stimulant drug-induced hyperthermia can result in many fatal complications such as hyponatremia, rhabdomyolysis, brain edema, disseminated intravascular coagulation and coma [244]. Hyperthermia is very common, especially when these drugs are ingested in crowded clubs with high ambient temperatures and excessive physical exertion [245]. A large number of hyperthermia-associated clinical cases caused by amphetamines and synthetic cathinones have been reported so far [246, 247]. These drugs can increase users’ body temperature over 40°C,

which may lead to life-threatening conditions [246]. Base on some surveys, more than 60% users of 4-MMC (mephedrone) have hyperthermic subjective effects [248]. Methcathinone and 4-CMC have also been reported to cause hyperthermia [11, 57]. Furthermore, the combination of these drugs induces an impairment of thermoregulation and promotes toxicity, resulting in more frequent and serious cases of hyperthermia [249, 250].

Results

1. Paper 1

Molecular Toxicological Mechanisms of Synthetic Cathinones on C2C12 Myoblasts

In this paper, we investigated the mechanisms of molecular toxicity for methylone, 4-MMC (mephedrone), 3-MMC, MDPV, α-PVP and naphyrone in C2C12 myoblast.

International Journal of
Molecular Sciences

MDPI

Article

Molecular Toxicological Mechanisms of Synthetic Cathinones on C2C12 Myoblasts

Xun Zhou [1], Dino Luethi [1], Gerda M. Sanvee [1], Jamal Bouitbir [1,2], Matthias E. Liechti [1,2] and Stephan Krähenbühl [1,2,*]

1 Division of Clinical Pharmacology & Toxicology, Department of Biomedicine, University Hospital Basel and University of Basel, 4031 Basel, Switzerland; Xun.Zhou@unibas.ch (X.Z.); dino.luethi@unibas.ch (D.L.); Gerda.Sanvee@unibas.ch (G.M.S.); Jamal.Bouitbir@unibas.ch (J.B.); Matthias.Liechti@unibas.ch (M.E.L.)
2 Swiss Centre for Applied Human Toxicology, 4031 Basel, Switzerland
* Correspondence: stephan.kraehenbuehl@usb.ch; Tel.: +41-612654715

Received: 31 January 2019; Accepted: 22 March 2019; Published: 28 March 2019

check for updates

Abstract: Synthetic cathinones are popular psychoactive substances that may cause skeletal muscle damage. In addition to indirect sympathomimetic myotoxicity, these substances could be directly myotoxic. Since studies in myocytes are currently lacking, the aim of the present study was to investigate potential toxicological effects by synthetic cathinones on C2C12 myoblasts (mouse skeletal muscle cell line). We exposed C2C12 myoblasts to 3-methylmethcathinone, 4-methylmethcathinone (mephedrone), 3,4-methylenedioxymethcathinone (methylone), 3,4-methylenedioxypyrovalerone (MDPV), alpha-pyrrolidinovalerophenone (α-PVP), and naphthylpyrovalerone (naphyrone) for 1 or 24 h before cell membrane integrity, ATP content, mitochondrial oxygen consumption, and mitochondrial superoxide production was measured. 3,4-Methylenedioxymethamphetamine (MDMA) was included as a reference compound. All investigated synthetic cathinones, as well as MDMA, impaired cell membrane integrity, depleted ATP levels, and increased mitochondrial superoxide concentrations in a concentration-dependent manner in the range of 50–2000 μM. The two pyrovalerone derivatives α-PVP and naphyrone, and MDMA, additionally impaired basal and maximal cellular respiration, suggesting mitochondrial dysfunction. Alpha-PVP inhibited complex I, naphyrone complex II, and MDMA complex I and III, whereas complex IV was not affected. We conclude that, in addition to sympathetic nervous system effects and strenuous muscle exercise, direct effects of some cathinones on skeletal muscle mitochondria may contribute to myotoxicity in susceptible synthetic cathinone drugs users.

Keywords: synthetic cathinones; skeletal muscle toxicity; mitochondria; electron transport chain

1. Introduction

Synthetic cathinones are derivatives of cathinone, the naturally occurring alkaloid found in the *Catha edulis* shrub, and represent one of the largest groups of new psychoactive substances (NPS), with more than one hundred different substances detected by the European Union Early Warning System between 2005 and 2017 [1]. As shown in Figure 1, cathinones are structurally closely related to amphetamines, such as 3, 4-methylenedioxymethamphetamine (MDMA, "ecstasy"). The main difference is a β-keto group in the side chain of the cathinones, which is not present in the amphetamines [2]. Even though the frequent use of synthetic cathinones in a recreational setting is a relatively new phenomenon, several of these substances were first synthesized during the twentieth century. For instance, the first synthesis of the frequently abused 4-methylmethcathinone (mephedrone) was published in 1929 [3]. Many additional synthetic cathinones have since been developed, mostly as

antidepressant or anorectic agents [4–9]. However, due to concerns about abuse liability, only a few of them were marketed.

Synthetic cathinones elicit their pharmacological effect mainly as substrates or inhibitors of monoamine transporters [10–15], and their use has been associated with sympathomimetic toxicity, which typically includes tachycardia, hypertension, raised body temperature, diaphoresis, mydriasis and agitation [16–20]. In rare cases, the use of synthetic cathinones may result in significant peripheral organ damage [21–23].

Amongst other toxicities, skeletal muscle damage has been linked to the use of cathinone and its synthetic derivatives [23–27], but the underlying mechanisms of toxicity are currently not fully elucidated. Previous studies in human hepatic cells [28–30], as well as in dopaminergic human neuroblastoma cells [31,32], showed that synthetic cathinones cause cellular stress and elicit mitochondrial dysfunction, leading to apoptosis and cell death. In order to investigate whether similar toxicological mechanisms also contribute to skeletal muscle toxicity, the in vitro myotoxicity of the synthetic cathinones (Figure 1) 3-methylmethcathinone (3-MMC), 4-methylmethcathinone (4-MMC, mephedrone), 3,4-methylenedioxy-N-methcathinone (methylone), 3,4-methylenedioxypyrovalerone (MDPV), alpha-pyrrolidinovalerophenone (α-PVP), and naphthylpyrovalerone (naphyrone) was studied in C2C12 myoblasts. 3,4-methylenedioxymethamphetamine (MDMA, "ecstasy") was included in the study as a non-cathinone reference compound with documented myotoxic effects [33–37].

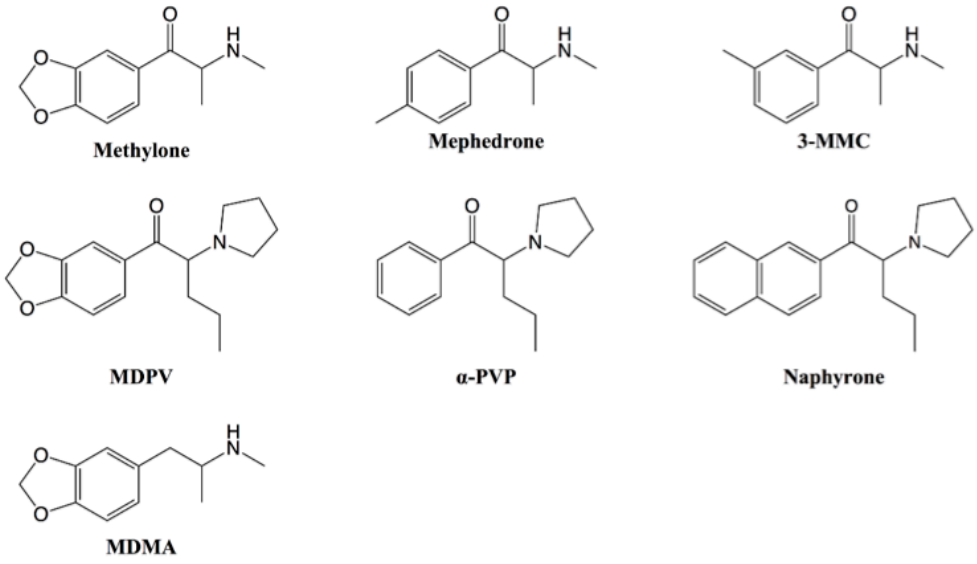

Figure 1. Structures of the synthetic cathinones included in the study and the reference substance 3,4-methylenedioxymethamphetamine (MDMA). MDPV: 3,4-methylenedioxypyrovalerone; α-PVP: alpha-pyrrolidinovalerophenone; 3-MMC: 3-methylmethcathinone

2. Results

2.1. Cell Viability and ATP Content

The intracellular ATP content was determined for the assessment of mitochondrial function and cell viability and the release of adenylate kinase (AK) as a marker of cell membrane integrity. After treatment for 24 h, all drugs proved to impair cell membrane integrity and to deplete ATP in a concentration-dependent manner in the range of 50–2000 μM (Figure 2). After exposure for 24 h, a significant depletion of ATP at 50 μM was observed for naphyrone, at 200 μM for mephedrone, at 500 μM for methylone, and ≥1 mM for the remaining drugs. The depletion of ATP was accompanied by cell membrane integrity loss for all drugs, reaching significance at slightly higher (methylone and MDPV), or similar concentrations (remaining drugs), at which ATP depletion occurred. The IC50

Int. J. Mol. Sci. **2019**, *20*, 1561

values for membrane toxicity were higher than for ATP depletion for 3-MMC, mephedrone, α-PVP, MDPV and naphyrone (Table 1).

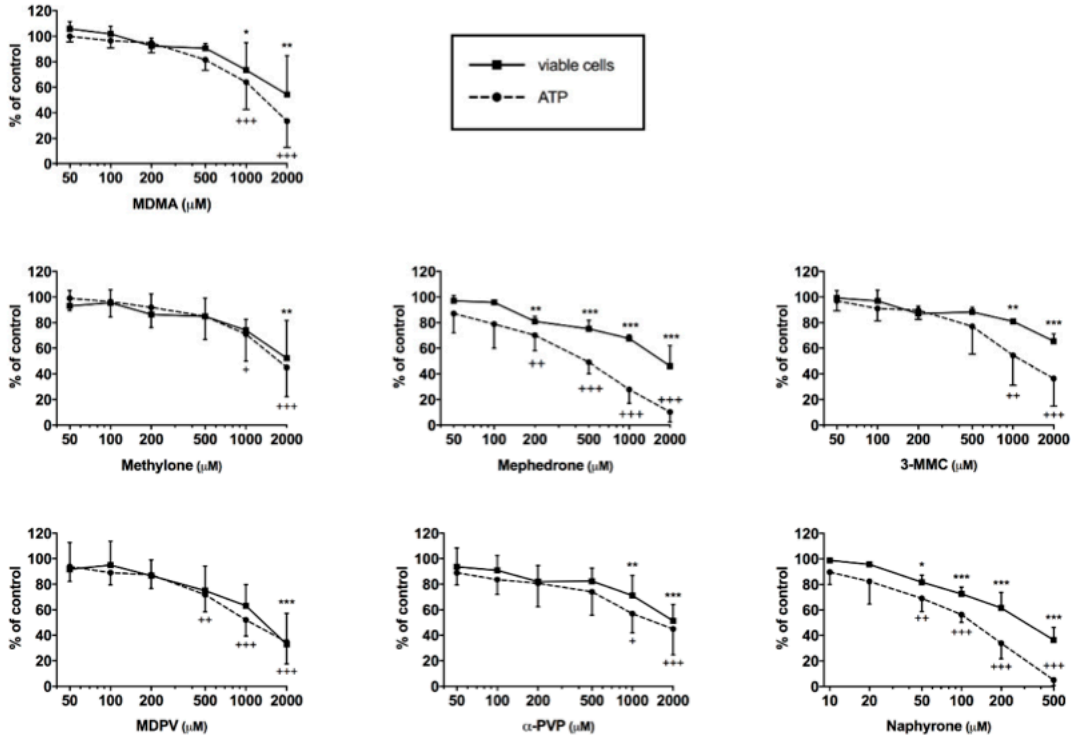

Figure 2. Intracellular ATP content and viable cells expressed by maintained cell membrane integrity after drug exposure for 24 h in C2C12 cells. Data are expressed as mean ± SEM of at least three independent experiments. Drug treatments were compared to vehicle control with ANOVA followed by Dunnett's test. Significance levels for cell viability are given as * $p < 0.05$, ** $p < 0.01$, *** $p < 0.001$. Significance levels for ATP content are given as + $p < 0.05$, ++ $p < 0.01$, +++ $p < 0.001$.

Table 1. Quantification (IC_{50}) of membrane toxicity and ATP depletion by the investigated synthetic cathinones and MDMA. Unit for IC_{50} is mM.

	MDMA	3-MMC	Mephedrone	Methylone	α-PVP	MDPV	Naphyrone
Membrane toxicity	0.74	>2	>2	1.10	1.04	>2	0.047
ATP depletion	0.88	1.08	0.53	1.16	0.94	1.01	0.021

2.2. *Effect on Cellular Oxygen Consumption*

A decrease in the cellular ATP content in the presence of glucose can result from an impaired function of the mitochondrial respiratory chain or impaired glycolysis [38,39]. In order to determine whether the depletion of ATP mediated by the synthetic cathinones was related to the interruption of the mitochondrial respiratory chain, the cellular oxygen consumption of treated C2C12 cells was assessed with a SeahorseXF24 analyzer. Basal, leak, and maximal respiration of the cells is shown in Figure 3. After treatment for 24 h, a decrease in basal respiration was observed for the pyrovalerone derivatives naphyrone and α-PVP, starting at 500 μM. In addition, both drugs decreased the maximal respiratory capacity of the cells at equal concentrations. α-PVP seemed to decrease the maximal oxygen consumption already at 200 μM, statistical significance was, however, not reached. The remaining drugs did not impair cellular respiration in the investigated concentration range with the exception of MDMA, which decreased the maximal respiratory capacity at concentrations ≥1 mM.

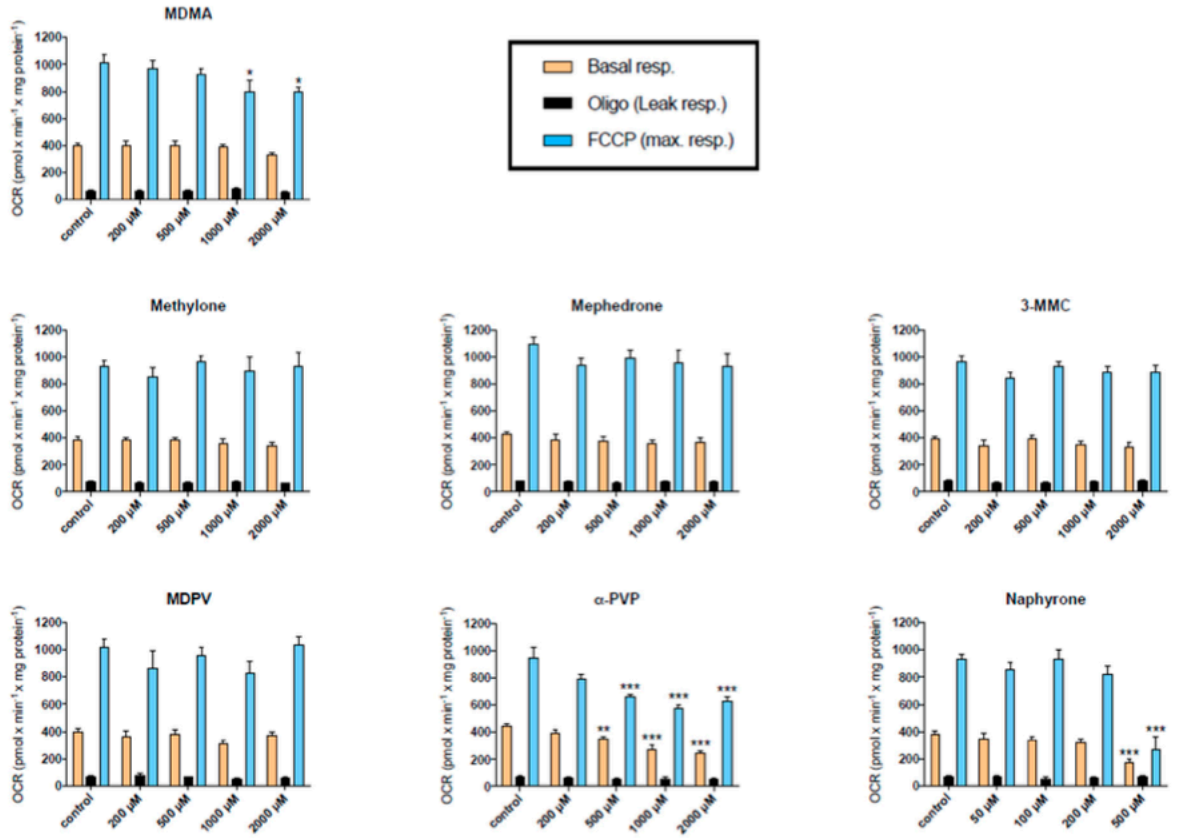

Figure 3. Oxygen consumption rate (OCR) in C2C12 cells after 24 h drug exposure. Basal respiration, leak respiration, and maximal respiration are expressed as mean ± SEM of at least three independent experiments. Drug treatments were compared to vehicle control with ANOVA followed by Dunnett's test. Significance levels are given as * $p < 0.05$, ** $p < 0.01$, *** $p < 0.001$.

Almost identical results were obtained after incubation of C2C12 myoblasts for 1 h (Figure S1). Similar to the incubations for 24 h, methylone, mephedrone, 3-MMC and MDPV did not impair cellular oxygen consumption. In contrast to the 24 h study, MDMA did not inhibit cellular oxygen consumption, whereas α-PVP and naphyrone inhibited oxygen consumption after 1 h starting at 1000 and 200 µM, respectively.

2.3. *Activity of Enzyme Complexes of the Mitochondrial Electron Transport Chain*

MDMA, and the pyrovalerone cathinones α-PVP and naphyrone, disrupted cellular respiration in C2C12 myoblasts in addition to decreasing ATP levels and cell viability. Therefore, the activity of the enzyme complexes of the mitochondrial electron transport chain was investigated in more detail using a high-resolution respirometry system (Oxygraph-2k). For each drug, the lowest concentration at which an impairment of cellular oxygen consumption became apparent was chosen for further investigation of the activity of the enzyme complexes. As shown in Figure 4, MDMA inhibited complex I (glutamate) and III (duroquinol), α-PVP complex I (glutamate) and naphyrone complex II (succinate). None of the compounds investigated impaired the activity of complex IV (TMPD/ascorbate). In the presence oligomycin, no stimulation of the respiration was observed compared to control values, excluding the uncoupling of oxidative phosphorylation. Interestingly, the oxygen consumption in the presence of succinate was low compared to the other substrates, indicating a low activity of complex II in C2C12 myoblasts.

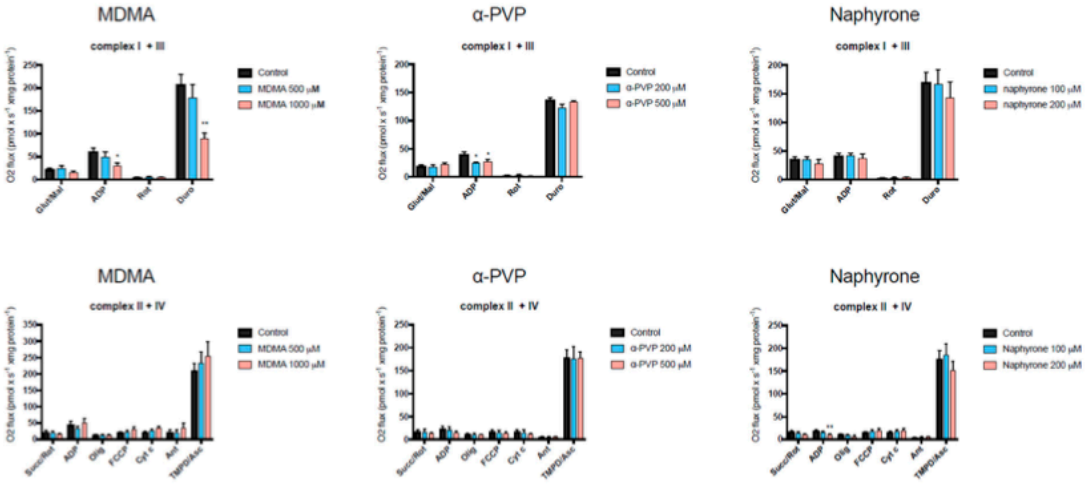

Figure 4. Effect on the activity of the enzyme complexes of the mitochondrial electron transport chain in C2C12 cells measured using a Oxygraph-2k-high-resolution respirometer. Data are expressed as mean ± SEM of at least four independent experiments. Treatment was compared to vehicle control with an unpaired two-tailed Student's *t*-test. Significance levels are given as * $p < 0.05$, ** $p < 0.01$

2.4. *Mitochondrial Superoxide Production*

The accumulation of reactive oxygen species (ROS) was one of the consequences of the impairment of the mitochondrial respiratory chain. All the drugs caused an increase in superoxide in a concentration dependent manner (Figure 5). Consistent with ATP depletion, naphyrone caused elevated superoxide concentrations at the lowest concentration (200 µM) among all drugs investigated. 3-Methylmethcathinone induced significant increase in superoxide production at 500 µM, and the remaining drugs at 1000 µM.

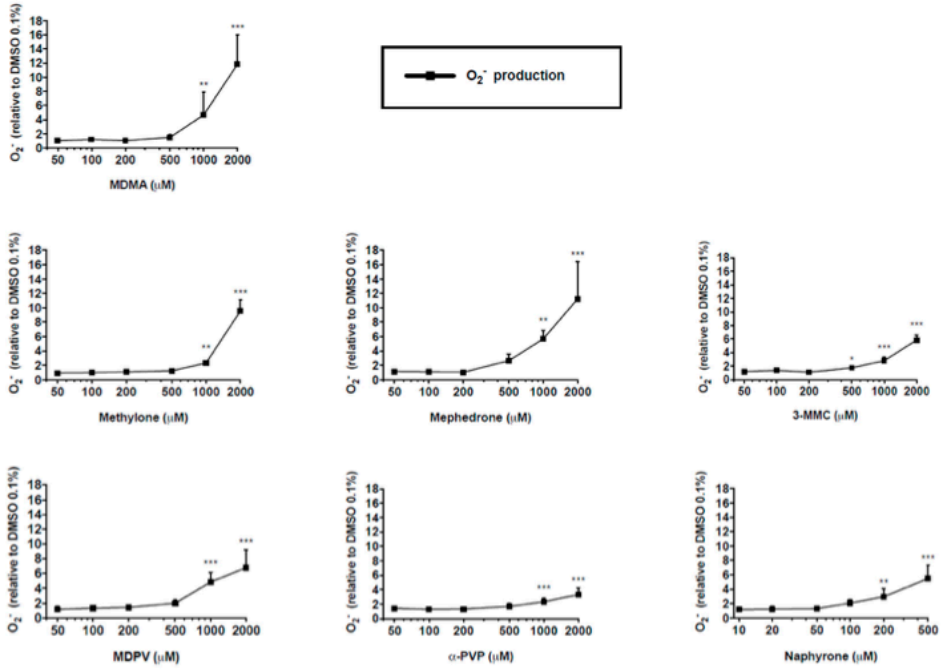

Figure 5. Mitochondrial superoxide production in C2C12 cells after 24 h drug treatment. Data are expressed as mean ± SEM of at least three independent experiments compared to vehicle control and were analyzed with ANOVA followed by Dunett's test. Significance levels are given as * $p < 0.05$, ** $p < 0.01$, *** $p < 0.001$.

It was surprising to observe that all the investigated compounds caused an increase in the mitochondrial superoxide concentration. One reason could be a low mitochondrial antioxidative capacity in mitochondria from C2C12 myoblasts. We therefore determined the protein content of superoxide dismutase 2 (SOD2), the enzyme which degrades intramitochondrial superoxide [40], in C2C12 myoblasts and myotubes after differentiation. As shown in Figure S2, the protein content of SOD2 was approximately 3 times lower in myoblasts than in myotubes, suggesting that impaired degradation could play a role in the accumulation of mitochondrial superoxide as observed in the presence of the compounds investigated.

3. Discussion

All of the investigated synthetic cathinones, as well as MDMA, depleted the cellular ATP pool and impaired cell membrane integrity in C2C12 myoblasts, but at concentrations (≥50 µM) that are not reached with ingestion of the typical doses. However, patients with preexisting mitochondrial diseases, or who ingested other myotoxic drugs, may be more sensitive to these drugs. Patients who ingested suprapharmacological doses may reach such concentrations [41]. Nevertheless, such studies are helpful to investigate the mechanisms of toxicity, for instance, mitochondrial toxicity [42]. Similar to previous results in HepG2 cells [30], all synthetic cathinones impaired cell membrane integrity at almost identical concentrations. Naphyrone was the most toxic compound investigated, which may be related to the reactivity of the naphthyl group. The direct comparison between MDMA and methylone (which differ only in the β-keto group in the side chain, see Figure 1) suggests no major role of the β-keto group regarding the toxicity in C2C12 myoblasts.

A decrease in ATP that precedes cell membrane integrity loss after drug treatment is reported to indicate that the mitochondria, as primary ATP-producing organelles, are targeted by these drugs [38,43]. Considering the IC50 values for ATP depletion and membrane integrity, a trend for ATP depletion preceding loss of cell membrane integrity was visible for 3-MMC, mephedrone, α-PVP, MDPV and naphyrone, but not for MDMA and methylone (Table 1). This possible indicator of mitochondrial toxicity was confirmed by the more detailed mitochondria-specific investigations, and for this reason, cellular respiration was assessed after exposing C2C12 myoblasts to the test drugs. Xenobiotics may disrupt cellular respiration either by inhibition of enzyme complexes of the electron transport chain, or by uncoupling the activity of the electron transport chain from ATP synthesis, or a combination thereof [38,43–45]. Such events may then lead to a decrease in ATP production, increased production of superoxide, disruption of $\Delta\psi m$, and eventually cell death by apoptosis or necrosis. The investigations of cellular respiration after pretreatment with the synthetic cathinones for 1 or 24 h revealed that only pretreatment with the two pyrovalerone derivatives α-PVP and naphyrone, but not with the pyrovalerone derivative MDPV or any of the other investigated substances, decreased basal respiration. In addition to the decrease in basal respiration, α-PVP and naphyrone impaired the maximal respiratory capacity at similar concentrations (500 to 1000 µM). Interestingly, MDMA was only toxic after 24 h but not at 1 h of incubation, suggesting that the toxicological mechanisms may be different between cathinones and MDMA.

Compared to vehicle control treatment, no difference in proton leak was observed for any of the tested compounds in the investigated concentration range, suggesting that the compounds did not directly uncouple oxidative phosphorylation. However, uncoupling of oxidative phosphorylation has previously been identified as an important contributor to MDMA-induced hyperthermia, which is attributable to activation (by phosphorylation) of the uncoupling protein 3 (UCP-3) in skeletal muscle [35,37,46]. The activation of UCP-3 has been proposed to be mediated by norepinephrine release, following activation of the sympathetic nervous system by MDMA [47]. Since we carried out our investigations in vitro, this mechanism was impossible, possibly explaining the lack of uncoupling of oxidative phosphorylation by the compounds investigated. Many cathinone designer drugs exert similar effects on the noradrenergic system as MDMA [10,11,14], and may therefore potentially cause hyperthermia mediated through UCP-3 activation in vivo as well. However, a direct uncoupling

effect of the prescription cathinone bupropion has previously been observed in human hepatoma cells [30], suggesting that some synthetic cathinones that were not investigated in the current study can have a direct uncoupling effect in skeletal muscle cells. Furthermore, since the mechanisms of cathinone-induced hyperthermia may differ from those of MDMA [48], they should be investigated in more detail in future studies.

The effect of MDMA, α-PVP, and naphyrone on the enzyme complexes of the mitochondrial electron transport chain was investigated in more detail to assess whether impairment of these complexes may be the underlying mechanism leading to disturbance of the electron transport chain. As shown in Figure 4, all three compounds impaired the activity of enzyme complexes of the electron transport chain. This observation may explain the decrease in the cellular oxygen consumption and ATP production observed for these substances.

The mitochondrial respiratory chain is a major source of ROS and complex I and III, and has been shown to be potential sites for ROS generation [49–51]. We therefore expected to detect an increase in mitochondrial ROS production for MDMA, α-PVP and naphyrone. To our surprise, we not only observed an increase in the cellular ROS content for these three compounds, but also for the other compounds investigated, which were not found to impair the electron transport chain. A possible reason could be a low antioxidative capacity in C2C12 myoblasts as suggested by a low expression of SOD2, the enzyme responsible for mitochondrial breakdown of superoxide [40].

The question arises as to why we observed ATP depletion for 3-MMC, mephedrone, MDPV and methylone without detecting mitochondrial dysfunction. In the presence of glucose, ATP can also be derived from glycolysis, which can also be impaired by toxicants [39]. Furthermore, the IC50 for impairment of membrane integrity and ATP depletion were close, suggesting that ATP depletion could have been a secondary event after disruption of membrane integrity.

4. Materials and Methods

4.1. Chemicals

3-MMC, MDMA, MDPV, methylone, mephedrone, and α-PVP were purchased as hydrochlorides from Lipomed (Arlesheim, Switzerland) with high-performance liquid chromatography (HPLC) purity >98.5%. Naphyrone hydrochloride was available from a previous study [11], after originally being synthesized as described by Meltzer et al. [52]. Drug stocks were made in autoclaved deionized water and were freshly prepared for each assay.

4.2. Cell Culture

C2C12 myoblasts were obtained from the American Type Culture Collection and kindly provided by Novartis (Basel, Switzerland). The cells were cultured in Dulbecco's Modified Eagle's Medium (DMEM) supplemented with 10% heat-inactivated fetal bovine serum at 37 °C in a humidified 5% CO_2 atmosphere [53]. When 70–80% confluency was reached, the cells were passaged with TrypLE Express reagent (Invitrogen, Basel, Switzerland). Undifferentiated C2C12 myoblasts were chosen for the current study due to the higher sensitivity to xenobiotics compared to differentiated C2C12 myotubes.

4.3. Plasma Membrane Integrity

As marker of membrane toxicity, cell membrane integrity loss expressed as adenylate kinase (AK) release, was determined with the ToxiLight BioAssay kit (Lonza, Basel, Switzerland) [38]. In brief, C2C12 myoblasts were seeded at a density of 50,000 cells per well in a 96-well plate. After attachment, the cells were treated with 100 µL of culture medium containing the test drugs (naphyrone at the concentrations of 10–500 µM, the remaining drugs at concentrations of 50–2000 µM). Triton X-100 (0.1%) was included as positive control inducing cell lysis. After 24 h, 20 µL of cell supernatant was transferred to a luminescence compatible 96-well plate and 100 µL of AK detection reagent was added to each well. After shaking of the plate at room temperature for 5 min, luminescence was measured

with a Tecan M200 Pro Infinity plate reader (Tecan, Männedorf, Switzerland). The percentage of intact cells (no cell membrane integrity loss) was calculated in relation to untreated cells and cells treated with Triton X-100, which were determined to represent 100% and 0% intact cells, respectively.

4.4. ATP Content

The intracellular ATP content representing the metabolic cell activity was measured using a CellTiter-Glo kit (Promega, Dübendorf, Switzerland) [38]. C2C12 myoblasts were seeded at a density of 50,000 cells per well in a 96-well plate. After attachment, the cells were treated with 100 µL of culture medium containing the test drugs (naphyrone at the concentrations of 10–500 µM, the remaining drugs at concentrations of 50–2000 µM). Triton X-100 (0.1%) was included as positive control inducing cell lysis. After 24 h, 50 µL of supernatant was removed from each well before 50 µL of CellTiter-Glo Reagent was added to the remaining cell culture medium at a ratio of 1:1 (*v*/*v*). After shaking of the plate at room temperature for 15 min, luminescence was measured with a Tecan M200 Pro Infinity plate reader (Tecan, Männedorf, Switzerland).

4.5. Oxygen Consumption

To determine whether synthetic cathinones target mitochondria, the oxygen consumption rate (OCR) of C2C12 myoblasts was measured with a Seahorse XF24 analyzer (Seahorse Biosciences, North Billerica, MA, USA). Briefly, 50,000 C2C12 cells per well were seeded in a Seahorse XF 24-well cell culture microplate coated with poly-D-lysine. The attached cells were then treated with a culture medium containing the test drugs (naphyrone at the concentrations of 50–500 µM, the remaining drugs at concentrations of 200–2000 µM) for 24 h. Thereafter, the culture medium was removed and the cells were washed twice with unbuffered DMEM (4 mM L-glutamate, 1 mM pyruvate, 4.1 g/L glucose, 63.3 mM sodium chloride, pH 7.4). After the second washing step, 750 µL of unbuffered DMEM was added to each well and the cells were incubated in a CO_2-free incubator for 40 min at 37 °C before they were transferred into the XF24 analyzer. After measuring the basal oxygen consumption rate, 1 µM oligomycin (inhibitor of F0F1ATPase), 1 µM carbonyl cyanide-4-(trifluoromethoxy)phenylhydrazone (FCCP; uncoupling agent), and 1 µM rotenone (complex I inhibitor) were successively added to the cells in order to measure proton leak, maximal cellular respiration, and extramitochondrial respiration, respectively. To adjust the OCR to the protein content, the cells were first fixed with 100 µL 50% (*w*/*v*) trichloroacetic acid added directly to the assay medium of each well for 1 h at 4 °C. Thereafter, the cells were washed with deionized water and treated with 0.4% (*w*/*v*, in 1% [*v*/*v*] acetic acid) sulforhodamine B. After 20 min, the cells were rapidly washed with 1% (*v*/*v*) acetic acid and the incorporated dye was solubilized with 100 µL of 10 mM TRIS base. The absorbance was then measured at 490 nm to obtain the amount of protein in relation to vehicle control.

4.6. Activity of Specific Enzyme Complexes of the Mitochondrial Electron Transport Chain

The activity of complex I and complex III of the mitochondrial respiratory chain was analyzed with an Oxygraph-2k high-resolution respirometer equipped with DataLab software (Oroboros Instruments, Innsbruck, Austria). Briefly, C2C12 cells were treated with either MDMA (1 mM), α-PVP (200 µM), or naphyrone (500 µM). After 24 h exposure, cells were resuspended in mitochondrial respiration medium MiR05 (0.5 mM EGTA, 3 mM magnesium chloride, 20 mM taurine, 10 mM potassium dihydrogen phosphate, 20 mM HEPES, 110 mM sucrose, 1 g/L fatty-acid free bovine serum albumin, and 60 mM lactobionic acid, pH 7.1) and a volume of 200 µL containing 2 million cells was transferred into the pre-calibrated Oxygraph chamber [54]. To permeabilize the cells, digitonin (10 µg per million cells) was added to the chamber. Then, the activity of complex I (NADH-CoQ reductase) was measured by adding L-glutamate and malate (10 and 2 mM, respectively) as substrates of the electron transport chain, followed by the addition of adenosine-diphosphate (ADP; 2.5 mM). To determine the activity complex III (CoQH2-cytochrome c reductase), complex I was inhibited with rotenone (0.5 µM) and duroquinol (0.5 mM) and was then added as a substrate of complex III.

4.7. Mitochondrial Superoxide Production

The MitoSOX red superoxide (O^{2-}) indicator (Invitrogen, Basel, Switzerland) was used for the assessment of oxidative stress in C2C12 cells treated with the test drugs. MitoSOX red is a live-cell permeant fluorogenic dye that targets the mitochondria and exhibits red fluorescence upon oxidation by superoxide. In brief, 50,000 cells were seeded at a density of 50,000 cells per well in a black clear-bottom 96-well plate. After attachment, the cells were treated with 100 µL of culture medium containing the test drugs (naphyrone at the concentrations of 10–500 µM, the remaining drugs at concentrations of 50–2000 µM). Amiodarone (20 µM) was included as a positive control. After 24 h, the cells were treated with 2.5 µM of MitoSOX reagent (100 µL per well) and incubated for 20 min at 37 °C and protected from light. Fluorescence was measured at 510/580 nm using a Tecan M200 Infinite Pro Infinity plate reader (Männedorf, Switzerland). The protein content was assessed with the Pierce Protein Assay kit (Thermo Scientific, Wohlen, Switzerland) and the fluorescence signal adjusted to protein content.

4.8. Statistics

Data are presented as mean ± SEM of at least three independent experiments and GraphPad Prism 7 (GraphPad Software, La Jolla, CA, USA) was used for statistical analysis. The activity of the enzyme complexes of the mitochondrial electron transport chain was compared to vehicle control with an unpaired two-tailed Student's *t*-test. For the remaining assays, statistical differences between control and test drugs were calculated with ANOVA followed by Dunett's test. p values below 0.05 were considered to be statistically significant.

5. Conclusions

All investigated synthetic cathinones, as well as MDMA, depleted ATP and elicited cell membrane integrity loss, and increased superoxide levels in C2C12 myoblasts in a concentration-dependent manner. The two pyrovalerone derivatives, α-PVP and naphyrone, additionally impaired basal and maximal cellular respiration, which suggests mitochondrial dysfunction. Therefore, in addition to sympathetic nervous system effects and strenuous muscle exercise, direct effects of some cathinones on skeletal muscle mitochondria may contribute to myotoxicity in susceptible cathinone users.

Supplementary Materials: The following are available online at http://www.mdpi.com/1422-0067/20/7/1561/s1.

Author Contributions: Study design: X.Z., D.L., S.K.; experiments: X.Z., D.L., G.M.S.; data interpretation: X.Z., D.L., G.M.S., J.B., M.E.L., S.K.; writing—original draft preparation: D.L., J.B., G.M.S.; writing—review and editing: D.L., M.E.L., S.K.; funding acquisition: X.Z., M.E.L., S.K.

Funding: The study was financially supported by a grant from the Swiss National Science Foundation to S.K. (SNF 31003A_156270).

Acknowledgments: X.Z. is a recipient of China Scholarship Council Stipendium of China.

Conflicts of Interest: The authors declare no conflict of interest.

References

1. European Monitoring Centre for Drugs and Drug Addiction. European Drug Report 2017. Available online: http://www.emcdda.europa.eu/system/files/publications/4541/TDAT17001ENN.pdf (accessed on 4 October 2018).
2. Prosser, J.M.; Nelson, L.S. The toxicology of bath salts: A review of synthetic cathinones. *J. Med. Toxicol.* **2012**, *8*, 33–42. [CrossRef] [PubMed]
3. Sanchez, S. Sur un homologue de l'ephedrine. *Bull. Soc. Chim. France* **1929**, *45*, 284–286.
4. Valente, M.J.; Guedes de Pinho, P.; de Lourdes Bastos, M.; Carvalho, F.; Carvalho, M. Khat and synthetic cathinones: A review. *Arch. Toxicol.* **2014**, *88*, 15–45. [CrossRef] [PubMed]

5. Soroko, F.E.; Mehta, N.B.; Maxwell, R.A.; Ferris, R.M.; Schroeder, D.H. Bupropion hydrochloride ((+/-) alpha-t-butylamino-3-chloropropiophenone HCl): A novel antidepressant agent. *J. Pharm. Pharmacol.* **1977**, *29*, 767–770. [CrossRef] [PubMed]
6. Seaton, D.A.; Duncan, L.J.; Rose, K.; Scott, A.M. Diethyl-propion in the treatment of "refractory" obesity. *Br. Med. J.* **1961**, *1*, 1009–1011. [CrossRef] [PubMed]
7. Cunningham, G. Diethylpropion in the treatment of obesity. *J. Coll. Gen. Pract.* **1963**, *6*, 347. [PubMed]
8. Canning, H.; Goff, D.; Leach, M.J.; Miller, A.A.; Tateson, J.E.; Wheatley, P.L. The involvement of dopamine in the central actions of bupropion, a new antidepressant [proceedings]. *Br. J. Pharmacol.* **1979**, *66*, 104p–105p. [PubMed]
9. Dal Cason, T.A.; Young, R.; Glennon, R.A. Cathinone: An investigation of several N-alkyl and methylenedioxy-substituted analogs. *Pharmacol. Biochem. Behav.* **1997**, *58*, 1109–1116. [CrossRef]
10. Simmler, L.D.; Rickli, A.; Hoener, M.C.; Liechti, M.E. Monoamine transporter and receptor interaction profiles of a new series of designer cathinones. *Neuropharmacology* **2014**, *79*, 152–160. [CrossRef]
11. Simmler, L.D.; Buser, T.A.; Donzelli, M.; Schramm, Y.; Dieu, L.H.; Huwyler, J.; Chaboz, S.; Hoener, M.C.; Liechti, M.E. Pharmacological characterization of designer cathinones in vitro. *Br. J. Pharmacol.* **2013**, *168*, 458–470. [CrossRef]
12. Rickli, A.; Hoener, M.C.; Liechti, M.E. Monoamine transporter and receptor interaction profiles of novel psychoactive substances: Para-halogenated amphetamines and pyrovalerone cathinones. *Eur. Neuropsychopharmacol.* **2015**, *25*, 365–376. [CrossRef]
13. Mayer, F.P.; Wimmer, L.; Dillon-Carter, O.; Partilla, J.S.; Burchardt, N.V.; Mihovilovic, M.D.; Baumann, M.H.; Sitte, H.H. Phase I metabolites of mephedrone display biological activity as substrates at monoamine transporters. *Br. J. Pharmacol.* **2016**, *173*, 2657–2668. [CrossRef]
14. Luethi, D.; Kolaczynska, K.E.; Docci, L.; Krahenbuhl, S.; Hoener, M.C.; Liechti, M.E. Pharmacological profile of mephedrone analogs and related new psychoactive substances. *Neuropharmacology* **2018**, *134*, 4–12. [CrossRef]
15. Baumann, M.H.; Ayestas, M.A., Jr.; Partilla, J.S.; Sink, J.R.; Shulgin, A.T.; Daley, P.F.; Brandt, S.D.; Rothman, R.B.; Ruoho, A.E.; Cozzi, N.V. The designer methcathinone analogs, mephedrone and methylone, are substrates for monoamine transporters in brain tissue. *Neuropsychopharmacology* **2012**, *37*, 1192–1203. [CrossRef]
16. Wood, D.M.; Davies, S.; Greene, S.L.; Button, J.; Holt, D.W.; Ramsey, J.; Dargan, P.I. Case series of individuals with analytically confirmed acute mephedrone toxicity. *Clin. Toxicol.* **2010**, *48*, 924–927. [CrossRef]
17. James, D.; Adams, R.D.; Spears, R.; Cooper, G.; Lupton, D.J.; Thompson, J.P.; Thomas, S.H. Clinical characteristics of mephedrone toxicity reported to the U.K. National Poisons Information Service. *Emerg. Med. J.* **2011**, *28*, 686–689. [CrossRef] [PubMed]
18. Beck, O.; Franzen, L.; Backberg, M.; Signell, P.; Helander, A. Intoxications involving MDPV in Sweden during 2010-2014: Results from the STRIDA project. *Clin. Toxicol.* **2015**, *53*, 865–873. [CrossRef]
19. Beck, O.; Franzen, L.; Backberg, M.; Signell, P.; Helander, A. Toxicity evaluation of alpha-pyrrolidinovalerophenone (α-PVP): Results from intoxication cases within the STRIDA project. *Clin. Toxicol.* **2016**, *54*, 568–575. [CrossRef] [PubMed]
20. Umebachi, R.; Aoki, H.; Sugita, M.; Taira, T.; Wakai, S.; Saito, T.; Inokuchi, S. Clinical characteristics of alpha-pyrrolidinovalerophenone (α-PVP) poisoning. *Clin. Toxicol.* **2016**, *54*, 563–567. [CrossRef] [PubMed]
21. Fröhlich, S.; Lambe, E.; O'Dea, J. Acute liver failure following recreational use of psychotropic "head shop" compounds. *Ir. J. Med. Sci.* **2011**, *180*, 263–264. [CrossRef] [PubMed]
22. Borek, H.A.; Holstege, C.P. Hyperthermia and multiorgan failure after abuse of "bath salts" containing 3, 4-methylenedioxypyrovalerone. *Ann. Emerg. Med.* **2012**, *60*, 103–105. [CrossRef] [PubMed]
23. Penders, T.M.; Gestring, R.E.; Vilensky, D.A. Excited delirium following use of synthetic cathinones (bath salts). *Gen. Hosp. Psychiatry* **2012**, *34*, 647–650. [CrossRef] [PubMed]
24. Ross, E.A.; Watson, M.; Goldberger, B. "Bath salts" intoxication. *N. Engl. J. Med.* **2011**, *365*, 967–968. [CrossRef] [PubMed]
25. Ross, E.A.; Reisfield, G.M.; Watson, M.C.; Chronister, C.W.; Goldberger, B.A. Psychoactive "bath salts" intoxication with methylenedioxypyrovalerone. *Am. J. Med.* **2012**, *125*, 854–858. [CrossRef]
26. Patel, N.B. Mechanism of action of cathinone: The active ingredient of khat (Catha Edulis). *East Afr. Med. J.* **2000**, *77*, 329–332. [CrossRef]

27. White, C.M. Mephedrone and 3,4-methylenedioxypyrovalerone (MDPV): Synthetic cathinones with serious health implications. *J. Clin. Pharmacol.* **2016**, *56*, 1319–1325. [CrossRef]
28. Valente, M.J.; Araujo, A.M.; Silva, R.; Bastos Mde, L.; Carvalho, F.; Guedes de Pinho, P.; Carvalho, M. 3,4-Methylenedioxypyrovalerone (MDPV): In vitro mechanisms of hepatotoxicity under normothermic and hyperthermic conditions. *Arch. Toxicol.* **2016**, *90*, 1959–1973. [CrossRef]
29. Valente, M.J.; Araujo, A.M.; Bastos Mde, L.; Fernandes, E.; Carvalho, F.; Guedes de Pinho, P.; Carvalho, M. characterization of hepatotoxicity mechanisms triggered by designer cathinone drugs (beta-keto amphetamines). *Toxicol. Sci.* **2016**, *153*, 89–102. [CrossRef]
30. Luethi, D.; Liechti, M.E.; Krahenbuhl, S. Mechanisms of hepatocellular toxicity associated with new psychoactive synthetic cathinones. *Toxicology* **2017**, *387*, 57–66. [CrossRef]
31. Valente, M.J.; Bastos, M.L.; Fernandes, E.; Carvalho, F.; Guedes de Pinho, P.; Carvalho, M. Neurotoxicity of beta-keto amphetamines: Deathly mechanisms elicited by methylone and MDPV in human dopaminergic SH-SY5Y cells. *ACS Chem. Neurosci.* **2017**, *8*, 850–859. [CrossRef]
32. Valente, M.J.; Amaral, C.; Correia-da-Silva, G.; Duarte, J.A.; Bastos, M.L.; Carvalho, F.; Guedes de Pinho, P.; Carvalho, M. Methylone and MDPV activate autophagy in human dopaminergic SH-SY5Y cells: A new insight into the context of beta-keto amphetamines-related neurotoxicity. *Arch. Toxicol.* **2017**, *91*, 3663–3676. [CrossRef] [PubMed]
33. Halachanova, V.; Sansone, R.A.; McDonald, S. Delayed rhabdomyolysis after ecstasy use. *Mayo Clin. Proc.* **2001**, *76*, 112–113. [CrossRef] [PubMed]
34. Duarte, J.A.; Leao, A.; Magalhaes, J.; Ascensao, A.; Bastos, M.L.; Amado, F.L.; Vilarinho, L.; Quelhas, D.; Appell, H.J.; Carvalho, F. Strenuous exercise aggravates MDMA-induced skeletal muscle damage in mice. *Toxicology* **2005**, *206*, 349–358. [CrossRef]
35. Carvalho, M.; Carmo, H.; Costa, V.M.; Capela, J.P.; Pontes, H.; Remiao, F.; Carvalho, F.; Bastos Mde, L. Toxicity of amphetamines: An update. *Arch. Toxicol.* **2012**, *86*, 1167–1231. [CrossRef]
36. Vanden Eede, H.; Montenij, L.J.; Touw, D.J.; Norris, E.M. Rhabdomyolysis in MDMA intoxication: A rapid and underestimated killer. "Clean" ecstasy, a safe party drug? *J. Emerg. Med.* **2012**, *42*, 655–658. [CrossRef]
37. Kelly, O.M.; McNamara, Y.M.; Manzke, L.H.; Meegan, M.J.; Porter, R.K. The preservation of in vivo phosphorylated and activated uncoupling protein 3 (UCP3) in isolated skeletal muscle mitochondria following administration of 3,4-methylenedioxymethamphetamine (MDMA aka ecstasy) to rats/mice. *Mitochondrion* **2012**, *12*, 110–119. [CrossRef] [PubMed]
38. Felser, A.; Blum, K.; Lindinger, P.W.; Bouitbir, J.; Krähenbühl, S. Mechanisms of hepatocellular toxicity associated with dronedarone—A comparison to amiodarone. *Toxicol. Sci.* **2013**, *131*, 480–490. [CrossRef] [PubMed]
39. Paech, F.; Bouitbir, J.; Krahenbuhl, S. Hepatocellular Toxicity Associated with Tyrosine Kinase Inhibitors: Mitochondrial Damage and Inhibition of Glycolysis. *Front. Pharmacol.* **2017**, *8*, 367. [CrossRef]
40. Flynn, J.M.; Melov, S. SOD2 in mitochondrial dysfunction and neurodegeneration. *Free Radic. Biol. Med.* **2013**, *62*, 4–12. [CrossRef]
41. Torrance, H.; Cooper, G. The detection of mephedrone (4-methylmethcathinone) in 4 fatalities in Scotland. *Forensic Sci Int.* **2010**, *202*, e62-3. [CrossRef]
42. Kamalian, L.; Chadwick, A.E.; Bayliss, M.; French, N.S.; Monshouwer, M.; Snoeys, J.; Park, B.K. The utility of HepG2 cells to identify direct mitochondrial dysfunction in the absence of cell death. *Toxicol. In Vitro* **2015**, *29*, 732–740. [CrossRef] [PubMed]
43. Fromenty, B.; Fisch, C.; Berson, A.; Letteron, P.; Larrey, D.; Pessayre, D. Dual effect of amiodarone on mitochondrial respiration. Initial protonophoric uncoupling effect followed by inhibition of the respiratory chain at the levels of complex I and complex II. *J. Pharmacol. Exp. Ther.* **1990**, *255*, 1377–1384. [PubMed]
44. Krähenbühl, S. Mitochondria: Important target for drug toxicity? *J. Hepatol.* **2001**, *34*, 334–336. [CrossRef]
45. Serviddio, G.; Bellanti, F.; Giudetti, A.M.; Gnoni, G.V.; Capitanio, N.; Tamborra, R.; Romano, A.D.; Quinto, M.; Blonda, M.; Vendemiale, G.; et al. Mitochondrial oxidative stress and respiratory chain dysfunction account for liver toxicity during amiodarone but not dronedarone administration. *Free Radic. Biol. Med.* **2011**, *51*, 2234–2242. [CrossRef]
46. Mills, E.M.; Banks, M.L.; Sprague, J.E.; Finkel, T. Pharmacology: Uncoupling the agony from ecstasy. *Nature* **2003**, *426*, 403–404. [CrossRef]

47. Mills, E.M.; Rusyniak, D.E.; Sprague, J.E. The role of the sympathetic nervous system and uncoupling proteins in the thermogenesis induced by 3,4-methylenedioxymethamphetamine. *J. Mol. Med.* **2004**, *82*, 787–799. [CrossRef]
48. Shortall, S.E.; Green, A.R.; Swift, K.M.; Fone, K.C.; King, M.V. Differential effects of cathinone compounds and MDMA on body temperature in the rat, and pharmacological characterization of mephedrone-induced hypothermia. *Br. J. Pharmacol.* **2013**, *168*, 966–977. [CrossRef]
49. Votyakova, T.V.; Reynolds, I.J. DeltaPsi(m)-Dependent and -independent production of reactive oxygen species by rat brain mitochondria. *J. Neurochem.* **2001**, *79*, 266–277. [CrossRef]
50. Drose, S.; Brandt, U. Molecular mechanisms of superoxide production by the mitochondrial respiratory chain. *Adv. Exp. Med. Biol.* **2012**, *748*, 145–169.
51. Antico Arciuch, V.G.; Elguero, M.E.; Poderoso, J.J.; Carreras, M.C. Mitochondrial regulation of cell cycle and proliferation. *Antioxid. Redox Signal.* **2012**, *16*, 1150–1180. [CrossRef]
52. Meltzer, P.C.; Butler, D.; Deschamps, J.R.; Madras, B.K. 1-(4-Methylphenyl)-2-pyrrolidin-1-yl-pentan-1-one (Pyrovalerone) analogues: A promising class of monoamine uptake inhibitors. *J. Med. Chem.* **2006**, *49*, 1420–1432. [CrossRef] [PubMed]
53. Bonifacio, A.; Sanvee, G.M.; Brecht, K.; Kratschmar, D.V.; Odermatt, A.; Bouitbir, J.; Krähenbühl, S. IGF-1 prevents simvastatin-induced myotoxicity in C2C12 myotubes. *Arch. Toxicol.* **2017**, *91*, 2223–2234. [CrossRef] [PubMed]
54. Pesta, D.; Gnaiger, E. High-resolution respirometry: OXPHOS protocols for human cells and permeabilized fibers from small biopsies of human muscle. *Methods Mol. Biol.* **2012**, *810*, 25–58. [PubMed]

Supplemental file

Methods

Cell line and maintenance for cells used for western blotting

C2C12 myoblasts (American Type Culture Collection, USA) were kindly provided by Novartis (Basel, Switzerland). Cells were cultured in Dulbecco's Modified Eagle Medium – GlutaMAX supplemented with 10% fetal bovine serum (FBS) and 1% HEPES (Gibco, UK). Cells were maintained at 37°C in a humidified 5% CO_2 cell culture incubator, were passaged using trypsin upon reaching approximately 60% confluency and seeded in appropriate well plates prior differentiation into myotubes. Two days after seeding the medium was replaced by differentiation medium (DM) containing DMEM-Glutamax and 1% HEPES supplemented with 2% horse serum (Gibco, UK) and 0.029 % insulin (stock: 10mg/mL) (Sigma-Aldrich, USA) for three days. They were then starved in DMEM-Glutamax and 1% HEPES supplemented with 2% horse serum (Gibco, UK), without insulin. Myoblasts and myotubes were then treated for 24 hours with DMSO 0.1 %.

Western Blotting

C2C12 myoblasts and myotubes were lysed with RIPA buffer (150 mM sodium chloride, 1.0% NP-40, 0.5% sodium deoxycholate, 0.1% sodium dodecyl sulphate, 50 mM Tris, pH 8.0) containing complete Mini protease inhibitor cocktail (Roche Diagnostics, Mannheim, Germany). Proteins (10 µg) were resolved by SDS-PAGE using commercially available 4–12% NuPAGE Bis-Tris gels (Invitrogen, Basel, Switzerland) and transferred using the Trans-Blot Turbo Blotting System (Bio-Rad, Cressier, Switzerland). The membranes were incubated with antibodies against SOD2 (#13194, cell signaling, 1/2000), and GAPDH (sc-365062, santa cruz, 1/6000). Membranes were probed with secondary antibodies conjugated to horse radish peroxidase (HRP). Immunoblots were developed using Clarity

Western ECL Substrate (Bio-Rad Laboratories, Hercules, USA). Protein expression was quantified using the Fusion Pulse TS device (Vilber Lourmat, Oberschwaben, Germany).

Figure Legends

Suppl. Fig. 1. Oxygen consumption rate (OCR) in C2C12 cells after 1 h drug exposure. Basal respiration, leak respiration, and maximal respiration are expressed as mean ± SEM of at least three independent experiments. Drug treatments were compared to vehicle control with ANOVA followed by Dunett's test. Significance levels are given as *p < 0.05, **p < 0.01, ***p < 0.001.

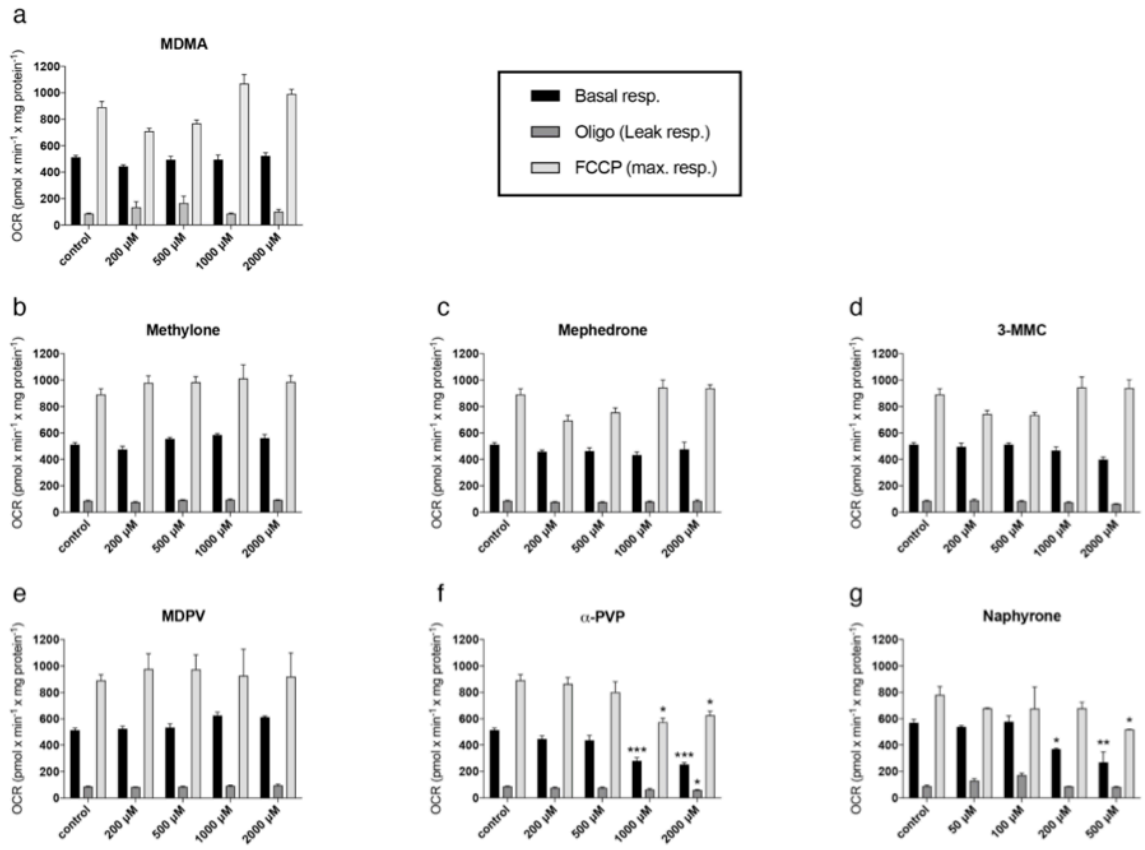

Suppl. Fig. 2. SOD2 protein expression in myoblasts and myotubes. Western blots showing the expression levels of SOD2 and GAPDH. The graph shows the quantification of SOD2 protein expression normalized against GAPDH. Data represent the mean±SEM. N= 3. * $p < 0.05$.

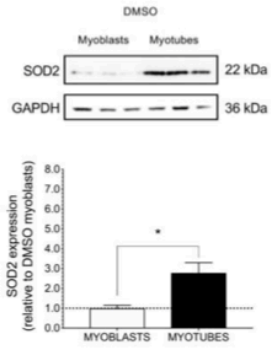

2. Paper 2

Para-Halogenation Affects Monoamine Transporter Inhibition Properties and Hepatocellular Toxicity of Amphetamines and Methcathinones

In this paper, we investigated the pharmacological perspective and hepatocellular toxicity of amphetamine, 4-FA, PCA, methcathinone, 4-FMC and 4-CMC in HepG2 cells.

frontiers in Pharmacology

ORIGINAL RESEARCH
published: 24 April 2019
doi: 10.3389/fphar.2019.00438

Para-Halogenation Affects Monoamine Transporter Inhibition Properties and Hepatocellular Toxicity of Amphetamines and Methcathinones

Dino Luethi[1]*, *Melanie Walter*[1], *Xun Zhou*[1], *Deborah Rudin*[1], *Stephan Krähenbühl*[1,2] and *Matthias E. Liechti*[1]

[1]Division of Clinical Pharmacology and Toxicology, Department of Biomedicine, University Hospital Basel, University of Basel, Basel, Switzerland, [2]Swiss Centre for Applied Human Toxicology (SCAHT), University of Basel, Basel, Switzerland

OPEN ACCESS

Edited by:
M Foster Olive,
Arizona State University,
United States

Reviewed by:
Thorsten Lau,
Central Institute for Mental Health,
Germany
David Pubill,
University of Barcelona, Spain

***Correspondence:**
Dino Luethi
dino.luethi@unibas.ch

Specialty section:
This article was submitted to Neuropharmacology, a section of the journal Frontiers in Pharmacology

Received: *06 February 2019*
Accepted: *05 April 2019*
Published: *24 April 2019*

Citation:
Luethi D, Walter M, Zhou X, Rudin D, Krähenbühl S and Liechti ME (2019) Para-Halogenation Affects Monoamine Transporter Inhibition Properties and Hepatocellular Toxicity of Amphetamines and Methcathinones. Front. Pharmacol. 10:438. doi: 10.3389/fphar.2019.00438

Halogenated derivatives of amphetamine-type stimulants are appearing on the drug market, often with altered pharmacological profile and sometimes different legal status compared to the non-halogenated substances. The aim of the present study was to investigate the pharmacological profile and hepatocellular toxicity of *para*-halogenated amphetamines and cathinones. The potential of amphetamine, 4-fluoroamphetamine, 4-chloroamphetamine, methcathinone, 4-fluoromethcathinone, and 4-chloromethcathinone to inhibit the monoamine transporters for norepinephrine, dopamine, and serotonin was determined in transporter-transfected human embryonic kidney 293 cells. Cell membrane integrity, ATP content, oxygen consumption rate, and superoxide levels were measured in human hepatoma HepG2 cells after exposure to the substances for 24 h. All compounds inhibited the norepinephrine transporter at submicromolar concentrations and the dopamine transporter at low micromolar concentrations. The selectivity of the compounds to inhibit the dopamine *versus* serotonin transporter decreased with increasing size of the *para*-substituent, resulting in potent serotonin uptake inhibition for the halogenated derivatives. All substances depleted the cellular ATP content at lower concentrations (0.25–2 mM) than cell membrane integrity loss occurred (≥0.5 mM), suggesting mitochondrial toxicity. The amphetamines and 4-chloromethcathinone additionally impaired the mitochondrial respiratory chain, confirming mitochondrial toxicity. The following toxicity rank order for the *para*-substituents was observed: chloride > fluoride > hydrogen. In conclusion, *para*-halogenation of stimulants increases the risk for serotonergic neurotoxicity. Furthermore, *para*-halogenation may increase hepatic toxicity mediated by mitochondrial impairment in susceptible users.

Keywords: amphetamine, cathinone, liver injury, mitochondria, monoamine, transporter

INTRODUCTION

Halogenation of illicit amphetamine-type substances represents a tool to create novel designer drugs in clandestine chemistry. Besides having an altered pharmacological profile (Rickli et al., 2015; Mayer et al., 2018; Luethi et al., 2018a), halogenated derivatives may emerge as uncontrolled substances, facilitating their distribution over the Internet. However, halogenation can also result in increased toxicity. For instance, the *para*-chlorinated derivative of amphetamine (4-chloroamphetamine) exerts an increased serotonergic toxicity when compared to the parent compound (Miller et al., 1986; Fuller, 1992; Colado et al., 1993). Other *para*-halogenated stimulants (**Figure 1**), such as 4-fluoroamphetamine (4-FA), 4-fluoromethcathinone (flephedrone), and 4-chloromethcathinone (clephedrone), have recently appeared on the recreational drug market (Brandt et al., 2010; Taschwer et al., 2014; Linsen et al., 2015; Odoardi et al., 2016; Grifell et al., 2017; Tomczak et al., 2018), but their pharmacological properties and toxicity are currently not well investigated.

Considering the lack of knowledge about the pharmacological and toxicological properties of the halogenated amphetamine and methcathinone (β-keto *N*-methylamphetamine) derivatives, the current study had two principle aims. First, we wanted to determine the effect of *para*-halogenation of amphetamine and methcathinone on the stimulant-type pharmacological potency of these compounds. For that, we obtained monoamine uptake inhibition profiles in monoamine transporter-transfected human embryonic kidney (HEK) 293 cells, which represent a widely used *in vitro* model to study transporter inhibition of stimulants. Second, we investigated the impact of *para*-halogenation of amphetamine and methcathinone on the toxicological profile of these compounds. Since liver injury is a potentially severe complication of amphetamine-type drug intake (Carvalho et al., 2012), we used HepG2 cells for this purpose. HepG2 cells represent a well-established human hepatoma cell line, which has previously been used to study hepatocellular toxicity of stimulants (Dias da Silva et al., 2013, 2015; Luethi et al., 2017). With this study, we aimed on the one hand to assess the hepatotoxic potential of these drugs and on the other hand to put this potential into perspective to their stimulant properties, which may put users at risk of sympathomimetic toxicity.

MATERIALS AND METHODS

Test Substances

Amphetamine, 4-fluoroamphetamine, methcathinone, 4-fluoromethcathinone, and 4-chloromethcathinone were purchased from Lipomed (Arlesheim, Switzerland) with HPLC purity of >98.5%. 4-Chloroamphetamine was purchased from Cayman Chemical (Ann Arbor, MI, USA) with a purity of >98%. All drugs were obtained as racemic hydrochloride salts.

Cell Line and Culture

Cell culture medium and supplements were purchased from Thermo Fisher Scientific (Basel, Switzerland). HEK 293 cells stably transfected with the human monoamine transporter for norepinephrine (hNET), dopamine (hDAT), or serotonin (hSERT; Tatsumi et al., 1997) were cultured in Dulbecco's Modified Eagle Medium (DMEM, 4.5 g/L glucose) supplemented with 10% non-heat inactivated fetal calf serum (FCS), 2 mM L-glutamine, 1 mM sodium pyruvate, and 1% MEM non-essential amino acids. Geneticin (250 µg/ml) was used as selection antibiotic. HepG2 cells were cultured in DMEM (1 g/L glucose) supplemented with 10% heat inactivated FCS, 10 mM HEPES buffer, 2 mM GlutaMAX, 1% MEM non-essential amino acids, and penicillin-streptomycin (10,000 U/ml corresponding to 10 mg/ml). Both cell lines were cultured at 37°C in a 5% CO_2 humidified atmosphere.

Monoamine Transport Inhibition

The monoamine uptake inhibition of the halogenated amphetamine and methcathinone derivatives was assessed at ambient temperature in transporter-transfected HEK 293 cells at concentrations in the range of 1 nM–900 µM as previously described (Luethi et al., 2018b). As summarized, the cells were detached from the cultivation flask and

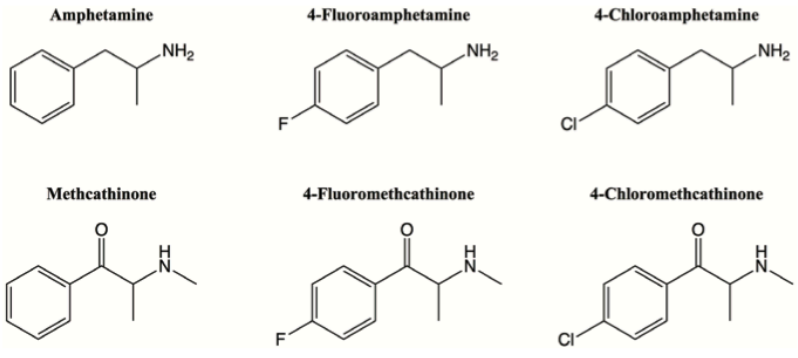

FIGURE 1 | *Para*-halogenated amphetamine and methcathinone derivatives.

resuspended in Krebs-Ringer Bicarbonate Buffer (Sigma-Aldrich, Buchs, Switzerland) at a density of 3 million cells per ml. The cell suspension was transferred into a round bottom 96-well plate (100 µl cell suspension per well) and incubated with the compounds of interest for 10 min before [^{3}H]norepinephrine (13.1 Ci/mmol, PerkinElmer, Schwerzenbach, Switzerland), [^{3}H] dopamine (30.0 Ci/mmol, PerkinElmer, Schwerzenbach, Switzerland), or [^{3}H]serotonin (80 Ci/mmol, Anawa, Zürich, Switzerland), which was added at a final concentration of 5 nM for another 10 min. The assay mixtures (100 µl per well) were then transferred into 0.5 ml centrifugation tubes, and the cells were separated from the supernatant through a silicone oil phase by centrifugation at 16,550 g for 3 min. The tubes were then snap frozen in liquid nitrogen, and the cell pellets were cut into 6 ml scintillation vials containing 0.5 ml lysis buffer (0.05 M TRIS-HCl, 50 mM NaCl, 5 mM EDTA, and 1% NP-40 in water). After vigorously shaking the vials for 1 h, 3 ml Ultima Gold (PerkinElmer, Schwerzenbach, Switzerland) was added, and the radioactivity was quantified by liquid scintillation counting using a Packard Tri-Carb Liquid Scintillation Counter 1900 TR. The uptake in the presence of transporter-specific inhibitors (10 µM nisoxetine for NET, 10 µM mazindol for DAT, and 10 µM fluoxetine for SERT) was assessed in order to determine non-specific uptake.

Cell Membrane Integrity

Cell membrane integrity loss was assessed with the ToxiLight BioAssay Kit (Lonza, Basel, Switzerland) as a marker of cytotoxicity. Briefly, HepG2 cells were seeded in a 96-well plate at a density of 25,000 cells per well. The following day, the cells were treated with 100 µl of the compounds of interest dissolved in medium (0.25, 0.5, 1.0, and 2.0 mM of each drug, and additionally, 0.1 mM of 4-fluoroamphetamine and 4-chloroamphetamine). Triton X-100 (0.5%) was chosen as positive control to induce cell lysis. After 24 h, 50 µl of the ToxiLight assay buffer was added to 20 µl of the supernatant of the drug treatments. After 5 min incubation under shaking, luminescence was measured with a M200 Pro Infinity plate reader (Tecan, Männedorf, Switzerland) and compared to medium control. The amount of viable cells (no cell membrane integrity loss) was calculated in relation to untreated cells and cells lysed with Triton X-100, which were determined to represent 100% and 0% viable cells, respectively.

ATP Content

The ATP content was assessed with the CellTiter-Glo Luminescent Cell Viability Assay (Promega, Dübendorf, Switzerland). Briefly, HepG2 cells were seeded in a 96-well plate at a density of 25,000 cells per well. The following day, the cells were treated with 100 µl of the test substances dissolved in medium (0.25, 0.5, 1.0, and 2.0 mM of each drug, and additionally, 0.1 mM of 4-fluoroamphetamine and 4-chloroamphetamine). Triton X-100 (0.5%) was chosen as positive control to induce cell lysis. After 24 h incubation, 50 µl of the supernatant was discarded, and 50 µl of CellTiter-Glo reagent was added to each well. The plate was then shaken for 15 min at room temperature to induce cell lysis. Thereafter, luminescence was measured with a M200 Pro Infinity plate reader (Tecan, Männedorf, Switzerland) and compared to medium control.

Oxygen Consumption

The cellular oxygen consumption rate (OCR) was measured with a Seahorse XF24 Analyzer (Seahorse Biosciences, North Billerica, MA, USA). Briefly, HepG2 cells were seeded in a poly-D-lysine coated Seahorse XF24 cell culture microplate at a density of 100,000 cells per well. The following day, the cells were treated with the compounds of interest dissolved in 100 µl culture medium. After 24 h incubation, the medium was removed, and the cells were washed twice with pre-warmed and unbuffered DMEM (4 mM L-glutamate, 1 mM pyruvate, 1 g/L glucose, 63.3 mM sodium chloride, pH 7.4). Thereafter, 750 µl of unbuffered DMEM was added to each well, and the plate was incubated in a CO_2 free incubator for 40 min at 37°C. The ports of the XF24 assay cartridge were then loaded with oligomycin, trifluoromethoxy carbonylcyanide phenylhydrazone (FCCP), or rotenone at a final assay concentration of 1 µM, and the cartridge was loaded into the Seahorse XF24 Analyzer. First, oligomycin was injected to inhibit mitochondrial phosphorylation, allowing a quantification of proton leak. Second, oxidative phosphorylation was uncoupled from ATP synthesis by FCCP to determine the maximal respiratory capacity of the cells. Third, rotenone was injected to inhibit complex I of the electron transport chain in order to assess for extramitochondrial respiration, which was then subtracted from basal, leak, and maximal respiration. The protein content was determined using sulforhodamine B staining. The cells were fixed with 100 µl trichloroacetic acid (50% [w/v]), added to each well of the assay plate. After 1 h at 4°C, the cells were washed with deionized water and stained with sulforhodamine B (0.4% [w/v], in 1% [v/v] acetic acid). After 20 min, the cells were rapidly washed with 1% (v/v) acetic acid, and the incorporated dye was solubilized with 100 µl of 10 mM TRIS base. The absorbance was then measured at 490 nm.

Oxidative Stress

Reactive oxygen species (ROS) production was determined with the mitochondrial superoxide (O_2^-) indicator MitoSOX (Thermo Fisher Scientific, Basel, Switzerland), which is a live-cell permeant fluorogenic dye that targets the mitochondria and exhibits red fluorescence upon oxidation by superoxide. Briefly, HepG2 cells were seeded in a 96-well plate at a density of 25,000 cells per well. The following day, the cells were treated with 100 µl of the test substances dissolved in medium (0.25, 0.5, 1.0, and 2.0 mM of each drug, and additionally, 0.1 mM of 4-fluoroamphetamine and 4-chloroamphetamine). Amiodarone (50 µM) was included as positive control. After 24 h incubation, 100 µl of MitoSOX reagent (2.5 µM) was added to each well for 10 min at 37°C protected from light. After that, fluorescence was measured at 510/580 nm with a M200 Pro Infinity plate

reader (Tecan, Männedorf, Switzerland). The protein content was assessed with the Pierce BCA Protein Assay Kit (Thermo Fisher Scientific, Basel, Switzerland).

Mechanisms of Cell Death

Annexin V, a Ca^{2+}-dependent phospholipid-binding protein that has a high affinity for phosphatidylserine, was used to determine the percentage of apoptotic cells. Phosphatidylserine is located in the inner cytoplasmic surface of intact cell membranes; in apoptotic cells, phosphatidylserine is translocated to the outer leaflet of the plasma membrane where annexin V binds to it. To assess the percentage of dead cells composed of necrotic and late apoptotic cells, propidium iodide, a red fluorescent dye not permeable to live and apoptotic cells but able to stain permeable necrotic cells by binding to the nucleic acid in the cell, was used. Briefly, 100,000 HepG2 cells per well were seeded in a 48-well plate and cultured overnight. The following day, the cells were treated with 250 µl of the compounds of interest dissolved in medium at concentrations selected based on ATP depletion and cell membrane disruption. Doxorubicin (0.5 µM) was included as positive control. After incubation for 24 h, the cells were harvested with 0.05% trypsin and washed with phosphate buffered saline (pH = 7.4). Afterward, 1 µl Alexa Fluor 488 annexin V staining (Molecular Probes, OR, USA) and 1 µl propidium iodide staining (Molecular Probes, OR, USA) were added to the cell suspension at a final concentration of 10 µg/ml. After 15 min incubation in the dark, the cells were analyzed with a CytoFLEX flow cytometer (Beckman Coulter, IN, USA) gating for 10,000 cells. The data were assessed using FlowJo software 10.08 (Tree Star, Ashland, OR, USA).

Statistics

All statistical analyses were performed using GraphPad Prism 7.0c (GraphPad Software, La Jolla, CA, USA). For toxicology assays, differences between control and test drugs were calculated with ANOVA followed by Dunett's test. p below 0.05 was considered statistically significant. Monoamine uptake data were fit by nonlinear regression to variable slope sigmoidal dose-response curves to assess IC_{50} values.

RESULTS

Monoamine Transporter Inhibition

Monoamine uptake inhibition curves are shown in **Figure 2**, and the corresponding IC_{50} values are listed in **Table 1**. For all amphetamines and methcathinones, most potent uptake inhibition was observed at NET (IC_{50} values in the range of 0.08–0.43 µM). The compounds displayed similar potential to inhibit dopamine uptake (IC_{50} values in the range of 1.6–6.6 µM) but differed greatly in their potential to inhibit serotonin uptake (IC_{50} values in the range of 0.5–54 µM). *Para*-fluorination increased the inhibition potency at the SERT *versus* DAT roughly one order of magnitude and *para*-chlorination roughly two orders of magnitude compared to the non-substituted amphetamine and methcathinone.

Cell Membrane Integrity and ATP Content

In comparison to the interaction with monoamine transporters, the toxicity on HepG2 cells occurred at substantially higher concentrations. A significant and concentration-dependent depletion of ATP was observed at 0.1 mM for 4-chloroamphetamine;

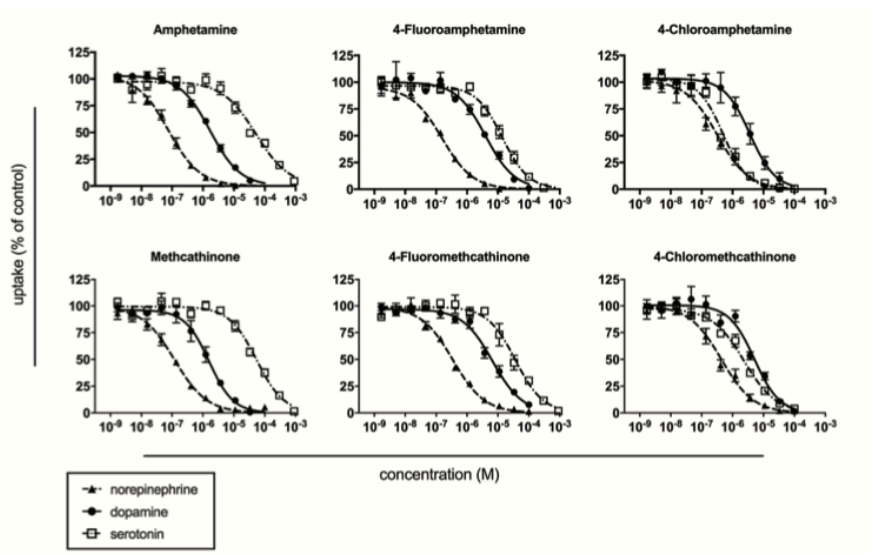

FIGURE 2 | Monoamine uptake inhibition in stably transfected HEK 293 cells that expressed the human NET, DAT, or SERT. Curves were fitted by non-linear regression, and corresponding IC_{50} values are shown in **Table 1**. The data are presented as the mean ± SEM of three experiments performed in triplicate.

TABLE 1 | Monoamine uptake inhibition.

	NET IC_{50} (μM)	DAT IC_{50} (μM)	SERT IC_{50} (μM)	DAT/SERT ratio
Amphetamine	0.078 (0.053–0.113)	1.7 (1.4–2.0)	51 (38–68)	30 (19–49)
4-Fluoroamphetamine	0.15 (0.12–0.21)	3.9 (2.6–5.8)	14 (11–17)	3.6 (1.9–6.5)
4-Chloroamphetamine	0.32 (0.20–0.51)	3.6 (2.6–5.1)	0.49 (0.37–0.65)	0.14 (0.07–0.25)
Methcathinone	0.12 (0.08–0.17)	1.6 (1.2–2.1)	54 (43–68)	34 (20–57)
4-Fluoromethcathinone	0.35 (0.26–0.46)	6.6 (5.2–8.4)	37 (28–49)	5.6 (3.3–9.4)
4-Chloromethcathinone	0.43 (0.30–0.62)	5.1 (3.6–7.2)	2.3 (1.8–3.0)	0.45 (0.25–0.83)

Values are means and 95% confidence intervals (CI). DAT/SERT ratio = 1/DAT IC_{50}: 1/SERT IC_{50}.

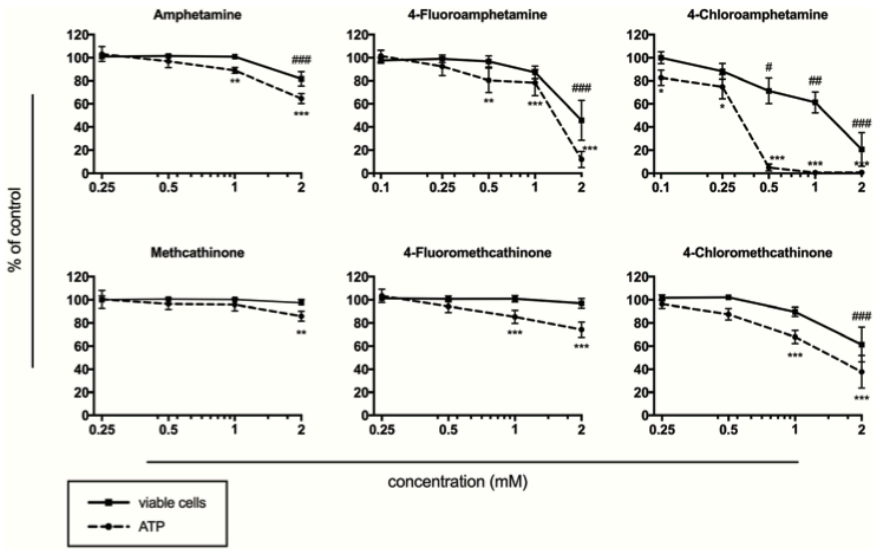

FIGURE 3 | Intracellular ATP content and viable cells expressed by maintained cell membrane integrity after drug exposure of HepG2 cells for 24 h. Data are expressed as mean ± SEM, and numbers in parentheses indicate the number of individual experiments performed in triplicate: amphetamine (4), 4-fluoroamphetamine (7), 4-chloroamphetamine (4), methcathinone (4), 4-fluoromethcathinone (4), and 4-chloromethcathinone (4). Significance levels are given as $^{*}p < 0.05$, $^{**}p < 0.01$, $^{***}p < 0.001$ (ATP content); $\#p < 0.05$, $\#\#p < 0.01$, $\#\#\#p < 0.001$ (viable cells).

at 0.5 mM for 4-fluoroamphetamine; at 1 mM for amphetamine, 4-fluoromethcathinone, and 4-chloromethcathinone; and at 2 mM for methcathinone (**Figure 3**). 4-Chloroamphetamine disrupted the cell membrane at 0.5 mM, whereas amphetamine, 4-fluoroamphetamine, and 4-chloromethcathinone caused significant cell membrane integrity loss at 2 mM (**Figure 3**). No cell membrane integrity loss was observed after 24 h exposure of HepG2 cells to methcathinone and 4-fluoromethcathinone at concentrations up to 2 mM.

Cellular Oxygen Consumption

The effect of halogenated amphetamine and methcathinone derivatives on cellular respiration is shown in **Figure 4**. Amphetamine and its *para*-halogenated derivatives decreased basal respiration in the range of 0.1–2 mM. 4-Fluoroamphetamine and 4-chloroamphetamine additionally decreased the maximal respiratory capacity at 1 and 0.1 mM, respectively. 4-Chloromethcathinone decreased maximal respiration at 1 mM and showed signs of uncoupling of cellular respiration from ATP synthesis at the same concentration. Methcathinone and 4-fluoromethcathinone did not disrupt cellular respiration in the investigated concentration range (≤2 mM).

Oxidative Stress

All test compounds induced a concentration-dependent increase in mitochondrial superoxide (**Figure 5**). A significant increase in mitochondrial superoxide was observed at 0.5 mM for 4-chloroamphetamine, at 1 mM for 4-fluoroamphetamine and 4-chloromethcathinone, and at 2 mM for amphetamine, methcathinone, and 4-fluoromethcathinone.

Mechanisms of Cell Death

The proportion of viable, apoptotic, and necrotic cells after treatment with the test drugs is shown in **Figure 6**. Using annexin V staining, a significant reduction in cell viability was observed for 4-fluoramphetamine and 4-chloromethcathinone starting at 1 mM and for 4-chloroamphetamine at 0.5 mM. Amphetamine, methcathinone, and 4-fluoromethcathinone did

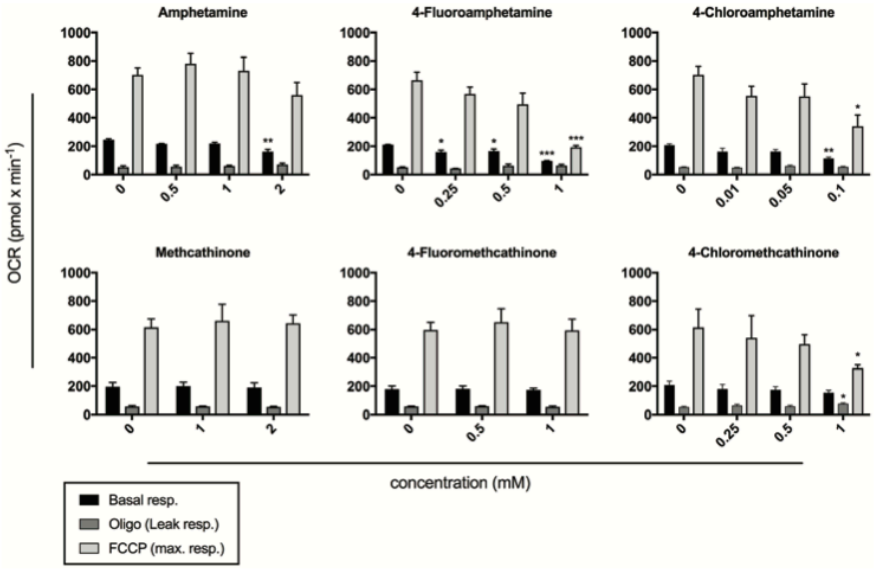

FIGURE 4 | Oxygen consumption rate (OCR) in HepG2 cells after drug exposure for 24 h. Basal respiration, leak respiration, and maximal respiration are expressed as mean ± SEM adjusted to protein content. Numbers in parentheses indicate the number of individual experiments performed in triplicate: amphetamine (3), 4-fluoroamphetamine (3), 4-chloroamphetamine (5), methcathinone (5), 4-fluoromethcathinone (5), and 4-chloromethcathinone (4). Significance levels are given as $^{*}p < 0.05$, $^{**}p < 0.01$, $^{***}p < 0.001$.

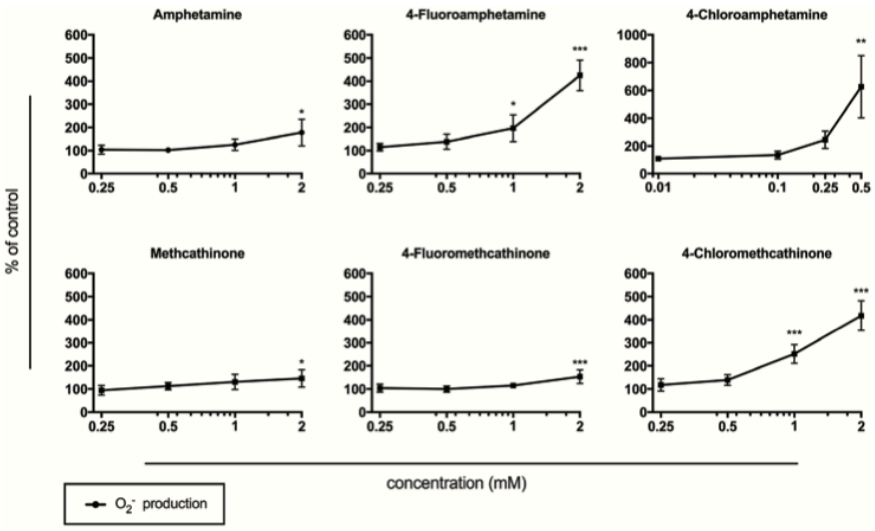

FIGURE 5 | Mitochondrial superoxide production in HepG2 cells after drug exposure for 24 h. Data are expressed as mean ± SEM adjusted to protein content. Numbers in parentheses indicate the number of individual experiments performed in triplicate: amphetamine (5), 4-fluoroamphetamine (4), 4-chloroamphetamine (3), methcathinone (5), 4-fluoromethcathinone (4), and 4-chloromethcathinone (3). Significance levels are given as $^{*}p < 0.05$, $^{**}p < 0.01$, $^{***}p < 0.001$.

not decrease cell viability at 2 mM. Apoptosis was the main mechanism of death for HepG2 cells treated with 4-fluoroamphetamine and 4-chloromethcathinone, whereas the majority of cells treated with 0.5 mM 4-chloroamphetamine underwent necrosis.

DISCUSSION

Pharmacological Perspective

Para-substituted amphetamines and methcathinones are monoamine transporter substrates (Rickli et al., 2015), elevating extracellular

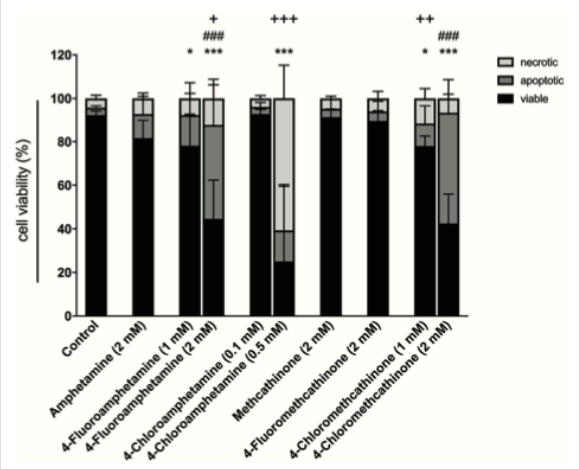

FIGURE 6 | Mechanisms of cell death in HepG2 cells after drug exposure for 24 h. Data are expressed as mean ± SEM, and numbers in parentheses indicate the number of individual experiments: amphetamine (7), 4-fluoroamphetamine (8), 4-chloroamphetamine (4), methcathinone (7), 4-fluoromethcathinone (7), and 4-chloromethcathinone (7). Significance levels are given as $^{*}p < 0.05$, $^{***}p < 0.001$ (viable cells); $\#\#\#p < 0.001$ (apoptotic cells); $+p < 0.05$, $++p < 0.01$, $+++p < 0.001$ (necrotic cells).

monoamine levels by inducing an efflux through reverse transport of the transporters (Rothman and Baumann, 2003; Sitte and Freissmuth, 2015). This subsequently results in inhibition of the monoamine uptake transport from the synaptic cleft.

Norepinephrine uptake inhibition was observed at submicromolar concentrations for all substances, and all compounds additionally inhibited the uptake of at least one other monoamine at low micromolar concentrations. As reported previously (Baumann et al., 2011; Simmler et al., 2014; Rickli et al., 2015; Suyama et al., 2016), *para*-halogenation reduced the selectivity for DAT over SERT, which is associated with a decreased abuse liability for amphetamine-type substances (Ritz et al., 1987; Kuhar et al., 1991; Baumann et al., 2000; Wee et al., 2005; Wee and Woolverton, 2006). *Para*-chlorination of amphetamine and methcathinone seems to reduce the selectivity for DAT over SERT in a similar manner as *para*-methylation (Luethi et al., 2018b). NET and DAT inhibition correlates with human effective doses, and SERT inhibition inversely correlates with human effective doses (Luethi and Liechti, 2018), indicating lower clinical potency for the halogenated amphetamine and methcathinone derivatives. However, the highly potent serotonergic activity coupled with considerably potent dopaminergic activity may explain the severe serotonergic neurotoxicity of 4-chloroamphetamine (Johnson et al., 1990). Currently, the neurotoxic potential of the corresponding methcathinone analog 4-chloromethcathinone is not well investigated.

Toxicological Perspective

Amphetamine-type stimulant-induced organ damage is multifaceted and so far not completely understood (Carvalho et al., 2012). The amphetamines and methcathinones investigated in this study potently interacted with monoaminergic systems, which regulate body temperature in a variety of ways (Docherty and Green, 2010). Thus, hyperthermia is a possible consequence of the use of these substances, which can rarely lead to potentially fatal complications such as rhabdomyolysis, acute renal failure, acidosis, or multiple organ failure including the liver (Kendrick et al., 1977; Henry, 1992; Kalant, 2001). In addition to systemic causes of organ damage, the results of this study suggest that direct cellular mechanisms of halogenated amphetamines and methcathinones may contribute to liver and probably other organ toxicity. As observed in other studies (Dias da Silva et al., 2013, 2015; Luethi et al., 2017), HepG2 cells proved to be a robust cell model with low susceptibility to stimulant toxicity, allowing the investigation of cellular mechanisms of toxicity in the absence of cell death (Kamalian et al., 2015). The drug concentrations used were therefore mostly outside of the pharmacologically relevant range. However, concentrations inducing toxic effects may be lower in primary cells (Gerets et al., 2012), and the toxic effects of stimulants may be enhanced by elevated temperature (Valente et al., 2016). With limited diffusion across the cell membrane under physiological conditions, amphetamine and structurally related compounds require active transport to enter cells (Freyberg et al., 2016). However, as monoamine transporters are mainly expressed in the brain (Kristensen et al., 2011), amphetamine-type drug uptake into the liver likely relies on other transporters. A previous study of the gene expression for various transporters revealed substantially decreased overall transporter expression in HepG2 cells compared to human liver tissue (Hilgendorf et al., 2007). This may be one of the reasons why these cells are more resistant to amphetamine-type drug toxicity. Therefore, reduced transporter expression in HepG2 cells may be one compared to primary cells. Therefore, even though this study provides information on possible cellular mechanisms that could contribute to clinical toxicity in stimulant users, it does not provide precise information about the toxic concentration range. Furthermore, organ-toxic drug levels and mechanisms of toxicity may vary considerably between users. For example, case reports of liver damage associated with the amphetamine derivative 3,4-methylenedioxymethamphetamine (MDMA) do not indicate strictly dose-dependent hepatotoxicity (Ellis et al., 1996). The present study therefore demonstrates underlying cellular mechanisms that may contribute to clinical toxicity in susceptible drug users. Both *para*-fluorination and *para*-chlorination increased the cytotoxicity of amphetamine and methcathinone, with a higher toxicity observed for amphetamines compared to the corresponding methcathinones. For all substances, a decrease in cellular ATP preceded the loss in cell membrane integrity, which points out the possibility of mitochondrial impairment. A more detailed investigation of the mitochondrial respiration revealed that the investigated amphetamines in fact interfered with mitochondrial function by decreasing basal respiration. In addition, both halogenated amphetamine derivatives additionally decreased the maximal respiratory capacity of HepG2 cells. While methcathinone and 4-fluoromethcathinone did not significantly alter cellular respiration, a decrease in the maximal respiration was observed for 4-chloromethcathinone. Furthermore, 4-chloromethcathinone

was the only compound to uncouple cellular respiration from ATP synthesis. Such uncoupling properties have previously been observed for the structurally similar fluorinated cathinone derivative bupropion (Luethi et al., 2017). Disruption of the mitochondrial respiratory chain is associated with increased ROS levels, with the enzyme complex I and III as potential sites for ROS generation (Votyakova and Reynolds, 2001; Antico Arciuch et al., 2012; Dröse and Brandt, 2012). Increased ROS levels may subsequently elicit toxicity by causing damage to various cellular components. A concentration-dependent increase in ROS was observed in HepG2 cells after treatment with all investigated compounds, which may be explained by the disruption of the mitochondrial electron transport chain. Additionally, impairment of the cellular antioxidant response could contribute to increased ROS levels; this was, however, not investigated in this study. Investigations of cell death revealed a concentration-dependent increase in apoptotic cells after treatment with 4-fluoroamphetamine and 4-chloromethcathinone; a concentration-dependent increase in necrotic cells was observed after treatment with 4-chloroamphetamine. These observations are consistent with the notion that ATP levels are a determinant of manifestation of cell death (Eguchi et al., 1997). As shown in this study, a decrease in ATP after 4-chloroamphetamine treatment is much more distinct when compared to the other compounds. At 0.5 mM, treatment with 4-chloroamphetamine caused an almost complete ATP depletion, explaining the high amount of necrotic cells at this concentration. The amount of necrotic and apoptotic cells after treatment with 2 mM amphetamine, methcathinone, and 4-fluoromethcathinone did not significantly differ from control incubations. As no concentrations higher than 2 mM were investigated in this study, no predictions about the amount of necrotic and apoptotic cells at higher concentrations or about dose-dependency can be made.

The investigations of this study were restricted to *para*-halogenated derivatives of amphetamine and methcathinone. Whether *ortho*- or *meta*-halogenation results similarly in increased hepatocellular toxicity remains to be investigated in a future study.

CONCLUSION

All investigated compounds inhibited norepinephrine uptake at submicromolar concentrations and dopamine uptake at low micromolar concentrations. In addition, *para*-fluorination and *para*-chlorination increased the potential to inhibit serotonin uptake, which could result in severe serotonergic neurotoxicity. In comparison to the non-halogenated compounds, *para*-halogenation of amphetamine and methcathinone furthermore increased the cytotoxicity of the respective derivatives in HepG2 cells. The results of this study suggest mitochondrial toxicity for amphetamine and its halogenated derivatives as well as for 4-chloromethcathinone. Methcathinone and 4-fluoromethcathinone may potentially disrupt mitochondrial function as well; however, this was not observed at investigated concentrations in this study (≤2 mM). The potent monoamine transporter inhibition potential of the substances indicates that adverse effects are most likely linked to sympathomimetic toxicity, which is consistent with clinical intoxication reports (Knippels et al., 2017; Wijers et al., 2017; Hondebrink et al., 2018). Direct cellular mechanisms, such as mitochondrial toxicity, may, however, additionally play a contributory role in susceptible users.

AUTHOR CONTRIBUTIONS

DL, SK, and ML designed the research. DL, MW, XZ, and DR conducted the research. DL, DR, SK, and ML analyzed the data. DL, SK, and ML wrote the manuscript with significant input from all the other authors.

FUNDING

This work was supported by the Federal Office of Public Health (grant no. 16.921318 to ML) and the Swiss National Science Foundation (grant no. 31003A_156270 to SK).

REFERENCES

Antico Arciuch, V. G., Elguero, M. E., Poderoso, J. J., and Carreras, M. C. (2012). Mitochondrial regulation of cell cycle and proliferation. *Antioxid. Redox Signal.* 16, 1150–1180. doi: 10.1089/ars.2011.4085

Baumann, M. H., Ayestas, M. A., Dersch, C. M., Brockington, A., Rice, K. C., and Rothman, R. B. (2000). Effects of phentermine and fenfluramine on extracellular dopamine and serotonin in rat nucleus accumbens: therapeutic implications. *Synapse* 36, 102–113.

Baumann, M. H., Clark, R. D., Woolverton, W. L., Wee, S., Blough, B. E., and Rothman, R. B. (2011). *In vivo* effects of amphetamine analogs reveal evidence for serotonergic inhibition of mesolimbic dopamine transmission in the rat. *J. Pharmacol. Exp. Ther.* 337, 218–225. doi: 10.1124/jpet.110.176271

Brandt, S. D., Sumnall, H. R., Measham, F., and Cole, J. (2010). Analyses of second-generation 'legal highs' in the UK: initial findings. *Drug Test. Anal.* 2, 377–382. doi: 10.1002/dta.155

Carvalho, M., Carmo, H., Costa, V. M., Capela, J. P., Pontes, H., Remiao, F., et al. (2012). Toxicity of amphetamines: an update. *Arch. Toxicol.* 86, 1167–1231. doi: 10.1007/s00204-012-0815-5

Colado, M. I., Murray, T. K., and Green, A. R. (1993). 5-HT loss in rat brain following 3,4-methylenedioxymethamphetamine (MDMA), p-chloroamphetamine and fenfluramine administration and effects of chlormethiazole and dizocilpine. *Br. J. Pharmacol.* 108, 583–589. doi: 10.1111/j.1476-5381.1993.tb12846.x

Dias da Silva, D., Arbo, M. D., Valente, M. J., Bastos, M. L., and Carmo, H. (2015). Hepatotoxicity of piperazine designer drugs: comparison of different *in vitro* models. *Toxicol. in vitro* 29, 987–996. doi: 10.1016/j.tiv.2015.04.001

Dias da Silva, D., Carmo, H., Lynch, A., and Silva, E. (2013). An insight into the hepatocellular death induced by amphetamines, individually and in combination: the involvement of necrosis and apoptosis. *Arch. Toxicol.* 87, 2165–2185. doi: 10.1007/s00204-013-1082-9

Docherty, J. R., and Green, A. R. (2010). The role of monoamines in the changes in body temperature induced by 3,4-methylenedioxymethamphetamine (MDMA, ecstasy) and its derivatives. *Br. J. Pharmacol.* 160, 1029–1044. doi: 10.1111/j.1476-5381.2010.00722.x

Dröse, S., and Brandt, U. (2012). Molecular mechanisms of superoxide production by the mitochondrial respiratory chain. *Adv. Exp. Med. Biol.* 748, 145–169. doi: 10.1007/978-1-4614-3573-0_6

Eguchi, Y., Shimizu, S., and Tsujimoto, Y. (1997). Intracellular ATP levels determine cell death fate by apoptosis or necrosis. *Cancer Res.* 57, 1835–1840.

Ellis, A. J., Wendon, J. A., Portmann, B., and Williams, R. (1996). Acute liver damage and ecstasy ingestion. *Gut* 38, 454–458. doi: 10.1136/gut.38.3.454

Freyberg, Z., Sonders, M. S., Aguilar, J. I., Hiranita, T., Karam, C. S., Flores, J., et al. (2016). Mechanisms of amphetamine action illuminated through optical monitoring of dopamine synaptic vesicles in Drosophila brain. *Nat. Commun.* 7, 1–15. doi: 10.1038/ncomms10652

Fuller, R. W. (1992). Effects of *p*-chloroamphetamine on brain serotonin neurons. *Neurochem. Res.* 17, 449–456. doi: 10.1007/BF00969891

Gerets, H. H., Tilmant, K., Gerin, B., Chanteux, H., Depelchin, B. O., Dhalluin, S., et al. (2012). Characterization of primary human hepatocytes, HepG2 cells, and HepaRG cells at the mRNA level and CYP activity in response to inducers and their predictivity for the detection of human hepatotoxins. *Cell Biol. Toxicol.* 28, 69–87. doi: 10.1007/s10565-011-9208-4

Grifell, M., Ventura, M., Carbon, X., Quintana, P., Galindo, L., Palma, A., et al. (2017). Patterns of use and toxicity of new *para*-halogenated substituted cathinones: 4-CMC (clephedrone), 4-CEC (4-chloroethcatinone) and 4-BMC (brephedrone). *Hum. Psychopharmacol.* 32, 1–9. doi: 10.1002/hup.2621

Henry, J. A. (1992). Ecstasy and the dance of death. *BMJ* 305, 5–6. doi: 10.1136/bmj.305.6844.5

Hilgendorf, C., Ahlin, G., Seithel, A., Artursson, P., Ungell, A. L., and Karlsson, J. (2007). Expression of thirty-six drug transporter genes in human intestine, liver, kidney, and organotypic cell lines. *Drug Metab. Dispos.* 35, 1333–1340. doi: 10.1124/dmd.107.014902

Hondebrink, L., Nugteren-Van Lonkhuyzen, J. J., Rietjens, S. J., Brunt, T. M., Venhuis, B., Soerdjbalie-Maikoe, V., et al. (2018). Fatalities, cerebral hemorrhage, and severe cardiovascular toxicity after exposure to the new psychoactive substance 4-fluoroamphetamine: a prospective cohort study. *Ann. Emerg. Med.* 71, 294–305. doi: 10.1016/j.annemergmed.2017.07.482

Johnson, M. P., Huang, X. M., Oberlender, R., Nash, J. F., and Nichols, D. E. (1990). Behavioral, biochemical and neurotoxicological actions of the alpha-ethyl homologue of p-chloroamphetamine. *Eur. J. Pharmacol.* 191, 1–10. doi: 10.1016/0014-2999(90)94090-K

Kalant, H. (2001). The pharmacology and toxicology of "ecstasy" (MDMA) and related drugs. *CMAJ* 165, 917–928.

Kamalian, L., Chadwick, A. E., Bayliss, M., French, N. S., Monshouwer, M., Snoeys, J., et al. (2015). The utility of HepG2 cells to identify direct mitochondrial dysfunction in the absence of cell death. *Toxicol. in vitro* 29, 732–740. doi: 10.1016/j.tiv.2015.02.011

Kendrick, W. C., Hull, A. R., and Knochel, J. P. (1977). Rhabdomyolysis and shock after intravenous amphetamine administration. *Ann. Intern. Med.* 86, 381–387. doi: 10.7326/0003-4819-86-4-381

Knippels, M. C. J., Essers, I. M. M., Magdelijns, F. J. H., and Van Twist, D. J. L. (2017). 'Ecstasy-light' - not as light as its name suggests: toxic effects of 4-fluoroamphetamine. *Ned. Tijdschr. Geneeskd.* 161, 1–3.

Kristensen, A. S., Andersen, J., Jorgensen, T. N., Sorensen, L., Eriksen, J., Loland, C. J., et al. (2011). SLC6 neurotransmitter transporters: structure, function, and regulation. *Pharmacol. Rev.* 63, 585–640. doi: 10.1124/pr.108.000869

Kuhar, M. J., Ritz, M. C., and Boja, J. W. (1991). The dopamine hypothesis of the reinforcing properties of cocaine. *Trends Neurosci.* 14, 299–302. doi: 10.1016/0166-2236(91)90141-G

Linsen, F., Koning, R. P., Van Laar, M., Niesink, R. J., Koeter, M. W., and Brunt, T. M. (2015). 4-Fluoroamphetamine in the Netherlands: more than a one-night stand. *Addiction* 110, 1138–1143. doi: 10.1111/add.12932

Luethi, D., Kaeser, P. J., Brandt, S. D., Krähenbühl, S., Hoener, M. C., and Liechti, M. E. (2018a). Pharmacological profile of methylphenidate-based designer drugs. *Neuropharmacology* 134, 133–140. doi: 10.1016/j.neuropharm.2017.08.020

Luethi, D., Kolaczynska, K. E., Docci, L., Krähenbühl, S., Hoener, M. C., and Liechti, M. E. (2018b). Pharmacological profile of mephedrone analogs and related new psychoactive substances. *Neuropharmacology* 134, 4–12. doi: 10.1016/j.neuropharm.2017.07.026

Luethi, D., and Liechti, M. E. (2018). Monoamine transporter and receptor interaction profiles *in vitro* predict reported human doses of novel psychoactive stimulants and psychedelics. *Int. J. Neuropsychopharmacol.* 21, 926–931. doi: 10.1093/ijnp/pyy047

Luethi, D., Liechti, M. E., and Krähenbühl, S. (2017). Mechanisms of hepatocellular toxicity associated with new psychoactive synthetic cathinones. *Toxicology* 387, 57–66. doi: 10.1016/j.tox.2017.06.004

Mayer, F. P., Burchardt, N. V., Decker, A. M., Partilla, J. S., Li, Y., Mclaughlin, G., et al. (2018). Fluorinated phenmetrazine "legal highs" act as substrates for high-affinity monoamine transporters of the SLC6 family. *Neuropharmacology* 134, 149–157. doi: 10.1016/j.neuropharm.2017.10.006

Miller, K. J., Anderholm, D. C., and Ames, M. M. (1986). Metabolic activation of the serotonergic neurotoxin *para*-chloroamphetamine to chemically reactive intermediates by hepatic and brain microsomal preparations. *Biochem. Pharmacol.* 35, 1737–1742. doi: 10.1016/0006-2952(86)90332-1

Odoardi, S., Romolo, F. S., and Strano-Rossi, S. (2016). A snapshot on NPS in Italy: distribution of drugs in seized materials analysed in an Italian forensic laboratory in the period 2013–2015. *Forensic Sci. Int.* 265, 116–120. doi: 10.1016/j.forsciint.2016.01.037

Rickli, A., Hoener, M. C., and Liechti, M. E. (2015). Monoamine transporter and receptor interaction profiles of novel psychoactive substances: *para*-halogenated amphetamines and pyrovalerone cathinones. *Eur. Neuropsychopharmacol.* 25, 365–376. doi: 10.1016/j.euroneuro.2014.12.012

Ritz, M. C., Lamb, R. J., Goldberg, S. R., and Kuhar, M. J. (1987). Cocaine receptors on dopamine transporters are related to self-administration of cocaine. *Science* 237, 1219–1223. doi: 10.1126/science.2820058

Rothman, R. B., and Baumann, M. H. (2003). Monoamine transporters and psychostimulant drugs. *Eur. J. Pharmacol.* 479, 23–40. doi: 10.1016/j.ejphar.2003.08.054

Simmler, L. D., Rickli, A., Hoener, M. C., and Liechti, M. E. (2014). Monoamine transporter and receptor interaction profiles of a new series of designer cathinones. *Neuropharmacology* 79, 152–160. doi: 10.1016/j.neuropharm.2013.11.008

Sitte, H. H., and Freissmuth, M. (2015). Amphetamines, new psychoactive drugs and the monoamine transporter cycle. *Trends Pharmacol. Sci.* 36, 41–50. doi: 10.1016/j.tips.2014.11.006

Suyama, J. A., Sakloth, F., Kolanos, R., Glennon, R. A., Lazenka, M. F., Negus, S. S., et al. (2016). Abuse-related neurochemical effects of *para*-substituted methcathinone analogs in rats: microdialysis studies of nucleus accumbens dopamine and serotonin. *J. Pharmacol. Exp. Ther.* 356, 182–190. doi: 10.1124/jpet.115.229559

Taschwer, M., Weiss, J. A., Kunert, O., and Schmid, M. G. (2014). Analysis and characterization of the novel psychoactive drug 4-chloromethcathinone (clephedrone). *Forensic Sci. Int.* 244, e56–e59. doi: 10.1016/j.forsciint.2014.09.007

Tatsumi, M., Groshan, K., Blakely, R. D., and Richelson, E. (1997). Pharmacological profile of antidepressants and related compounds at human monoamine transporters. *Eur. J. Pharmacol.* 340, 249–258. doi: 10.1016/S0014-2999(97)01393-9

Tomczak, E., Wozniak, M. K., Kata, M., Wiergowski, M., Szpiech, B., and Biziuk, M. (2018). Blood concentrations of a new psychoactive substance 4-chloromethcathinone (4-CMC) determined in 15 forensic cases. *Forensic Toxicol.* 36, 476–485. doi: 10.1007/s11419-018-0427-8

Valente, M. J., Araujo, A. M., Silva, R., Bastos Mde, L., Carvalho, F., Guedes De Pinho, P., et al. (2016). 3,4-Methylenedioxypyrovalerone (MDPV): *in vitro* mechanisms of hepatotoxicity under normothermic and hyperthermic conditions. *Arch. Toxicol.* 90, 1959–1973. doi: 10.1007/s00204-015-1653-z

Votyakova, T. V., and Reynolds, I. J. (2001). Deltapsi(m)-dependent and -independent production of reactive oxygen species by rat brain mitochondria. *J. Neurochem.* 79, 266–277. doi: 10.1046/j.1471-4159.2001.00548.x

Wee, S., Anderson, K. G., Baumann, M. H., Rothman, R. B., Blough, B. E., and Woolverton, W. L. (2005). Relationship between the serotonergic activity and reinforcing effects of a series of amphetamine analogs. *J. Pharmacol. Exp. Ther.* 313, 848–854. doi: 10.1124/jpet.104.080101

Wee, S., and Woolverton, W. L. (2006). Self-administration of mixtures of fenfluramine and amphetamine by rhesus monkeys. *Pharmacol. Biochem. Behav.* 84, 337–343. doi: 10.1016/j.pbb.2006.05.022

Wijers, C. H., Van Litsenburg, R. T., Hondebrink, L., Niesink, R. J., and Croes, E. A. (2017). Acute toxic effects related to 4-fluoroamphetamine. *Lancet* 389:600. doi: 10.1016/S0140-6736(17)30281-7

Conflict of Interest Statement: The authors declare that the research was conducted in the absence of any commercial or financial relationships that could be construed as a potential conflict of interest.

3. Paper 3

Para-halogenation of Amphetamine and Methcathinone Increases the Mitochondrial Toxicity in Undifferentiated and Differentiated SH-SY5Y Cells

In this paper, we investigated the mitochondrial toxicity of amphetamine, 4-FA, PCA, methcathinone, 4-FMC and 4-CMC in undifferentiated and differentiated SH-SY5Y cells.

International Journal of
Molecular Sciences

MDPI

Article

Para-Halogenation of Amphetamine and Methcathinone Increases the Mitochondrial Toxicity in Undifferentiated and Differentiated SH-SY5Y Cells

Xun Zhou [1,2], Jamal Bouitbir [1,2,3], Matthias E. Liechti [1,2], Stephan Krähenbühl [1,2,3,*] and Riccardo V. Mancuso [1,2]

1 Division of Clinical Pharmacology & Toxicology, University Hospital Basel, 4031 Basel, Switzerland; xun.zhou@unibas.ch (X.Z.); jamal.bouitbir@unibas.ch (J.B.); matthias.liechti@usb.ch (M.E.L.); riccardo.mancuso@unibas.ch (R.V.M.)
2 Department of Biomedicine, University of Basel, 4031 Basel, Switzerland
3 Swiss Centre for Applied Human Toxicology, 4031 Basel, Switzerland
* Correspondence: stephan.kraehenbuehl@usb.ch; Tel.: +41-61-265-4715

Received: 14 March 2020; Accepted: 15 April 2020; Published: 18 April 2020

Abstract: Halogenation of amphetamines and methcathinones has become a common method to obtain novel psychoactive substances (NPS) also called "legal highs". The *para*-halogenated derivatives of amphetamine and methcathinone are available over the internet and have entered the illicit drug market but studies on their potential neurotoxic effects are rare. The primary aim of this study was to explore the neurotoxicity of amphetamine, methcathinone and their *para*-halogenated derivatives 4-fluoroamphetamine (4-FA), 4-chloroamphetamine (PCA), 4-fluoromethcathinone (4-FMC), and 4-chloromethcathinone (4-CMC) in undifferentiated and differentiated SH-SY5Y cells. We found that 4-FA, PCA, and 4-CMC were cytotoxic (decrease in cellular ATP and plasma membrane damage) for both cell types, whereby differentiated cells were less sensitive. IC_{50} values for cellular ATP depletion were in the range of 1.4 mM for 4-FA, 0.4 mM for PCA and 1.4 mM for 4-CMC. The rank of cytotoxicity observed for the *para*-substituents was chloride > fluoride > hydrogen for both amphetamines and cathinones. Each of 4-FA, PCA and 4-CMC decreased the mitochondrial membrane potential in both cell types, and PCA and 4-CMC impaired the function of the electron transport chain of mitochondria in SH-SY5Y cells. 4-FA, PCA, and 4-CMC increased the ROS level and PCA and 4-CMC induced apoptosis by the endogenous pathway. In conclusion, *para*-halogenation of amphetamine and methcathinone increases their neurotoxic properties due to the impairment of mitochondrial function and induction of apoptosis. Although the cytotoxic concentrations were higher than those needed for pharmacological activity, the current findings may be important regarding the uncontrolled recreational use of these compounds.

Keywords: amphetamine; methcathinone; mitochondria; neurotoxicity; *para*-halogenation

1. Introduction

Amphetamine is a potent central nervous system (CNS) stimulant, which is or has been used for the treatment of attention deficit hyperactivity disorder (ADHD), narcolepsy, and body weight control under restricted medical prescription [1]. The predominant pharmacological action of amphetamine is to promote the release from [2] and inhibition of the reuptake of catecholamines into presynaptic nerve terminals [3], causing an increase in the catecholamine concentration in the synaptic clefts of mainly dopaminergic and noradrenergic neurons. A series of structurally similar psychoactive substances were derived from amphetamine after 1877 when it was first synthesized. Methcathinone, an amphetamine derivative, is currently used widely as a recreational drug [4]. Since amphetamine and

methcathinone are illicit for recreational use in most countries, many derivatives of these compounds were synthesized as novel psychoactive substances (NPS) and labeled "legal highs" [5]. Halogenation has been recognized as a possible method to create "legal highs" form amphetamine and derivatives [6], and as a method to enhance their membrane binding and permeation characteristics [7]. Many reports have documented how halogenated amphetamine derivatives such as 4-chloroamphetamine (PCA, also called *para*-chloroamphetamine; 4-CA), 4-fluoroamphetamine (4-FA), and methcathinone derivatives such as 4-chloromethcathinone (4-CMC) and 4-fluoromethcathinone (4-FMC) have lately reached the market (Figure S1) [8–12].

However, halogenation also has the potential to increase the toxicity of the original compounds [13]. It is well known that the brain, skeletal muscle, and the liver are the most important target organs of the toxicity of psychoactive substances [14]. Accordingly, the use of amphetamines and methcathinones can lead to the impairment of cognitive function, addiction, convulsions, rhabdomyolysis and acute liver failure [15–17]. Our previous research has shown that the *para*-halogenated derivatives of amphetamine and methcathinone caused hepatotoxicity [18] and myotoxicity [19] mainly by impairing mitochondrial function due to disruption of the mitochondrial respiratory chain, which is associated with an increase in the intracellular level of reactive oxygen species (ROS).

To date, systematic toxicological investigations of the *para*-halogenated derivatives of amphetamine and methcathinone in human neuron-like cells are missing. Based on these considerations, the aim of the current study was to investigate the in vitro mechanisms causing neurotoxicity of amphetamine, 4-FA, PCA, methcathinone, 4-FMC, and 4-CMC, using the well-established SH-SY5Y cell model in the differentiated and undifferentiated states [20–22].

2. Results

2.1. Cell Differentiation

As the first step in our study, we validated our protocol of differentiation of SH-SY5Y cells by immunohistofluorescence (Figure S2). Microtubule-associated protein 2 (MAP2) and neurofilament heavy polypeptide (NF-H) are well-known markers of differentiation of SH-SY5Y cells [20]. In undifferentiated SH-SY5Y cells, MAP2 was distributed strongly within the perinuclear area, but weakly in the neurites, and the expression of NF-H was restricted mainly to the cell soma (Figure S2A) [20]. Moreover, the neuritic processes were short and almost undetectable in undifferentiated cells. A different pattern of immunoreactivity and cell morphology was observed in ATRA/BDNF-differentiated SH-SY5Y cells (Figure S2B). MAP2 and NF-H expression was not only restricted to the cell soma but strongly present in the neurites as well, indicating the typical differentiation of SH-SY5Y cells to neuron-like cells. Finally, differentiated SH-SY5Y cells showed phenotypical characteristics of neurons, in particular a pyramidal body shape with longer projections, similar to dendrites and axons [22].

2.2. Cell Membrane Integrity and ATP Content

The release of adenylate kinase (AK) was measured as a marker for cell membrane integrity, and the intracellular ATP content was assessed to determine mitochondrial function (Figures 1 and 2, respectively). Undifferentiated and differentiated SH-SY5Y cells were treated with increasing concentrations of amphetamine, 4-FA, PCA, methcathinone, 4-FMC, and 4-CMC (see Figure S1 for the chemical structures of these compounds). All of these compounds were membrane toxic and decreased the intracellular ATP content in a concentration-dependent manner, with the exception of methcathinone and 4-FMC, which did not show any toxicity up to 2000 µM.

Int. J. Mol. Sci. **2020**, *21*, 2841

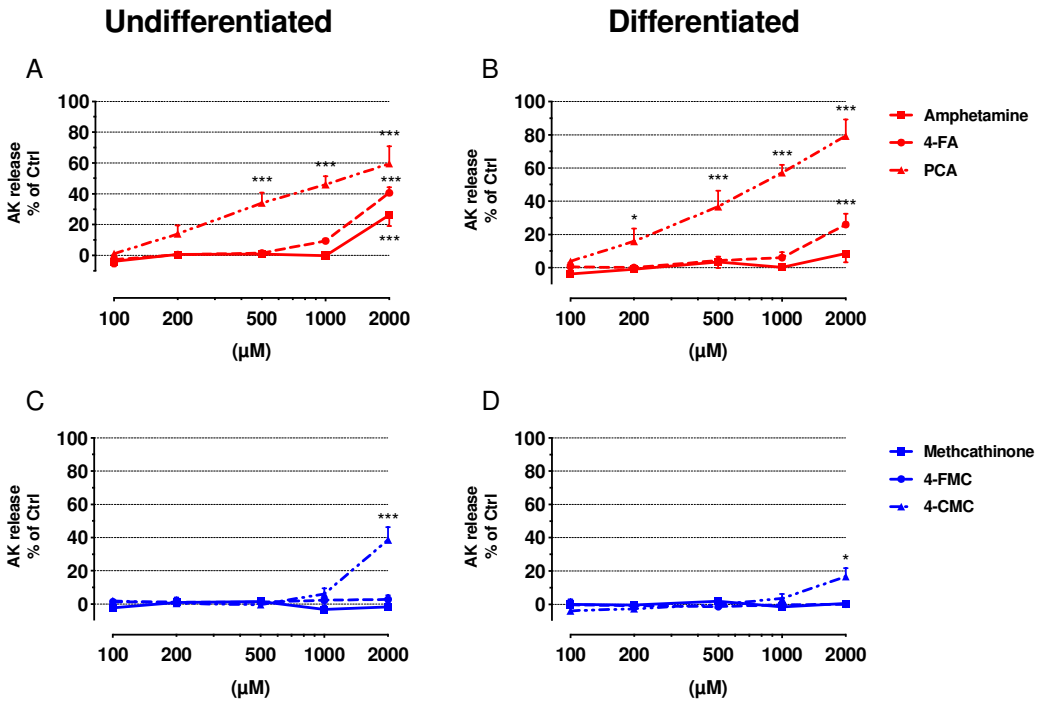

Figure 1. Plasma membrane integrity in undifferentiated and differentiated SH-SY5Y cells. (**A**)Undifferentiated and (**B**) differentiated SH-SY5Y cells were exposed to amphetamine, 4-FA and PCA for 24 h. (**C**) Undifferentiated and (**D**) differentiated SH-SY5Y cells were exposed to methcathinone, 4-FMC and 4-CMC for 24 h. Data are expressed as percentage of release of adenylate kinase (AK) compared to control (controls: DMSO 0.1% set as 0%, Triton X set as 100%). Data are expressed as mean ± SEM of eight independent experiments. Statistical differences were calculated with one-way ANOVA followed by the Dunnett's test, (*) $p \leq 0.05$ and (***) $p \leq 0.001$ versus 0.1% DMSO control.

The exposure of undifferentiated SH-SY5Y to amphetamine, 4-FA, and 4-CMC for 24 h was significantly membrane toxic at 2000 µM, whereas PCA was toxic already at 500 µM (Figure 1A,C). A similar pattern was observed in differentiated cells for 4-FA, PCA, and 4-CMC, but not for amphetamine (Figure 1B,D). Moreover, membrane toxicity of PCA in differentiated cells started already at 200 µM (Figure 1A,B). The intracellular ATP content started to decrease in undifferentiated cells at 200 µM for PCA, at 500 µM for 4-FA and 4-CMC, and at 1000 µM for amphetamine, whereas methcathinone and 4-FMC were not toxic up to 2000 µM (Figure 2A,C). In differentiated cells, only PCA (starting at 500 µM), 4-FA (starting at 1000 µM) and 4-CMC (starting at 1000 µM) were toxic, whereas amphetamine, methcathinone and 4-FMC did not significantly decrease the cellular ATP pool (Figure 2C,D). Table 1 presents the IC_{50} values of cellular membrane toxicity and ATP depletion for the compounds investigated. The values show a more pronounced effect regarding the diminution of the cellular ATP content as compared to the membrane toxicity, a pattern suggesting mitochondrial toxicity.

Table 1. Quantification (IC_{50}) of membrane toxicity (MT) and ATP depletion (ATP) by *para*-halogenated amphetamine (Amph) and methcathinone (MC) derivatives in undifferentiated (und), and differentiated (diff) SH-SY5Y cells.

Drug	**Amph**		**4-FA**		**PCA**		**MC**		**4-FMC**		**4-CMC**	
Cell	und	diff	und	diff	und	diff	und	diff	und	diff	und	diff
MT (IC_{50}) [mM]	>2	>2	>2	>2	1.17	0.77	>2	>2	>2	>2	>2	>2
ATP (IC_{50}) [mM]	>2	>2	1.44	1.41	0.42	0.39	>2	>2	>2	>2	1.43	1.33

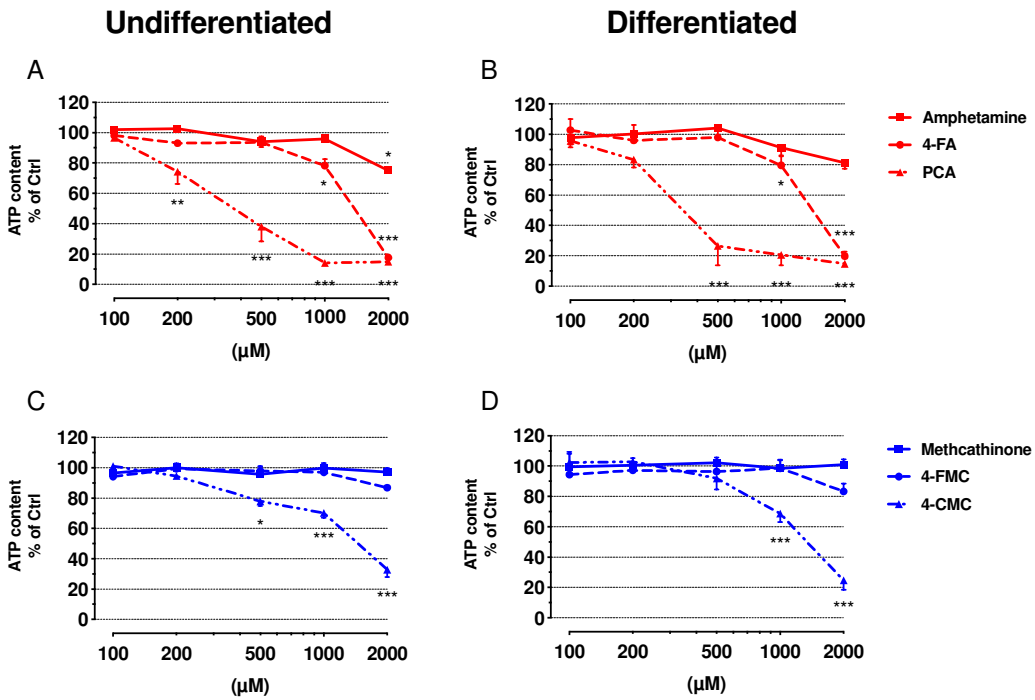

Figure 2. Intracellular ATP content in undifferentiated and differentiated SH-SY5Y cells. (**A**) Undifferentiated and (**B**) differentiated SH-SY5Y cells were exposed to amphetamine, 4-FA and PCA for 24 h. (**C**) Undifferentiated and (**D**) differentiated SH-SY5Y cells were exposed to methcathinone, 4-FMC and 4-CMC for 24 h. Data are expressed as percentage of ATP content compared to control (controls: DMSO 0.1% set as 100%, Triton X set as 0%. Data are expressed as mean ± SEM of eight independent experiments. Statistical differences were calculated with one-way ANOVA followed by the Dunnett's test, (*) $p \leq 0.05$, (**) $p \leq 0.01$ and (***) $p \leq 0.001$ versus 0.1% DMSO control.

2.3. Mitochondrial Membrane Potential

In order to confirm mitochondrial toxicity, we determined the mitochondrial membrane potential ($\Delta\psi_m$) using JC-1 staining. Mitochondrial toxicants have been shown to decrease the mitochondrial membrane potential in SH-SY5Y cells [23]. Each of 4-FA, PCA and 4-CMC decreased the $\Delta\psi_m$ in a concentration-dependent manner in both cell models (Figure 3A–D), whereas amphetamine, methcathinone and 4-FMC were not toxic up to 2000 µM. Similar to cytotoxicity, PCA was the most toxic compound investigated, starting to decrease $\Delta\psi_m$ at 500 µM in undifferentiated and at 200 µM in differentiated SH-SY5Y cells exposed for 24 h (Figure 3A,B). In comparison to the amphetamines, the methcathinones were less toxic.

These data confirmed our results obtained for the depletion of the cellular ATP content and indicated that 4-FA, PCA and 4-CMC are mitochondrial toxicants.

2.4. Cellular Oxygen Consumption

In order to understand the mechanism of mitochondrial toxicity, we determined the cellular oxygen consumption by SH-SY5Y cells having been exposed for 24 h to the test compounds using a Seahorse XF96 analyzer. After having obtained the basal respiration, oligomycin was injected to inhibit complex V allowing the determination of the leak respiration as a measure of the uncoupling of oxidative phosphorylation. This was followed by the addition of FCCP to obtain the maximal respiration and the complex I inhibitor rotenone to obtain the non-mitochondrial respiration. Basal respiration, leak respiration and maximal respiration are shown in Figure 4. As can be seen in all Figures (Figure 4A–L), FCCP did not stimulate basal respiration in differentiated and even inhibited basal respiration in undifferentiated cells. None of the drugs stimulated the leak respiration, suggesting

Int. J. Mol. Sci. **2020**, *21*, 2841

that there was no uncoupling of oxidative phosphorylation. PCA showed a concentration-dependent effect on basal respiration and respiration in the presence of FCCP in differentiated cells, reaching statistical significance at 100 µM (Figure 4F). In undifferentiated cells, the effect of PCA was not clearly concentration-dependent but reached statistical significance already at 50 µM (Figure 4E). Similarly, 4-CMC was toxic for undifferentiated and differentiated SH-SY5Y cells, reaching statistical significance for basal and stimulated respiration at 500 µM in undifferentiated (Figure 4K) and at 200 µM in differentiated SH-SY5Y cells (Figure 4L). A trend to decrease basal and stimulated respiration in both cell types with 4-FMC was shown, but without reaching significance up to 1000 µM (Figure 4I,J). In comparison, amphetamine, 4-FA, and methcathinone did not affect the oxidative metabolism of SH-SY5Y cells.

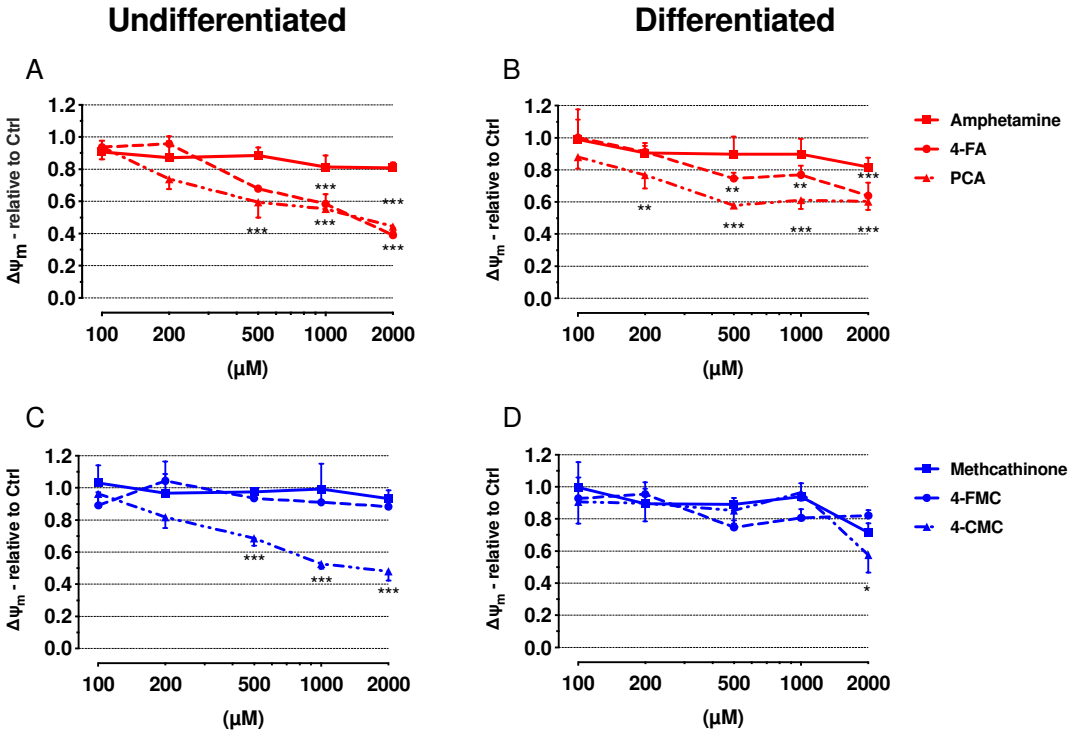

Figure 3. Mitochondrial membrane potential in undifferentiated and differentiated SH-SY5Y cells. Mitochondrial membrane potential was measured by JC-1 staining after exposure to drugs in undifferentiated and differentiated SH-SY5Y cells for 24 h. (**A**) Undifferentiated and (**B**) differentiated SH-SY5Y cells were exposed to amphetamine, 4-FA and PCA for 24 h. (**C**) Undifferentiated and (**D**) differentiated SH-SY5Y cells were exposed to methcathinone, 4-FMC and 4-CMC for 24 h. Data are expressed as mean ± SEM of five independent experiments. Statistical differences were calculated with one-way ANOVA followed by the Dunnett's test, (*) $p \leq 0.05$, (**) $p \leq 0.01$ and (***) $p \leq 0.001$ versus 0.1% DMSO control.

These data confirmed mitochondrial toxicity of PCA and 4-CMC, but not of 4-FA. They show that halogenation is critical for the toxicity of these compounds and that the addition of chlorine in the *p*-position is more toxic than fluoride.

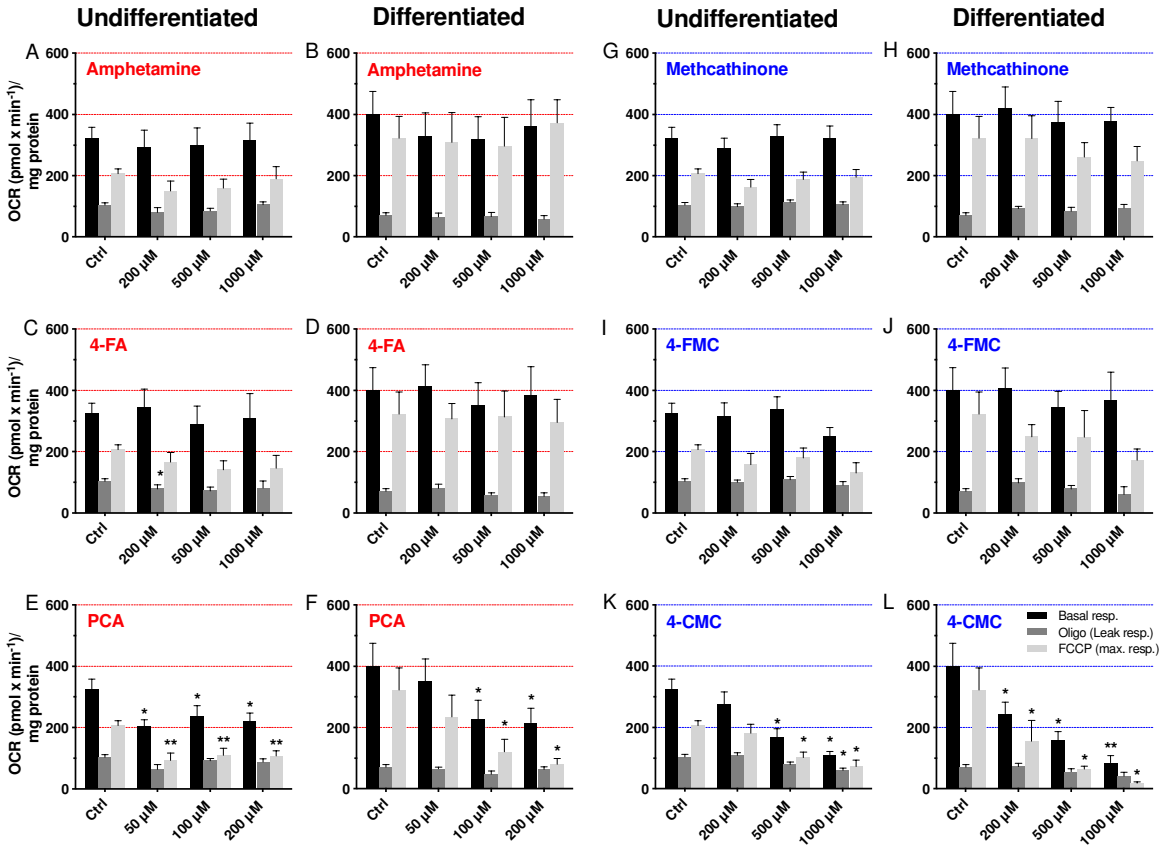

Figure 4. Oxygen consumption by undifferentiated and differentiated SH-SY5Y cells expressed as basal, leak, and maximal respiration. Undifferentiated and differentiated SH-SY5Y cells were exposed to (**A**,**B**) amphetamine, (**C**,**D**) 4-FA, (**E**,**F**) PCA, (**G**,**H**) methcathinone, (**I**,**J**) 4-FMC, and (**K**,**L**) 4-CMC for 24 h. Data are expressed as mean ± SEM of seven independent experiments. Statistical differences were calculated with one-way ANOVA followed by the Dunnett's test, (*) $p \leq 0.05$, (**) $p \leq 0.01$ versus 0.1% DMSO control.

2.5. Mitochondrial Superoxide Production

Toxicants inhibiting the function of the mitochondrial electron transport chain can increase the production of mitochondrial ROS [19,24]. Therefore, we determined mitochondrial production of the superoxide anion in undifferentiated and differentiated SH-SY5Y cells exposed to test drugs for 24 h (Figure 5).

In both undifferentiated and differentiated SH-SY5Y cells exposed to 4-FA, mitochondrial superoxide production started to increase at the highest concentration of 2000 µM (Figure 5A,B). Concerning PCA, only undifferentiated SH-SY5Y cells showed a significant increase of the cellular ROS content, which started at 500 µM (Figure 5A), whereas the differentiated cells were more resistant with a trend for an increase at 2000 µM (Figure 5B). The exposure to 4-CMC increased the superoxide anion content in both cell models starting at 2000 µM (Figure 5C,D). The other drugs investigated did not increase the mitochondrial superoxide production in the investigated concentration range (up to 2000 µM).

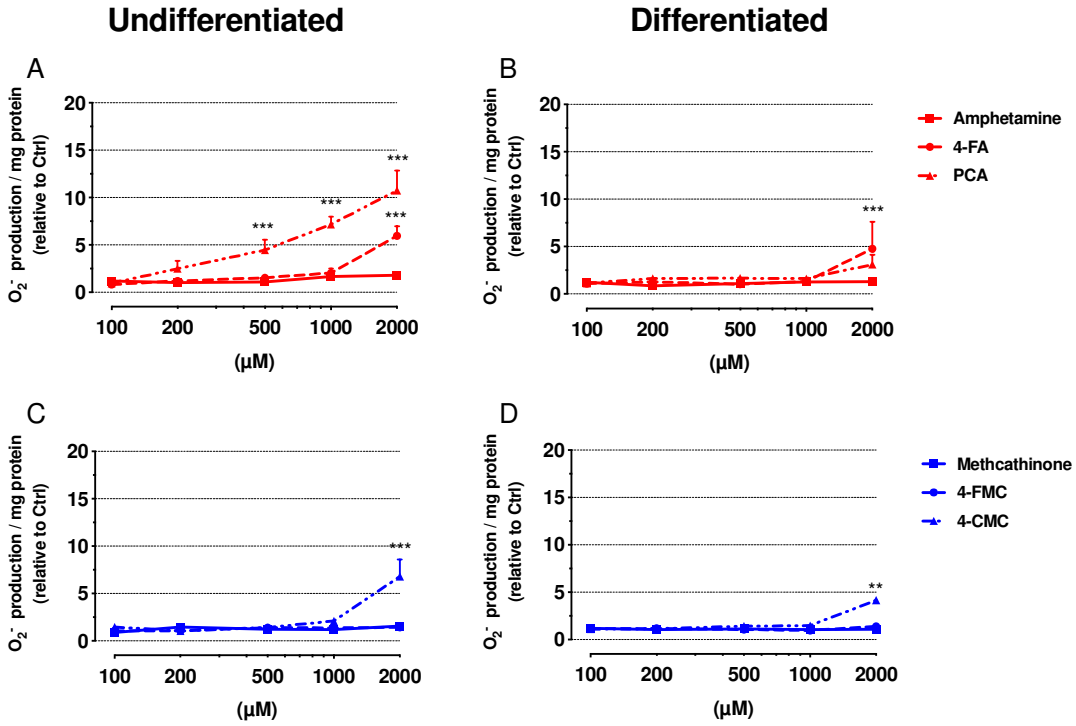

Figure 5. Mitochondrial superoxide accumulation was measured in undifferentiated and differentiated SH-SY5Y cells after exposure to drugs for 24 h. (**A**) Undifferentiated and (**B**) differentiated SH-SY5Y cells were exposed to amphetamine, 4-FA and PCA for 24 h. (**C**) Undifferentiated and (**D**) differentiated SH-SY5Y cells were exposed to methcathinone, 4-FMC and 4-CMC for 24 h. Data are expressed as mean ± SEM of five independent experiments. Statistical differences were calculated with one-way ANOVA followed by the Dunnett's test, (**) $p \leq 0.01$ and (***) $p \leq 0.001$ versus 0.1% DMSO control.

2.6. Mechanisms of Cell Death

When the mitochondrial damage becomes too large, cells undergo apoptosis or necrosis, depending on the cellular ATP content [25]. In order to investigate the mechanism of cell death, we assessed the externalization of phosphatidylserine by annexin V binding, and the permeability of the cell membrane to propidium iodide (PI), as markers of apoptosis and necrosis, respectively. H_2O_2 (500 µM) was used as a positive control (Figure 6) [26]. In undifferentiated SH-SY5Y cells exposed for 6 h, PCA increased necrosis starting at 200 µM, reaching statistical significance at 500 µM (Figure 6A). 4-CMC induced apoptosis starting at 1000 µM and reached statistical significance at 2000 µM. Similar to PCA, 4-FA also increased necrosis (starting at 2000 µM), whereas the other compounds did not induce apoptosis or necrosis up to 2000 µM. In differentiated SH-SY5Y cells, PCA induced necrosis starting at 100 µM, reaching statistical significance at 500 µM (Figure 6B). 4-CMC induced apoptosis starting at 500 µM, reaching statistical significance at 1000 µM, and necrosis starting at 2000 µM. 4-FA induced necrosis starting at 2000 µM, whereas the other compounds were ineffective. The shorter incubation time (6 h versus 24 h) was selected to focus on the early apoptosis phase rather than on necrosis.

To confirm the activation of apoptotic pathways and to find out the mechanism of activation, we assessed the activation of caspases 3 and 9 in the presence of 4-CMC at 6 h of incubation. We chose 4-CMC for these experiments, since only 4-CMC, and not PCA or 4-FA, induced apoptosis of SH-SY5Y cells at 6 h of incubation. Caspase 9 is activated in response to the intrinsic apoptotic pathway, whereas caspase 3 is an executioner caspase [27,28]. The intrinsic pathway can be defined as the mitochondrial pathway, since damaged mitochondria release cytochrome *c*, which activates caspase 9 [29]. To confirm that 4-CMC causes apoptosis and to assess by which pathway, we determined the expression of cleaved caspase 3 and 9 by immunoblotting after drug exposure for 6 h (Figure 7A,B) [30].

Int. J. Mol. Sci. **2020**, *21*, 2841

Amiodarone (50 µM) and MDMA (500 µM) were used as negative controls regarding the induction of apoptosis. As shown in Figure 7A, 2000 µM 4-CMC increased the abundance of cleaved caspase 3 in both undifferentiated and differentiated SH-SY5Y cells, confirming the results obtained with the annexin V assay. Moreover, 4-CMC increased the expression of cleaved caspase 9 at 2000 µM in both differentiated and undifferentiated SH-SY5Y cells (Figure 7B).

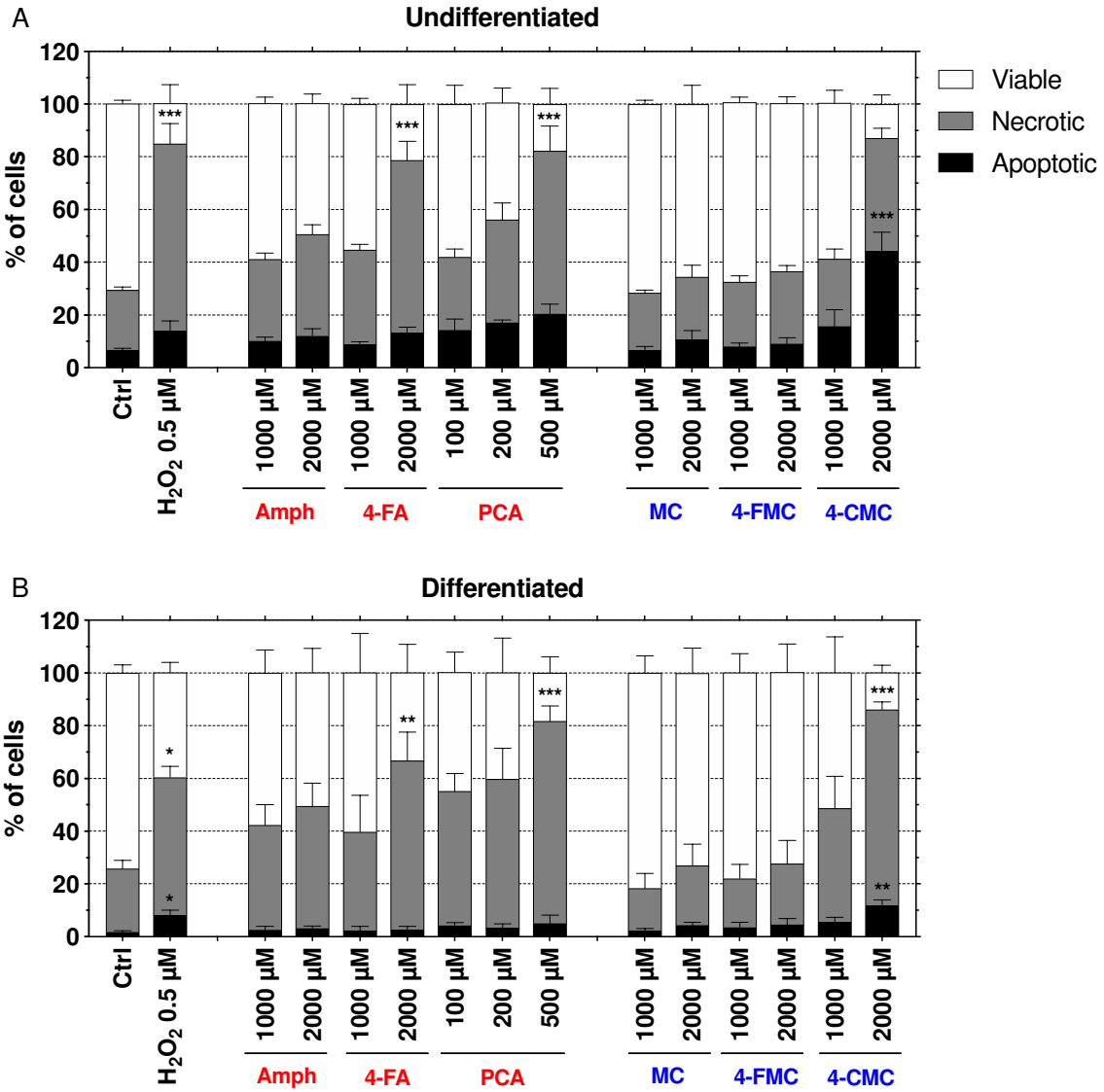

Figure 6. Mechanisms of cell death of undifferentiated and differentiated SH-SY5Y cells exposed to toxicants for 6 h. (**A**) Undifferentiated and (**B**) differentiated SH-SY5Y cells were exposed to amphetamine (Amph), 4-FA, PCA, methcathinone (MC), 4-FMC, and 4-CMC for 6 h. Data is expressed as mean ± SEM of six independent experiments. Statistical differences were calculated with one-way ANOVA followed by the Dunnett's test, (*) $p \leq 0.05$, (**) $p \leq 0.01$ and (***) $p \leq 0.001$ versus 0.1% DMSO control.

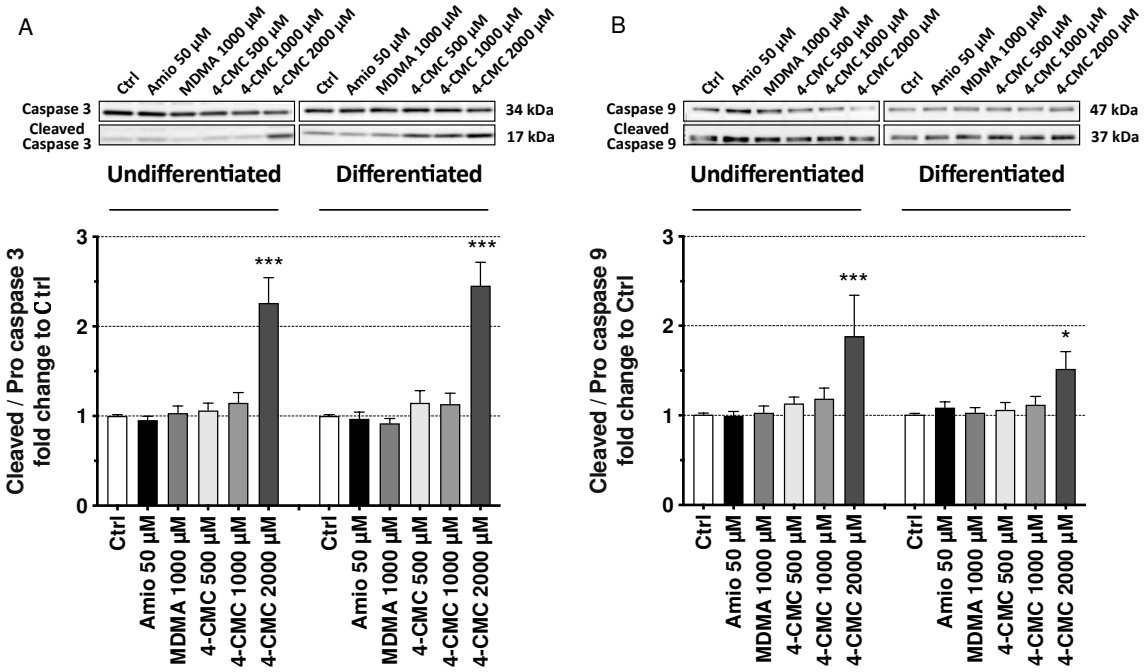

Figure 7. Effects on markers of apoptosis in undifferentiated and differentiated SH-SY5Y cells exposed to drugs for 6 h. (**A**) Activation of caspase 3 and (**B**) activation of caspase 9. Data are expressed as mean ± SEM of eight independent experiments for each drug concentration. Statistical differences were calculated with one-way ANOVA followed by the Dunnett's test, (*) $p \leq 0.05$, and (***) $p \leq 0.001$ versus 0.1% DMSO control.

3. Discussion

We found that both halogenated amphetamines were cytotoxic (membrane damage and/or ATP depletion) for undifferentiated and differentiated SH-SY5Y cells, with a similar concentration-dependent pattern. Among the halogenated methcathinones, only 4-CMC showed plasma membrane toxicity and ATP depletion. Amphetamine was cytotoxic at the highest concentration investigated, whereas methcathinone was not cytotoxic up to 2 mM. The rank of cytotoxicity observed for the *para*-substituents was chloride > fluoride > hydrogen for both amphetamines and cathinones. Both PCA and 4-CMC impaired the function of the mitochondrial electron transport chain and increased mitochondrial superoxide production. In general, differentiated SH-SY5Y were less sensitive to the chemicals investigated than undifferentiated cells.

The amphiphilic nature of amphetamines and methcathinones enables them to cross the blood-brain barrier and to reach the neurons, their site of pharmacological action. As known from case reports and as shown in the current study, this has not only an impact on the pharmacological effect but also on the neurotoxicity of these compounds. Halogenation in the *para*-position not only increases lipophilicity of these chemicals but also blocks *para*-hydroxylation, prolonging the pharmacological and toxicological effects of these compounds in vivo [31].

In the current investigations, 4-FA, PCA and 4-CMC decreased the cellular ATP content at lower concentrations than impairing membrane integrity (Table 1 and Table S1). This is a typical feature of toxicants that impair mitochondrial function [32,33] and is in line with our previous investigations on the hepatocellular toxicity of amphetamine, methcathinone and their *para*-halogenated forms [3,13,34,35]. A decrease in the cellular ATP content is also one of the first hints of mitochondrial perturbation, since mitochondria are the main site of ATP production in most cells, although glycolysis may also contribute when glucose is available [36]. The significant drop in the $\Delta\psi_m$, which appeared at similar concentrations as the decrease in the cellular ATP pool (Table S1), confirmed that mitochondria are the target of the *p*-halogenated amphetamine compounds and of 4-CMC [37]. These findings are consistent

with the observations of Chen et al., who investigated the toxicity of amphetamines in a pulmonary artery model [18,38] and of Luethi et al., who studied the mechanisms of hepatocellular toxicity associated with new synthetic cathinones [18,38]. Investigations of the effects on mitochondrial respiration revealed that PCA and 4-CMC reduced basal and maximal respiration of both undifferentiated and differentiated SH-SY5Y cells, whereby PCA was slightly more toxic than 4-CMC. While amphetamine and methcathinone were not toxic up to 2000 µM, the fluorinated derivatives decreased basal and maximal respiration by trend in both cell types studied. The toxicity rank order of the substituents in the *p*-position for disturbing mitochondrial function was therefore for both amphetamines and methcathinones (Cl > F > H), which was also the case for cytotoxicity. The current study revealed a decrease in oxygen consumption by SH-SY5Y cells in the presence of 4-FA, PCA and 4-CMC, indicating impaired function of the electron transport chain. The results do not, however, allow to conclude which enzyme complexes of the electron transport chain are affected. In a previous study, we have shown that the amphetamine-like MDMA reduced the activity of complexes I and III, and the cathinones α-pyrrolidinopentiophenone (α-PVP) and naphyrone complex I and complex II, respectively, in C2C12 cells, a mouse skeletal muscle cell line [19]. Inhibition of complex I and/or complex III could explain the results obtained in the current study.

Defective mitochondrial respiration can lead to an increase in mitochondrial ROS levels [3,39]. It is known that the neurotoxicity of amphetamines is at least partially due to an increased cellular ROS accumulation caused by oxidative deamination of catecholamines, depletion of antioxidant systems and/or mitochondrial dysfunction [24,40–44]. In addition, Naserzadeh et al. have shown that 4-methylmethcathinone (4-MMC), a new and popular drug of abuse, increases mitochondrial ROS levels and damages the outer mitochondrial membrane in mitochondria obtained from the hippocampus, cortex, and cerebellum of rats [45]. In the current study, we observed a significant increase in the mitochondrial ROS content in the presence of 4-FA, PCA and 4-CMC in undifferentiated SH-SY5Y cells, which is in line with the studies mentioned above.

Mitochondrial ROS generation can have different consequences for cells, eventually leading to oxidation of DNA, membrane lipids and proteins and finally cell death. Superoxide generated mainly by complex I or III within the mitochondria can be degraded by superoxide dismutase 2 (SOD2) to H_2O_2, which can leave the mitochondria and oxidize KEAP1 in the cytoplasm [46]. This process stabilizes and activates NRF2, a nuclear transcription factor, which stimulates the transcription of genes associated with antioxidative defense, such as SOD2 and many others [47]. An additional defense mechanism that can be activated by ROS-induced accumulation of misfolded proteins and/or organelle damage is autophagy [48]. We have shown in a recent study that 4-CMC stimulates autophagy in SH-SY5Y cells [49], demonstrating the activation of antioxidative defense mechanisms. If mitochondrial superoxide generation is too extensive, mitochondrial superoxide accumulation can lead to an opening of the permeability transition pore (mPTP), which is associated with a drop in the mitochondrial membrane potential and release of cytochrome *c* into the cytoplasm with induction of apoptosis [50,51]. This is in line with the activation of caspases 9 and 3 observed in the current study, which proves the stimulation of the endogenous apoptotic pathway by 4-CMC.

When compared to differentiated cells, the effects of PCA and 4-CMC were less accentuated than in undifferentiated cells and the effect of 4-FA was not significant. In agreement with these findings, Schneider et al. showed that the regulation of glycolysis and oxidative phosphorylation is modulated during cell differentiation, which can affect the way cells respond to toxicants causing oxidative stress [52]. In line with this notion, ATRA-induced cell differentiation has been shown to confer resistance to compounds inducing oxidative stress [53]. However, despite an increase in antioxidative capacity during the differentiation of SH-SY5Y cells [20,22,24], treatment with PCA and 4-CMC caused high enough cellular ROS levels to induce apoptosis.

There are reports in the literature that show how the use of methamphetamine is linked to the development of Parkinson's syndrome. In an epidemiological study, an increased risk to develop Parkinson's syndrome by a factor of 1.5–3 has been reported in amphetamine consumers [54,55].

Parkinson's syndrome develops due to a loss of dopaminergic neurons in the nigrostriatal system, which may be caused by mitochondrial damage [56]. Therefore, the current study suggests that *para*-halogenation of amphetamines and methcathinones may increase this risk. If confirmed, this is an important finding, which may have an impact on the use of these compounds.

In comparison to their pharmacological activity, which is observed in the high nanomolar to low micromolar range, depending on the compound and the pharmacological effect considered [3], cytotoxicity was detected at clearly higher concentrations in the current study. Plasma concentrations reached for amphetamine after a pharmacological dose are in the low micromolar range [57] and PCA started to be toxic at 50 to 100 micromolar. A possible explanation for this discrepancy between pharmacological activity and toxicity may be that cell lines as used in the current study may be less sensitive to toxicants than primary cells. This has for instance been shown for human hepatocyte cell lines and primary human hepatocytes [58]. Furthermore, patients presenting with neurotoxicity usually have ingested higher than pharmacological doses of these compounds, may have ingested other toxic drugs and/or alcohol and may have an elevated body temperature. It has recently been shown that the hepatocellular toxicity of the synthetic cathinone 3,4-methylenedioxypyrovalerone is more accentuated at higher temperatures [59]. In addition, since amphetamine has a volume of distribution in the range of 3 L/kg [57], it can be assumed that the concentrations in the brain are higher than those in plasma. Taken together, these factors may be sufficient to explain the gap between the concentrations associated with a pharmacological activity and toxic effects observed for these compounds in the current in vitro investigations.

4. Materials and Methods

4.1. Chemicals

Amphetamine, 4-fluoroamphetamine (4-FA), methcathinone, 4-fluoromethcathinone (4-FMC), 4-chloromethcathinone (4-CMC), and 3,4-methylenedioxymethamphetamine (MDMA) were purchased from Lipomed (Arlesheim, Switzerland). 4-Chloroamphetamine (PCA) was purchased from Cayman Chemical (Ann Arbor, MI, USA). All drugs were racemic hydrochloride salts with a HPLC purity of >98%. Test drugs were dissolved in DMSO and stored at -20 °C, then serially diluted in DMSO to avoid precipitation, followed by dilution in medium or assay buffer. The final DMSO concentration during the experiment was 0.1%.

4.2. Cell Culture and Differentiation

SH-SY5Y cells were obtained from the European Collection of Authenticated Cell Cultures (ECACC, RRID:CVCL_0019) (Sigma-Aldrich, Buchs, Switzerland). Undifferentiated SH-SY5Y cells were cultured in high glucose Dulbecco's Modified Eagle's Medium (DMEM) (Thermo Fischer Scientific, Basel, Switzerland) supplemented with 15% heat-inactivated fetal bovine serum (FBS) (Thermo Fischer Scientific, Basel, Switzerland), 2 mM L-glutamine (Thermo Fischer Scientific, Basel, Switzerland), and 1 mM sodium pyruvate (Thermo Fischer Scientific, Basel, Switzerland) at 37 °C in a humidified 5% CO_2 atmosphere. Confluent cells (70–80%) were passaged using Gibco™ Trypsin-EDTA (0.05%) reagent (Invitrogen, Basel, Switzerland). Neuron-like differentiation of SH-SY5Y cells were induced as described previously [20]. Briefly, SH-SY5Y cells were seeded into collagen-coated plates (Thermo Fischer Scientific, Basel, Switzerland) at 10,000 cells/cm^2. Following overnight growth, the medium was replaced by culture medium supplemented with 10 µM all-trans-retinoic acid (ATRA) (Sigma-Aldrich, Buchs, Switzerland) and the plates were incubated for five days. Finally, medium was replaced by DMEM supplemented with 50 ng/mL brain-derived neurotrophic factor (BDNF) (Sigma-Aldrich, Buchs, Switzerland) and incubated for 7 days [20]. To avoid phenotypic alterations, differentiated SH-SY5Y cells were used between the 14th and 16th passage [22,60].

4.3. Cell Differentiation Determined by Microscopy

To validate the differentiation protocol, we performed immunofluorescence experiments in order to check cell morphology and the expression of differentiation markers. Undifferentiated SH-SY5Y cells were seeded into ibiTreat µ-Slide (Vitaris, Baar, Switzerland) one day before the assessment. Differentiated SH-SY5Y cells were grown into collagen-coated µ-Slide (Vitaris, Baar, Switzerland). For the staining procedure, cells were fixed with 100 µL of fixation buffer (3.7% paraformaldehyde in PBS) for 20 min at room temperature (RT). Then, cell permeabilization was achieved by adding 0.1% Triton® X-100 in PBS solution for 10 min. Finally, the cells were blocked for 20 min in blocking solution (10% goat serum, 0.1% Triton® X-100 in PBS). Afterwards, the primary antibody cocktail (anti-MAP2 clone Poly18406, RRID:AB_256545, diluted 1:500, anti-neurofilament H clone SMI31, RRID:AB_2566782, diluted 1:200 in blocking solution) (BioLegend, San Diego, CA, USA) was added at RT for 1 h. Then, the cells were washed with PBS and the secondary antibody cocktail (FITC anti-rabbit clone Poly4064, RRID:AB_893531, diluted 1:250, Alexa Fluor® 647 Goat anti-mouse IgG polyclonal, RRID:AB_2563045, diluted 1:100, and 1.8 µM Hoechst 33258 in blocking solution) (BioLegend, San Diego, CA, USA) was added to each well and the slide was incubated at RT for 1 h with light protection [20]. Samples were maintained in PBS and investigated using an Olympus IX83 microscope (Olympus, Shinjuku, Japan).

4.4. Cell Membrane Integrity

Membrane toxicity was assessed by measuring adenylate kinase (AK) release using the ToxiLight Bioassay kit (Lonza, Basel, Switzerland) according to the manufacturer's protocol [19]. Briefly, undifferentiated SH-SY5Y (50,000 cells/well) and differentiated SH-SY5Y (25,000 cells/well) cells were exposed to different concentrations of amphetamine, 4-FA, PCA, methcathinone, 4-FMC, and 4-CMC (100 µM, 200 µM, 500 µM, 1000 µM, and 2000 µM). Triton® X-100 (0.1%) was used as a positive control to induce cell lysis. After 24 h of exposure, 20 µL of cell supernatant was transferred into a luminescence compatible 96-well plate and 50 µL of AK detection reagent was added to each well. The plate was incubated for 5 min at RT. The luminescence was measured on an M200 Pro Infinity plate reader (Tecan, Männedorf, Switzerland). The percentage of intact cells (no cell membrane integrity loss) was calculated in relation to DMSO-treated and Triton® X-100 treated cells, representing 100% and 0% of intact cells, respectively.

4.5. ATP Content

The intracellular ATP content was measured using the CellTiter-Glo® kit (Promega, Dübendorf, Switzerland) according to the manufacturer's protocol [19]. Undifferentiated and differentiated neuronal SH-SY5Y cells were prepared as described above. Briefly, 80 µL assay buffer was added to each 96-well containing 80 µL culture medium. After 15 min of incubation at RT, the ATP content was determined by luminescence measurement using an M200 Pro Infinity plate reader (Tecan, Männedorf, Switzerland). All data were normalized to control incubations containing DMSO 0.1%.

4.6. Mitochondrial Membrane Potential

The mitochondrial membrane potential ($\Delta\psi_m$) was determined using the cationic dye 5,5,6,6-tetrachloro-1,1,3,3-tetraethylbenzimidazolylcarbocyanine iodide (JC-1) kit (Abcam, Cambridge, UK) according to the manufacturer's protocol [23]. Undifferentiated and differentiated SH-SY5Y cells were seeded as described above (cell membrane integrity assay) in black costar 96-well plates and exposed to test drugs for 24 h. Carbonyl cyanide-*p*-trifluoromethoxyphenylhydrazone (FCCP, 100 µM) was used as a positive control. FCCP is an uncoupler of mitochondrial oxidative phosphorylation and therefore decreases $\Delta\psi_m$ [23]. FCCP was added to the cells for 4 h. The medium was removed and the cells were washed with 100 µL/well of 1X dilution buffer from the JC-1 kit. The working JC-1 solution (20 µM JC-1 in 1X Dilution Buffer) was freshly prepared and 100 µL was added into each well. The plate was incubated for 10 min at 37 °C with light protection. Then, the wells were washed twice with

1X dilution buffer solution. The fluorescence was measured by an M200 Infinite Pro plate reader (Tecan, Männedorf, Switzerland) at an excitation wavelength of 475 nm for both aggregate and monomer forms. The emission wavelength was set at 530 nm and at 590 nm for monomer and aggregate forms, respectively. The ratio of the fluorescence intensities between aggregates and monomers was considered as $\Delta\psi_m$. All data were normalized to control incubations containing DMSO 0.1%.

4.7. Oxygen Consumption

To measure the changes in mitochondrial respiration after test drug exposure, the mitochondrial oxygen consumption rate (OCR) was measured with a Seahorse XF96 analyzer (Seahorse Biosciences, North Billerica, MA, USA). Undifferentiated and differentiated SH-SY5Y cells were cultured in XF96 Cell Culture Microplates (Seahorse Biosciences, North Billerica, MA, USA), which were pre-coated with the cell adhesive Corning™ Cell-Tak (22.4 µg/mL, Corning, New York, NY, USA). The attached cells were treated with culture medium containing the test drugs (PCA at a concentration of 50–200 µM and the remaining drugs at concentrations of 200–100 µM) for 24 h. Upon treatment, the culture medium was replaced with 175 µL per well of unbuffered medium (4 mM L-glutamate, 1 mM pyruvate, 1 g/L glucose, and 63.3 mM sodium chloride, pH 7.4). Thereafter, the cells were equilibrated for 40 min in a CO_2-free incubator at 37 °C, and the plate was transferred into the XF96 analyzer. Basal oxygen consumption rates were measured prior to the automated injection of an inhibitor of F_0F_1ATPase (oligomycin 1 µM). In order to assess the maximal respiratory capacity, 1 µM FCCP was applied, which uncouples the activity of the electron transport chain from ATP synthesis. Finally, followed by the addition of an electron transport chain complex I inhibitor (rotenone 1 µM), the non-mitochondrial respiration rate was obtained [61]. OCR was automatically recorded by the Wave software (Seahorse Biosciences, North Billerica, MA, USA), and data were normalized to protein content. The protein content was determined using the Pierce BCA Protein Assay kit (Thermo Fisher Scientific, Basel, Switzerland). OCR was expressed as pmol O_2 per minute per mg of protein.

4.8. Mitochondrial Superoxide Production

Mitochondrial superoxide production was determined using the MitoSOX™ Red fluorophore probe (Thermo Fisher Scientific, Basel, Switzerland). MitoSOX is a living-cell permeant fluorogenic dye commonly used for the detection of superoxide within mitochondria. In brief, undifferentiated and differentiated SH-SY5Y cells were cultured and treated in black clear-bottom 96-well plates [3]. Amiodarone (50 µM) was used as a positive control [62]. The cells were treated with the test drugs at concentrations of 100–2000 µM for 24 h at 37 °C in a CO_2 incubator and then washed twice with PBS. Subsequently, the medium was replaced by 100 µL PBS containing the MitoSOX reagent (2.5 µM) and incubated for 10 min at 37 °C with light protection. The fluorescence was measured at 510/580 nm using an M200 Infinite Pro plate reader (Tecan, Männedorf, Switzerland). The results were normalized to the protein content using the Pierce BCA Protein Assay kit (Thermo Fisher Scientific, Basel, Switzerland).

4.9. Annexin V/Propidium Iodide Staining

Apoptosis (early and late apoptosis/necrosis) was determined using the Alexa Fluor® 488 annexin V/propidium iodide (PI) staining kit, according to the manufacturer's protocol (Vybrant TM Apoptosis Assay Kit #2) (Gibco Life Technologies, Paisley, UK) [63] and was followed by flow cytometric acquisition using a Cytoflex cytometer (Beckman Coulter, Indianapolis, IN, USA). Briefly, undifferentiated and differentiated SH-SY5Y cells were seeded into a 24-well plates and exposed to amphetamine, 4-FA, methcathinone, 4-FMC, or 4-CMC (1000 µM and 2000 µM), or PCA (100 µM, 200 µM, and 500 µM) for 6 h at 37 °C. This shorter incubation time (6 h versus 24 h) was selected to focus on the early apoptosis phase rather than on necrosis. Following incubation, the cells were detached and transferred into a V-well plate. The cells were pelleted and washed twice with PBS, then 100 µL of 1X annexin-binding buffer containing 5 µL of Alexa Fluor® 488 annexin V, 1 µL of PI (100 µg/mL), and 0.5 µL of anti-CD29-APC (clone TS2/16) (BioLegend, San Diego, CA, USA) was added to each well. CD29 is a member of the

integrin family which is expressed on the plasma membrane of undifferentiated and differentiated SH-SY5Y cells. Thereafter, the plate was incubated at 4 °C for 15 min with light protection. For the flow cytometry gating strategy, singlets were first identified by a forward scatter area (FSC-A) and forward scatter height (FSC-H) gate, and then by an FSC-A and a side scatter area (SSC-A) gate. Intact SH-SY5Y cells were distinguished from cell debris through staining with anti-CD29-APC in a FL-5 and an SCC-A gate. Samples were analyzed using FlowJo software (Tree Star, Ashland, OR, USA).

4.10. Western Blotting

Undifferentiated and differentiated SH-SY5Y cells were grown into a 6-well plate and treated with 4-CMC (500 µM, 1000 µM, and 2000 µM) for 6 h. Amiodarone 50 µM and MDMA 1000 µM were used as negative controls [62,64]. After treatment, cells were washed twice with cold PBS buffer (pH 7.4) and incubated with 70 µL of cell lysis buffer (radioimmunoprecipitation assay (RIPA) buffer supplemented with complete protease inhibitor (Roche Diagnostics, Mannheim, Germany)) for 15 min on ice. Then, the cell lysates were collected into Eppendorf tubes and centrifuged at 1600 *g* for 20 min. The supernatants were collected and the protein concentration was quantified using the Pierce BCA Pierce Protein Assay kit (Thermo Fisher Scientific, Basel, Switzerland). The protein extracts (18 µg per lane) were loaded, separated by SDS/PAGE using 4–12% NuPAGE Bis-Tris gels (Invitrogen, Basel, Switzerland), and then transferred to nitrocellulose membranes by the Trans-Blot Turbo Blotting System (Bio-Rad, Cressier, Switzerland). After protein transfer, membranes were first incubated with blocking buffer (5% non-fat dry milk in PBS containing 0.1% Tween-20 (Sigma-Aldrich, Buchs, Switzerland)) for 1 h at RT, and then incubated overnight at 4 °C with the following primary antibodies diluted in blocking solution: anti-cleaved caspase 3 (diluted 1:500, ab32042, RRID:AB_725947, Abcam, Cambridge, UK), anti-caspase 3 (diluted 1:500, 8G10, RRID:AB_2069872, Cell Signaling Technology, Danvers, USA), anti-caspase 9 (diluted 1:2000, ab52298, RRID:AB_868689, Abcam, Cambridge, UK) for full and cleaved forms, and anti-glyceraldehyde 3-phosphate dehydrogenase (GAPDH) (sc-365062, RRID:AB_10847862, Santa Cruz Biotechnology, Dallas, TX, USA). The amount of GAPDH was used to correct for different loading. Thereafter, the nitrocellulose membranes were washed three times with PBS and incubated with secondary antibodies (Santa Cruz Biotechnology, Dallas, TX, USA) diluted at 1:2000 in blocking solution for 1 h at RT. Membranes were then washed, and protein bands were developed using the ClarityTM Western ECL Substrate (Bio-Rad Laboratories, San Diego, CA, USA). Protein expression was quantified using the Fusion Pulse TS device (Vilber Lourmat, Oberschwaben, Germany).

4.11. Statistics

GraphPad Prism 8.3.0 (GraphPad Software, La Jolla, CA, USA) was used for all statistical analyses. The data are presented as the mean ± standard error mean (SEM) of at least three independent experiments. Statistical differences between the DMSO 0.1% control group and test drugs were calculated with one-way ANOVA followed by the Dunnett's test. A p-value < 0.05 was considered to indicate a statistically significant difference.

5. Conclusions

In conclusion, *para*-halogenation of amphetamine and methcathinone increases mitochondrial toxicity associated with these drugs. The *para*-chlorinated and fluorinated forms were toxic on undifferentiated and differentiated SH-SY5Y cells in a concentration-dependent fashion, whereby the amphetamine derivatives showed higher toxicity than the methcathinone counterparts. Moreover, differentiated SH-SY5Y cells were less susceptible to the toxic effects of the compounds investigated, possibly due to stronger antioxidative capacity. Although the cytotoxic concentrations were higher than those needed for pharmacological activity, mitochondrial dysfunction may represent a major mechanism for neural toxicity associated with these compounds.

Supplementary Materials: Supplementary materials can be found at http://www.mdpi.com/1422-0067/21/8/2841/s1. Figure S1: Chemical structures, Figure S2: Differentiation of SH-SY5Y cells, Table S1: Summary of the toxicity.

Author Contributions: Study design: X.Z., R.V.M., and S.K.; experiments: X.Z., J.B., and R.V.M.; data interpretation: X.Z., J.B., R.V.M., and S.K.; writing—original draft preparation: X.Z., J.B., and R.V.M.; writing—review & editing: J.B., R.V.M., M.E.L., and S.K.; funding acquisition: X.Z. and S.K. All authors have read and agreed to the published version of the manuscript.

Funding: The research was funded by a grant from the Swiss National Science Foundation to S.K. (SNF 31003A_156270). X.Z. is a recipient of the China Scholarship Council Stipendium of the P.R. China.

Conflicts of Interest: The authors declare no conflict of interest

References

1. Heal, D.J.; Smith, S.L.; Gosden, J.; Nutt, D.J. Amphetamine, past and present-a pharmacological and clinical perspective. *J. Psychopharmacol.* **2013**, *27*, 479–496. [CrossRef] [PubMed]
2. Sulzer, D.; Sonders, M.S.; Poulsen, N.W.; Galli, A. Mechanisms of neurotransmitter release by amphetamines: A review. *Prog. Neurobiol.* **2005**, *75*, 406–433. [CrossRef] [PubMed]
3. Luethi, D.; Walter, M.; Zhou, X.; Rudin, D.; Krahenbuhl, S.; Liechti, M.E. Para-halogenation affects monoamine transporter inhibition properties and hepatocellular toxicity of amphetamines and methcathinones. *Front. Pharmacol.* **2019**, *10*, 438. [CrossRef] [PubMed]
4. Calkins, R.F.; Aktan, G.B.; Hussain, K.L. Methcathinone: the next illicit stimulant epidemic? *J. Psychoact. Drugs* **1995**, *27*, 277–285. [CrossRef] [PubMed]
5. Kesha, K.; Boggs, C.L.; Ripple, M.G.; Allan, C.H.; Levine, B.; Jufer-Phipps, R.; Doyon, S.; Chi, P.; Fowler, D.R. Methylenedioxypyrovalerone ("bath salts"), related death: case report and review of the literature. *J. Forensic Sci.* **2013**, *58*, 1654–1659. [CrossRef]
6. Neumann, C.S.; Fujimori, D.G.; Walsh, C.T. Halogenation strategies in natural product biosynthesis. *Chem. Biol.* **2008**, *15*, 99–109. [CrossRef]
7. Gerebtzoff, G.; Li-Blatter, X.; Fischer, H.; Frentzel, A.; Seelig, A. Halogenation of drugs enhances membrane binding and permeation. *Chembiochem* **2004**, *5*, 676–684. [CrossRef]
8. Brandt, S.D.; Sumnall, H.R.; Measham, F.; Cole, J. Analyses of second-generation 'legal highs' in the UK: initial findings. *Drug Test. Anal.* **2010**, *2*, 377–382. [CrossRef]
9. Grifell, M.; Ventura, M.; Carbon, X.; Quintana, P.; Galindo, L.; Palma, A.; Fornis, I.; Gil, C.; Farre, M.; Torrens, M. Patterns of use and toxicity of new para-halogenated substituted cathinones: 4-CMC (clephedrone), 4-CEC (4-chloroethcatinone) and 4-BMC (brephedrone). *Hum. Psychopharmacol. Clin. Exp.* **2017**, *32*, e2621. [CrossRef]
10. Linsen, F.; Koning, R.P.; van Laar, M.; Niesink, R.J.; Koeter, M.W.; Brunt, T.M. 4-Fluoroamphetamine in the Netherlands: more than a one-night stand. *Addiction* **2015**, *110*, 1138–1143. [CrossRef]
11. Tomczak, E.; Wozniak, M.K.; Kata, M.; Wiergowski, M.; Szpiech, B.; Biziuk, M. Blood concentrations of a new psychoactive substance 4-chloromethcathinone (4-CMC) determined in 15 forensic cases. *Forensic Toxicol.* **2018**, *36*, 476–485. [CrossRef] [PubMed]
12. Archer, R.P. Fluoromethcathinone, a new substance of abuse. *Forensic Sci. Int.* **2009**, *185*, 10–20. [CrossRef] [PubMed]
13. Fuller, R.W. Effects ofp-chloroamphetamine on brain serotonin neurons. *Neurochem. Res.* **1992**, *17*, 449–456. [CrossRef] [PubMed]
14. Yamamoto, B.K.; Moszczynska, A.; Gudelsky, G.A. Amphetamine toxicities: Classical and emerging mechanisms. *Ann. New York Acad. Sci.* **2010**, *1187*, 101–121. [CrossRef] [PubMed]
15. Sinha, A.; Lewis, O.; Kumar, R.; Yeruva, S.L.; Curry, B.H. Amphetamine abuse related acute myocardial infarction. *Case Rep. Cardiol.* **2016**, 1–6. [CrossRef] [PubMed]
16. Berman, S.M.; Kuczenski, R.; McCracken, J.T.; London, E.D. Potential adverse effects of amphetamine treatment on brain and behavior: a review. *Mol. Psychiatry* **2009**, *14*, 123–142. [CrossRef]
17. Kalix, P. The pharmacology of khat. *Gen. Pharmacol. Vasc. Syst.* **1984**, *15*, 179–187. [CrossRef]
18. Luethi, D.; Liechti, M.E.; Krähenbühl, S. Mechanisms of hepatocellular toxicity associated with new psychoactive synthetic cathinones. *Toxicology* **2017**, *387*, 57–66. [CrossRef]
19. Zhou, X.; Luethi, D.; Sanvee, G.M.; Bouitbir, J.; Liechti, M.E.; Krahenbuhl, S. Molecular Toxicological Mechanisms of Synthetic Cathinones on C2C12 Myoblasts. *Int. J. Mol. Sci.* **2019**, *20*, 1561. [CrossRef]

20. Encinas, M.; Iglesias, M.; Liu, Y.; Wang, H.; Muhaisen, A.; Ceña, V.; Gallego, C.; Comella, J.X. Sequential treatment of sh-sy5y cells with retinoic acid and brain-derived neurotrophic factor gives rise to fully differentiated, neurotrophic factor-dependent, human neuron-like cells. *J. Neurochem.* **2000**, *75*, 991–1003. [CrossRef]
21. Agholme, L.; Lindstrom, T.; Kagedal, K.; Marcusson, J.; Hallbeck, M. An in vitro model for neuroscience: differentiation of SH-SY5Y cells into cells with morphological and biochemical characteristics of mature neurons. *J. Alzheimer's Dis.* **2010**, *20*, 1069–1082. [CrossRef] [PubMed]
22. Kovalevich, J.; Langford, D. Considerations for the use of SH-SY5Y neuroblastoma cells in neurobiology. *Methods Mol. Biol.* **2013**, *1078*, 9–21. [CrossRef] [PubMed]
23. Song, M.S.; Ryu, P.D.; Lee, S.Y. Kv3.4 is modulated by HIF-1α to protect SH-SY5Y cells against oxidative stress-induced neural cell death. *Sci. Rep.* **2017**, *7*, 2075. [CrossRef] [PubMed]
24. Wang, Y.; Nartiss, Y.; Steipe, B.; McQuibban, G.A.; Kim, P.K. ROS-induced mitochondrial depolarization initiates PARK2/PARKIN-dependent mitochondrial degradation by autophagy. *Autophagy* **2012**, *8*, 1462–1476. [CrossRef] [PubMed]
25. Tsujimoto, Y. Apoptosis and necrosis: Intracellular ATP level as a determinant for cell death modes. *Cell Death Differ.* **1997**, *4*, 429. [CrossRef] [PubMed]
26. Wang, C.-M.; Yang, C.-Q.; Cheng, B.-H.; Chen, J.; Bai, B. Orexin-A protects SH-SY5Y cells against H2O2-induced oxidative damage via the PI3K/MEK1/2/ERK1/2 signaling pathway. *Int. J. Immunopathol. Pharmacol.* **2018**, *32*, 2058738418785739. [CrossRef] [PubMed]
27. Thornberry, N.A.; Lazebnik, Y. Caspases: Enemies within. *Science* **1998**, *281*, 1312–1316. [CrossRef]
28. Ashkenazi, A.; Dixit, V.M. Death receptors: Signaling and modulation. *Science* **1998**, *281*, 1305–1308. [CrossRef]
29. Wang, C.; Youle, R.J. The role of mitochondria in apoptosis. *Annu. Rev. Genet.* **2009**, *43*, 95–118. [CrossRef]
30. Elmore, S. Apoptosis: A review of programmed cell death. *Toxicol. Pathol.* **2007**, *35*, 495–516. [CrossRef]
31. Nielsen, I.M.; Dubnick, B. Amphetamines and Related Compounds. In Proceedings of the Mario Negri Institute for Pharmacological Research; Raven Press: New York, NY, USA, 1970; p. 63.
32. Barbosa, D.J.; Capela, J.P.; Feio-Azevedo, R.; Teixeira-Gomes, A.; Bastos Mde, L.; Carvalho, F. Mitochondria: Key players in the neurotoxic effects of amphetamines. *Arch. Toxicol.* **2015**, *89*, 1695–1725. [CrossRef] [PubMed]
33. Paumard, P.; Vaillier, J.; Coulary, B.; Schaeffer, J.; Soubannier, V.; Mueller, D.M.; Brèthes, D.; Rago, J.-P.D.; Velours, J. The ATP synthase is involved in generating mitochondrial cristae morphology. *Embo J.* **2002**, *21*, 221–230. [CrossRef] [PubMed]
34. Colado, M.I.; Murray, T.K.; Green, A.R. 5-HT loss in rat brain following 3,4-methylenedioxymethamphetamine (MDMA), p-chloroamphetamine and fenfluramine administration and effects of chlormethiazole and dizocilpine. *Br. J. Pharmacol.* **1993**, *108*, 583–589. [CrossRef] [PubMed]
35. Miller, K.J.; Anderholm, D.C.; Ames, M.M. Metabolic activation of the serotonergic neurotoxin para-chloroamphetamine to chemically reactive intermediates by hepatic and brain microsomal preparations. *Biochem Pharm.* **1986**, *35*, 1737–1742. [CrossRef]
36. Hyun, D.H.; Hunt, N.D.; Emerson, S.S.; Hernandez, J.O.; Mattson, M.P.; Cabo, R.D. Up-regulation of plasma membrane-associated redox activities in neuronal cells lacking functional mitochondria. *J. Neurochem.* **2007**, *100*, 1364–1374. [CrossRef]
37. Volobueva, A.S.; Melnichenko, A.A.; Grechko, A.V.; Orekhov, A.N. Mitochondrial genome variability: the effect on cellular functional activity. *Ther. Clin. Risk Manag.* **2018**, *14*, 237–245. [CrossRef]
38. Zorova, L.D.; Popkov, V.A.; Plotnikov, E.Y.; Silachev, D.N.; Pevzner, I.B.; Jankauskas, S.S.; Babenko, V.A.; Zorov, S.D.; Balakireva, A.V.; Juhaszova, M. Mitochondrial membrane potential. *Anal. Biochem.* **2018**, *552*, 50–59. [CrossRef]
39. Zorov, D.B.; Juhaszova, M.; Sollott, S.J. Mitochondrial reactive oxygen species (ROS) and ROS-induced ROS release. *Physiol. Rev.* **2014**, *94*, 909–950. [CrossRef]
40. Halpin, L.E.; Collins, S.A.; Yamamoto, B.K. Neurotoxicity of methamphetamine and 3, 4-methylenedioxymethamphetamine. *Life Sci.* **2014**, *97*, 37–44. [CrossRef]
41. Carvalho, M.; Carmo, H.; Costa, V.M.; Capela, J.P.; Pontes, H.; Remião, F.; Carvalho, F.; de Lourdes Bastos, M. Toxicity of amphetamines: an update. *Arch. Toxicol.* **2012**, *86*, 1167–1231. [CrossRef]

42. Yamamoto, B.K.; Bankson, M.G. Amphetamine neurotoxicity: cause and consequence of oxidative stress. *Crit. Rev. Neurobiol.* **2005**, *17*. [CrossRef] [PubMed]
43. Valente, M.J.o.; Bastos, M.d.L.; Fernandes, E.; Carvalho, F.l.; Guedes de Pinho, P.; Carvalho, M.R. Neurotoxicity of β-keto amphetamines: deathly mechanisms elicited by methylone and MDPV in human dopaminergic SH-SY5Y cells. *ACS Chem. Neurosci.* **2017**, *8*, 850–859. [CrossRef] [PubMed]
44. Mammucari, C.; Rizzuto, R. Signaling pathways in mitochondrial dysfunction and aging. *Mech. Ageing Dev.* **2010**, *131*, 536–543. [CrossRef] [PubMed]
45. Naserzadeh, P.; Taghizadeh, G.; Atabaki, B.; Seydi, E.; Pourahmad, J. A comparison of mitochondrial toxicity of mephedrone on three separate parts of brain including hippocampus, cortex and cerebellum. *Neurotoxicology* **2019**, *73*, 40–49. [CrossRef] [PubMed]
46. Roos, N.J.; Duthaler, U.; Bouitbir, J.; Krahenbuhl, S. The uricosuric benzbromarone disturbs the mitochondrial redox homeostasis and activates the NRF2 signaling pathway in HepG2 cells. *Free Radic. Biol. Med.* **2020**, *152*, 216–226. [CrossRef]
47. Ma, Q. Role of nrf2 in oxidative stress and toxicity. *Annu. Rev. Pharm. Toxicol.* **2013**, *53*, 401–426. [CrossRef]
48. Guo, F.; Liu, X.; Cai, H.; Le, W. Autophagy in neurodegenerative diseases: pathogenesis and therapy. *Brain Pathol.* **2018**, *28*, 3–13. [CrossRef]
49. Zhou, X.; Bouitbir, J.; Liechti, M.E.; Krähenbühl, S.; Mancuso, R.V. Hyperthermia Increases Neurotoxicity Associated with Novel Methcathinones. *Cells* **2020**, *9*, 965. [CrossRef]
50. Liu, X.; Kim, C.N.; Yang, J.; Jemmerson, R.; Wang, X. Induction of apoptotic program in cell-free extracts:Requirement for datp and cytochrome c. *Cell* **1996**, *86*, 147–157. [CrossRef]
51. Green, D.R.; Reed, J.C. Mitochondria and apoptosis. *Science* **1998**, *281*, 1309–1312. [CrossRef]
52. Schneider, L.; Giordano, S.; Zelickson, B.R.; Johnson, M.S.; Benavides, G.A.; Ouyang, X.; Fineberg, N.; Darley-Usmar, V.M.; Zhang, J. Differentiation of SH-SY5Y cells to a neuronal phenotype changes cellular bioenergetics and the response to oxidative stress. *Free Radic. Biol. Med.* **2011**, *51*, 2007–2017. [CrossRef] [PubMed]
53. Cheung, Y.T.; Lau, W.K.W.; Yu, M.S.; Lai, C.S.W.; Yeung, S.C.; So, K.F.; Chang, R.C.C. Effects of all-trans-retinoic acid on human SH-SY5Y neuroblastoma as in vitro model in neurotoxicity research. *Neurotoxicology* **2009**, *30*, 127–135. [CrossRef] [PubMed]
54. Lappin, J.M.; Darke, S.; Farrell, M. Methamphetamine use and future risk for Parkinson's disease: Evidence and clinical implications. *Drug Alcohol Depend.* **2018**, *187*, 134–140. [CrossRef]
55. Lopes, F.M.; Schröder, R.; da Frota Júnior, M.L.C.; Zanotto-Filho, A.; Müller, C.B.; Pires, A.S.; Meurer, R.T.; Colpo, G.D.; Gelain, D.P.; Kapczinski, F. Comparison between proliferative and neuron-like SH-SY5Y cells as an in vitro model for Parkinson disease studies. *Brain Res.* **2010**, *1337*, 85–94. [CrossRef] [PubMed]
56. Karbowski, M.; Neutzner, A. Neurodegeneration as a consequence of failed mitochondrial maintenance. *Acta Neuropathol.* **2012**, *123*, 157–171. [CrossRef] [PubMed]
57. Dolder, P.C.; Strajhar, P.; Vizeli, P.; Hammann, F.; Odermatt, A.; Liechti, M.E. Pharmacokinetics and Pharmacodynamics of Lisdexamfetamine Compared with D-Amphetamine in Healthy Subjects. *Front. Pharmacol.* **2017**, *8*, 617. [CrossRef] [PubMed]
58. Gerets, H.H.; Tilmant, K.; Gerin, B.; Chanteux, H.; Depelchin, B.O.; Dhalluin, S.; Atienzar, F.A. Characterization of primary human hepatocytes, HepG2 cells, and HepaRG cells at the mRNA level and CYP activity in response to inducers and their predictivity for the detection of human hepatotoxins. *Cell Biol. Toxicol.* **2012**, *28*, 69–87. [CrossRef]
59. Valente, M.J.; Araujo, A.M.; Silva, R.; Bastos Mde, L.; Carvalho, F.; Guedes de Pinho, P.; Carvalho, M. 3,4-Methylenedioxypyrovalerone (MDPV): in vitro mechanisms of hepatotoxicity under normothermic and hyperthermic conditions. *Arch. Toxicol.* **2016**, *90*, 1959–1973. [CrossRef]
60. Shipley, M.M.; Mangold, C.A.; Szpara, M.L. Differentiation of the SH-SY5Y human neuroblastoma cell line. *J. Vis. Exp.* **2016**, *108*, 53193. [CrossRef]
61. Haylett, W.; Swart, C.; van der Westhuizen, F.; van Dyk, H.; van der Merwe, L.; van der Merwe, C.; Loos, B.; Carr, J.; Kinnear, C.; Bardien, S. Altered mitochondrial respiration and other features of mitochondrial function in parkin-mutant fibroblasts from parkinson's disease patients. *Parkinson's Dis.* **2016**, *2016*, 1819209. [CrossRef]

62. Felser, A.; Blum, K.; Lindinger, P.W.; Bouitbir, J.; Krahenbuhl, S. Mechanisms of hepatocellular toxicity associated with dronedarone-a comparison to amiodarone. *Toxicol. Sci.* **2013**, *131*, 480–490. [CrossRef] [PubMed]
63. Demchenko, A.P. Beyond annexin V: Fluorescence response of cellular membranes to apoptosis. *Cytotechnology* **2013**, *65*, 157–172. [CrossRef] [PubMed]
64. Barbosa, D.J.; Capela, J.P.; Silva, R.; Ferreira, L.M.; Branco, P.S.; Fernandes, E.; Bastos, M.L.; Carvalho, F. "Ecstasy"-induced toxicity in SH-SY5Y differentiated cells: role of hyperthermia and metabolites. *Arch. Toxicol.* **2014**, *88*, 515–531. [CrossRef] [PubMed]

4. Paper 4

Hyperthermia Increases Neurotoxicity Associated with Novel Methcathinones

In this paper, we investigated the role of hyperthermia on methcathinone, 4-CMC, and 4-MMC induced neurotoxicity in undifferentiated SH-SY5Y cells.

cells

MDPI

Article

Hyperthermia Increases Neurotoxicity Associated with Novel Methcathinones

Xun Zhou [1,2], Jamal Bouitbir [1,2,3], Matthias E. Liechti [1,2], Stephan Krähenbühl [1,2,3,*] and Riccardo V. Mancuso [1,2]

1 Division of Clinical Pharmacology & Toxicology, University Hospital Basel, 4031 Basel, Switzerland; xun.zhou@unibas.ch (X.Z.); jamal.bouitbir@unibas.ch (J.B.); matthias.liechti@usb.ch (M.E.L.); riccardo.mancuso@unibas.ch (R.V.M.)
2 Department of Biomedicine, University of Basel, 4031 Basel, Switzerland
3 Swiss Centre for Applied Human Toxicology, 4031 Basel, Switzerland
* Correspondence: stephan.kraehenbuehl@usb.ch; Tel.: +41-61-265-4715

Received: 24 February 2020; Accepted: 9 April 2020; Published: 14 April 2020

Abstract: Hyperthermia is one of the severe acute adverse effects that can be caused by the ingestion of recreational drugs, such as methcathinones. The effect of hyperthermia on neurotoxicity is currently not known. The primary aim of our study was therefore to investigate the effects of hyperthermia (40.5 °C) on the neurotoxicity of methcathinone (MC), 4-chloromethcathinone (4-CMC), and 4-methylmethcathinone (4-MMC) in SH-SY5Y cells. We found that 4-CMC and 4-MMC were cytotoxic (decrease in cellular ATP and plasma membrane damage) under both hyper- (40.5 °C) and normothermic conditions (37 °C), whereby cells were more sensitive to the toxicants at 40.5 °C. 4-CMC and 4-MMC impaired the function of the mitochondrial electron transport chain and increased mitochondrial formation of reactive oxygen species (ROS) in SH-SY5Y cells, which were accentuated under hyperthermic conditions. Hyperthermia was associated with a rapid expression of the 70 kilodalton heat shock protein (Hsp70), which partially prevented cell death after 6 h of exposure to the toxicants. After 24 h of exposure, autophagy was stimulated by the toxicants and by hyperthermia but could only partially prevent cell death. In conclusion, hyperthermic conditions increased the neurotoxic properties of methcathinones despite the stimulation of protective mechanisms. These findings may be important for the understanding of the mechanisms and clinical consequences of the neurotoxicity associated with these compounds.

Keywords: autophagy; hyperthermia; methcathinone; mitochondria; neurotoxicity

1. Introduction

New psychoactive substances (NPSs) are a broad group of drugs of abuse that are not controlled by classic international drug laws [1]. The abuse of NPSs is a major problem worldwide, since NPSs can elicit serious toxic effects on users [2]. In recent years, several synthetic cathinones, designated as "legal highs", have emerged and their use as recreational drugs has grown rapidly [3]. Structurally, synthetic cathinones are β-keto-amphetamine derivatives, with pharmacological and toxicological properties similar to amphetamines [3]. Synthetic cathinones, such as methcathinone (MC), 4-chloromethcathinone (4-CMC), and 4-methylmethcathinone (4-MMC, mephedrone) (see Figure S1 for chemical structures), have recently been recognized by the European Monitoring Centre for Drugs and Drug Addiction (EMCDDA) as emerging NPSs [4–6].

Despite clinical studies with and initial use of some synthetic cathinones for the treatment of depression, appetite suppression, or smoking-cessation, none of these compounds have been approved for one of these indications, mainly due to their adverse effect profile [7]. Relevant adverse effects

reported for synthetic cathinones include anxiety, paranoia, depression, stroke, seizures, hyperthermia, heart failure, liver failure, and even death [7,8].

Hyperthermia, also reported as "overheating", is one of the prominent acute severe adverse effects of stimulant drug abuse, and one of the primary causes of death [9,10]. According to clinical case reports, drug-induced hyperthermia can result in many potentially fatal complications, such as hyponatremia, rhabdomyolysis, cerebral edema, disseminated intravascular coagulation, and coma [11]. Drug-induced hyperthermia can be caused by several factors. Most psychostimulant drugs can directly increase metabolic heat production by central and/or peripheral mechanisms as well as decrease heat dissipation [9,10]. Several clinical cases of hyperthermia induced by synthetic cathinones have been reported so far [12] and a large number of animal studies have been performed in mice and rats to investigate the effect of these compounds on the body temperature [13]. Polysubstance abuse may contribute to methcathinone-induced hyperthermia. Additionally, a drug that may accidentally or deliberately be used in combination with cathinones is 3,4-methylenedioxymethamphetamine (MDMA), an amphetamine derivative with well-known effects on thermoregulation [9,14]. In addition, environmental effects that users face in dancing clubs where these drugs are usually consumed may contribute as well as to hyperthermia associated with methcathinones and MDMA [15,16].

While the capacity of cathinones and many other recreational drugs to increase the body and brain temperature is well established, the effects of hyperthermia on neurotoxicity associated with these drugs is currently less well known [13]. Barbosa et al. investigated the effect of ecstasy and ecstasy metabolites on SH-SY5Y cells under normothermic (37 °C) and hyperthermic (40 °C) conditions [17]. They found that the metabolites were more toxic than the parent compound and that the toxicity increased with higher temperature. The aim of the current study was to investigate in vitro the role of hyperthermia on methcathinone-induced neurotoxicity using the well-established SH-SY5Y neuronal cell model [18].

2. Materials and Methods

2.1. Chemicals and Cell Culture

Amphetamine, 4-fluoroamphetamine (4-FA), methcathinone (MC), 4-fluoromethcathinone (4-FMC), 4-chloromethcathinone (4-CMC), 4-methylmethcathinone (4-MMC), and 3,4-methylenedioxymethamphetamine (MDMA) were purchased from Lipomed (Arlesheim, Switzerland). 4-Chloroamphetamine (PCA) was purchased from Cayman Chemical (Ann Arbor, MI, USA). All drugs were racemic hydrochloride salts with an HPLC purity of >98%. Test drugs were dissolved in dimethyl sulfoxide (DMSO) and stored at −20 °C. The final DMSO concentration during the experiment was 0.1%.

The SH-SY5Y human neuroblastoma cell line was purchased from European Collection of Authenticated Cell Cultures (RRID:CVCL_0019, ECACC) (Sigma-Aldrich, Buchs, Switzerland). SH-SY5Y cells were cultured in a 5% CO_2 incubator at 37 (normothermic conditions) or 40.5 °C (hyperthermic conditions) in high glucose Dulbecco's Modified Eagle's Medium (DMEM) (Thermo Fischer Scientific, Basel, Switzerland) containing 15% heat-inactivated fetal bovine serum (FBS) (Thermo Fischer Scientific, Basel, Switzerland), 2 mM L-glutamine (Thermo Fischer Scientific, Basel, Switzerland), and 1 mM sodium pyruvate (Thermo Fischer Scientific, Basel, Switzerland).

2.2. Cell Membrane Toxicity

The release of adenylate kinase (AK) into the cell medium was assessed as a marker to measure plasma membrane integrity. We used the ToxiLight Bioassay Kit (Lonza, Basel, Switzerland) according to the manufacturer's protocol. In brief, SH-SY5Y cells (50,000 cells per well) were seeded into a 96-well Costar polystyrene plate and left to grow overnight. Afterwards, the medium was removed, and the cells were exposed to different concentrations of PCA (from 100 to 1000 μM), amphetamine, 4-FA, MC, 4-FMC, 4-CMC, and 4-MMC (from 200 to 2000 μM). Triton X-100 (0.1%) was used as a positive control to

induce cell lysis. MDMA (500 µM and 1000 µM) was used as a control drug, which is known to induce hyperthermia in vivo [9]. The plate was incubated at 37 and 40.5 °C in 5% CO_2 and saturated humidity for 6 and 24 h. Then, 20 µL of cell supernatant was transferred into a luminescence-compatible 96-well plate followed by the addition of 50 µL of AK detection reagent. The plate was incubated at room temperature (RT) for 5 min, and the luminescence was measured with a M200 Pro Infinity plate reader (Tecan, Männedorf, Switzerland). All data were normalized to DMSO 0.1%-treated cells (control).

2.3. Intracellular ATP Content

Changes in the intracellular ATP content were measured using the CellTiter-Glo® kit from Promega (Dübendorf, Switzerland) according to the manufacturer's protocol. SH-SY5Y cells were treated as described above. After 6 and 24 h of treatment, 80 µL of assay buffer was added to each well containing SH-SY5Y cells in 80 µL of culture medium. The plate was shaken for 2 min at 350 rpm, followed by 15 min of incubation at RT. The ATP content was determined by luminescence measurement using a M200 Pro Infinity plate reader (Tecan, Männedorf, Switzerland). All data were normalized to DMSO 0.1%-treated cells (control).

2.4. Mitochondrial Membrane Potential

The mitochondrial membrane potential ($\Delta\psi m$) was measured using the JC-10 Mitochondrial Membrane Potential Assay Kit (Abcam, Cambridge, UK) according to the manufacturer's protocol. In healthy cells, JC-10 concentrates in the mitochondrial matrix where it forms red fluorescent aggregates, whereas, in apoptotic and necrotic cells where the $\Delta\psi m$ decreases, JC-10 diffuses out of mitochondria, changes to a monomeric form, and stains cells with green fluorescence [19]. SH-SY5Y cells were seeded into black Costar 96-well plates at 50,000 cells per well. Upon incubation with different concentrations of the synthetic methcathinones (200–2000 µM) at 37 or 40.5 °C for 24 h, the supernatant was removed and the cells were rinsed with PBS. Then, 50 µL of JC-10 dye-loading solution was added to each well and the plate was incubated for 15 min at 37 °C and 5% CO_2 with light protection. Carbonyl cyanide-*p*-trifluoromethoxyphenylhydrazone (FCCP, 100 µM) was used as a positive control. FCCP is an uncoupler of mitochondrial oxidative phosphorylation and therefore decreases $\Delta\psi m$ [20]. SH-SY5 cells were exposed to FCCP for 4 h.

The fluorescence was measured using a Tecan M200 Infinite Pro plate reader (Tecan, Männedorf, Switzerland) at 490/525 nm for the aggregates, and at 540/590 nm for monomeric forms. The ratio of the fluorescence intensities between aggregates and monomers was considered as an indicator of $\Delta\psi m$. Data were normalized to control incubations containing DMSO 0.1%.

2.5. Mitochondrial Oxygen Consumption

In order to assess the changes in mitochondrial respiration due to hyperthermia in the presence of test drugs, the mitochondrial oxygen consumption rate (OCR) was measured with a Seahorse XF96 analyzer (Seahorse Biosciences, North Billerica, MA, USA). SH-SY5Y cells were seeded at a density of 50,000 cells per well into XF96 Cell Culture Microplates (Seahorse Biosciences, North Billerica, MA, USA) coated with the cell adhesive Corning™ Cell-Tak (22.4 µg/mL) (Corning, New York, USA). SH-SY5Y cells were left to grow overnight and then treated with different concentrations of test drugs (200, 500, and 1000 µM) for 24 h at 37 and 40.5 °C. Before the measurement, SH-SY5Y cells were rinsed twice with unbuffered DMEM medium (4 mM L-glutamate, 1000 µM pyruvate, 1 g/L glucose, and 63.3 mM sodium chloride, pH 7.4) and equilibrated in a CO_2-free incubator for 30 min. First, basal oxygen consumption was measured, then the leak respiratory rate after automated injection of an ATP synthase inhibitor (oligomycin 1 µM). Maximal OCR was determined by adding FCCP (1 µM). Finally, the non-mitochondrial respiration rate was obtained by the addition of an electron transport chain complex I inhibitor (rotenone 1 µM). OCR was automatically recorded by the Wave software (Seahorse Biosciences, North Billerica, MA, USA), and data were normalized to the protein content

determined using the Pierce BCA Protein Assay kit (Thermo Fisher Scientific, Basel, Switzerland). OCR was expressed as pmol O_2 per minute per mg of protein.

2.6. Mitochondrial Superoxide Production

Mitochondrial superoxide production was assessed using the MitoSOX™ Red fluorophore probe (Thermo Fisher Scientific, Basel, Switzerland). SH-SY5Y cells were seeded into a black 96-well plate at a density of 50,000 cells per well, treated with the synthetic methcathinones at different concentrations (from 200 to 2000 µM), and incubated for 24 h at 37 or 40.5 °C. Amiodarone (50 µM) was used as a positive control [21]. MDMA (500 and 1000 µM) was used as a control drug known to induce hyperthermia in vivo [9]. Upon treatment, the medium was removed, and the cells were rinsed with PBS. Next, 100 µL of PBS containing MitoSOX reagent (2.5 µM) was added to each well and the plate was incubated for 10 min at 37 °C with light protection. The fluorescence was measured using a Tecan M200 Infinite Pro plate reader (Tecan, Männedorf, Switzerland) at 510/580 nm. The results were normalized to the protein content quantified by the Pierce BCA Protein Assay kit (Thermo Fisher Scientific, Basel, Switzerland) and to DMSO 0.1%-treated control cells.

2.7. Apoptosis

Apoptosis (early and late apoptosis/necrosis) was determined using the Alexa Fluor® 488 annexin V/propidium iodide (PI) staining kit, according to the manufacturer's protocol (Vybrant TM Apoptosis Assay Kit #2) (Gibco Life Technologies, Paisley, UK) and followed by flow cytometric acquisition using a Cytoflex cytometer (Beckman Coulter, Indianapolis, IN, USA). Briefly, SH-SY5Y cells were seeded into a 48-well plate at a density of 200,000 cells per well and left to grow overnight. The cells were treated with MC, 4-CMC, 4-MMC at 1000 and 2000 µM, and MDMA at 500 and 1000 µM, for 6 and for 24 h at 37 and 40.5 °C. H_2O_2 (500 µM) was used as a positive control for apoptosis [22]. The 6-h incubation time was selected to focus on the early apoptosis phase rather than on the necrosis. On the day of measurement, the cells were transferred into a V-well plate, pelleted, and washed twice with PBS. Then, 100 µL of 1× Annexin-Binding Buffer containing 5 µL of Alexa Fluor® 488 annexin V, 1 µL of PI (100 µg/mL), and 0.5 µL of anti-CD29-APC (RRID:AB_314323, clone TS2/16) (BioLegend, San Diego, CA, USA) was added to each well. CD29 is a member of the integrin family expressed on the membrane of SH-SY5Y cells [23]. Thereafter, the plate was incubated at 4 °C for 15 min with light protection. For the flow cytometry gating strategy, singlets were first identified by a forward scatter area (FSC-A) and forward scatter height (FSC-H) gate, and then by an FSC-A and side scatter area (SSC-A) gate. Intact SH-SY5Y cells were distinguished from cell debris by staining with anti-CD29-APC in a FL5-A/SCC-A dot plot. Samples were analyzed using FlowJo software, Tree Star (RRID:SCR_008520) (Ashland, OR, USA).

2.8. Western Blotting

SH-SY5Y cells were seeded into 6-well plates and left to grow overnight. For the assessment of Hsp70, caspase 3, LC3 I, and LC3 II, cells were treated with methcathinones (MC, 4-CMC, and 4-MMC) at the concentrations of 1000 and 2000 µM, and with MDMA at 500 and 1000 µM at 37 or 40.5 °C. Concanamycin A (100 nM) and bafilomycin A (100 nM) (Tocris Bioscience, Abingdon, UK) were used as positive controls for the inhibition of autophagy [24]. Hsp70 and caspase 3 were quantified after 6 h of incubation, LC3 I and LC3 II were quantified after 24 h of incubation. Upon treatment, cells were lysed using radioimmunoprecipitation assay (RIPA) buffer with complete protease inhibitor (Roche Diagnostics, Mannheim, Germany) on ice for 15 min and then centrifuged to obtain protein samples. Following the collection of supernatants, BCA Pierce assay was used to quantify the protein concentration of each sample. Afterwards, a total of 18 µg protein per sample was loaded and run onto a 4–12% SDS-PAGE gel and then electroblotted onto a nitrocellulose membrane. The membrane was blocked with 5% non-fat milk in TBST buffer (4 mM Tris base saline containing 0.1% Tween-20, pH 7.5) for 1 h at RT, and then incubated with primary antibody anti-heat shock protein 70

(Hsp70, 1:1000 dilution, ab2787 Abcam, RRID:AB_303300, Cambridge, UK), anti-cleaved caspase 3 (1:500 dilution, ab32042, RRID:AB_725947, Abcam, Cambridge, UK), anti-caspase 3 (1:500 dilution, 8G10, RRID:AB_2069872, Cell Signaling Technology, Danvers, USA), anti-LC3 I/II (1:1000 dilution, 12741s, RRID:AB_2617131, Cell Signaling Technology, Danvers, USA), and anti-glyceraldehyde 3-phosphate dehydrogenase (GAPDH) (1:5000 dilution, sc-365062, RRID:AB_10847862, Santa Cruz Biotechnology, Dallas, USA) overnight at 4 °C. After washing three times with TBST buffer, the membrane was incubated with a secondary antibody (1:2000 dilution, Santa Cruz Biotechnology, USA) for 1 h at RT. Then, signals were developed by the enhanced chemiluminescence (ECL) kit (Bio-Rad Laboratories, Hercules, USA). Protein expression was quantified by the Fusion Pulse TS device (Vilber Lourmat, Oberschwaben, Germany).

2.9. Fluorescence Microscopy with Acridine Orange Staining

Acidic vesicular organelles (AVOs) are autolysosomes and autophagosomes and can be measured as markers of the late autophagic process [25,26]. To detect AVOs, cells were stained with acridine orange (AO) according to published protocols [25,26]. AO is a lysosomotropic dye, its fluorescence emission is pH dependent, green at neutral pH and bright yellow to red within acidic organelles [25,26]. SH-SY5Y cells were seeded into ibiTreat µ-Slide (Vitaris, Baar, Switzerland) and exposed to 1000 µM of the synthetic methcathinones for 24 h at 37 °C or 40.5 °C. Then, the cell culture medium was replaced by AO staining solution (0.5 µg/mL acridine orange in culture medium), and the µ-Slide was incubated for 20 min at 37 °C with light protection. The samples were rinsed three times with pre-warmed medium and pictures were acquired by an Olympus IX83 microscope (Olympus, Shinjuku, Japan).

2.10. Flow Cytometry with Acridine Orange Staining

To quantify the formation of AVOs, we detected the intensity of AO fluorescence by flow cytometry. AVOs stained with AO emit red fluorescence (FL3-A, 690/50 nm BP); the increase in the intensity of red fluorescence (AO+ events) is proportional to the volume and number of AVOs [25,26]. SH-SY5Y cells were seeded into a 48-well plate at a density of 200,000 cells per well and left to grow overnight. Cells were treated with MC, 4-CMC, and 4-MMC at 1000 and 2000 µM, and MDMA at 500 and 1000 µM, for 24 h, at 37 or 40.5 °C. On the day of measurement, SH-SY5Y cells were transferred and pelleted into a V-well plate, then washed twice with PBS. Afterwards, the cells were incubated with 100 µL of AO staining solution (0.5 µg/mL in PBS) for 20 min at 37 °C with light protection. SH-SY5Y cells were analyzed with a CytoFLEX flow cytometer (Beckman Coulter, IN, USA). For the flow cytometry gating strategy, singlets were first identified by an FSC-A/FSC-H gate, and then by an FSC-A/SSC-A gate. AO+ cells were identified in an SSC-A/FL3-A dot plot, in comparison to DMSO 0.1%-treated cells (control). Results were analyzed using the FlowJo software (Tree Star, Ashland, OR, USA).

2.11. Statistics

Experimental data are presented as the mean ± SEM of at least five independent experiments. Statistical comparisons were performed with one-way ANOVA followed by *t*-tests. Statistical significance was considered at $P \leq 0.05$. GraphPad Prism 8.3.0 (RRID:SCR_002798) (GraphPad Software, La Jolla, CA, USA) was used for all statistical analyses.

3. Results

3.1. Cell Membrane Integrity and ATP Content

In order to obtain an overview of the effect of hyperthermia on amphetamine- and methcathinone-induced neurotoxicity, we first determined the release of AK and the intracellular ATP content in SH-SY5Y after 24 h of drug exposure under normothermic (37 °C) and hyperthermic conditions (40.5 °C). AK release is commonly used as a marker of cell membrane integrity, whereas the intracellular ATP content represents a marker of energy metabolism. SH-SY5Y cells were exposed

to increasing concentrations of amphetamine, 4-fluoroamphetamine (4-FA), 4-chloroamphetamine (PCA), methcathinone (MC), 4-fluoromethcathinone (4-FMC), 4-chloromethcathinone (4-CMC), and 4-methylmethcathinone (4-MMC) (see Figure S1 for chemical structures). MDMA was also included due its widespread use and its known effects on body temperature.

As shown in Figure 1 for methcathinones and MDMA and in Figure S2 for the amphetamines, all of these compounds were membrane toxic and decreased the intracellular ATP content in a concentration-dependent manner. Exceptions were MC and 4-FMC, which did not show any significant toxicity up to 2000 µM (Figure 1). 4-FA and PCA were membrane toxic starting at 1000 and 500 µM, respectively, at both temperatures investigated (Figure S2A), whereas 4-CMC, 4-MMC, and MDMA were significantly more toxic at 40.5 °C, with membrane toxicity starting at 1000 µM at this temperature (Figure 1A).

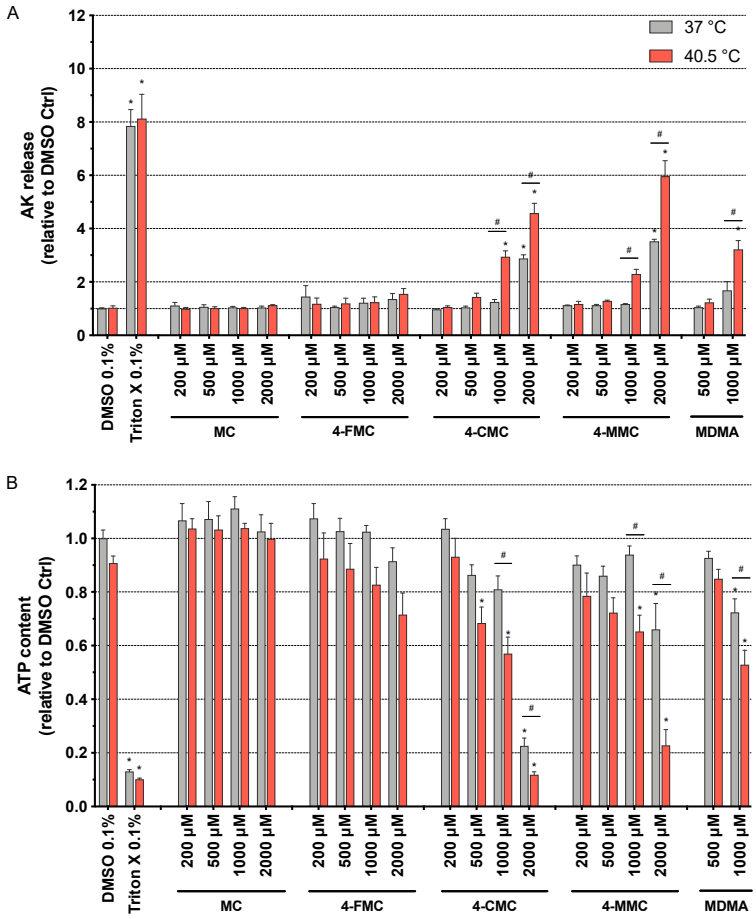

Figure 1. (**A**) Plasma membrane integrity and (**B**) intracellular ATP content assessed in SH-SY5Y cells after 24 h of exposure at 37 and 40.5 °C to methcathinone (MC), 4-fluoromethcathinone (4-FMC), 4-chloromethcathinone (4-CMC), 4-methylmethcathinone (4-MMC) (200-2000 µM), and 3,4-methylenedioxymethamphetamine (MDMA) (500 and 1000 µM). Dimethyl sulfoxide (DMSO) and Triton X were used as negative and positive controls, respectively. Data are expressed relative to the DMSO control as the mean ± SEM of eight independent experiments. Statistical comparisons were performed with one-way ANOVA followed by *t*-tests (*$P \leq 0.05$ versus control at the same temperature; $^{\#}P \leq 0.05$ versus the same concentration at a different temperature).

The intracellular ATP content in SH-SY5Y cells started to decrease at 2000 µM for 4-FA, 4-CMC, and 4-MMC, and at 1000 µM for MDMA at normothermic conditions, whereas at 40.5 °C, it started to decrease at 2000 µM for amphetamine; 1000 µM for 4-FA, MDMA, and 4-MMC; at 200 µM for PCA; and at 500 µM for 4-CMC (Figure 1B and Figure S2B). 4-FA, 4-CMC, 4-MMC, and MDMA were significantly

more toxic under hyperthermic conditions (Figure 1B and Figure S2B), in line with the findings of the AK assessment experiments. Moreover, the drugs investigated showed a more pronounced toxicity regarding the decrease in the intracellular ATP content when compared to membrane toxicity, a pattern suggesting mitochondrial toxicity (Table S1).

Based on these first screenings, we decided to investigate the effect of hyperthermia on the neurotoxicity associated with the synthetic methcathinones MC, 4-CMC, and 4-MMC in more detail.

3.2. Mitochondrial Membrane Potential

In order to understand the mechanism of temperature-increased mitochondrial toxicity, we determined the Δψm by staining SH-SY55 cells with the JC-10 dye [21]. Our data indicated that MC did not change the Δψm significantly up to 2000 µM (Figure S3A). Similarly, MDMA was associated with a numeric drop in the Δψm but without reaching statistical significance (Figure S3D). In contrast, 4-CMC and 4-MMC decreased the Δψm in a concentration-dependent manner at both temperature conditions (Figure S3B and S3C), reaching statistical significance at 2000 and 1000 µM, respectively. In contrast to AK release and ATP depletion, the Δψm did not show a more accentuated decrease at 40.5 °C compared to 37 °C.

3.3. Mitochondrial Oxygen Consumption

The observed decrease in intracellular ATP and Δψm could be caused by impaired mitochondrial function. We therefore assessed the oxygen consumption rate (OCR) by exposing SH-SY5Y cells for 24 h at 37 and 40.5 °C to the test compounds using a Seahorse XF96 analyzer. While MC was not toxic, 4-CMC (1000 µM), 4-MMC (1000 µM), and MDMA (500 µM) significantly decreased mitochondrial basal and FCCP-stimulated respiration at 37 °C (Figure 2). In comparison, at 40.5 °C, all compounds investigated started to be toxic already at 200 µM for both basal and FCCP-stimulated respiration (Figure 2). We also recorded the leak respiration, which is the cellular uptake of oxygen in the presence of the F_1F_0-ATP synthase inhibitor oligomycin. An increase in the leak respiration would indicate uncoupling of oxidative phosphorylation. Since none of the compounds investigated stimulated leak respiration, we can exclude uncoupling as a reason for the observed decrease in Δψm.

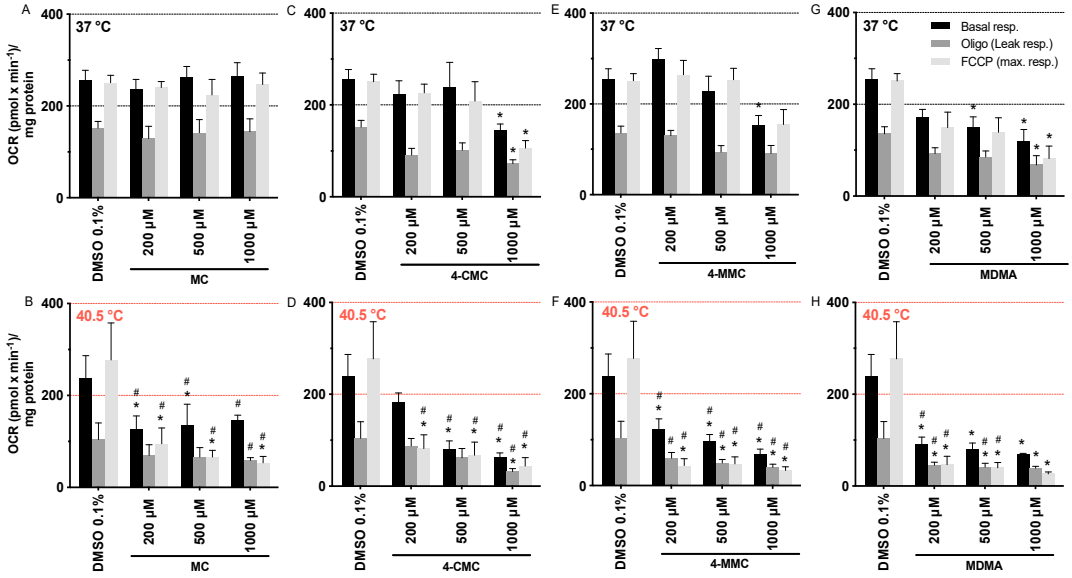

Figure 2. Oxygen consumption rate of SH-SY5Y cells at 37 and 40.5 °C expressed as basal, leak, and maximal respiration. SH-SY5Y cells were exposed for 24 h to (**A,B**) MC, (**C,D**) 4-CMC (**E,F**) 4-MMC, and (**G,H**) MDMA. Data are expressed as mean ± SEM of eight independent experiments. Statistical comparisons were performed with one-way ANOVA followed by *t*-tests (*$P \leq 0.05$ versus control at the same temperature; $^{\#}P \leq 0.05$ versus the same concentration at a different temperature).

In contrast to the effect on the mitochondrial membrane potential, these data showed that hyperthermic conditions clearly increased the mitochondrial toxicity of MC, 4-CMC, 4-MMC, and MDMA. Furthermore, halogenation and methylation in the *p*-position increased the toxicity of the methcathinones in comparison to hydrogen in this position.

3.4. Mitochondrial Superoxide Production

To further investigate the potential involvement of mitochondria in the observed toxicity, we determined the mitochondrial ROS production. The inhibition of complex I and III of the electron transport chain can increase the production of mitochondrial superoxide [27,28]. Mitochondrial ROS were measured in SH-SY5Y cells exposed to methcathinones for 24 h at 37 and at 40.5 °C. Concerning normothermic conditions, only 4-CMC showed a significant increase of the mitochondrial ROS content, which started at 2000 µM. At 40.5 °C, the superoxide anion content increased significantly starting at 2000 µM for MC, and at 1000 µM for 4-CMC, 4-MMC, and MDMA (Figure 3).

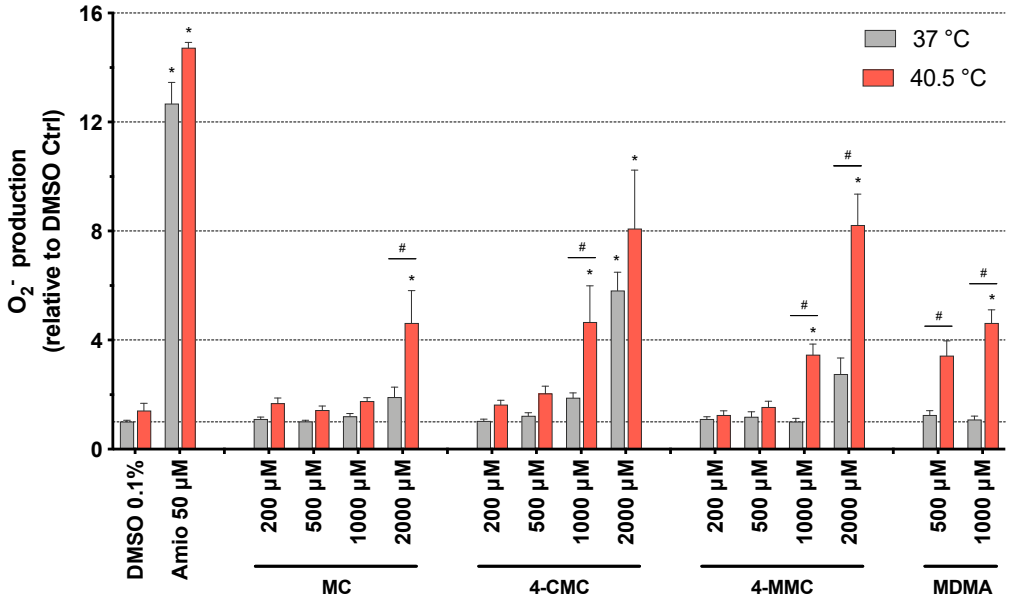

Figure 3. Mitochondrial superoxide production in SH-SY5Y cells at 37 and 40.5 °C after 24 h of exposure to MC, 4-CMC, 4-MMC (200–2000 µM), and MDMA (500 and 1000 µM). DMSO and amiodarone were used as negative and positive controls, respectively. Data are expressed relative to DMSO control as mean ± SEM of six independent experiments run in quadruplicate. Statistical comparisons were performed with one-way ANOVA followed by *t*-tests (*$P \leq 0.05$ versus control at the same temperature; #$P \leq 0.05$ versus the same concentration at a different temperature).

3.5. Cell Death Mechanisms

Inhibition of oxidative phosphorylation with a decrease in the cellular ATP content and intracellular accumulation of ROS could initiate cell death mechanisms, such as apoptosis and/or necrosis [29]. To clarify whether hyperthermia can affect such events in drug-treated SH-SY5Y cells, we analyzed the proportion of apoptotic and necrotic cells after treatment with test compounds at 37 and 40.5 °C for 6 and 24 h.

As expected, H_2O_2 at 0.5 µM increased the number of apoptotic and necrotic cells at both temperatures (Figure 4A). At 37 °C, after 6 h of incubation, 4-CMC increased the percentage of apoptotic cells significantly, starting at 1000 µM (Figure 4A). In comparison, the other compounds tested increased the percentage of apoptotic cells only numerically, without reaching statistical significance. 4-CMC and 4-MMC increased the percentage of necrotic cells starting at 1000 and 2000 µM, respectively, and MDMA starting at 1000 µM. Similar results were obtained for caspase 3 activation at

37 °C (Figure 4B). 4-CMC and 4-MMC increased caspase 3 cleavage starting at 1000 µM, whereas the other compounds tested increased caspase 3 cleavage only numerically. In comparison, at 40.5 °C, the effect of the compounds investigated on the percentage of apoptotic cells (Figure 4A) and caspase 3 cleavage (Figure 4B) was less accentuated than at 37 °C. 4-CMC induced apoptosis, necrosis, and caspase 3 cleavage at 2000 µM, whereas the other compounds were not associated with significant increases in the induction of apoptosis, necrosis, or caspase 3 cleavage up to 2000 µM. After 24 h of incubation at 37 °C, none of the substances tested induced apoptosis, but 4-CMC and 4-MMC induced necrosis starting at 2000 µM (Figure S4). At 40.5 °C, the picture was not different from 37 °C, but the extent of necrosis was numerically more accentuated.

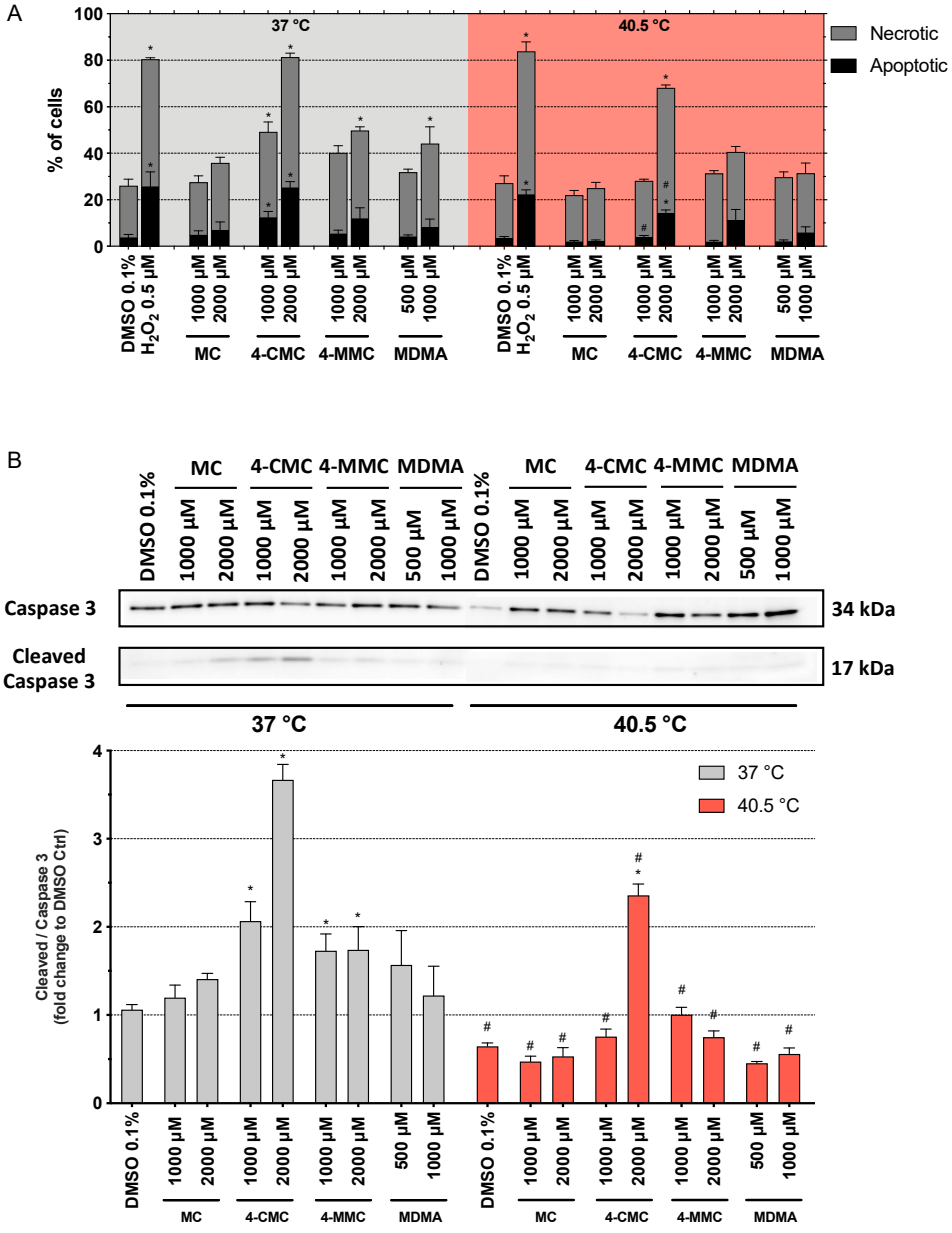

Figure 4. Mechanisms of cell death after 6 h of exposure at 37 and 40.5 °C to MC, 4-CMC, 4-MMC (1000 and 2000 µM), and MDMA (500 and 1000 µM). DMSO and H_2O_2 were used as negative and positive controls, respectively. (**A**) Percentage of necrotic and apoptotic cells. (**B**) Activation of caspase 3. Data are expressed as mean ± SEM of six independent experiments. Statistical comparisons were performed with one-way ANOVA followed by *t*-tests (*$P \leq 0.05$ versus control at the same temperature; $^{\#}P \leq 0.05$ versus the same concentration at a different temperature).

The data suggested a shift from apoptosis to necrosis at the higher temperature and with longer incubation. In order to obtain a better understanding of this shift, we also determined the AK release and ATP content in the presence of the methcathinone derivatives after 6 h of incubation (Figure S5). The ATP content dropped, and the AK release increased only at the highest 4-CMC concentrations at both temperatures investigated, which is compatible with the increase in cell necrosis observed with this compound.

To better understand the effects of hyperthermia on the cell death pathways, we measured the expression of Hsp70 protein in SH-SY5Y cells after 6 h of exposure to the synthetic methcathinones. Hsp70 are a family of proteins, which protect the cells from stress by helping cellular proteins to retain their native conformation or to regain their function after misfolding due to an increased temperature. Hsp70 proteins are usually upregulated by heat stress and toxic chemicals [30]. As expected, Hsp70 expression was significantly increased at 40.5 °C compared to 37 °C for all compounds tested as well as for DMSO-treated control cells (Figure 5). In comparison to control incubations, the compounds investigated did not influence Hsp70 expression at 37 or 40.5 °C.

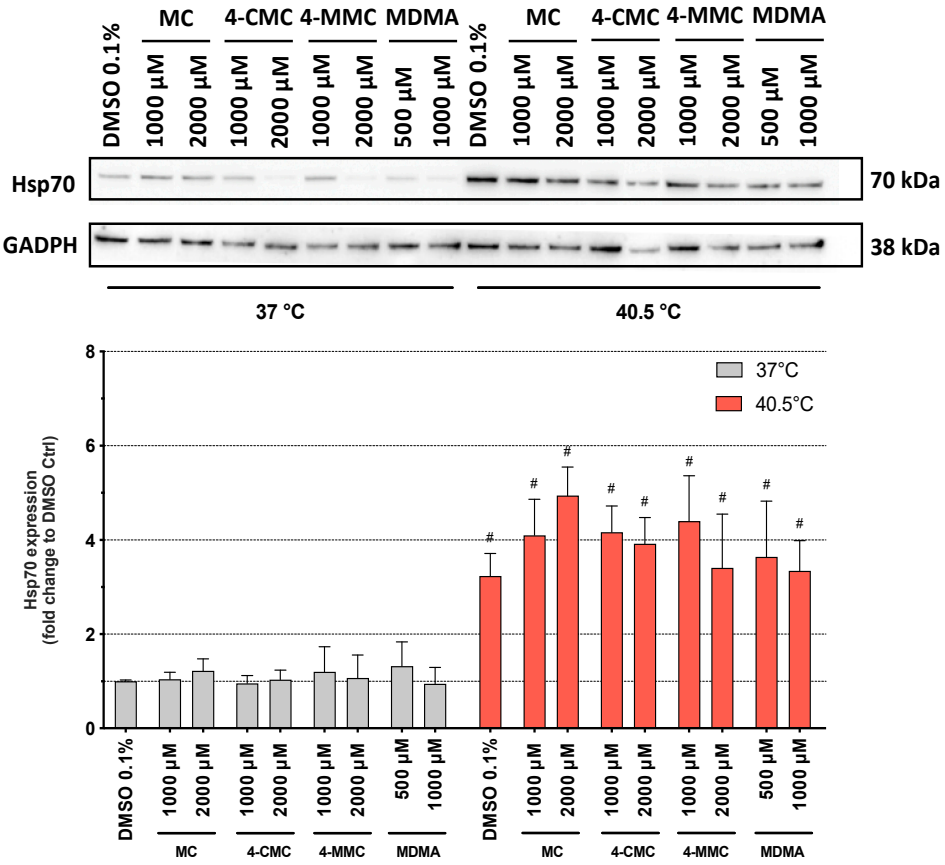

Figure 5. Expression of 70 kilodalton heat shock protein (Hsp70) in SH-SY5Y cells after 6 h of exposure at 37 and 40.5 °C to MC, 4-CMC, 4-MMC (200–2000 µM), and MDMA (500 and 1000 µM). Data are expressed relative to the DMSO control as mean ± SEM of six independent experiments. Statistical comparisons were performed with one-way ANOVA followed by *t*-tests ($^{\#}P \leq 0.05$ versus the same concentration at a different temperature).

3.6. Detection of Autophagy

Autophagy is a physiological catabolic process used by most cells to remove misfolded proteins or entire organelles in order to maintain proteo- and homeostasis. It is triggered mainly by starvation, cell insults, and DNA damage [31]. Hyperthermic conditions, exposure to mitochondrial toxicants, and cellular ROS accumulation can generate misfolded proteins, which can affect the cellular metabolism [32].

In order to explore whether hyperthermia and/or methcathinones can promote autophagy in SH-SY5Y cells, we analyzed the expression of autophagy-related protein microtubule-associated protein 1A/1B-light chain 3 (LC3) by Western blots [25]. LC3 is a component of the autophagosome membranes in mammalian cells, and it is a validated marker for the assessment of early autophagy [33]. During the first phase of autophagy, the cytosolic form of LC3 (LC3 I) is cleaved and conjugated with phosphatidylethanolamine to form LC3 II, which is then translocated into autophagosome membranes. An increase in the LC3 II/LC3 I ratio therefore reflects autophagosome formation [34]. SH-SY5Y cells were exposed at 37 and 40.5 °C to MC, 4-CMC, 4-MMC (1000 and 2000 µM), and MDMA (500 and 1000 µM). After 24 h of incubation at 37 °C, all test compounds showed a concentration-dependent increase in the LC3 II/LC3 I ratio compared to control conditions, which reached statistical significance for 2000 µM 4-CMC and for 2000 µM 4-MMC (Figure 6). Under hyperthermic conditions, the effect of the test compounds on the LC3 II/LC3 I ratio was similar but more accentuated for 4-CMC and 4-MMC as compared to 37 °C.

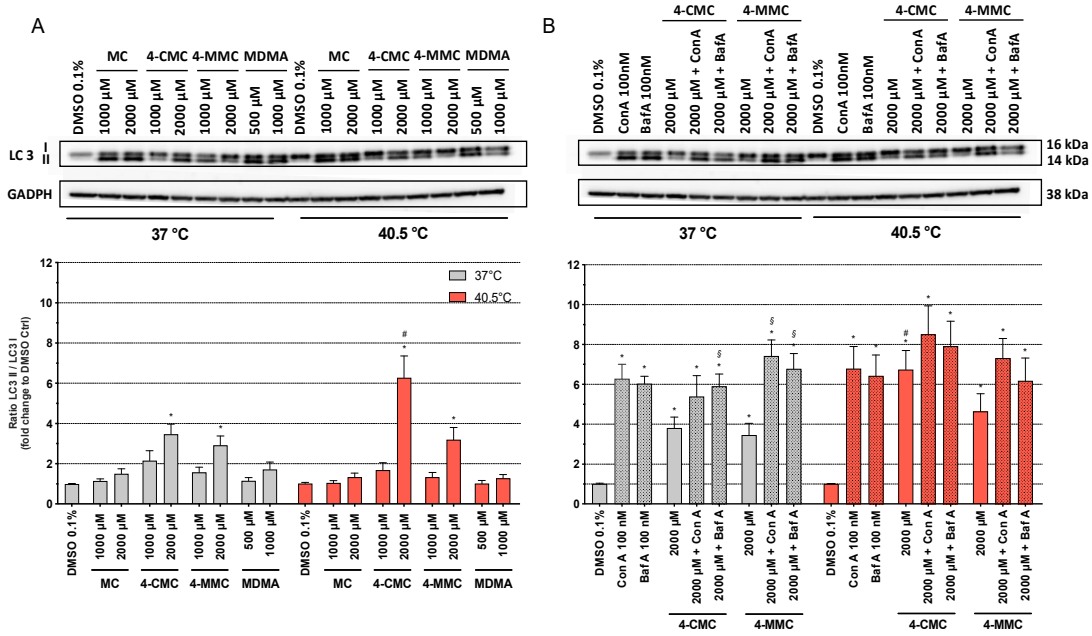

Figure 6. Protein expression of microtubule-associated protein 1A/1B-light chain 3 (LC3) I and LC3 II in SH-SY5Y cells after 24 h of exposure at 37 and 40.5 °C to (**A**) MC, 4-CMC, 4-MMC (200–2000 µM), and MDMA (500 and 1000 µM) and (**B**) in the presence of the autophagy inhibitors concanamycin A (100 nM) and bafilomycin A (100 nM). Data are expressed as the ratio of LC3 II/LC3 I relative to the DMSO control of six independent experiments. Statistical comparisons were performed with one-way ANOVA followed by paired *t*-test (*$P \leq 0.05$ versus DMSO control at the same temperature; $^{\#}$ $P \leq 0.05$ versus the same concentration at a different temperature; $^{\S}P \leq 0.05$ versus incubations containing 4-CMC or 4-MMC without concanamycin A or bafilomycin A).

In order to investigate whether the observed increase in the LC3 II/LC3 I ratio in the presence of 4-CMC and 4-MMC was due to increased phagosome formation or decreased degradation, we investigated the effect of the two autophagy inhibitors concanamycin A and bafilomycin A on the LC3 II/LC3 I ratio. Concanamycin A and bafilomycin A impair the fusion of autophagosomes and lysosomes by inhibiting the vacuolar H^+ ATPase and therefore the acidification of organelles, which increases LC3 II expression [24]. As shown in Figure 6A, in the absence of concanamycin A and bafilomycin A, treatment with 2000 µM 4-CMC or 4-MMC significantly increased the LC3 II/LC3 I ratio both at 37 and 40.5 °C compared to control incubations, with 40.5 °C being more effective than 37 °C. As shown in Figure 6B, as expected, concanamycin A and bafilomycin A increased the LC3 II/LC3 I ratio at both temperatures compared to the DMSO control. At 37 °C, concanamycin A and bafilomycin

A increased the LC3 II/LC3 I ratio in the presence of 4-CMC or 4-MMC compared to the respective control incubations (2000 µM 4-CMC or 4-MMC). At 40.5 °C, this effect was less prominent and did not reach statistical significance. Importantly, the LC3 II/LC3 I ratios of incubations containing only concanamycin A or bafilomycin A and of incubations containing concanamycin A or bafilomycin A in combination with 4-CMC or 4-MMC were not different at both temperatures. Since concanamycin A and bafilomycin A block autosome degradation, the LC3 II/LC3 I ratio in the presence of these inhibitors reflects autophagosome formation, which was obviously not different between incubations containing only concanamycin A or bafilomycin A and incubations containing concanamycin A or bafilomycin A in combination with 4-CMC or 4-MMC. The results therefore suggest that the observed increase in the LC3 II/LC3 I ratio in the presence of 4-CMC and 4-MMC reflects impaired autophagosome degradation and not formation.

To further study the autophagy, we assessed the formation of acidic vesicular organelles (AVOs) [25], which is a hallmark of late autophagy [26]. Microscopic analysis of SH-SY5Y cells exposed for 24 h at 37 and 40.5 °C to MC, 4-CMC, and 4-MMC (1000 µM) showed an accumulation of AO dye within acidic compartments (Figure 7A). All the tested drugs increased the formation and size of the AVOs at both temperature conditions. Moreover, 4-CMC and 4-MMC at hyperthermic conditions affected the morphology of the cells, with a reduction of neuritic processes (Figure 7A). To confirm the effect of the investigated compounds on AVO formation, SH-SY5Y cells were exposed for 24 h at 37 and 40.5 °C to MC and 4-MMC (1000 and 2000 µM) and to 4-CMC (500 and 1000 µM) and AVOs were quantified by flow cytometry (Figure 7B). At 37 °C, 4-CMC and 4-MMC showed a significantly increased percentage of AO+ cells at 1000 µM compared to control incubations. Compared to 37 °C, exposure to 4-CMC and 4-MMC at 40.5 °C was associated with more AVO formation (Figure 7B), and 4-CMC significantly increased AVO abundance at 40.5 °C already at 500 µM.

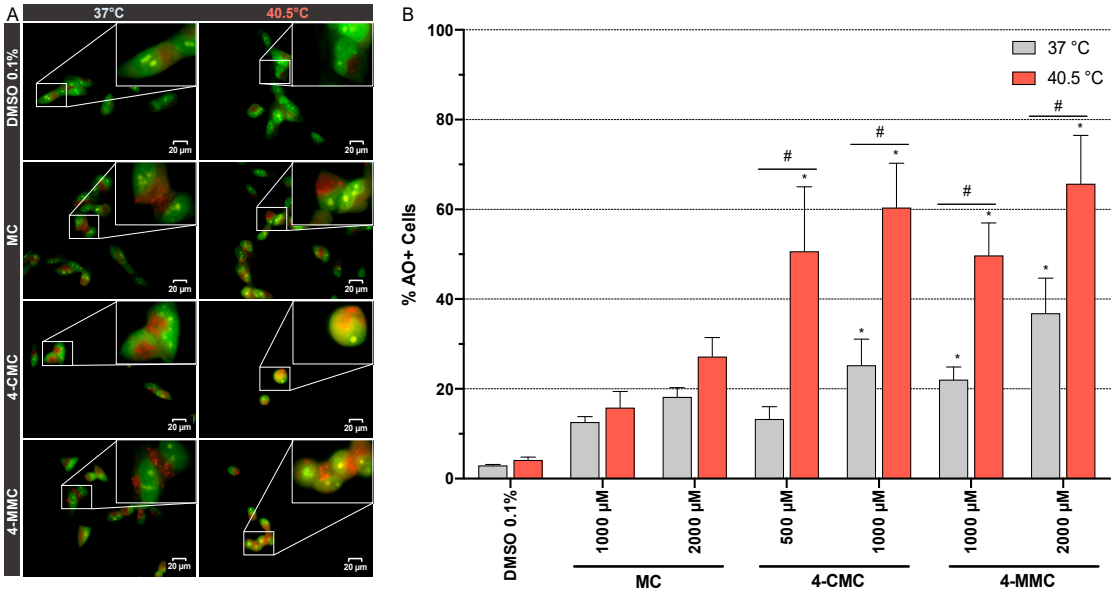

Figure 7. (**A**) Fluorescence microscopy visualization of acidic vesicular organelles (AVOs) stained with acridine orange (AO). SH-SY5Y cells were exposed to MC, 4-CMC, and 4-MMC (1000 µM) for 24 h at 37 and 40.5 °C. Scale bar 20 µm, magnification 60×. (**B**) Flow cytometric quantification of AVOs. SH-SY5Y cells were exposed to MC (1000 and 2000 µM), 4-CMC (500 and 1000 µM), and 4-MMC (1000 and 2000 µM) for 24 h at 37 and 40.5 °C. Data are expressed as mean ± SEM of five independent experiments. Statistical comparisons were performed with one-way ANOVA followed by *t*-tests (* $P \leq 0.05$ versus control at the same temperature; $^{\#}P \leq 0.05$ versus the same concentration at a different temperature).

4. Discussion

Barbosa et al. [17] have shown in a previous study that the toxicity of ecstasy and ecstasy metabolites on differentiated SH-SY5Y cells is increased at hyperthermic (40 °C) compared to normothermic (37 °C) conditions. Similarly, in the present study, we demonstrated that hyperthermic conditions increase the cytotoxicity of methcathinones by inducing apoptotic and necrotic cell death. The loss in cell membrane integrity was preceded by a decrease in cellular ATP content, a typical feature of mitochondrial toxicants [21,35]. We could confirm our previous investigations on the hepatocellular and muscle toxicity observed with these drugs [27,36].

The choice of the higher temperature was based on the study of Barbosa et al. [17] and on clinical reports suggesting that body temperatures ≥40 °C are associated with severe complications, such as intravascular coagulation, rhabdomyolysis, renal and multiorgan failure, and even death, in patients having ingested ecstasy or other psychostimulants [9,10].

The mitochondrial toxicity of the methcathinones studied was confirmed by the investigation of their effect on mitochondrial respiration. For all compounds studied, a prominent reduction of basal and FCCP-induced respiration was observed at 40.5 °C compared to 37 °C. Mitochondrial toxicants that reduce the OCR, which indicates an impairment of the electron transport chain, can result in a decrease in $\Delta\psi m$ and an increase in mitochondrial generation of ROS [37], which we observed in the current study. In agreement with the results of the current study, previous in vitro investigations have shown that synthetic methcathinones increase the production of ROS and nitrogen reactive species in human dopaminergic SH-SY5Y cells [25]. Moreover, animal studies revealed that methcathinones increase the expression of the antioxidant enzymes superoxide dismutase, catalase, and glutathione peroxidase in response to ROS accumulation [38].

Mitochondrial impairment and ROS accumulation can lead to the opening of the mitochondrial permeability transition pore (mPTP), and subsequently to the release of cytochrome *c* into the cytoplasm, which is followed by caspase activation and apoptosis [39,40]. In our study, exposure to 4-CMC and 4-MMC already induced apoptosis and/or necrosis at both temperature conditions after 6 h of incubation.

Surprisingly, after 6 h of incubation, the compounds investigated were more toxic at normothermic conditions than under hyperthermic conditions, whereas, after 24 h, the temperature shift from 37 to 40.5 °C clearly increased the toxicity of the methcathinones studied. These findings suggested the induction of defensive mechanisms that could protect the cells during the first hours of the caloric insult. We therefore determined the expression of Hsp70 proteins, which are molecular chaperones synthesized in response to a heat shock [41]. As shown in Figure 5, hyperthermic conditions increased the expression of Hsp70 proteins, independently of the exposure to the compounds tested. Already after 6 h at 40.5 °C, the expression of Hsp70 was significantly higher than under normothermic conditions. These proteins, which assist in the folding and assembly of newly synthesized proteins as well as refolding of misfolded and aggregated proteins, act in an ATP-controlled fashion [42]. Importantly, Hsp70 proteins can inhibit mitochondrial cytochrome *c* release, apoptosome formation, and caspase activation [43,44]. The results of the current study suggest that at the 6-h time point, the induction of HSP70 partially prevented not only the cellular damage induced by heat but also the toxic insult by the methcathinones investigated.

However, because of the ongoing ROS-induced protein and organelle damage and the associated decrease in the cellular ATP content, this defensive system may be not able to counteract the cellular insults. Autophagy is an additional defensive mechanism, which may be stimulated under these conditions. In support of this assumption, it has been shown that 3-fluoromethcathinone (3-FMC), another synthetic methcathinone, activates autophagy in the neuronal cell line HT22 [45]. Autophagy is an evolutionarily conserved process, which plays a pivotal role in maintaining the viability of eukaryotic organisms by regulating the intracellular balance between anabolism and catabolism [46]. Autophagy is activated as a protective mechanism when cells are not able to respond to nutrient stress, the accumulation of misfolded proteins, and/or organelle damage [47]. In our investigations, LC3 II,

an early marker of autophagy [48], was overexpressed in SH-SY5Y cells after exposure to 4-CMC under both temperature conditions. Furthermore, we demonstrated the stimulation of autophagy directly by the visualization of acidic vesicular organelles (AVOs) in SH-SY5Y cells exposed to 4-CMC and 4-MMC, which is a marker of late autophagy. Similar to the induction of HSP70, hyperthermic conditions also increased the formation of AVOs, suggesting that the activation of the cellular defense systems is tightly coordinated.

In comparison to their pharmacological activity, which is observed in the high nanomolar to micromolar range depending on the compound and the pharmacological effect considered [49], cytotoxicity was detected at higher concentrations in the current study. For 4-CMC, blood concentrations reached approximately 1 micromolar with non-toxic pharmacological doses and up to 10 micromolar in patients with intoxications [50]. In the current study, we started to see an impairment of cellular oxygen uptake at 200 micromolar for MC, 4-CMC, and 4-MMC. A possible explanation for this discrepancy between pharmacological activity and in vitro toxicity may be that the cell lines used in the current study may be less sensitive to toxicants than primary cells. This has, for instance, been shown for hepatotoxicants, which are typically less toxic for human hepatocyte cell lines than for primary human hepatocytes [51,52]. Furthermore, patients presenting with neurotoxicity have usually ingested doses higher than the pharmacological doses of these compounds and may have ingested additional toxic drugs and/or alcohol. Finally, the brain/plasma concentration ratio for 4-MMC is >1, indicating that the drug penetrates the blood–brain barrier easily and that the concentration reached in the brain is higher than in plasma [53].

Interestingly, many studies have shown a link between autophagy and neurodegenerative diseases [31,54,55]. A prevalent pathological feature of many neurodegenerative diseases, such as Alzheimer's disease (AD), Parkinson's disease (PD), and Huntington disease (HD), is in fact the aggregation of misfolded proteins, which may result from the production of defective proteins and/or impaired function of the protein quality control systems. Our studies suggest that repetitive ingestion of neurotoxic drugs, such as methcathinones, and other neurotoxic neurostimulants may aggravate or even provoke such conditions.

5. Conclusions

In conclusion, 4-CMC and 4-MMC are mitochondrial toxicants whose toxicity is increased by shifting the temperature from 37 to 40.5 °C. SH-SY5Y cells exposed to 40.5 °C activate cellular defense mechanisms, such as the expression of Hsp70 proteins, which can partially prevent early apoptosis and necrosis. With time, the activation of additional defense mechanisms, such as autophagy, is necessary to prevent cell dysfunction and cell death. Mitochondrial toxicity, which is accentuated by hyperthermia, represents an important mechanism of the neural toxicity of these compounds.

Supplementary Materials: The following are available online at http://www.mdpi.com/2073-4409/9/4/965/s1, Figure S1: Chemical structures of amphetamine and methcathinone derivatives, Figure S2: Plasma membrane integrity and intracellular ATP content of SH-SY5Y cells exposed to amphetamine and amphetamine derivatives, Figure S3: Mitochondrial membrane potential in SH-SY5YX cells exposed to methcathinone derivatives, Figure S4: Percentage of viable, necrotic and apoptotic cells after 24 h of exposure to methcathinone derivatives, Figure S5: Plasma membrane integrity and intracellular ATP content of SH-SY5Y cells exposed for 6 h to methcathinone derivatives, Table S1: IC_{50} values of membrane toxicity and ATP depletion of SH-SY5Y cells exposed to methcathinone derivatives.

Author Contributions: Study design: X.Z., R.V.M., S.K.; experiments: X.Z., J.B., R.V.M.; data interpretation: X.Z., J.B., R.V.M., S.K.; writing—original draft preparation: X.Z., J.B., R.V.M.; writing—review and editing: J.B., R.V.M., M.E.L., S.K.; funding acquisition: X.Z., S.K. All authors have read and agreed to the published version of the manuscript.

Funding: The research was funded by a grant from the Swiss National Science Foundation to S.K. (SNF 31003A_156270). X.Z. is a recipient of China Scholarship Council Stipendium of the P.R. China.

Conflicts of Interest: The authors declare no conflict of interest.

References

1. Smith, J.P.; Sutcliffe, O.B.; Banks, C.E. An overview of recent developments in the analytical detection of new psychoactive substances (NPSs). *Analyst* **2015**, *140*, 4932–4948. [CrossRef]
2. Madras, B.K. The Growing Problem of New Psychoactive Substances (NPS). *Curr. Top. Behav. Neurosci.* **2017**, *32*, 1–18. [PubMed]
3. Valente, M.J.; Guedes de Pinho, P.; de Lourdes Bastos, M.; Carvalho, F.; Carvalho, M. Khat and synthetic cathinones: A review. *Arch. Toxicol.* **2014**, *88*, 15–45. [CrossRef]
4. Taschwer, M.; Weiβ, J.A.; Kunert, O.; Schmid, M.G. Analysis and characterization of the novel psychoactive drug 4-chloromethcathinone (clephedrone). *Forensic Sci. Int.* **2014**, *244*, e56–e59. [CrossRef]
5. Griffiths, P.; Lopez, D.; Sedefov, R.; Gallegos, A.; Hughes, B.; Noor, A.; Royuela, L. Khat use and monitoring drug use in Europe: The current situation and issues for the future. *J. Ethnopharmacol.* **2010**, *132*, 578–583. [CrossRef] [PubMed]
6. Schifano, F.; Napoletano, F.; Arillotta, D.; Zangani, C.; Gilgar, L.; Guirguis, A.; Corkery, J.M.; Vento, A. The clinical challenges of synthetic cathinones. *Br. J. Clin. Pharmacol.* **2019**, *86*, 410–419. [CrossRef] [PubMed]
7. Prosser, J.M.; Nelson, L.S. The toxicology of bath salts: A review of synthetic cathinones. *J. Med. Toxicol.* **2012**, *8*, 33–42. [CrossRef] [PubMed]
8. Paillet-Loilier, M.; Cesbron, A.; Le Boisselier, R.; Bourgine, J.; Debruyne, D. Emerging drugs of abuse: Current perspectives on substituted cathinones. *Subst. Abuse Rehabil.* **2014**, *5*, 37–52. [PubMed]
9. Liechti, M.E. Effects of MDMA on body temperature in humans. *Temperature* **2014**, *1*, 192–200. [CrossRef]
10. Callaway, C.W.; Clark, R.F. Hyperthermia in psychostimulant overdose. *Ann. Emerg. Med.* **1994**, *24*, 68–76. [CrossRef]
11. Halpern, P.; Moskovich, J.; Avrahami, B.; Bentur, Y.; Soffer, D.; Peleg, K. Morbidity associated with MDMA (ecstasy) abuse: A survey of emergency department admissions. *Hum. Exp. Toxicol.* **2011**, *30*, 259–266. [CrossRef]
12. Zaami, S.; Giorgetti, R.; Pichini, S.; Pantano, F.; Marinelli, E.; Busardò, F.P. Synthetic cathinones related fatalities: An update. *Eur. Rev. Med. Pharmacol. Sci.* **2018**, *22*, 268–274. [PubMed]
13. Angoa-Pérez, M.; Anneken, J.H.; Kuhn, D.M. Neurotoxicology of synthetic cathinone analogs. *Curr. Top. Behav. Neurosci.* **2017**, *32*, 209–230.
14. Camilleri, A.M.; Caldicott, D. Underground pill testing, down under. *Forensic Sci. Int.* **2005**, *151*, 53–58. [CrossRef]
15. Parrott, A.C. MDMA (3, 4-Methylenedioxymethamphetamine) or ecstasy: The neuropsychobiological implications of taking it at dances and raves. *Neuropsychobiology* **2004**, *50*, 329–335. [CrossRef] [PubMed]
16. Parrott, A.C.; Rodgers, J.; Buchanan, T.; Ling, J.; Heffernan, T.; Scholey, A.B. Dancing hot on Ecstasy: Physical activity and thermal comfort ratings are associated with the memory and other psychobiological problems reported by recreational MDMA users. *Hum. Psychopharmacol.* **2006**, *21*, 285–298. [CrossRef] [PubMed]
17. Barbosa, D.J.; Capela, J.P.; Silva, R.; Ferreira, L.M.; Branco, P.S.; Fernandes, E.; Bastos, M.L.; Carvalho, F. "Ecstasy"-induced toxicity in SH-SY5Y differentiated cells: Role of hyperthermia and metabolites. *Arch Toxicol.* **2014**, *88*, 515–531. [CrossRef]
18. Kovalevich, J.; Langford, D. Considerations for the use of SH-SY5Y neuroblastoma cells in neurobiology. *Methods Mol. Biol.* **2013**, *1078*, 9–21.
19. Kysenius, K.; Brunello, C.A.; Huttunen, H.J. Mitochondria and NMDA receptor-dependent toxicity of berberine sensitizes neurons to glutamate and rotenone injury. *PLoS One* **2014**, *9*, e107129. [CrossRef]
20. Song, M.S.; Ryu, P.D.; Lee, S.Y. Kv3.4 is modulated by HIF-1α to protect SH-SY5Y cells against oxidative stress-induced neural cell death. *Sci. Rep.* **2017**, *7*, 2075. [CrossRef]
21. Felser, A.; Blum, K.; Lindinger, P.W.; Bouitbir, J.; Krähenbühl, S. Mechanisms of hepatocellular toxicity associated with dronedarone-a comparison to amiodarone. *Toxicol. Sci.* **2013**, *131*, 480–490. [CrossRef] [PubMed]
22. Wang, C.-M.; Yang, C.-Q.; Cheng, B.-H.; Chen, J.; Bai, B. Orexin-A protects SH-SY5Y cells against H2O2-induced oxidative damage via the PI3K/MEK1/2/ERK1/2 signaling pathway. *Int. J. Immunopathol. Pharmacol.* **2018**, *32*, 2058738418785739. [CrossRef]

23. Ferlemann, F.C.; Menon, V.; Condurat, L.; Rössler, J. Surface marker profiling of SH-SY5Y cells enables small molecule screens identifying BMP4 as a modulator of neuroblastoma differentiation. *Sci. Rep.* **2017**, *7*. [CrossRef] [PubMed]
24. Yano, K.; Yanagisawa, T.; Mukae, K.; Niwa, Y.; Inoue, Y.; Moriyasu, Y. Dissection of autophagy in tobacco BY-2 cells under sucrose starvation conditions using the vacuolar H+-ATPase inhibitor concanamycin A and the autophagy-related protein Atg8. *Plant Signal Behav.* **2015**, *10*, e1082699. [CrossRef] [PubMed]
25. Valente, M.J.; Amaral, C.; Correia-da-Silva, G.; Duarte, H.A. Methylone and MDPV activate autophagy in human dopaminergic SH-SY5Y cells: A new insight into the context of β-keto amphetamines-related neurotoxicity. *Arch. Toxicol.* **2017**, *91*, 3663–3676. [CrossRef] [PubMed]
26. Thomé, M.P.; Filippi-Chiela, E.C.; Villodre, E.S.; Migliavaca, C.B.; Onzi, G.R.; Felipe, K.B.; Lenz, G. Ratiometric analysis of Acridine Orange staining in the study of acidic organelles and autophagy. *J.Cell Sci.* **2016**, *129*, 4622–4632. [CrossRef]
27. Zhou, X.; Luethi, D.; Sanvee, G.M.; Bouitbir, J.; Liechti, M.E.; Krähenbühl, S. Molecular Toxicological Mechanisms of Synthetic Cathinones on C2C12 Myoblasts. *Int. J. Mol. Sci.* **2019**, *20*, 1561. [CrossRef]
28. Wang, Y.; Nartiss, Y.; Steipe, B.; McQuibban, G.A.; Kim, P.K. ROS-induced mitochondrial depolarization initiates PARK2/PARKIN-dependent mitochondrial degradation by autophagy. *Autophagy* **2012**, *8*, 1462–1476. [CrossRef]
29. Eguchi, Y.; Shimizu, S.; Tsujimoto, Y. Intracellular ATP levels determine cell death fate by apoptosis or necrosis. *Cancer Res.* **1997**, *57*, 1835–1840.
30. Sharma, D.; Masison, D.C. Hsp70 structure, function, regulation and influence on yeast prions. *Protein Pept. Lett.* **2009**, *16*, 571–581. [CrossRef]
31. Guo, F.; Liu, X.; Cai, H.; Le, W. Autophagy in neurodegenerative diseases: Pathogenesis and therapy. *Brain Pathol.* **2018**, *28*, 3–13. [CrossRef]
32. Katschinski, D.M.; Boos, K.; Schindler, S.G.; Fandrey, J. Pivotal role of reactive oxygen species as intracellular mediators of hyperthermia-induced apoptosis. *J. Biolog. Chem.* **2000**, *275*, 21094–21098. [CrossRef] [PubMed]
33. Kuma, A.; Matsui, M.; Mizushima, N. LC3, an autophagosome marker, can be incorporated into protein aggregates independent of autophagy: Caution in the interpretation of LC3 localization. *Autophagy* **2007**, *3*, 323–328. [CrossRef]
34. Tanida, I.; Ueno, T.; Kominami, E. LC3 and Autophagy. *Methods Mol. Biol.* **2008**, *445*, 77–88. [PubMed]
35. Fromenty, B.; Fisch, C.; Berson, A.; Letteron, P.; Larrey, D.; Pessayre, D. Dual effect of amiodarone on mitochondrial respiration. Initial protonophoric uncoupling effect followed by inhibition of the respiratory chain at the levels of complex I and complex II. *J. Pharmacol. Exp. Ther.* **1990**, *255*, 1377–1384. [PubMed]
36. Luethi, D.; Liechti, M.E.; Krähenbühl, S. Mechanisms of hepatocellular toxicity associated with new psychoactive synthetic cathinones. *Toxicology* **2017**, *387*, 57–66. [CrossRef] [PubMed]
37. Bae, Y.S.; Oh, H.; Rhee, S.G.; Yoo, Y.D. Regulation of reactive oxygen species generation in cell signaling. *Mol. Cells* **2011**, *32*, 491–509. [CrossRef] [PubMed]
38. López-Arnau, R.; Martinez-Clemente, J.; Rodrigo, T.; Pubill, D.; Camarasa, J.; Escubendo, E. Neuronal changes and oxidative stress in adolescent rats after repeated exposure to mephedrone. *Toxicol. Appl. Pharmacol.* **2015**, *286*, 27–35. [CrossRef]
39. Liu, X.; Kim, C.N.; Yang, J.; Jemmerson, R.; Wang, X. Induction of apoptotic program in cell-free extracts:Requirement for datp and cytochrome c. *Cell* **1996**, *86*, 147–157. [CrossRef]
40. Green, D.R.; Reed, J.C. Mitochondria and apoptosis. *Science* **1998**, *281*, 1309–1312. [CrossRef]
41. He, Z.; Sun, X.; Ma, Z.; Fu, J.; Huang, B.; Liu, F.; Chen, Y.; Deng, T.; Han, X.; Sun, D. Heat shock protein 70 protects mouse against post-infection irritable bowel syndrome via up-regulating intestinal gammadelta T cell's Th17 response. *Cell Biosci.* **2018**, *8*, 38. [CrossRef] [PubMed]
42. Mayer, M.; Bukau, B. Hsp70 chaperones: Cellular functions and molecular mechanism. *Cell. Mol. Life Sci.* **2005**, *62*, 670. [CrossRef]
43. Stankiewicz, A.R.; Lachapelle, G.; Foo, C.P.; Radicioni, S.M.; Mosser, D.D. Hsp70 inhibits heat-induced apoptosis upstream of mitochondria by preventing Bax translocation. *J. Biol. Chem.* **2005**, *280*, 38729–38739. [CrossRef] [PubMed]
44. Li, C.Y.; Lee, J.S.; Ko, Y.G.; Kim, J.I.; Seo, J.S. Heat shock protein 70 inhibits apoptosis downstream of cytochrome c release and upstream of caspase-3 activation. *J. Biol. Chem.* **2000**, *275*, 25665–25671. [CrossRef] [PubMed]

45. Siedlecka-Kroplewska, K.; Wrońska, A.; Stasiłojć, G.; Kmieć, Z. The designer drug 3-fluoromethcathinone induces oxidative stress and activates autophagy in HT22 neuronal cells. *Neurotox Res.* **2018**, *34*, 388–400. [CrossRef] [PubMed]
46. Khandia, R.; Dadar, M.; Munjal, A.; Dhama, K.; Karthik, K.; Tiwari, R.; Yatoo, M.I.; Iqbal, H.M.N.; Pal Singh, K.; Joshi, S.K.; et al. A comprehensive review of autophagy and its various roles in infectious, non-infectious, and lifestyle diseases: Current knowledge and prospects for disease prevention, novel drug design, and therapy. *Cells* **2019**, *8*, 674. [CrossRef] [PubMed]
47. Kroemer, G.; Levine, B. Autophagic cell death: The story of a misnomer. *Nat. Rev. Mol Cell Biol.* **2008**, *9*, 1004–1010. [CrossRef]
48. Tanida, I.; Minematsu-Ikeguchi, N.; Ueno, T.; Kominami, E. Lysosomal turnover, but not a cellular level, of endogenous LC3 is a marker for autophagy. *Autophagy* **2005**, *1*, 84–91. [CrossRef]
49. Luethi, D.; Walter, W.; Zhou, X.; Rudin, D.; Krähenbühl, S.; Liechti, M.E. Para-Halogenation Affects Monoamine Transporter Inhibition Properties and Hepatocellular Toxicity of Amphetamines and Methcathinones. *Front. Pharmacol.* **2019**, *10*, 438. [CrossRef]
50. Tomczak, E.; Woźniak, M.K.; Kata, M.; Wiergowski, M.; Szpiech, B.; Biziuk, M. Blood concentrations of a new psychoactive substance 4-chloromethcathinone (4-CMC) determined in 15 forensic cases. *Forensic Toxicol.* **2018**, *36*, 476–485. [CrossRef]
51. Berger, B.; Donzelli, M.; Maseneni, S.; Boess, F.; Roth, A.; Krähenbühl, S.; Haschke, M. Comparison of Liver Cell Models Using the Basel Phenotyping Cocktail. *Front. Pharmacol.* **2016**, *7*, 443. [CrossRef] [PubMed]
52. Gerets, H.H.; Tilmant, K.; Gerin, B.; Chanteux, H.; Depelchin, B.O.; Dhalluin, S.; Atienzar, F.A. Characterization of primary human hepatocytes, HepG2 cells, and HepaRG cells at the mRNA level and CYP activity in response to inducers and their predictivity for the detection of human hepatotoxins. *Cell. Biol. Toxicol.* **2012**, *28*, 69–87. [CrossRef]
53. Calinski, D.M.; Kisor, D.F.; Sprague, J.E. A review of the influence of functional group modifications to the core scaffold of synthetic cathinones on drug pharmacokinetics. *Psychopharmacology (Berl)* **2019**, *236*, 881–890. [CrossRef]
54. Turturici, G.; Sconzo, G.; Geraci, F. Hsp70 and its molecular role in nervous system diseases. *Biochem. Res. Int.* **2011**, *2011*, 618127. [CrossRef] [PubMed]
55. Penke, B.; Bogár, F.; Crul, T.; Sántha, M.; Tóth, M.E.; Vígh, L. Heat shock proteins and autophagy pathways in neuroprotection: From molecular bases to pharmacological interventions. *Int. J. Mol. Sci.* **2018**, *19*, 325. [CrossRef] [PubMed]

Discussion

Abuse of psychostimulant drugs is becoming a more and more serious problem in the world [251]. Clinical case reports have shown that the abuse of psychostimulant drugs can result in significant organ damage in users, affecting the liver, muscle and/or brain [79, 124, 252-257]. Another important acute side effect due to the use of psychostimulant drugs is hyperthermia, which is a contributing factor to several acute complications and which can lead to a fatal outcome [243, 246]. Therefore, we aimed to assess the toxicological mechanisms of psychostimulant drugs in vitro (muscle, liver and neuronal cells), and to assess how hyperthermic conditions may affect the toxicity of these drugs in neuron cells.

In our studies, we used concentrations of drugs ranging from 100 µM to 2000 µM. In some fatality cases, the plasma concentrations of these NPS reached 22.00 mg/L (~125 µM, 4-MMC), 18.50 mg/L (105 µM, MDMA), 3.13 mg/L (17.78 µM, methylone), 0.64 mg/L (~3.64 µM, α-PVP), 0.30 mg/L (~1.70 µM, 3-MMC), 0.17 mg/L (~0.97 µM, MDPV) [52, 247, 258-260]. These concentrations are quite lower than the highest drug concentration used by us *in vitro* (2000 µM). There are two reasons for using high concentrations: (1) high concentrations were used to elucidate the molecular toxicological mechanisms of these drugs, since *in vivo* their effects can be observed only at higher concentrations than *in vivo* [73]. (2) users often use these drugs for a long time, in this regard, in our experimental settings we used higher concentrations for shorter exposure time, a common research method *in vitro* [261]. It has also to be taken into account that we used cell lines for our investigations, which may be less sensitive than primary cells. Furthermore, only serum concentrations have been determined (or post mortem blood concentrations), which may not reflect the concentrations in the brain.

1. Effect of *para*-halogenation on amphetamines and cathinones

Our current studies suggested that the toxicity rank order of these *para*-halogenated amphetamines and methcathinones is the following: Cl >F >H. According to the IC_{50} values of membrane integrity in HepG2 cells, and undifferentiated and differentiated SH-SY5Y cells, we found that PCA impairs the cell membrane at lower concentrations than the other investigated drugs, followed by 4-FA. Amphetamine showed the highest IC_{50}. Moreover, the results in these three cell types have shown that fluorinated and chlorinated forms of amphetamine can induce mitochondrial dysfunction, however, amphetamine showed mitochondrial toxicity only in HepG2 cells. A similar result for the *para*-halogenated forms of cathinone was observed. 4-CMC can cause cell membrane integrity loss in HepG2 cells,

undifferentiated and differentiated SH-SY5Y cells, while no effect was observed for 4-FMC and MC at concentrations up to 2 mM. Besides that, only 4-CMC was a mitochondrial toxicant among all the *para*-halogenated cathinones. Taken together, both *p*-F and *p*-Cl increase the cytotoxicity of amphetamine and methcathinone.

This finding could be explained by the data of Fuller et al. [45]. *para*-Halogenated amphetamine derivatives are more lipophilic, they show longer half-life, and also are more potent inhibitors of the monoamine oxidase, again following the order Cl >F >H.

In addition to the toxicity rank (Cl >F >H), *para*-halogenation has other effects on drugs. Based on our pharmacological experiments, *para*-halogenated phenylethylamines may enhance serotonergic effects [262]. One feasible explanation is that the *para*-halogenation prevents *para*-hydroxylation, and then prolongs the half-life of the compound, enhancing its clinical effects [263]. For *para*-halogenated amphetamines and methcathinones, inhibition of norepinephrine uptake was observed at sub-micromolar concentrations. Other authors reported that the *para*-halogenation reduces the selectivity towards DAT over SERT [19, 264-266]. PCA and 4-CMC were considered to reduce the selectivity towards SERT and DAT in a similar manner as *para*-methylation [267]. The inhibition of NET and DAT correlated with human effective doses, while SERT inhibition was inversely correlated with human effective doses [268], suggesting that the clinical effects of halogenation are low. However, the highly potent serotonergic activity and fairly strong dopaminergic activity can be a possible explanation of the severe serotonergic neurotoxicity of PCA [269]. Furthermore, it has been reported that amphetamines can enhance users' risk of developing Parkinson's syndrome 1.5 to 3 times [270, 271]. Parkinson's syndrome develops due to the loss of dopaminergic neurons in the nigrostriatal system, which may be induced by mitochondrial damage [272]. As a result, current research suggests that the halogenation of stimulant drugs may increase this risk. If confirmed, this will be an important finding which could have an impact on the use of these halogenated compounds.

2. Mitochondrial mechanism of toxicity

The mechanism beyond the organ damage induced by NPS is not completely clear yet [273]. Mitochondria are known as energy generators for cells, and as well as a primary target in drug toxicity, due to their structural and functional characteristics [164, 274].

In our current studies, we found that amphetamine, 4-FA and PCA are among all the amphetamines tested *in vitro* mitochondrial toxicants. Moreover, high concentrations of 4-FA can trigger apoptosis in HepG2 cells, and PCA can induce apoptosis in undifferentiated and differentiated SH-SY5Y cells. For the investigated synthetic cathinones, 4-CMC can cause mitochondrial dysfunction and apoptosis in HepG2 cells, undifferentiated and differentiated SH-SY5Y cells. 4-MMC showed as well mitochondrial toxicity in undifferentiated SH-SY5Y cells. Besides that, α-PVP and naphyrone were also strong toxicants in C2C12 myoblasts, affecting their mitochondrial function. In more detail, a decrease in the ATP content prior to cell membrane integrity loss after drug exposure suggests that the mitochondria are a target of these drugs [275, 276]. We found that the IC_{50} values of ATP content decrease were lower than the IC_{50} values of membrane toxicity (MT) after amphetamine, 4-FA, PCA and 4-CMC exposure in HepG2 cells, and for α-PVP and naphyrone in C2C12 cells. This effect was observed for 4-FA, PCA, 4-MMC and 4-CMC in undifferentiated SH-SY5Y cells, as well for 4-FA, PCA and 4-CMC in differentiated SH-SY5Y cells. It is known that the decrease of the cellular ATP content and the $\Delta\psi m$ are considered as markers of the perturbation of mitochondria [277]. We found that a significant reduction of the $\Delta\psi m$ at similar concentrations of the depletion of the cellular ATP, after 4-FA, PCA and 4-CMC exposure. Additionally, the decrease of cellular ATP and $\Delta\psi m$ can be associated with the impairment and/or uncoupling of the mitochondrial respiratory chain [164]. In HepG2 cells, amphetamine decreased the basal respiratory capacity, whereas 4-FA, PCA and 4-CMC decreased both basal and maximal respiration. For C2C12 cells, α-PVP and naphyrone not only impaired basal respiratory capacity, but also decreased the maximal respiration at similar concentrations after treatment for 1 or 24 h. α-PVP and naphyrone impaired the activity of enzyme complexes of the ETC. α-PVP inhibited complex I, and naphyrone inhibited complex II. Our data in undifferentiated and differentiated SH-SY5Y cells demonstrated that PCA and 4-CMC reduced basal and maximal respiration, while 4-MMC only impaired the basal respiratory capacity in undifferentiated SH-SY5Y cells. 4-CMC exposure resulted in decrease of the leak and maximal respiration at a lower concentration than 4-MMC in undifferentiated SH-SY5Y cells. This indicates that 4-CMC is slightly more toxic than 4-MMC [278].

It is well known that the neurotoxicity of amphetamines and synthetic cathinones can be linked with the accumulation of cellular ROS [79, 135, 273, 279-283]. Since the enzyme

complexes I and III of the ETC are potential sites for ROS formation, the increase in ROS levels may cause disruption of the mitochondrial respiratory chain, damage of various cellular components and result in mitochondrial toxicity [187, 284, 285]. Concentration-dependent increases in ROS were also observed after treatment with amphetamine, 4-FA, PCA and 4-CMC in HepG2 cells. PCA and 4-CMC promoted the ROS production in undifferentiated and differentiated SH-SY5Y cells, while 4-FA and 4-CMC increased the ROS level only in undifferentiated SH-SY5Y cells. In C2C12 cells, as expected, α-PVP and naphyrone led to an increase of mitochondrial ROS level. Additionally, the *in vivo* data shown by Naserzadeh et al. suggest that 4-MMC could promote mitochondrial ROS production and impair the outer mitochondrial membrane [286]. This result is consistent with our observations of 4-MMC. In conclusion, NPS-induced mitochondrial dysfunction is related to the inhibition of mitochondrial oxidative metabolism. Furthermore, the impairment of the cellular antioxidant response could contribute to the increase in ROS levels. These findings are in agreement with a recent report of Chen et al., showing the toxicity of amphetamines in a pulmonary artery model [124, 287].

The release of cytochrome *c* from mitochondria can trigger the activation of caspases, suggesting that ROS play an important role in apoptosis [288]. We further investigated cell death mechanisms in HepG2 cells. As shown in our study, a concentration-dependent increase in apoptotic and necrotic cells appear after treatment with 4-FA. These observations are in accordance with the effect on the cellular ATP level [289]. The assessment of ATP content after PCA exposure showed a decrease in the ATP content at a lower concentration than for 4-FA and amphetamine. Treatment with 0.5 mM PCA resulted in almost complete depletion of ATP, indicating a large number of necrotic cells at this concentration. After treatment with 2 mM amphetamine and 4-FA, the amount of necrotic and apoptotic cells showed no significant difference from the control incubation. In undifferentiated and differentiated SH-SY5Y cells, PCA and 4-CMC also caused a large amount of ROS accumulation and further triggered apoptosis. In this regard, the generation of mitochondrial ROS can result in opening of the mitochondrial permeability transition pore (mPTP), which is linked to a drop of the mitochondrial membrane potential and the release of cytochrome *c* into the cytoplasm where it may activate the caspase pathway [207, 290]. Further studies supported this finding; we found that 4-CMC induce apoptosis *via* the activation of caspase 9 and 3, the endogenous apoptotic pathway.

3. Non-mitochondrial mechanism of toxicity

In addition to mitochondrial dysfunction, other mechanisms can decrease the cellular ATP content and lead to cytotoxicity. In our studies, a drop in the cellular ATP content was observed after methcathinone and 4-FMC exposure in HepG2 cells, while 3-MMC, MDPV and methylone resulted in cytotoxicity with a non-mitochondrial mechanism in C2C12 cells.

Data generated in our studies demonstrated that methcathinone, 4-FMC, 3-MMC, MDPV and methylone could cause ATP depletion without impairing the function of the mitochondrial respiratory chain and the activity of enzyme complexes of the mitochondrial ETC. One possible reason why these drugs induced ATP depletion without detecting mitochondrial dysfunction is that when glucose is present in cells, ATP can also originate from glycolysis, which may be impaired by these drugs [291]. In addition, the IC_{50} values of impaired membrane integrity and ATP depletion are close, indicating that ATP depletion may be a secondary event after disrupting membrane integrity [291]. To our surprise, we also observed the increase of cellular ROS level for 3-MMC, MDPV and methylone, without impairment of the ETC. One of the possible reasons is that low expression of SOD2 results in low antioxidant capacity of C2C12 myoblasts and HepG2 cells [291, 292].

4. Effect of NPS on Different Cell Types

In our studies, the concentrations of NPS used were much higher than the concentrations pharmacologically relevant (<50 μM). Exposure to pharmacological concentration of drugs in primary liver cells and HepG2 cells does not induce toxicity [261]. It is possible that HepG2 cells are robust cell model with low level of transporter and enzyme expression [293], suggesting lower susceptibility to hepatotoxic toxicity than primary liver cells. Moreover, these NPS require active transport to enter cells *in vivo,* it is hard to simulate under experiment conditions *in vitro* due to the limited ability to diffuse across cell membranes [294]. In addition, these NPS can elevate temperature *in vivo*, the toxicity of these NPS may be underestimate *in vitro* [123].

Of note, comparing the effects of NPS in undifferentiated and differentiated SH-SY5Y cells, most of the tested NPS have shown less toxicity in differentiated SH-SY5Y

cells. We can explain that due to cell differentiation, which may modulate the regulation of glycolysis and oxidative phosphorylation, affecting the way cells respond to toxicants-induced oxidative stress [282, 295-297]. Moreover, differentiated SH-SY5Y cells have stronger stimulation of mitochondrial respiration capacity with uncoupling and a higher bioenergetic reserve capacity [297], and differentiated cells may express more SOD enzymes compared to the undifferentiated SH-SY5Y cells [297].

For C2C12 cells, our data showed that naphyrone is a strong toxicant of the mitochondrial function, while MDPV and 4-MMC can cause cytotoxicity through a non-mitochondrial mechanism. Whereas in HepG2 cells naphyrone, MDPV and 4-MMC induced all mitochondrial toxicity by impairing the ETC [124]. These findings seem to point out that the mechanisms of NPS-induced toxicity may vary considerably within different organs.

Taken together, our results in different cell lines show the following rank of sensitivity to NPS-induced mitochondrial toxicity: HepG2 cells <SH-SY5Y cells <C2C12 cells.

5. Hyperthermia

Drug-induced hyperthermia can be caused by several factors. Most psychostimulant drugs can direct increase metabolic heat production and/or decrease heat dissipation [246, 298]. Moreover, drug-induced serotonin syndrome and adrenergic receptor stimulation are also considered as important factors in hyperthermia [246]. MDMA is a very popular amphetamine, its use is associated with body temperature increase. There are three possible mechanisms of MDMA-induced hyperthermia. First, MDMA can cause serotonin release and result in a serotonin syndrome [299]. Second, the increase of dopamine release due to the interaction of MDMA with D_1 receptors [300]. Third, the adrenergic receptor stimulation can lead to mitochondria uncoupling and vasoconstriction [246]. However, to date there are only few studies about the hyperthermia caused by other drugs.

In order to evaluate the possible mechanism of NPS-induced hyperthermia, we explored the pharmacological effects of *para*-substituted amphetamines and methcathinones. They are monoamine transporter substrates [266], which can elevate the extracellular monoamine levels by reversing transporting transporters [301, 302]. This further results in

inhibition of monoamine uptake transport from the synaptic cleft. The *para*-halogenated amphetamines and methcathinones in our study interacted effectively with monoaminergic systems, which regulate body temperature in a variety of ways [303]. In our opinion, hyperthermia could be a possible manifestation of using these substances.

To further investigate the role of hyperthermia on the neurotoxicity induced by these drugs, we first assess the cell membrane integrity of undifferentiated SH-SY5Y cells exposed to these substances at 37 °C or 40.5 °C. Our data demonstrated that high temperatures increased the cytotoxicity and mitochondrial impairment of the synthetic cathinones 4-CMC and 4-MMC. These results were further supported by the data on the mitochondrial respiration. Our results showed that methcathinone, 4-CMC and 4-MMC decreased MMP with a temperature-dependent effect and depleted OCR at low concentrations after incubation at 40.5 °C for 24 h, compared to 37 °C. The inhibition of the complexes of the ETC is likely to increase the production of ROS [304]. In *in vivo* studies, methcathinones can also increase ROS levels and expression of the antioxidant enzymes, superoxide dismutase, catalase, and glutathione peroxidase [305]. In our study, data of ROS production showed that methcathinone, 4-MMC, MDMA as well as low concentration of 4-CMC have significantly elevated the generation of ROS at hyperthermic conditions compared to normothermic conditions. It indicates that a possible reason for hyperthermia-enhanced neurotoxicity is the promotion of ROS production. Moreover, the collapse of the MMP and the accumulation of ROS can be associated with the opening of the mPTP and the initiation of apoptosis *via* the activation of caspases [306].

Apoptosis is a programmed form of cellular death, which is distinct from necrosis as it can occur under physiological and pathological conditions [307]. However, we observed that hyperthermia decreased apoptosis in cells exposed to drugs when compared to 37 °C condition. We tested the expression of Hsp 70, proteins that are considered the cellular defence system against the damage of hyperthermia, and we found that the expression of Hsp 70 was significantly higher at 40.5 °C after 6 h drugs exposure compared with normothermic conditions. These results further supported that hyperthermia activates the Hsp 70 to avoid cell death mechanisms [308]. Furthermore, Hsp 70 proteins can also inhibit the activation caspases [309, 310]. These findings are consistent with our results on the activation of caspase 3.

However the accumulation of protein aggregates and ROS may reach a level where this defensive mechanism is not anymore able to act, consequently, autophagic cell death (ACD) may happen, as shown with 3-fluoromethcathinone (3-FMC) in the neuronal cell line HT22 [311]. In our studies, an enhancement of expression in the marker of early autophagy LC3 II was observed in undifferentiated SH-SY5Y cells after 4-CMC exposure at hyperthermic condition. The flux of autophagy was confirmed by the autophagic inhibitors concanamycin A and bafilomycin A [312]. Moreover, acridine orange (AO) staining showed the formation of acidic vacuolar organelles (AVOs). Our findings show that hyperthermia increased the level of AVOs after exposure of 4-CMC and 4-MMC. This result may have potential significance in some neurodegenerative diseases [313-315].

In conclusion, hyperthermia increases cytotoxicity and mitochondrial dysfunction of methcathinones. However, it also can activate cellular defense mechanism by inducing the expression of Hsp 70 proteins. The accumulation of misfolded proteins and damaged organelles drastically promote autophagic death processes.

Conclusion

In conclusion, our studies demonstrate that in the amphetamine group drugs, 4-FA and PCA show mitochondrial toxicity in HepG2 cells, undifferentiated and differentiated SH-SY5Y cells, while amphetamine has potential mitochondrial toxicity in HepG2 cells. Moreover, high concentrations of 4-FA can trigger apoptosis in HepG2 cells, while PCA can induce apoptosis in undifferentiated and differentiated SH-SY5Y cells. Furthermore, we also found that the toxicity rank for the *para*-substituents: chloride >fluoride >hydrogen.

Concerning the synthetic cathinones, α-PVP and naphyrone strongly affect mitochondria in C2C12 cells. The inhibition of the ETC results in downstream effects like ATP depletion and ROS production. Additionally, 4-CMC is a strong mitochondrial toxicant in HepG2 cells, undifferentiated and differentiated SH-SY5Y cells. 4-MMC is also associated with mitochondrial dysfunctions in undifferentiated SH-SY5Y cells. For 4-MMC and 4-CMC, hyperthermic conditions may increase cytotoxicity and mitochondrial impairment, resulting in autophagic death processes in undifferentiated SH-SY5Y cells. In contrast, 3-MMC, MDPV, methylone, methcathinone and 4-FMC may affect mainly glycolysis rather than mitochondria.

Outlook

Pharmacological and toxicological study on NPS currently abused is highly valuable, and it could further support clinical research and improve the understanding of NPS-induced toxicity.

We demonstrated that several amphetamines and synthetic cathinones can cause mitochondrial toxicity by inhibiting the mitochondrial ETC and oxidative stress. However, there are some NPS that can decrease the ATP content without impairing the mitochondrial function. The impairment on glycolysis, may be studied in more detail. Furthermore, investigations whether methcathinones can cause mitophagy or impair autophagic processes may have a high impact for a better understanding of neurodegenerative diseases.

As we investigated the pharmacology and toxicology effect of these NPS drugs only *in vitro*, it would be interesting to do some studies of these NPS drugs *in vivo*. This will allow us to test low drug concentrations and multiple exposures to simulate the actual use of these NPS and evaluate the systemic effects of these drugs. Moreover, we could study *ex vivo* primary liver, muscle and neuron cells, as better models than cell lines. Finally, we could also use SOD2 or NRF2 knock-out mouse models to investigate the susceptibility to oxidative stress.

References

References

1. Margolis, R.D. and J.E. Zweben, *Treating patients with alcohol and other drug problems: An integrated approach*. 1998: American Psychological Association.
2. Barkley, R.A., G.J. DuPaul, and D.F. Connor, *Stimulants*, in *Practitioner's guide to psychoactive drugs for children and adolescents*. 1999, Springer. p. 213-247.
3. Dickenson, A. and J. Ghandehari, *Anti-convulsants and anti-depressants*, in *Analgesia*. 2006, Springer. p. 145-177.
4. Nichols, D.E., *Hallucinogens.* Pharmacology & therapeutics, 2004. **101**(2): p. 131-181.
5. Hoffer, A. and H. Osmond, *The hallucinogens*. 2013: Elsevier.
6. Madras, B.K., *The growing problem of new psychoactive substances (NPS)*, in *Neuropharmacology of New Psychoactive Substances (NPS)*. 2016, Springer. p. 1-18.
7. Bright, S., *New and emerging drugs.* Melbourne: Australian Drug Foundation, 2013.
8. Neumann, C.S., D.G. Fujimori, and C.T. Walsh, *Halogenation strategies in natural product biosynthesis.* Chemistry & Biology, 2008. **15**: p. 99-109.
9. Neumann, C.S., D.G. Fujimori, and C.T. Walsh, *Halogenation strategies in natural product biosynthesis.* Chemistry & biology, 2008. **15**(2): p. 99-109.
10. Gerebtzoff, G., et al., *Halogenation of drugs enhances membrane binding and permeation.* ChemBioChem, 2004. **5**(5): p. 676-684.
11. Grifell, M., et al., *Patterns of use and toxicity of new para‐halogenated substituted cathinones: 4‐CMC (clephedrone), 4‐CEC (4‐chloroethcatinone) and 4‐BMC (brephedrone).* Human Psychopharmacology: Clinical and Experimental, 2017. **32**(3): p. e2621.
12. Odoardi, S., F.S. Romolo, and S. Strano-Rossi, *A snapshot on NPS in Italy: Distribution of drugs in seized materials analysed in an Italian forensic laboratory in the period 2013–2015.* Forensic science international, 2016. **265**: p. 116-120.
13. Linsen, F., et al., *4‐Fluoroamphetamine in the Netherlands: more than a one‐night stand.* Addiction, 2015. **110**(7): p. 1138-1143.
14. Taschwer, M., et al., *Analysis and characterization of the novel psychoactive drug 4-chloromethcathinone (clephedrone).* Forensic science international, 2014. **244**: p. e56-e59.
15. Brandt, S.D., et al., *Analyses of second‐generation 'legal highs' in the UK: Initial findings.* Drug testing and analysis, 2010. **2**(8): p. 377-382.
16. Miller, K.J., D.C. Anderholm, and M.M. Ames, *Metabolic activation of the serotonergic neurotoxin para-chloroamphetamine to chemically reactive intermediates by hepatic and brain microsomal preparations.* Biochemical pharmacology, 1986. **35**(10): p. 1737-1742.
17. Fuller, R.W., *Effects ofp-chloroamphetamine on brain serotonin neurons.* Neurochemical research, 1992. **17**(5): p. 449-456.
18. Colado, M., T. Murray, and A. Green, *5‐HT loss in rat brain following 3, 4‐methylenedioxymethamphetamine (MDMA), p‐chloroamphetamine and fenfluramine administration and effects of chlormethiazole and dizocilpine.* British journal of pharmacology, 1993. **108**(3): p. 583-589.
19. Suyama, J.A., et al., *Abuse-related neurochemical effects of para-substituted methcathinone analogs in rats: microdialysis studies of nucleus accumbens dopamine*

and serotonin. Journal of Pharmacology and Experimental Therapeutics, 2016. **356**(1): p. 182-190.
20. Steinkellner, T., et al., *The ugly side of amphetamines: short- and long-term toxicity of 3,4-methylenedioxymethamphetamine (MDMA, 'Ecstasy'), methamphetamine and D-amphetamine.* Biological Chemistry, 2011. **392**: p. 103-105.
21. Sulzer, D., et al., *Mechanisms of neurotransmitter release by amphetamines: A review.* Progress in neurobiology, 2005. **75**(6): p. 406-433.
22. Edeleano, L., *Ueber einige Derivate der Phenylmethacrylsäure und der Phenylisobuttersäure.* Berichte der deutschen chemischen Gesellschaft, 1887. **20**(1): p. 616-622.
23. Freudenmann, R.W., F. Öxler, and S. Bernschneider ‐ Reif, *The origin of MDMA (ecstasy) revisited: the true story reconstructed from the original documents.* Addiction, 2006. **101**(9): p. 1241-1245.
24. Biel, J. and B. Bopp, *Amphetamines: Structure-activity relationships*, in *Stimulants*. 1978, Springer. p. 1-39.
25. Iversen, L.L., S.D. Iversen, and S.H. Snyder, *Handbook of psychopharmacology*. Vol. 8. 1977: Plenum Publishing Corporation.
26. Fleckenstein, A.E., et al., *New insights into the mechanism of action of amphetamines.* Annu. Rev. Pharmacol. Toxicol., 2007. **47**: p. 681-698.
27. Yamamoto, B.K., A. Moszczynska, and G.A. Gudelsky, *Amphetamine toxicities: classical and emerging mechanisms.* Annals of the New York Academy of Sciences, 2010. **1187**: p. 101-121.
28. Brown, J.M., G.R. Hanson, and A.E. Fleckenstein, *Methamphetamine rapidly decreases vesicular dopamine uptake.* Journal of neurochemistry, 2000. **74**(5): p. 2221-2223.
29. Greene, S.L., F. Kerr, and G. Braitberg, *Amphetamines and related drugs of abuse.* Emergency Medicine Australasia, 2008. **20**(5): p. 391-402.
30. medicine, T.u.S.o. *Amphetamines (Drug Class)*. 2016, September, 20; Available from: http://tmedweb.tulane.edu/pharmwiki/doku.php/amphetamines.
31. Berman, S.M., et al., *Potential adverse effects of amphetamine treatment on brain and behavior: a review.* Molecular psychiatry, 2009. **14**(2): p. 123-142.
32. Bradley, C., *The behavior of children receiving benzedrine.* American journal of Psychiatry, 1937. **94**(3): p. 577-585.
33. Board, I.N.C., *Report of the International Narcotics Control Board 2004: 2005*. 2005: United Nations Publications.
34. Grinspoon, L. and J.B. Bakalar, *Can drugs be used to enhance the psychotherapeutic process?* American Journal of Psychotherapy, 1986. **40**(3): p. 393-404.
35. Morgan, C.J., et al., *Harms and benefits associated with psychoactive drugs: findings of an international survey of active drug users.* Journal of Psychopharmacology, 2013. **27**(6): p. 497-506.
36. Hysek, C.M., et al., *MDMA enhances emotional empathy and prosocial behavior.* Social cognitive and affective neuroscience, 2013. **9**(11): p. 1645-1652.
37. Hysek, C.M., et al., *Pharmacokinetic and pharmacodynamic effects of methylphenidate and MDMA administered alone or in combination.* International journal of neuropsychopharmacology, 2014. **17**(3): p. 371-381.
38. Capela, J.P., et al., *Molecular and cellular mechanisms of ecstasy-induced neurotoxicity: an overview.* Molecular neurobiology, 2009. **39**(3): p. 210-271.

39. Hondebrink, L., et al., *Fatalities, cerebral hemorrhage, and severe cardiovascular toxicity after exposure to the new psychoactive substance 4-fluoroamphetamine: a prospective cohort study.* Annals of emergency medicine, 2018. **71**(3): p. 294-305.
40. Rösner, P., et al., *Isomeric fluoro-methoxy-phenylalkylamines: a new series of controlled-substance analogues (designer drugs).* Forensic science international, 2005. **148**(2-3): p. 143-156.
41. Nugteren-van Lonkhuyzen, J.J., et al., *Pharmacokinetics, pharmacodynamics and toxicology of new psychoactive substances (NPS): 2C-B, 4-fluoroamphetamine and benzofurans.* Drug and alcohol dependence, 2015. **157**: p. 18-27.
42. Marona-Lewicka, D., et al., *Psychostimulant-like effects of p-fluoroamphetamine in the rat.* European journal of pharmacology, 1995. **287**(2): p. 105-113.
43. Nagai, F., R. Nonaka, and K.S.H. Kamimura, *The effects of non-medically used psychoactive drugs on monoamine neurotransmission in rat brain.* European journal of pharmacology, 2007. **559**(2-3): p. 132-137.
44. Wee, S., et al., *Relationship between the serotonergic activity and reinforcing effects of a series of amphetamine analogs.* Journal of Pharmacology and Experimental Therapeutics, 2005. **313**(2): p. 848-854.
45. Fuller, R., et al., *Comparison of 4-chloro-, 4-bromo-and 4-fluoroamphetamine in rats: drug levels in brain and effects on brain serotonin metabolism.* Neuropharmacology, 1975. **14**(10): p. 739-746.
46. Altman, H.J., et al., *The effects of p-chloroamphetamine, a depletor of brain serotonin, on the performance of rats in two types of positively reinforced complex spatial discrimination tasks.* Behavioral and neural biology, 1989. **52**(2): p. 131-144.
47. Liechti, M.E., *Novel psychoactive substances (designer drugs): overview and pharmacology of modulators of monoamine signalling.* Swiss medical weekly, 2015. **145**: p. w14043.
48. Szendrei, K., *The chemistry of khat.* Bull Narc, 1980. **32**(3): p. 5-35.
49. Kalix, P., *Cathinone, a natural amphetamine.* Pharmacology & toxicology, 1992. **70**(2): p. 77-86.
50. Valente, M.J., et al., *Khat and synthetic cathinones: a review.* Archives of toxicology, 2014. **88**(1): p. 15-45.
51. Roman-Urrestarazu, A., et al., *European Monitoring Centre for Drugs and Drug Addiction: European Monitoring Centre for Drugs and Drug Addiction has a vital role in the UK's ability to respond to illicit drugs and organised crime.* Bmj, 2018. **362**.
52. Blum, K., et al., *Hypothesizing that designer drugs containing cathinones ("bath salts") have profound neuro-inflammatory effects and dangerous neurotoxic response following human consumption.* Medical hypotheses, 2013. **81**(3): p. 450-455.
53. Simmler, L., et al., *Pharmacological characterization of designer cathinones in vitro.* British journal of pharmacology, 2013. **168**(2): p. 458-470.
54. Majchrzak, M., et al., *The newest cathinone derivatives as designer drugs: an analytical and toxicological review.* Forensic toxicology, 2018. **36**(1): p. 33-50.
55. Belhadj-Tahar, H. and N. Sadeg, *Methcathinone: a new postindustrial drug.* Forensic science international, 2005. **153**(1): p. 99-101.
56. Sikk, K. and P. Taba, *Methcathinone "kitchen chemistry" and permanent neurological damage*, in *International review of neurobiology*. 2015, Elsevier. p. 257-271.

57. Emerson, T.S. and J.E. Cisek, *Methcathinone: a Russian designer amphetamine infiltrates the rural midwest.* Annals of emergency medicine, 1993. **22**(12): p. 1897-1903.
58. L'Italien, Y., J. Weston, and H. Park, *Toxicity studies on AL-464. Research Department, Parke, Davis and Co., December 1954, and methylaminoprepiophenone compounds# 2802865.* US Patent Office. August, 1957. **13**.
59. DeRuiter, J., et al., *Methcathinone and designer analogues: synthesis, stereochemical analysis, and analytical properties.* Journal of chromatographic science, 1994. **32**(12): p. 552-564.
60. Gygi, M.P., J.W. Gibb, and G.R. Hanson, *Methcathinone: an initial study of its effects on monoaminergic systems.* Journal of Pharmacology and Experimental Therapeutics, 1996. **276**(3): p. 1066-1072.
61. Sanchez, S., *Sur un homologue de l'ephedrine.* Bull. Soc. Chim. Fr, 1929. **45**: p. 284-286.
62. Papaseit, E., et al., *Clinical pharmacology of the synthetic cathinone mephedrone*, in *Neuropharmacology of New Psychoactive Substances (NPS)*. 2016, Springer. p. 313-331.
63. Brunt, T.M., et al., *Instability of the ecstasy market and a new kid on the block: mephedrone.* Journal of psychopharmacology, 2011. **25**(11): p. 1543-1547.
64. Van Hout, M.C. and T. Bingham, *"A Costly Turn On": Patterns of use and perceived consequences of mephedrone based head shop products amongst Irish injectors.* International Journal of Drug Policy, 2012. **23**(3): p. 188-197.
65. Sedefov, R. and A. Gallegos, *EMCDDA risk assessments: report on the risk assessment of mephedrone in the framework of the council decision on new psychoactive substances.* 2011.
66. EMCDDA, E., *EU Drug Markets Report: Strategic Overview*, 2016, Lisbon.
67. Reuter, P. and B. Pardo, *New psychoactive substances: Are there any good options for regulating new psychoactive substances?* International Journal of Drug Policy, 2017. **40**: p. 117-122.
68. Bäckberg, M., et al., *Characteristics of analytically confirmed 3-MMC-related intoxications from the Swedish STRIDA project.* Clinical Toxicology, 2015. **53**(1): p. 46-53.
69. Ameline, A., et al., *Determination of a threshold fatal 3-MMC concentration in human: mission impossible.* Psychopharmacology, 2019. **236**(3): p. 865-867.
70. Daveluy, A., et al., *Poisoning by synthetic cathinones: Consumption behaviour and clinical description from 11 cases recorded by the Addictovigilance Centre of Bordeaux.* Toxicologie analytique et clinique, 2017. **29**(1): p. 34-40.
71. Sande, M., *Characteristics of the use of 3-MMC and other new psychoactive drugs in Slovenia, and the perceived problems experienced by users.* International Journal of Drug Policy, 2016. **27**: p. 65-73.
72. Adamowicz, P., et al., *3-Methylmethcathinone—Interpretation of blood concentrations based on analysis of 95 cases.* Journal of analytical toxicology, 2016. **40**(4): p. 272-276.
73. da Silva, D.D., et al., *The new psychoactive substance 3-methylmethcathinone (3-MMC or metaphedrone) induces oxidative stress, apoptosis, and autophagy in primary rat hepatocytes at human-relevant concentrations.* Archives of toxicology, 2019. **93**(9): p. 2617-2634.

74. Kelly, J.P., *Cathinone derivatives: a review of their chemistry, pharmacology and toxicology.* Drug Test Analysis, 2011. **3**: p. 439-453.
75. Karila, L., et al., *The effects and risks associated to mephedrone and methylone in humans: a review of the preliminary evidences.* Brain research bulletin, 2016. **126**: p. 61-67.
76. Dependence, W.E.C.o.D. and W.H. Organization, *WHO Expert Committee on Drug Dependence: thirty-sixth report*. Vol. 991. 2015: World Health Organization.
77. Bossong, M., J. Van Dijk, and R. Niesink, *Methylone and mCPP, two new drugs of abuse?* Addiction biology, 2005. **10**(4): p. 321-323.
78. López‐Arnau, R., et al., *Comparative neuropharmacology of three psychostimulant cathinone derivatives: butylone, mephedrone and methylone.* British journal of pharmacology, 2012. **167**(2): p. 407-420.
79. Prosser, J.M. and L.S. Nelson, *The toxicology of bath salts: a review of synthetic cathinones.* Journal of Medical Toxicology, 2012. **8**(1): p. 33-42.
80. Westphal, F., et al., *Mass and NMR spectroscopic characterization of 3, 4-methylenedioxypyrovalerone: a designer drug with α-pyrrolidinophenone structure.* Forensic Science International, 2009. **190**(1-3): p. 1-8.
81. Zuba, D. and B. Byrska, *Prevalence and co‐existence of active components of 'legal highs'*. Drug testing and analysis, 2013. **5**(6): p. 420-429.
82. Baumann, M.H., et al., *Powerful cocaine-like actions of 3, 4-methylenedioxypyrovalerone (MDPV), a principal constituent of psychoactive 'bath salts' products.* Neuropsychopharmacology, 2013. **38**(4): p. 552.
83. Coppola, M. and R. Mondola, *3, 4-methylenedioxypyrovalerone (MDPV): chemistry, pharmacology and toxicology of a new designer drug of abuse marketed online.* Toxicology letters, 2012. **208**(1): p. 12-15.
84. Drug Enforcement Administration, D.o.J., *Schedules of controlled substances: temporary placement of three synthetic cathinones in Schedule I. Final Order.* Federal register, 2011. **76**(204): p. 65371.
85. Murray, B.L., C.M. Murphy, and M.C. Beuhler, *Death following recreational use of designer drug "bath salts" containing 3, 4-methylenedioxypyrovalerone (MDPV).* Journal of Medical Toxicology, 2012. **8**(1): p. 69-75.
86. Eshleman, A.J., et al., *Substituted methcathinones differ in transporter and receptor interactions.* Biochemical pharmacology, 2013. **85**(12): p. 1803-1815.
87. Fleckenstein, A.E., J.W. Gibb, and G.R. Hanson, *Differential effects of stimulants on monoaminergic transporters: pharmacological consequences and implications for neurotoxicity.* European journal of pharmacology, 2000. **406**(1): p. 1-13.
88. Katselou, M., et al., *α-PVP ("flakka"): a new synthetic cathinone invades the drug arena.* Forensic Toxicology, 2016. **34**(1): p. 41-50.
89. Nagai, H., et al., *Sudden death after sustained restraint following self-administration of the designer drug α-pyrrolidinovalerophenone.* International journal of cardiology, 2014. **172**(1): p. 263-265.
90. Wurita, A., et al., *Postmortem distribution of α-pyrrolidinobutiophenone in body fluids and solid tissues of a human cadaver.* Legal medicine, 2014. **16**(5): p. 241-246.
91. Drug Enforcement Administration, D.o.J., *Schedules of controlled substances: temporary placement of 10 synthetic cathinones into Schedule I. Final order.* Federal register, 2014. **79**(45): p. 12938.

92. Schifano, F., et al., *Mephedrone (4-methylmethcathinone;'meow meow'): chemical, pharmacological and clinical issues.* Psychopharmacology, 2011. **214**(3): p. 593-602.
93. Heffe, W., *Die STEVENS‐Umlagerung von Allyl‐phenacyl‐ammoniumsalzen.* Helvetica Chimica Acta, 1964. **47**(5): p. 1289-1292.
94. Vardakou, I., et al., *Naphyrone: a "legal high" not legal any more.* Drug and chemical toxicology, 2012. **35**(4): p. 467-471.
95. Meltzer, P.C., et al., *1-(4-Methylphenyl)-2-pyrrolidin-1-yl-pentan-1-one (Pyrovalerone) analogues: a promising class of monoamine uptake inhibitors.* Journal of medicinal chemistry, 2006. **49**(4): p. 1420-1432.
96. Brandt, S.D., et al., *The naphyrone story: The alpha or beta‐naphthyl isomer?* Drug testing and analysis, 2010. **2**(10): p. 496-502.
97. Archer, R., *Fluoromethcathinone, a new substance of abuse.* Forensic Science International, 2009. **185**(1-3): p. 10-20.
98. Brandt, S., *4‐Fluoromethcathinone (flephedrone; 4‐FMC). Critical Review Report. Agenda item 4.16. Expert Committee on Drug Dependence. Thirty‐sixth Meeting. Geneva, 16‐20 June 2014 (World Health Organization).* 2014.
99. Zetterqvist, A.V., J. Merlo, and S. Mulinari, *Complaints, complainants, and rulings regarding drug promotion in the United Kingdom and Sweden 2004–2012: A quantitative and qualitative study of pharmaceutical Industry self-regulation.* PLoS medicine, 2015. **12**(2).
100. Tomczak, E., et al., *Blood concentrations of a new psychoactive substance 4-chloromethcathinone (4-CMC) determined in 15 forensic cases.* Forensic toxicology, 2018. **36**(2): p. 476-485.
101. Wiergowski, M., et al., *Identification of novel psychoactive substances 25B-NBOMe and 4-CMC in biological material using HPLC-Q-TOF-MS and their quantification in blood using UPLC–MS/MS in case of severe intoxications.* Journal of Chromatography B, 2017. **1041**: p. 1-10.
102. Penders, T.M., R.E. Gestring, and D.A. Vilensky, *Excited delirium following use of synthetic cathinones (bath salts).* General hospital psychiatry, 2012. **34**(6): p. 647-650.
103. Peroutka, S.J., H. Newman, and H. Harris, *Subjective effects of 3, 4-methylenedioxymethamphetamine in recreational users.* Neuropsychopharmacology, 1988. **1**(4): p. 273-277.
104. Cohen, R.S., *Subjective reports on the effects of the MDMA (" ecstasy") experience in humans.* Progress in neuro-psychopharmacology & biological psychiatry, 1995.
105. Duarte, J.A., et al., *Strenuous exercise aggravates MDMA-induced skeletal muscle damage in mice.* Toxicology, 2005. **206**(3): p. 349-358.
106. Kelly, O.M., et al., *The preservation of in vivo phosphorylated and activated uncoupling protein 3 (UCP3) in isolated skeletal muscle mitochondria following administration of 3, 4-methylenedioxymethamphetamine (MDMA aka ecstasy) to rats/mice.* Mitochondrion, 2012. **12**(1): p. 110-119.
107. Ostapowicz, G., et al., *Results of a prospective study of acute liver failure at 17 tertiary care centers in the United States.* Annals of internal medicine, 2002. **137**(12): p. 947-954.
108. Andreu, V., et al., *Ecstasy: a common cause of severe acute hepatotoxicity.* Journal of hepatology, 1998. **29**(3): p. 394-397.

109. Milroy, C., J. Clark, and A. Forrest, *Pathology of deaths associated with" ecstasy" and" eve" misuse.* Journal of clinical pathology, 1996. **49**(2): p. 149-153.
110. Garbino, J., et al., *Ecstasy ingestion and fulminant hepatic failure: liver transplantation to be considered as a last therapeutic option.* Veterinary and human toxicology, 2001. **43**(2): p. 99-102.
111. Ibranyi, E. and J. Schönléber, *Acute liver failure caused by Ecstasy.* Orvosi hetilap, 2003. **144**(29): p. 1455-1456.
112. Ellis, A., et al., *Acute liver damage and ecstasy ingestion.* Gut, 1996. **38**(3): p. 454-458.
113. Lange-Brock, N., et al., *Acute liver failure following the use of ecstasy (MDMA).* Zeitschrift fur Gastroenterologie, 2002. **40**(8): p. 581-586.
114. Brauer, R., et al., *Liver transplantation for the treatment of fulminant hepatic failure induced by the ingestion of ecstasy.* Transplant international, 1997. **10**(3): p. 229-233.
115. Kamijo, Y., et al., *Acute liver failure following intravenous methamphetamine.* Veterinary and human toxicology, 2002. **44**(4): p. 216-217.
116. Zalis, E.G. and L.F. Parmley, *Fatal amphetamine poisoning.* Archives of internal medicine, 1963. **112**(6): p. 822-826.
117. El-Tawil, O.S., et al., *d-Amphetamine-induced cytotoxicity and oxidative stress in isolated rat hepatocytes.* Pathophysiology, 2011. **18**(4): p. 279-285.
118. da Silva, D.D., E. Silva, and H. Carmo, *Cytotoxic effects of amphetamine mixtures in primary hepatocytes are severely aggravated under hyperthermic conditions.* Toxicology in Vitro, 2013. **27**(6): p. 1670-1678.
119. Song, B.-J., et al., *Mechanisms of MDMA (ecstasy)-induced oxidative stress, mitochondrial dysfunction, and organ damage.* Current pharmaceutical biotechnology, 2010. **11**(5): p. 434-443.
120. Da Silva, D.D., et al., *An insight into the hepatocellular death induced by amphetamines, individually and in combination: the involvement of necrosis and apoptosis.* Archives of toxicology, 2013. **87**(12): p. 2165-2185.
121. Fröhlich, S., E. Lambe, and J. O'Dea, *Acute liver failure following recreational use of psychotropic "head shop" compounds.* Irish journal of medical science, 2011. **180**(1): p. 263-264.
122. Valente, M.J., et al., *Editor's Highlight: Characterization of hepatotoxicity mechanisms triggered by designer cathinone drugs (β-Keto Amphetamines).* Toxicological Sciences, 2016. **153**(1): p. 89-102.
123. Valente, M.J., et al., *3, 4-Methylenedioxypyrovalerone (MDPV): in vitro mechanisms of hepatotoxicity under normothermic and hyperthermic conditions.* Archives of toxicology, 2016. **90**(8): p. 1959-1973.
124. Luethi, D., M.E. Liechti, and S. Krähenbühl, *Mechanisms of hepatocellular toxicity associated with new psychoactive synthetic cathinones.* Toxicology, 2017. **387**: p. 57-66.
125. Baylen, C.A. and H. Rosenberg, *A review of the acute subjective effects of MDMA/ecstasy.* Addiction, 2006. **101**(7): p. 933-947.
126. Cruickshank, C.C. and K.R. Dyer, *A review of the clinical pharmacology of methamphetamine.* Addiction, 2009. **104**(7): p. 1085-1099.
127. McKenna, D.J. and S.J. Peroutka, *Neurochemistry and neurotoxicity of 3, 4‐methylenedioxymethamphetamine (MDMA, "ecstasy").* Journal of Neurochemistry, 1990. **54**(1): p. 14-22.

128. Seiden, L., *Neurotoxicity of methamphetamine and related drugs.* Psychopharmacology: The third generation of progress, 1987: p. 359-366.
129. Berman, S., et al., *Abuse of amphetamines and structural abnormalities in brain.* Annals of the New York Academy of Sciences, 2008. **1141**: p. 195.
130. Seiden, L.S. and K.E. Sabol, *Methamphetamine and methylenedioxymethamphetamine neurotoxicity: possible mechanisms of cell destruction.* NIDA Res Monogr, 1996. **163**: p. 251-276.
131. Baumann, M.H., X. Wang, and R.B. Rothman, *3, 4-Methylenedioxymethamphetamine (MDMA) neurotoxicity in rats: a reappraisal of past and present findings.* Psychopharmacology, 2007. **189**(4): p. 407-424.
132. Dunnick, J.K. and S.L. Eustis, *Decreases in spontaneous tumors in rats and mice after treatment with amphetamine.* Toxicology, 1991. **67**(3): p. 325-332.
133. Kita, T., G.C. Wagner, and T. Nakashima, *Current research on methamphetamine-induced neurotoxicity: animal models of monoamine disruption.* Journal of pharmacological sciences, 2003. **92**(3): p. 178-195.
134. Yamamoto, B.K., A. Moszczynska, and G.A. Gudelsky, *Amphetamine toxicities Classical and emerging mechanisms.* Annals of the New York Academy of Sciences, 2010. **1187**: p. 101.
135. Angoa-Pérez, M., J.H. Anneken, and D.M. Kuhn, *Neurotoxicology of synthetic cathinone analogs*, in *Neuropharmacology of New Psychoactive Substances (NPS)*. 2016, Springer. p. 209-230.
136. Yaffe, D. and O. Saxel, *Serial passaging and differentiation of myogenic cells isolated from dystrophic mouse muscle.* Nature, 1977. **270**(5639): p. 725-727.
137. Blau, H.M., et al., *Plasticity of the differentiated state.* Science, 1985. **230**(4727): p. 758-766.
138. Hu, Y., et al., *Lepidopteran DALP, and its mammalian ortholog HIC-5, function as negative regulators of muscle differentiation.* Proceedings of the National Academy of Sciences, 1999. **96**(18): p. 10218-10223.
139. Rajan, S., et al., *Analysis of early C2C12 myogenesis identifies stably and differentially expressed transcriptional regulators whose knock-down inhibits myoblast differentiation.* American Journal of Physiology-Heart and Circulatory Physiology, 2011.
140. Casas-Delucchi, C.S., et al., *Histone acetylation controls the inactive X chromosome replication dynamics.* Nature communications, 2011. **2**(1): p. 1-11.
141. ATCC, *C2C12 (ATCC® CRL-1772™).* 2016.
142. Knowles, B.B. and D.P. Aden, *Human hepatoma derived cell line, process for preparation thereof, and uses therefor*, 1983, Google Patents.
143. Castell, J.V. and M.J. Gmez-Lechn, *In vitro methods in pharmaceutical research*. 1996: Elsevier.
144. López-Terrada, D., et al., *Hep G2 is a hepatoblastoma-derived cell line.* Human pathology, 2009. **40**(10): p. 1512.
145. Castell, J.V., et al., *Hepatocyte cell lines: their use, scope and limitations in drug metabolism studies.* Expert opinion on drug metabolism & toxicology, 2006. **2**(2): p. 183-212.
146. Ihrke, G., et al., *WIF-B cells: an in vitro model for studies of hepatocyte polarity.* The Journal of Cell Biology, 1993. **123**(6): p. 1761-1775.

147. Mersch-Sundermann, V., et al., *Use of a human-derived liver cell line for the detection of cytoprotective, antigenotoxic and cogenotoxic agents.* Toxicology, 2004. **198**(1-3): p. 329-340.
148. ATCC, *Hep G2 [HEPG2] (ATCC® HB-8065™).* 2016.
149. Biedler, J.L., L. Helson, and B.A. Spengler, *Morphology and growth, tumorigenicity, and cytogenetics of human neuroblastoma cells in continuous culture.* Cancer research, 1973. **33**(11): p. 2643-2652.
150. Agholme, L., et al., *An in vitro model for neuroscience: differentiation of SH-SY5Y cells into cells with morphological and biochemical characteristics of mature neurons.* Journal of Alzheimer's Disease, 2010. **20**(4): p. 1069-1082.
151. Jämsä, A., et al., *The retinoic acid and brain-derived neurotrophic factor differentiated SH-SY5Y cell line as a model for Alzheimer's disease-like tau phosphorylation.* Biochemical and biophysical research communications, 2004. **319**(3): p. 993-1000.
152. Cheung, Y.-T., et al., *Effects of all-trans-retinoic acid on human SH-SY5Y neuroblastoma as in vitro model in neurotoxicity research.* Neurotoxicology, 2009. **30**(1): p. 127-135.
153. Koriyama, Y., et al., *Glyceraldehyde caused Alzheimer's disease-like alterations in diagnostic marker levels in SH-SY5Y human neuroblastoma cells.* Scientific reports, 2015. **5**(1): p. 1-7.
154. Kovalevich, J. and D. Langford, *Considerations for the use of SH-SY5Y neuroblastoma cells in neurobiology*, in *Neuronal cell culture*. 2013, Springer. p. 9-21.
155. ATCC, *SH-SY5Y (ATCC® CRL-2266™).* 2016.
156. Encinas, M., et al., *Sequential treatment of SH‐SY5Y cells with retinoic acid and brain‐derived neurotrophic factor gives rise to fully differentiated, neurotrophic factor‐dependent, human neuron‐like cells.* Journal of neurochemistry, 2000. **75**(3): p. 991-1003.
157. Kou, W., D. Luchtman, and C. Song, *Eicosapentaenoic acid (EPA) increases cell viability and expression of neurotrophin receptors in retinoic acid and brain-derived neurotrophic factor differentiated SH-SY5Y cells.* European journal of nutrition, 2008. **47**(2): p. 104-113.
158. Nunnari, J. and A. Suomalainen, *Mitochondria: in sickness and in health.* Cell, 2012. **148**(6): p. 1145-1159.
159. Kujoth, G.C., et al., *Mitochondrial DNA mutations, oxidative stress, and apoptosis in mammalian aging.* Science, 2005. **309**(5733): p. 481-484.
160. Iwasawa, R., et al., *Fis1 and Bap31 bridge the mitochondria–ER interface to establish a platform for apoptosis induction.* The EMBO journal, 2011. **30**(3): p. 556-568.
161. Voelker, D.R., *Genetic and biochemical analysis of non-vesicular lipid traffic.* Annual review of biochemistry, 2009. **78**: p. 827-856.
162. De Stefani, D., et al., *A forty-kilodalton protein of the inner membrane is the mitochondrial calcium uniporter.* Nature, 2011. **476**(7360): p. 336.
163. McFarland, R. and D. Turnbull, *Batteries not included: diagnosis and management of mitochondrial disease.* Journal of internal medicine, 2009. **265**(2): p. 210-228.
164. Krähenbühl, S., *Mitochondria: important target for drug toxicity?* Journal of hepatology, 2001. **34**(2): p. 334-336.
165. Voet, D., J.G. Voet, and C.W. Pratt, *Fundamentals of biochemistry: life at the molecular level.* Hoboken: Wiley, 2006: p. 547-556.

166. Lewis, M.T., et al., *Quantification of Mitochondrial Oxidative Phosphorylation in Metabolic Disease: Application to Type 2 Diabetes.* International journal of molecular sciences, 2019. **20**(21): p. 5271.
167. Koopman, W.J., P.H. Willems, and J.A. Smeitink, *Monogenic mitochondrial disorders.* New England Journal of Medicine, 2012. **366**(12): p. 1132-1141.
168. Zickermann, V., et al., *Functional implications from an unexpected position of the 49-kDa subunit of NADH: ubiquinone oxidoreductase.* Journal of Biological Chemistry, 2003. **278**(31): p. 29072-29078.
169. Saraste, M., *Oxidative phosphorylation at the fin de siecle.* Science, 1999. **283**(5407): p. 1488-1493.
170. Bleier, L. and S. Dröse, *Superoxide generation by complex III: from mechanistic rationales to functional consequences.* Biochimica et Biophysica Acta (BBA)-Bioenergetics, 2013. **1827**(11-12): p. 1320-1331.
171. Bruno, C., et al., *A stop-codon mutation in the human mtDNA cytochrome c oxidase I gene disrupts the functional structure of complex IV.* The American Journal of Human Genetics, 1999. **65**(3): p. 611-620.
172. Taanman, J.-W., *Human cytochrome c oxidase: structure, function, and deficiency.* Journal of bioenergetics and biomembranes, 1997. **29**(2): p. 151-163.
173. Hatefi, Y., *The mitochondrial electron transport and oxidative phosphorylation system.* Annual review of biochemistry, 1985. **54**(1): p. 1015-1069.
174. Nicholls, D. and S. Ferguson, *Bioenergetics 3 Academic Press.* London, United Kingdom [Google Scholar], 2002.
175. Mitchell, P. and J. Moyle, *Estimation of membrane potential and pH difference across the cristae membrane of rat liver mitochondria.* European journal of biochemistry, 1969. **7**(4): p. 471-484.
176. Berg, J., *Tymoczko JL, Stryer L.* Biochemistry, 2002.
177. Ferrick, D.A., A. Neilson, and C. Beeson, *Advances in measuring cellular bioenergetics using extracellular flux.* Drug discovery today, 2008. **13**(5-6): p. 268-274.
178. Dranka, B.P., et al., *Assessing bioenergetic function in response to oxidative stress by metabolic profiling.* Free Radical Biology and Medicine, 2011. **51**(9): p. 1621-1635.
179. Perry, C.G., et al., *Methods for assessing mitochondrial function in diabetes.* Diabetes, 2013. **62**(4): p. 1041-1053.
180. Rose, S., et al., *Oxidative stress induces mitochondrial dysfunction in a subset of autism lymphoblastoid cell lines in a well-matched case control cohort.* PloS one, 2014. **9**(1).
181. Mitchell, P., *Coupling of phosphorylation to electron and hydrogen transfer by a chemi-osmotic type of mechanism.* Nature, 1961. **191**(4784): p. 144-148.
182. Mitchell, P., *Chemiosmotic coupling in oxidative and photosynthetic phosphorylation.* Biological Reviews, 1966. **41**(3): p. 445-501.
183. Martínez-Reyes, I., et al., *TCA cycle and mitochondrial membrane potential are necessary for diverse biological functions.* Molecular cell, 2016. **61**(2): p. 199-209.
184. Nicholls, D.G. and M.W. Ward, *Mitochondrial membrane potential and neuronal glutamate excitotoxicity: mortality and millivolts.* Trends in neurosciences, 2000. **23**(4): p. 166-174.
185. Perry, S.W., et al., *Mitochondrial membrane potential probes and the proton gradient: a practical usage guide.* Biotechniques, 2011. **50**(2): p. 98-115.

186. Szabadkai, G. and M.R. Duchen, *Mitochondria: the hub of cellular Ca2+ signaling.* Physiology, 2008. **23**(2): p. 84-94.
187. Votyakova, T.V. and I.J. Reynolds, *$\Delta \Psi m$ - Dependent and - independent production of reactive oxygen species by rat brain mitochondria.* Journal of neurochemistry, 2001. **79**(2): p. 266-277.
188. Boveris, A. and E. Cadenas, *Mitochondrial production of superoxide anions and its relationship to the antimycin insensitive respiration.* FEBS letters, 1975. **54**(3): p. 311-314.
189. Sorgato, M.C., et al., *Oxygen radicals and hydrogen peroxide in rat brain mitochondria.* FEBS letters, 1974. **45**(1-2): p. 92-95.
190. Droge, W., *Free radicals in the physiological control of cell function.* Physiological reviews, 2002. **82**(1): p. 47-95.
191. Willcox, J.K., S.L. Ash, and G.L. Catignani, *Antioxidants and prevention of chronic disease.* Critical reviews in food science and nutrition, 2004. **44**(4): p. 275-295.
192. Pacher, P., J.S. Beckman, and L. Liaudet, *Nitric oxide and peroxynitrite in health and disease.* Physiological reviews, 2007. **87**(1): p. 315-424.
193. Genestra, M., *Oxyl radicals, redox-sensitive signalling cascades and antioxidants.* Cellular signalling, 2007. **19**(9): p. 1807-1819.
194. Halliwell, B., *Biochemistry of oxidative stress.* Biochemical society transactions, 2007. **35**(5): p. 1147-1150.
195. Zuo, L., et al., *Biological and physiological role of reactive oxygen species–the good, the bad and the ugly.* Acta physiologica, 2015. **214**(3): p. 329-348.
196. Quinton, M.S. and B.K. Yamamoto, *Causes and consequences of methamphetamine and MDMA toxicity.* The AAPS journal, 2006. **8**(2): p. E337-E337.
197. Lockshin, R.A. and Z. Zakeri, *Apoptosis, autophagy, and more.* The international journal of biochemistry & cell biology, 2004. **36**(12): p. 2405-2419.
198. Ulukaya, E., C. Acilan, and Y. Yilmaz, *Apoptosis: why and how does it occur in biology?* Cell biochemistry and function, 2011. **29**(6): p. 468-480.
199. Leist, M., et al., *Intracellular adenosine triphosphate (ATP) concentration: a switch in the decision between apoptosis and necrosis.* The Journal of experimental medicine, 1997. **185**(8): p. 1481-1486.
200. Cotter, T.G. and M. Al-Rubeai, *Cell death (apoptosis) in cell culture systems.* Trends in biotechnology, 1995. **13**(4): p. 150-155.
201. Kumar, V., et al., *Robbins and Cotran pathologic basis of disease, professional edition e-book*. 2014: elsevier health sciences.
202. Kerr, J.F., A.H. Wyllie, and A.R. Currie, *Apoptosis: a basic biological phenomenon with wideranging implications in tissue kinetics.* British journal of cancer, 1972. **26**(4): p. 239-257.
203. Majno, G. and I. Joris, *Apoptosis, oncosis, and necrosis. An overview of cell death.* The American journal of pathology, 1995. **146**(1): p. 3.
204. Cory, S. and J.M. Adams, *The Bcl2 family: regulators of the cellular life-or-death switch.* Nature Reviews Cancer, 2002. **2**(9): p. 647-656.
205. Nair, P., et al., *Apoptosis initiation through the cell-extrinsic pathway*, in *Methods in enzymology*. 2014, Elsevier. p. 99-128.
206. Pereira, W. and G. Amarante - Mendes, *Apoptosis: a programme of cell death or cell disposal?* Scandinavian journal of immunology, 2011. **73**(5): p. 401-407.

207. Green, D.R. and J.C. Reed, *Mitochondria and apoptosis.* Science, 1998. **281**(5381): p. 1309-1312.
208. McIlwain, D.R., T. Berger, and T.W. Mak, *Caspase functions in cell death and disease.* Cold Spring Harbor perspectives in biology, 2013. **5**(4): p. a008656.
209. Ashkenazi, A. and V.M. Dixit, *Death receptors: signaling and modulation.* science, 1998. **281**(5381): p. 1305-1308.
210. Samraj, A.K., et al., *Loss of caspase-9 provides genetic evidence for the type I/II concept of CD95-mediated apoptosis.* Journal of Biological Chemistry, 2006. **281**(40): p. 29652-29659.
211. Acehan, D., et al., *Three-dimensional structure of the apoptosome: implications for assembly, procaspase-9 binding, and activation.* Molecular cell, 2002. **9**(2): p. 423-432.
212. Shiozaki, E.N., J. Chai, and Y. Shi, *Oligomerization and activation of caspase-9, induced by Apaf-1 CARD.* Proceedings of the National Academy of Sciences, 2002. **99**(7): p. 4197-4202.
213. Thornberry, N.A. and Y. Lazebnik, *Caspases: enemies within.* Science, 1998. **281**(5381): p. 1312-1316.
214. Cryns, V. and J. Yuan, *Proteases to die for.* Genes & development, 1998. **12**(11): p. 1551-1570.
215. Salvesen, G.S., *Caspases: opening the boxes and interpreting the arrows*, 2002, Nature Publishing Group.
216. Ghavami, S., et al., *Apoptosis and cancer: mutations within caspase genes.* Journal of medical genetics, 2009. **46**(8): p. 497-510.
217. Porter, A.G. and R.U. Jänicke, *Emerging roles of caspase-3 in apoptosis.* Cell death & differentiation, 1999. **6**(2): p. 99-104.
218. Clarke, P. and K.L. Tyler, *Apoptosis in animal models of virus-induced disease.* Nature Reviews Microbiology, 2009. **7**(2): p. 144-155.
219. Klionsky, D.J., *Autophagy.* Current Biology, 2005. **15**(8): p. R282-R283.
220. Yorimitsu, T. and D.J. Klionsky, *Autophagy: molecular machinery for self-eating.* Cell Death & Differentiation, 2005. **12**(2): p. 1542-1552.
221. Aredia, F. and A.I. Scovassi, *Manipulation of autophagy in cancer cells: an innovative strategy to fight drug resistance.* Future medicinal chemistry, 2013. **5**(9): p. 1009-1021.
222. Kadowaki, M. and T. Kanazawa, *Amino acids as regulators of proteolysis.* The Journal of nutrition, 2003. **133**(6): p. 2052S-2056S.
223. Petiot, A., et al., *Diversity of signaling controls of macroautophagy in mammalian cells.* Cell structure and function, 2002. **27**(6): p. 431-441.
224. Ogier-Denis, E. and P. Codogno, *Autophagy: a barrier or an adaptive response to cancer.* Biochimica et Biophysica Acta (BBA)-Reviews on Cancer, 2003. **1603**(2): p. 113-128.
225. Mizushima, N., Y. Ohsumi, and T. Yoshimori, *Autophagosome formation in mammalian cells.* Cell structure and function, 2002. **27**(6): p. 421-429.
226. Klionsky, D.J. and S.D. Emr, *Autophagy as a regulated pathway of cellular degradation.* Science, 2000. **290**(5497): p. 1717-1721.
227. Dunn Jr, W., *Studies on the mechanisms of autophagy: maturation of the autophagic vacuole.* The Journal of cell biology, 1990. **110**(6): p. 1935-1945.

228. Lawrence, B.P. and W.J. Brown, *Autophagic vacuoles rapidly fuse with pre-existing lysosomes in cultured hepatocytes.* Journal of Cell Science, 1992. **102**(3): p. 515-526.
229. Gordon, P.B. and P.O. Seglen, *Prelysosomal convergence of autophagic and endocytic pathways.* Biochemical and biophysical research communications, 1988. **151**(1): p. 40-47.
230. Liou, W., et al., *The autophagic and endocytic pathways converge at the nascent autophagic vacuoles.* The Journal of cell biology, 1997. **136**(1): p. 61-70.
231. Nixon, R.A., et al., *Extensive involvement of autophagy in Alzheimer disease: an immuno-electron microscopy study.* Journal of Neuropathology & Experimental Neurology, 2005. **64**(2): p. 113-122.
232. Brunk, U.T. and A. Terman, *The mitochondrial‐lysosomal axis theory of aging: accumulation of damaged mitochondria as a result of imperfect autophagocytosis.* European Journal of Biochemistry, 2002. **269**(8): p. 1996-2002.
233. Larsen, K.E. and D. Sulzer, *Autophagy in neurons a review.* Histology and histopathology, 2002.
234. Tolkovsky, A.M., et al., *Mitochondrial disappearance from cells: a clue to the role of autophagy in programmed cell death and disease?* Biochimie, 2002. **84**(2-3): p. 233-240.
235. Hornung, J., H. Koppel, and P. Clarke, *Endocytosis and autophagy in dying neurons: an ultrastructural study in chick embryos.* Journal of Comparative Neurology, 1989. **283**(3): p. 425-437.
236. Baehrecke, E., *Autophagic programmed cell death in Drosophila.* Cell Death & Differentiation, 2003. **10**(9): p. 940-945.
237. Uchiyama, Y., *Autophagic cell death and its execution by lysosomal cathepsins.* Archives of histology and cytology, 2001. **64**(3): p. 233-246.
238. Nixon, R.A., A.M. Cataldo, and P.M. Mathews, *The endosomal-lysosomal system of neurons in Alzheimer's disease pathogenesis: a review.* Neurochemical research, 2000. **25**(9-10): p. 1161-1172.
239. Krampe, B. and M. Al-Rubeai, *Cell death in mammalian cell culture: molecular mechanisms and cell line engineering strategies.* Cytotechnology, 2010. **62**(3): p. 175-188.
240. Gozuacik, D. and A. Kimchi, *Autophagy as a cell death and tumor suppressor mechanism.* Oncogene, 2004. **23**(16): p. 2891-2906.
241. Hansen, M., D.C. Rubinsztein, and D.W. Walker, *Autophagy as a promoter of longevity: insights from model organisms.* Nature Reviews Molecular Cell Biology, 2018. **19**(9): p. 579-593.
242. Callaway, C.W. and R.F. Clark, *Hyperthermia in psychostimulant overdose.* Annals of Emergency Medicine, 1994. **24**(1): p. 68-76.
243. Green, A.R., E. O'Shea, and M.I. Colado, *A review of the mechanisms involved in the acute MDMA (ecstasy)-induced hyperthermic response.* European Journal of Pharmacology, 2004. **500**: p. 3-13.
244. Halpern, P., et al., *Morbidity associated with MDMA (ecstasy) abuse: a survey of emergency department admissions. .* Human & Experimental Toxicology, 2011. **30**(4): p. 259-266.
245. Parrott, A.C., *MDMA and temperature: a review of the thermal effects of 'Ecstasy' in humans.* Drug and Alcohol Dependence, 2012. **121**(1-2): p. 1-9.

246. Liechti, M.E., *Effects of MDMA on body temperature in humans.* Temperature, 2014. **1**(3): p. 192-200.
247. Zaami, S., et al., *Synthetic cathinones related fatalities: an update.* Eur Rev Med Pharmacol Sci, 2018. **22**(1): p. 268-274.
248. Winstock, A., et al., *Mephedrone: use, subjective effects and health risks.* Addiction, 2011. **106**(11): p. 1991-1996.
249. Baggott, M., et al., *Chemical analysis of ecstasy pills.* JAMA, 2000. **284**(17): p. 2190.
250. Camilleri, A.M. and D. Caldicott, *Underground pill testing, down under.* Forensic Sci Int, 2005. **151**(1): p. 53-58.
251. Smith, D.E. and C.M. Fischer, *An analysis of 310 cases of acute high-dose methamphetamine toxicity in Haight-Ashbury.* Clinical toxicology, 1970. **3**(1): p. 117-124.
252. White, C.M., *Mephedrone and 3, 4 ‐ Methylenedioxypyrovalerone (MDPV): synthetic cathinones with serious health implications.* The Journal of Clinical Pharmacology, 2016. **56**(11): p. 1319-1325.
253. Marinetti, L.J. and H.M. Antonides, *Analysis of synthetic cathinones commonly found in bath salts in human performance and postmortem toxicology: method development, drug distribution and interpretation of results.* Journal of analytical toxicology, 2013. **37**(3): p. 135-146.
254. Coppola, M. and R. Mondola, *Synthetic cathinones: chemistry, pharmacology and toxicology of a new class of designer drugs of abuse marketed as "bath salts" or "plant food".* Toxicology letters, 2012. **211**(2): p. 144-149.
255. Connell, P.H., *Amphetamine psychosis.* British medical journal, 1957. **1**(5018): p. 582.
256. Derlet, R.W., et al., *Amphetamine toxicity: experience with 127 cases.* The Journal of emergency medicine, 1989. **7**(2): p. 157-161.
257. Steinkellner, T., et al., *The ugly side of amphetamines: short-and long-term toxicity of 3, 4-methylenedioxymethamphetamine (MDMA,'Ecstasy'), methamphetamine and D-amphetamine.* Biological chemistry, 2011. **392**(1-2): p. 103-115.
258. Papaseit, E., et al., *Mephedrone concentrations in cases of clinical intoxication.* Current pharmaceutical design, 2017. **23**(36): p. 5511-5522.
259. De Letter, E.A., et al., *Interpretation of a 3, 4-methylenedioxymethamphetamine (MDMA) blood level: discussion by means of a distribution study in two fatalities.* Forensic science international, 2004. **141**(2-3): p. 85-90.
260. Turcant, A., et al., *A 6-year review of new psychoactive substances at the Centre antipoison Grand-Ouest d'Angers: Clinical and biological data.* Toxicologie Analytique et Clinique, 2017. **29**(1): p. 18-33.
261. Gerets, H., et al., *Characterization of primary human hepatocytes, HepG2 cells, and HepaRG cells at the mRNA level and CYP activity in response to inducers and their predictivity for the detection of human hepatotoxins.* Cell biology and toxicology, 2012. **28**(2): p. 69-87.
262. Fuller, R.W., *Structure-activity relationships among the halogenated amphetamines.* Ann. NY Acad. Sci, 1978. **305**: p. 147.
263. Thornton, S.L., R.R. Gerona, and C.A. Tomaszewski, *Psychosis from a bath salt product containing flephedrone and MDPV with serum, urine, and product quantification.* Journal of Medical Toxicology, 2012. **8**(3): p. 310-313.

264. Baumann, M.H., et al., *In vivo effects of amphetamine analogs reveal evidence for serotonergic inhibition of mesolimbic dopamine transmission in the rat.* Journal of Pharmacology and Experimental Therapeutics, 2011. **337**(1): p. 218-225.
265. Simmler, L., et al., *Monoamine transporter and receptor interaction profiles of a new series of designer cathinones.* Neuropharmacology, 2014. **79**: p. 152-160.
266. Rickli, A., M.C. Hoener, and M.E. Liechti, *Monoamine transporter and receptor interaction profiles of novel psychoactive substances: para-halogenated amphetamines and pyrovalerone cathinones.* European Neuropsychopharmacology, 2015. **25**(3): p. 365-376.
267. Luethi, D., et al., *Pharmacological profile of mephedrone analogs and related new psychoactive substances.* Neuropharmacology, 2018. **134**: p. 4-12.
268. Luethi, D. and M.E. Liechti, *Monoamine transporter and receptor interaction profiles in vitro predict reported human doses of novel psychoactive stimulants and psychedelics.* International Journal of Neuropsychopharmacology, 2018. **21**(10): p. 926-931.
269. Johnson, M.P., et al., *Behavioral, biochemical and neurotoxicological actions of the α-ethyl homologue of p-chloroamphetamine.* European journal of pharmacology, 1990. **191**(1): p. 1-10.
270. Lappin, J.M., S. Darke, and M. Farrell, *Methamphetamine use and future risk for Parkinson's disease: Evidence and clinical implications.* Drug and alcohol dependence, 2018. **187**: p. 134-140.
271. Lopes, F.M., et al., *Comparison between proliferative and neuron-like SH-SY5Y cells as an in vitro model for Parkinson disease studies.* Brain research, 2010. **1337**: p. 85-94.
272. Karbowski, M. and A. Neutzner, *Neurodegeneration as a consequence of failed mitochondrial maintenance.* Acta neuropathologica, 2012. **123**(2): p. 157-171.
273. Carvalho, M., et al., *Toxicity of amphetamines: an update.* Archives of toxicology, 2012. **86**(8): p. 1167-1231.
274. Wallace, K.B. and A. Starkov, *Mitochondrial targets of drug toxicity.* Annual review of pharmacology and toxicology, 2000. **40**(1): p. 353-388.
275. Felser, A., et al., *Mechanisms of hepatocellular toxicity associated with dronedarone—a comparison to amiodarone.* Toxicological sciences, 2013. **131**(2): p. 480-490.
276. Fromenty, B., et al., *Dual effect of amiodarone on mitochondrial respiration. Initial protonophoric uncoupling effect followed by inhibition of the respiratory chain at the levels of complex I and complex II.* Journal of Pharmacology and Experimental Therapeutics, 1990. **255**(3): p. 1377-1384.
277. Hyun, D.H., et al., *Up‐regulation of plasma membrane‐associated redox activities in neuronal cells lacking functional mitochondria.* Journal of neurochemistry, 2007. **100**(5): p. 1364-1374.
278. Volobueva, A.S., et al., *Mitochondrial genome variability: the effect on cellular functional activity.* Therapeutics and clinical risk management, 2018. **14**: p. 237-245.
279. Halpin, L.E., S.A. Collins, and B.K. Yamamoto, *Neurotoxicity of methamphetamine and 3, 4-methylenedioxymethamphetamine.* Life sciences, 2014. **97**(1): p. 37-44.
280. Yamamoto, B.K. and M.G. Bankson, *Amphetamine neurotoxicity: cause and consequence of oxidative stress.* Critical Reviews™ in Neurobiology, 2005. **17**(2).

281. Valente, M.J.o., et al., *Neurotoxicity of β-keto amphetamines: deathly mechanisms elicited by methylone and MDPV in human dopaminergic SH-SY5Y cells.* ACS chemical neuroscience, 2017. **8**(4): p. 850-859.
282. Wang, Y., et al., *ROS-induced mitochondrial depolarization initiates PARK2/PARKIN-dependent mitochondrial degradation by autophagy.* Autophagy, 2012. **8**(10): p. 1462-1476.
283. Mammucari, C. and R. Rizzuto, *Signaling pathways in mitochondrial dysfunction and aging.* Mech Ageing Dev, 2010. **131**(7-8): p. 536-543.
284. Antico Arciuch, V.G., et al., *Mitochondrial regulation of cell cycle and proliferation.* Antioxidants & redox signaling, 2012. **16**(10): p. 1150-1180.
285. Turrens, J.F., *Superoxide production by the mitochondrial respiratory chain.* Bioscience reports, 1997. **17**(1): p. 3-8.
286. Naserzadeh, P., et al., *A comparison of mitochondrial toxicity of mephedrone on three separate parts of brain including hippocampus, cortex and cerebellum.* Neurotoxicology, 2019. **73**: p. 40-49.
287. Zorova, L.D., et al., *Mitochondrial membrane potential.* Analytical biochemistry, 2018. **552**: p. 50-59.
288. Simon, H.-U., A. Haj-Yehia, and F. Levi-Schaffer, *Role of reactive oxygen species (ROS) in apoptosis induction.* Apoptosis, 2000. **5**(5): p. 415-418.
289. Eguchi, Y., S. Shimizu, and Y. Tsujimoto, *Intracellular ATP levels determine cell death fate by apoptosis or necrosis.* Cancer research, 1997. **57**(10): p. 1835-1840.
290. Liu, X., et al., *Induction of apoptotic program in cell-free extracts:Requirement for datp and cytochrome c.* Cell, 1996. **86**: p. 147–157.
291. Paech, F., J. Bouitbir, and S. Krähenbühl, *Hepatocellular toxicity associated with tyrosine kinase inhibitors: mitochondrial damage and inhibition of glycolysis.* Frontiers in pharmacology, 2017. **8**: p. 367.
292. Flynn, J.M. and S. Melov, *SOD2 in mitochondrial dysfunction and neurodegeneration.* Free Radical Biology and Medicine, 2013. **62**: p. 4-12.
293. Hilgendorf, C., et al., *Expression of thirty-six drug transporter genes in human intestine, liver, kidney, and organotypic cell lines.* Drug Metabolism and Disposition, 2007. **35**(8): p. 1333-1340.
294. Freyberg, Z., et al., *Mechanisms of amphetamine action illuminated through optical monitoring of dopamine synaptic vesicles in Drosophila brain.* Nature communications, 2016. **7**(1): p. 1-15.
295. Encinas, M., et al., *Sequential treatment of sh-sy5y cells with retinoic acid and brain-derived neurotrophic factor gives rise to fully differentiated, neurotrophic factor-dependent, human neuron-like cells.* Journal of Neurochemistry, 2000. **75**: p. 991–1003.
296. Kovalevich, J. and D. Langford, *Considerations for the use of SH-SY5Y neuroblastoma cells in neurobiology.* Methods in Molecular Biology, 2013. **1078**: p. 9-21.
297. Schneider, L., et al., *Differentiation of SH-SY5Y cells to a neuronal phenotype changes cellular bioenergetics and the response to oxidative stress.* Free Radical Biology and Medicine, 2011. **51**(11): p. 2007-2017.
298. McAllen, K.J. and D.R. Schwartz, *Adverse drug reactions resulting in hyperthermia in the intensive care unit.* Critical Care Medicine, 2010. **38**(6 Suppl): p. S244-252.

299. Silins, E., J. Copeland, and P. Dillon, *Qualitative review of serotonin syndrome, ecstasy (MDMA) and the use of other serotonergic substances: hierarchy of risk.* Australian & New Zealand Journal of Psychiatry, 2007. **41**(8): p. 649-655.
300. Mechan, A.O., et al., *The pharmacology of the acute hyperthermic response that follows administration of 3, 4 - methylenedioxymethamphetamine (MDMA, 'ecstasy') to rats.* British journal of pharmacology, 2002. **135**(1): p. 170-180.
301. Rothman, R.B. and M.H. Baumann, *Monoamine transporters and psychostimulant drugs.* European journal of pharmacology, 2003. **479**(1-3): p. 23-40.
302. Sitte, H.H. and M. Freissmuth, *Amphetamines, new psychoactive drugs and the monoamine transporter cycle.* Trends in pharmacological sciences, 2015. **36**(1): p. 41-50.
303. Docherty, J. and A. Green, *The role of monoamines in the changes in body temperature induced by 3, 4 - methylenedioxymethamphetamine (MDMA, ecstasy) and its derivatives.* British journal of pharmacology, 2010. **160**(5): p. 1029-1044.
304. Burrows, K.B., G. Gudelsky, and B.K. Yamamoto, *Rapid and transient inhibition of mitochondrial function following methamphetamine or 3,4-methylenedioxymethamphetamine administration.* European Journal of Pharmacology, 2000. **398**: p. 11-18.
305. López-Arnau, R., et al., *Neuronal changes and oxidative stress in adolescent rats after repeated exposure to mephedrone.* Toxicology and applied pharmacology, 2015. **286**(1): p. 27-35.
306. Chen, Q., et al., *Production of reactive oxygen species by mitochondria: central role of complex III.* The journal of biological chemistry, 2003. **278**(38): p. 36027-36031.
307. Kerr, J.F.R., A.H. Wyllie, and A.R. Currie, *Apoptosis: A basic biological phenomenon with wide- ranging implications in tissue kinetics.* British Journal of Cancer, 1972. **26**(4): p. 239-257.
308. Harmon, B.V., et al., *Cell death induced in a murine mastocytoma by 42–47°c heating in vitro: Evidence that the form of death changes from apoptosis to necrosis above a critical heat load.* International Journal of Radiation Biology, 1990. **58**(5): p. 845-858.
309. Stankiewicz, A.R., et al., *Hsp70 inhibits heat-induced apoptosis upstream of mitochondria by preventing Bax translocation.* Journal of Biological Chemistry, 2005. **280**(46): p. 38729-38739.
310. Li, C.-Y., et al., *Heat shock protein 70 inhibits apoptosis downstream of cytochrome c release and upstream of caspase-3 activation.* Journal of Biological Chemistry, 2000. **275**(33): p. 25665-25671.
311. Siedlecka-Kroplewska, K., et al., *The designer drug 3-fluoromethcathinone induces oxidative stress and activates autophagy in HT22 neuronal cells.* Neurotoxicity research, 2018. **34**(3): p. 388-400.
312. Kaini, R.R., et al., *Autophagy regulates lipolysis and cell survival through lipid droplet degradation in androgen - sensitive prostate cancer cells.* The Prostate, 2012. **72**(13): p. 1412-1422.
313. Guo, F., et al., *Autophagy in neurodegenerative diseases: pathogenesis and therapy.* Brain Pathology, 2018. **28**(1): p. 3-13.
314. Turturici, G., G. Sconzo, and F. Geraci, *Hsp70 and its molecular role in nervous system diseases.* Biochemistry research international, 2011. **2011**.

315. Penke, B., et al., *Heat shock proteins and autophagy pathways in neuroprotection: from molecular bases to pharmacological interventions.* International journal of molecular sciences, 2018. **19**(1): p. 325.